2023 *Oceanography* Supplement

FRONTIERS IN OCEAN OBSERVING

EMERGING TECHNOLOGIES FOR UNDERSTANDING AND MANAGING A CHANGING OCEAN

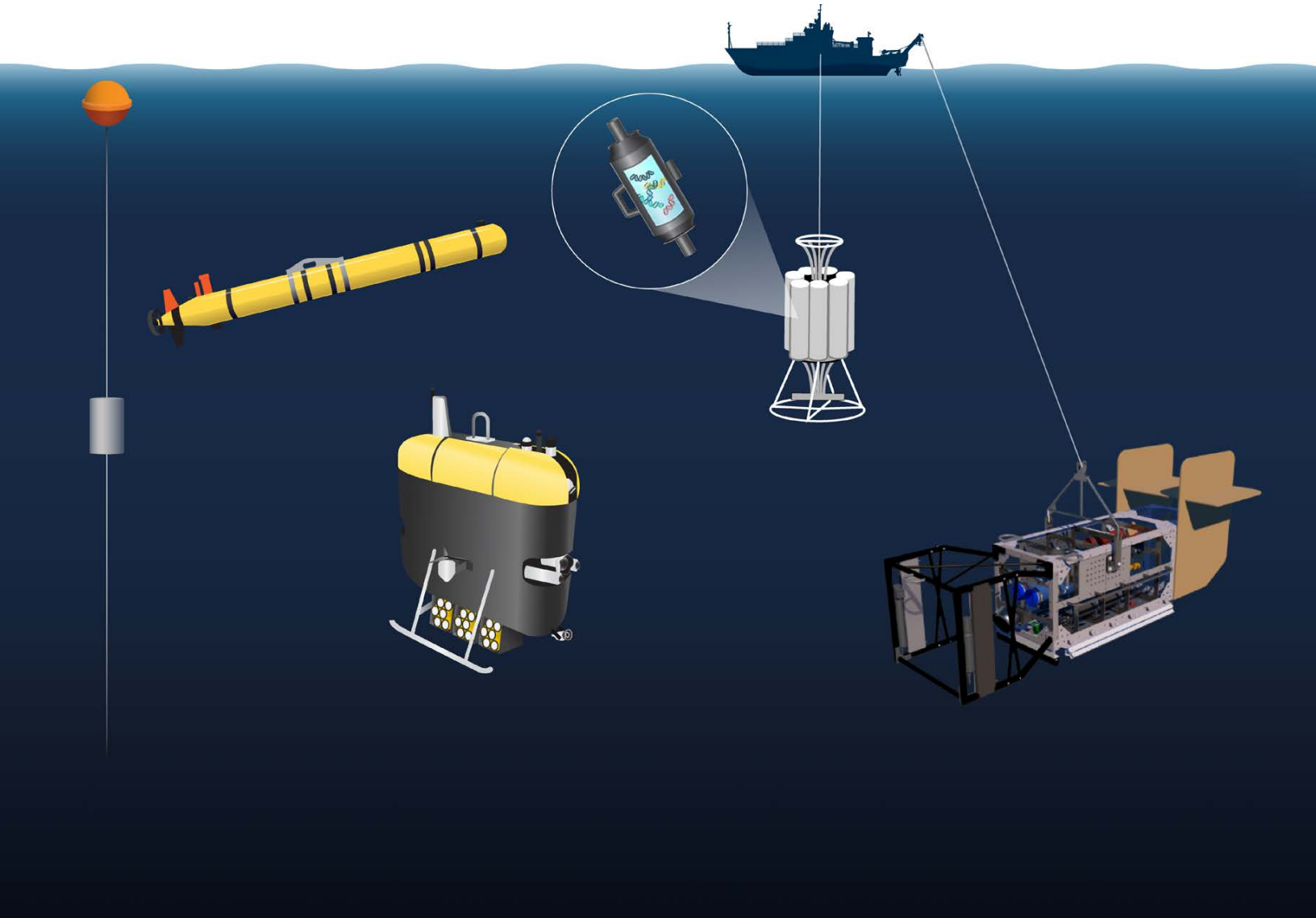

ABOUT THIS PUBLICATION

Support for this publication is provided by Ocean Networks Canada, the National Oceanic and Atmospheric Administration's Global Ocean Monitoring and Observing Program, and the Partnership for Observation of the Global Ocean.

Published by The Oceanography Society

Single printed copies are available upon request from info@tos.org.

PREFERRED CITATION

Kappel, E.S., V. Cullen, M.J. Costello, L. Galgani, C. Gordó-Vilaseca, A. Govindarajan, S. Kouhi, C. Lavin, L. McCartin, J.D. Müller, B. Pirenne, T. Tanhua, Q. Zhao, and S. Zhao, eds. 2023. *Frontiers in Ocean Observing: Emerging Technologies for Understanding and Managing a Changing Ocean*. *Oceanography* 36(Supplement 1), https://doi.org/10.5670/oceanog.2023.s1.

ON THE FRONT COVER. A depiction of some of the many platforms that scientists use to sample and sense the ocean, including (from left to right) moorings, autonomous underwater vehicles, CTD rosettes, and towed vehicles (not to scale). See Govindarajan et al. (2023, in this supplement) to read about how these platforms can be used to sample environmental DNA for studies of the mesopelagic ocean. *Illustration by Natalie Renier, Woods Hole Oceanographic Institution*

ON THIS PAGE. A Biogeochemical Argo float. For details, see Boyd et al. (2023, in this supplement). *Photo credit: David Luquet, licensed under CC BY-SA 4.0 by Thomas Boniface*

CONTENTS

MULTI-HAZARD WARNING SYSTEMS: OCEAN OBSERVATIONS FOR COASTAL HAZARD WARNING

TECHNOLOGY: ENVIRONMENTAL DNA

INTRODUCTION TO FRONTIERS IN OCEAN OBSERVING

By Ellen S. Kappel, Mark John Costello, Luisa Galgani, Cesc Gordó-Vilaseca, Annette Govindarajan, Soroush Kouhi, Charles Lavin, Luke McCartin, Jens Daniel Müller, Benoît Pirenne, Toste Tanhua, Qianshuo Zhao, and Shiye Zhao

In this second supplement to *Oceanography* on frontiers in ocean observing, articles describe the many creative and promising ways in which scientists are now sampling and studying the ocean and its constituents, from carbon dioxide and oxygen, environmental DNA (eDNA), plastics, and microplastics, to coral reefs, fish, and whole ecosystems. These papers show, for example, how acoustic techniques are critical components for early warning of natural hazards such as earthquakes, tsunamis, and landslides and how they play significant roles in investigations such as determining how ocean soundscapes may be used to monitor coral reef ecosystem health. Several articles demonstrate the application of long-used technologies for new and important data-gathering purposes, while others describe how data collected by multiple technologies deployed simultaneously have improved monitoring of threats such as harmful algal blooms and oil spills. Some authors detail the application of eDNA analyses, especially to midwater environments, where they are providing new insights, in combination with other sampling and sensing methods. Modeling is a key aspect of several of the studies, where ocean observing data serve as critical inputs and for validation. These innovative observing technologies and analytical techniques are advancing our understanding of the world ocean and supporting its sustainable use and management.

Similar to last year's supplement, we invited potential authors to submit letters of interest aligned with the priorities of the UN Decade of Ocean Science for Sustainable Development (2021–2030), though topics were further narrowed into specific themes. In addition, this year each topic had guest editors, some of whom are early career scientists. The idea was that this supplement would provide an opportunity for a senior scientist to mentor one from the next generation and for early career scientists to gain some experience as guest editors for a journal.

OCEAN-CLIMATE NEXUS

THEME: Observations for Marine Carbon Dioxide Removal
GUEST EDITORS: Toste Tanhua and Jens Daniel Müller

How ocean observations and emerging technologies are helping to identify potential marine carbon dioxide removal (mCDR) opportunities and to measure the effectiveness of mCDR actions, including studies evaluating the potential adverse effects of human interventions on biodiversity and ecosystem function.

ECOSYSTEMS AND THEIR DIVERSITY

THEME: Patterns and Trends in Ocean Biodiversity Under Climate Change
GUEST EDITORS: Mark John Costello, Qianshuo Zhao, Charles Lavin, and Cesc Gordó-Vilaseca

Ocean observing efforts that record environmental and related biodiversity changes occurring in different ecosystems, from the coasts to the deep ocean and from the tropics to the high latitudes, and that address the link between observations and policy.

OCEAN POLLUTANTS

THEME: Assessing the Damage Caused by Marine Plastic Pollution
GUEST EDITORS: Luisa Galgani and Shiye Zhao

Both classical oceanographic approaches and new techniques for quantifying marine plastic pollution as well as its long-term consequences on ecosystems and climate through their interaction with natural elements of the marine environment.

MULTI-HAZARD WARNING SYSTEMS

THEME: Ocean Observations for Coastal Hazard Warning
GUEST EDITORS: Benoît Pirenne and Soroush Kouhi

Observations and monitoring, forecasting, alerting, and hazard research together with the systems developed around them and their applications in coastal communities.

TECHNOLOGY

THEME: Environmental DNA Technology
GUEST EDITORS: Annette Govindarajan and Luke McCartin

Recent developments in all aspects of eDNA technology and interpretive approaches relevant for observing and studying animal biodiversity, especially in the ocean midwater environment.

We thank Ocean Networks Canada, the US National Oceanic and Atmospheric Administration's Global Ocean Monitoring and Observing Program, and the Partnership for Observation of the Global Ocean for generously supporting publication of this supplement to *Oceanography*.

ARTICLE DOI. https://doi.org/10.5670/oceanog.2023.s1.1

Operational Monitoring of Open-Ocean Carbon Dioxide Removal Deployments: Detection, Attribution, and Determination of Side Effects

By Philip W. Boyd*, Hervé Claustre*, Louis Legendre*, Jean-Pierre Gattuso, and Pierre-Yves Le Traon (*equal first authors)

Human activities are causing a sustained increase in the concentration of carbon dioxide (CO_2) and other greenhouse gases in the atmosphere. The resulting harmful effects on Earth's climate require decarbonizing the economy and, given the slow pace and inherent limitations of decarbonization of some industries such as aviation, also the active removal and safe sequestration of CO_2 away from the atmosphere (i.e., carbon dioxide removal or CDR; NASEM, 2022). Limiting global warming to 1.5°C—a target that may already have been exceeded—would require CDR on the order of 100–1,000 Gt CO_2 over the twenty-first century (IPCC, 2018).

Natural terrestrial and ocean processes already remove about half of human CO_2 emissions from the atmosphere, with half of this amount (i.e., a quarter of the total) ending up in the ocean. These natural processes slow down global warming; without the continuous removal of atmospheric CO_2 since the beginning of the Industrial Era (1750), the present (2022) level of 420 ppm would have been reached in the 1980s. In the ocean, CO_2 combines with water (H_2O) to form dissolved inorganic carbon (DIC: CO_2 gas, H_2CO_3, and HCO_3^- and CO_3^{2-} ions), and photosynthetic organisms use some of the DIC to synthesize the organic matter that is the basis of pelagic marine food webs. Marine organic carbon exists in both particulate and dissolved forms (POC and DOC, respectively). A number of physical, chemical, and biological processes, collectively called ocean carbon pumps, transfer carbon from surface waters downward and store it in the ocean as DIC and refractory (i.e., long-lived) DOC and POC in the ocean. Some of this storage takes place on climatically significant timescales and is called carbon sequestration. Sequestration of DIC can occur at any depth, but its potential is higher at greater depths.

There is increasing discussion of implementing marine CDR (mCDR) approaches, which range from methods based on natural processes to more industrial techniques (NASEM, 2022). Here, we focus on open-ocean mCDR approaches, including alkalinization (i.e., adding alkaline substances, such as olivine or lime, to seawater to enhance the ocean's chemical uptake of CO_2 from the atmosphere) and nutrient fertilization (i.e., adding a nutrient that limits phytoplankton photosynthesis, such as iron, to surface waters to enhance the photosynthetic uptake of DIC), which aim to enhance DIC sequestration resulting from increased CO_2 influx from the atmosphere.

There is a growing body of literature on various aspects of mCDR approaches. Published mCDR studies have addressed the appropriateness of implementation, testing the efficiency of sequestering CO_2 and/or assessing detrimental ecological effects (laboratory/mesocosm studies, field trials), and identifying potential deployment sites. Such pilot studies are precursors to possible future mCDR deployments (NASEM, 2022), which should only occur in cases where the pilot studies indicate that mCDR would not unduly disrupt marine ecosystems. In contrast, this paper addresses the situation where mCDRs are to be deployed at scales commensurate with the target of removing gigatons of atmospheric carbon.

Here, considering information from satellites and autonomous platforms combined with artificial intelligence (AI) and models (Figure 1), we describe a future operational monitoring system for the detection, attribution, and determination of side effects of open-ocean mCDR deployments. We mainly address the monitoring challenge described in NASEM (2022), based upon the current and expected readiness of observational platforms and sensors. This approach ensures that the proposed monitoring system would be tractable and deployable. The assessment of future mCDR deployments will include three components, together referred to as MRV: measurement or monitoring

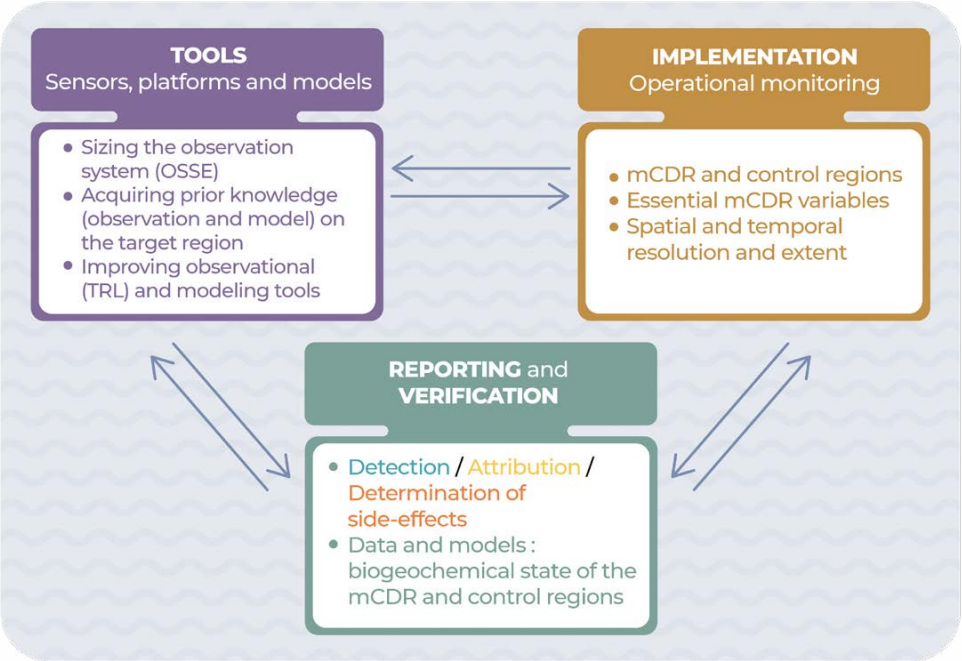

FIGURE 1. The three main components of a marine carbon dioxide removal (mCDR) monitoring system are the tools to be used, field implementation, and reporting and verification. These would interact, and thus progressively improve, prior to and during the long-term mCDR deployment. The development of tools would be accelerated by the urgency created by the mCDR deployments. Connections between the three objectives of the monitoring system (i.e., detection, attribution, and determination of side effects) and the monitored variables are described under "Monitoring mCDR Deployments" in the text. OSSE = Observation System Simulation Experiment. TRL = Technological Readiness Level. *Licensed under CC BY-SA 4.0 by Thomas Boniface*

(M) as described in this study, reporting (R) of the resulting data to a certified authority, and verification (V) by this authority, using data and models, that any deployment is successful at increasing CO_2 influx from the atmosphere and enhancing its sequestration in the ocean. Successful verification of removal and sequestration will result in certification of the mCDR. The last two MRV components are mentioned in the last section of the study.

Our study for this "Frontiers in Ocean Observing" supplement of *Oceanography* focuses on the observational aspects of the monitoring of open-ocean mCDR deployments, with less emphasis on the corresponding, essential modeling components. We nevertheless briefly describe the latter where necessary.

OBJECTIVES OF AN mCDR MONITORING SYSTEM

Monitoring is essential in order to quantify the effectiveness (removal) and durability (sequestration) of carbon storage resulting from open-ocean mCDR deployments and to identify environmental impacts (NASEM, 2022). Here, we examine three objectives of a future open-ocean mCDR monitoring system. Our definitions of detection and attribution are consistent with those in the Glossary of the Intergovernmental Panel on Climate Change (IPCC, 2021).

Detection. To quantify the amount of carbon sequestered as DIC. This will require quantification of metrics that document both the amount of carbon removed, based on models that assimilate accurate in situ measurements of carbon system variables, and the durability of its removal (i.e., long-term [decadal] estimates of air-sea CO_2 exchanges).

Attribution. To assign the detected carbon sequestration solely to a particular mCDR deployment. Attribution requires an understanding of the processes that jointly determine the success or failure of the given mCDR deployment and must thus address the influence of complex drivers in the carbon cycle to demonstrate additionality (see next section). Attribution addresses the proportion of carbon sequestration that can be attributed to an mCDR deployment, even if there are contributions by other drivers within the carbon cycle. This will involve advanced modeling capabilities that simulate the state of the coupled physical and biogeochemical ocean and its modification by the mCDR deployment.

Determination of Side Effects. To identify and quantify ecological impacts of the mCDR and ensure that they do not exceed the impacts expected from the pilot studies.

The mCDR deployments will necessarily modify the ocean, but intended and unintended ecological impacts are poorly known. This will require monitoring ecological variables in at least the upper 1,000 m as well as deeper, including at the seafloor where benthic systems could be affected. Side effects would be assessed through modeling studies of the impacts of biogeochemical changes on marine ecosystems. Unacceptable ecological side effects, acute or chronic, may lead to the termination of an mCDR deployment.

MODEL VALIDATION, EXCLUSION, AND ADDITIONALITY

To achieve these three objectives, model simulations will be run, with and without mCDR. In order to fulfill this role, simulations will have to capture many ongoing changes in the ocean that include those due to climate change, the hysteresis effects from climate change, the effects of other mCDR (and terrestrial CDR), and the effects of emissions reductions on the ocean carbon cycle. It will require advanced modeling capabilities that could effectively simulate the state of the coupled physical and biogeochemical ocean and its changes under the different mCDR scenarios. Such models pose many scientific and technological challenges that impede the development of Digital Twins of the Ocean (DTO). The DTO will combine next-generation ocean modeling, artificial intelligence, and high-performance computing to create digital replicas of the ocean that are regularly informed and improved with observations. Some of the observations will be used in the models, and others will be kept for model validation.

Extensive validation of these models and their improvements (e.g., optimization of model parameters) will be needed well in advance of and during mCDR deployments. Confirming that the simulations are consistent with observations will require the initiation of monitoring a long time before any mCDR deployment. During this pre-deployment period, no mCDR could be undertaken in the mCDR-intended region.

However, there may be cases where model validation could not be undertaken well in advance of the mCDR deployments, for example, where a deployment would take place without prior, long-term consultation with the authority to which monitoring would be reported. In such a case, the results of model simulations run with and without mCDR could be compared with observations made in the mCDR-deployment region and one or more control regions (with long-term time-series observations) where conditions would be comparable to those in the selected mCDR region and where no mCDR of any type would be deployed. Of course, control regions will eventually become "contaminated" by the spread of DIC—via ocean circulation—from mCDR deployed elsewhere (e.g., Boyd and Bressac, 2016), but they could be used for model validation before this occurs and even after.

Failure to implement either pre-deployment periods or control regions would make attribution impossible and therefore compromise the monitoring of all mCDR deployments in a given ocean region. In addition, an open registry or metadatabase of the mCDR pilot studies and deployments would be very useful in this context. It would provide information, in particular for modelers, on the location and depth of each activity and key information on its technical aspects (e.g., for alkalinization, the mineral type, timing, and amount of alkalinity added).

Furthermore, we assume here the desirable exclusion principle, whereby the deployment of one type of mCDR in a given ocean region excludes the possibility of deploying other types there. This principle stems from the likelihood that multiple-type deployments in a given region, especially as mCDR deployments aim to sequester carbon at the gigaton scale,[1] would make attribution of individual deployments impossible (Boyd and Bressac, 2016). Exclusion is also important because multiple-type deployments could potentially cause interactive side effects that were not anticipated by single-type mCDR pilot studies.

Pre-deployment periods or control regions—in situ or in models—are also needed to assess the additionality of mCDR deployments, defined in IPCC (2022) as: "The property of being additional. Mitigation is additional if the greenhouse gas emission reductions or removals would not have occurred in the absence of the associated policy intervention or activity." Thus, additionality is the requirement that the net increase in the air-to-sea CO_2 flux due to an mCDR deployment (i.e., based on detection and attribution) exceeds the flux in the absence of this mCDR.

Monitoring for additionality will be especially challenging as the change in net carbon flux into the ocean and the magnitude of carbon sequestration caused by an mCDR deployment will be very small compared to natural air-sea carbon fluxes and the magnitude of the ocean carbon sink. In addition, the models will need to take into account the inherent uncertainties of field measurements. This will pose challenges for both observation and modeling.

[1] The intended gigaton-scale magnitude of mCDR deployments would be much larger than existing multiple overlapping uses and perturbations. For example, global marine capture fisheries and aquaculture harvested 112 Mt of animals and 36 Mt of seaweeds (fresh weight) in marine waters in 2020 (FAO, 2022), which represented ~0.02 GtC yr^{-1}.

GENERAL REQUIREMENTS FOR AN mCDR MONITORING SYSTEM

Guidelines for monitoring were set for the Global Ocean Observing system (GOOS) in the context of the Framework for Ocean Observation (FOO; Tanhua et al., 2019). A key element of the FOO is its organization and coordination around essential ocean variables (EOVs) rather than specific observing systems. The mCDR operational system described here differs from the GOOS observations, but also focuses on EOVs.

We advocate that "essential mCDR variables" would include most current EOVs (see GOOS, 2021), along with more detailed data on lower atmosphere CO_2 concentration and oceanic DIC used to estimate air-sea CO_2 flux. Variables would also include wind speed, which has a strong influence on air-sea gas exchange.

The effects of mCDR deployments on carbon capture and sequestration will accumulate over time. Consequently, meeting the three objectives discussed above will require long-term monitoring.

Given the remote nature and carbon-sequestration target of open-ocean mCDR deployments, monitoring their effects will require systems with at least the following characteristics to efficiently address the objectives of detection, attribution, and determination of side effects:

- Calibrated sensors on autonomous platforms, that is, satellites (Figure 2) and in situ robots (see Box 1)
- Sampling over large surface areas to address horizontal eddy diffusion and transport
- Recurrent long-term measurements, commensurate with the duration of mCDR deployments
- Quasi-simultaneous estimates of air-sea CO_2 exchange and concentrations of DIC, particulate inorganic carbon (PIC), DOC, and POC from surface to depth to monitor the fate of the additional carbon

Air-sea CO_2 flux cannot be measured directly over large areas; it would be estimated by modeling. To do so, at least two parameters of the carbonate system should be measured in the water column. These parameters include pH, total DIC, total alkalinity (TA), and CO_2 partial pressure (pCO_2). Detecting changes in the carbonate system is challenging, and detecting a superimposed mCDR effect would be very difficult.

The monitoring system would combine satellite remote sensing (Figure 2) and long-term regional in situ measurements. The latter would be performed with autonomous robots (see Box 1), as described by Chai et al. (2020). Biogeochemical data would subsequently be analyzed using AI and assimilated in models. The integration of these platforms, analyzing their data with AI, and combining the data with models is already partly implemented in open-ocean research (e.g., Claustre et al., 2021) and could be readily applicable to monitor open-ocean mCDR deployments.

FIGURE 2. One of the numerous satellites used for mCDR monitoring, PACE (Plankton, Aerosol, Cloud, ocean Ecosystem, to be launched in early 2024) will be equipped with a hyperspectral spectrometer that could be used for assessing possible ecological side effects of mCDR deployments (e.g., changes in phytoplankton community composition). *This figure is a derivative of https://commons.wikimedia.org/wiki/File:PACE_Spacecraft_beauty2.jpg by NASA, in the public domain.*

Ideally, the observational and modeling components of the mCDR monitoring system should be in place prior to an mCDR deployment. If this is impossible, data collected by the global networks of Biogeochemical-Argo (BGC-Argo) floats (Figure 3) and ocean color satellites (Figure 2) could document natural variability and contribute to the validation/calibration of models required for attribution.

COMPONENTS OF AN mCDR MONITORING SYSTEM

Satellites and underwater robots operate autonomously, making relatively high-frequency measurements over several years. Present-day BGC-Argo floats (Figure B1) can achieve 300 profiles of up to 13 different variables[2] during their lifetimes, for example, profiling every five days over four years. Horizontally, satellites (Figure 2) cover large surfaces (with a spatial resolution of up to 4 × 4 km), and

[2] Temperature, salinity, dissolved O_2, pH, dissolved NO_3, chlorophyll *a*, particulate backscattering coefficient (b_{bp}), colored dissolved organic matter (CDOM), downwelling irradiance, upwelling radiance, particle size spectra, particles and plankton 100–2,00 µm, optical sediment trap (transmissometer).

BOX 1. ROBOTS TO MONITOR mCDR DEPLOYMENTS

The word "robots" refers here to autonomous vehicles and platforms, which include:

- Buoyancy-driven robots, encompassing
  - Biogeochemical (BGC)-Argo floats (Figures B1 and B2)
  - BGC-gliders (Figure B3)
- Uncrewed surface vehicles (USVs; Figure B4)

Floats and USVs could rendezvous for data intercomparison and transfer (Figure B5). In the future, USVs could intercept and reposition floats to maintain them in the best monitoring locations or create "virtual moorings."

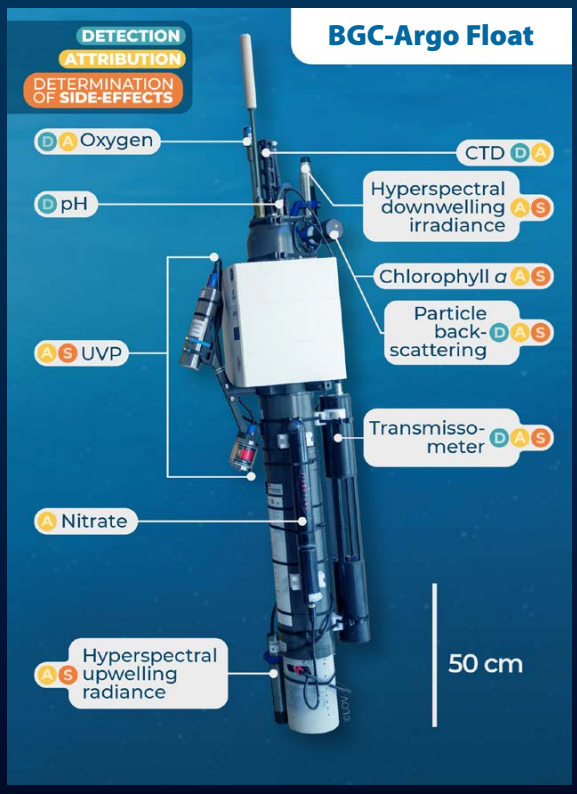

FIGURE B1. A jumbo biogeochemical profiling float (BGC-Argo float, REFINE type NKE CTS5) can provide profiles every five days over four years. Sensors are identified that contribute to the three mCDR monitoring objectives (detection, attribution, and determination of side effects). *Photo credit: David Luquet, used with his permission. Licensed under CC BY-SA 4.0 by Thomas Boniface*

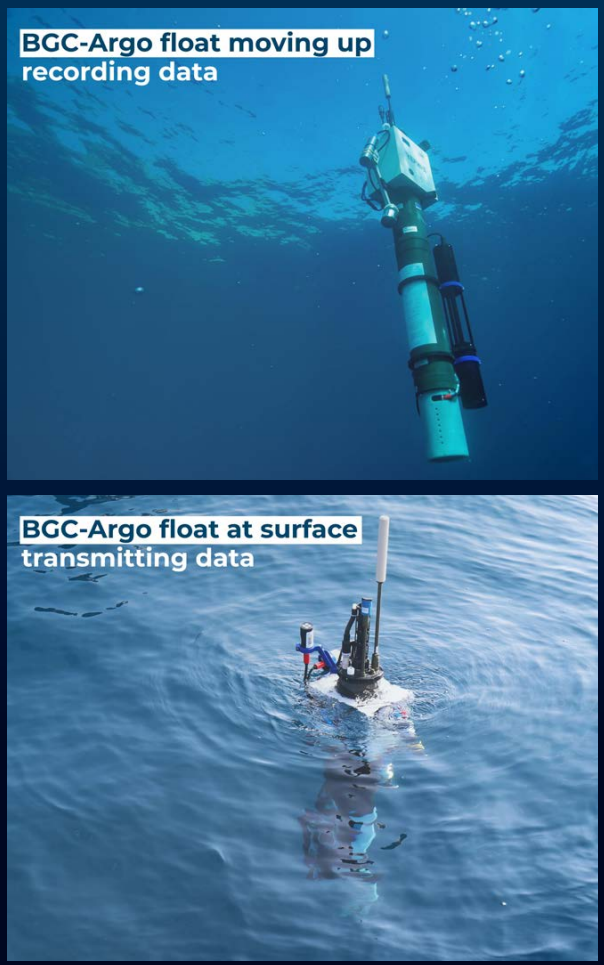

FIGURE B2. BGC-Argo floats record variables from 2,000 m depth to the surface, where data are rapidly transmitted to a satellite. The floats then descend to a parking depth (e.g., 1,000 m) where they stay for 10 days before initiating the next vertical profile. During the parking phase, floats have the potential to monitor key properties for mCDR such as wind (passive acoustic) and particle flux (transmissometer used as optical sediment trap). *Photo credits: (top) David Luquet and (bottom) Thomas Boniface, used with their permissions. Licensed under CC BY-SA 4.0 by Thomas Boniface.*

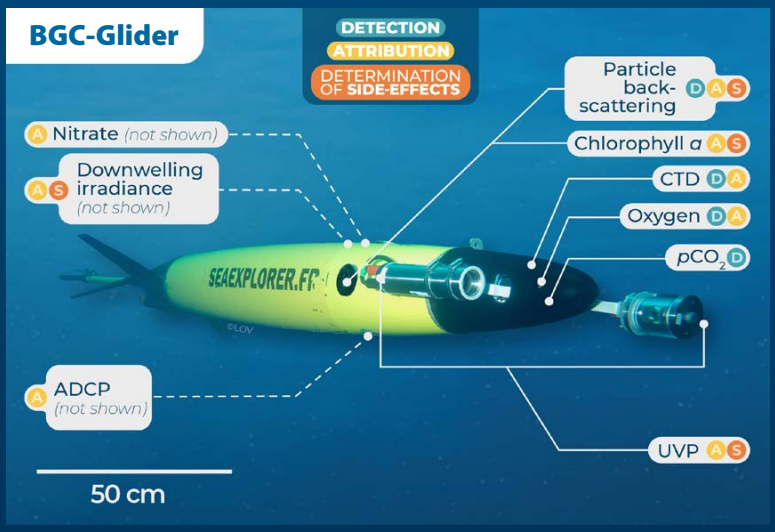

FIGURE B3. Biogeochemical SEAEXPLORER underwater glider (BGC-glider) equipped with almost the same array of sensors as BGC-Argo floats (Figure B1). Sensors are identified for the three mCDR monitoring objectives (detection, attribution, and determination of side effects). Such gliders can typically dive to 1,000 m depth and stay at sea up to 100 days. *Photo credit: David Luquet, used with his permission. Licensed under CC BY-SA 4.0 by Thomas Boniface*

FIGURE B4. A saildrone, a USV powered by wind and solar energy, with identification of sensors for the three mCDR monitoring objectives (detection, attribution, and determination of side effects). USVs would be key in acquiring accurate pCO_2 measurements for mCDR monitoring. The USVs could be deployed as fleets of intercommunicating platforms for pCO_2 measurements, and some could also rendezvous with BGC-Argo floats (Figure B5). Another type of USV, the waveglider (not shown), is powered by wave motion and solar energy. *This work is a derivative of https://commons.wikimedia.org/wiki/File:SD_1036.jpg by NOAA and Saildrone, in the public domain.*

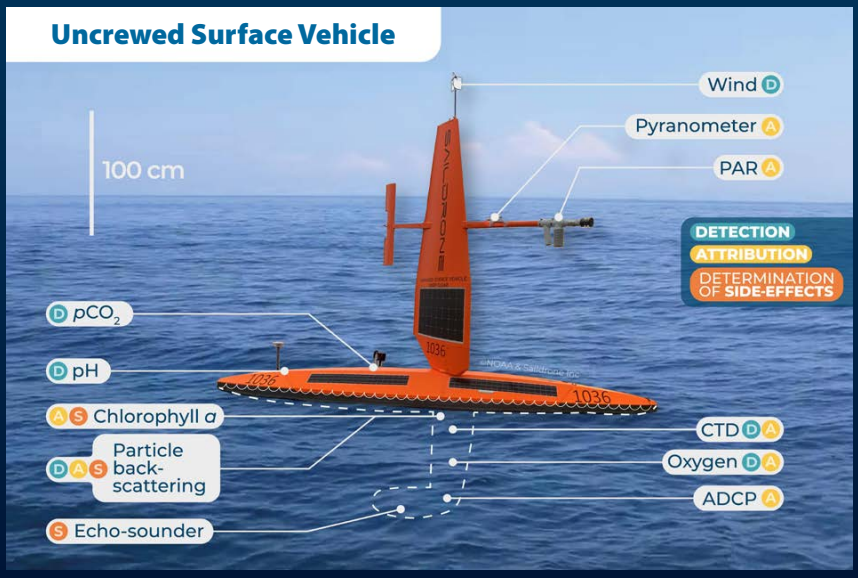

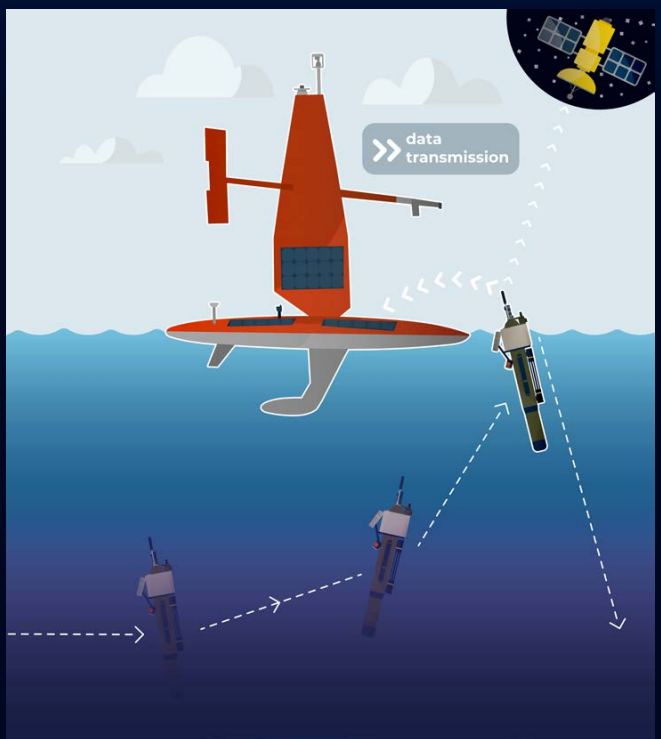

FIGURE B5. During a rendezvous between a saildrone and a surfacing BCG-Argo float, the USV would record data from the float and simultaneously make pCO_2 measurements. Data files too large to be transmitted to satellites by the float (e.g., particle and plankton images) could be transferred to the USV for later downloading when it returns to port. *Licensed under CC BY-SA 4.0 by Thomas Boniface*

floats can be operated as fleets with strong interoperability of measurements (Figure 3). Vertically, remote sensing investigates the ocean skin (the upper 10–100 μ) for some variables (e.g., temperature) and deeper waters for others (e.g., ocean color), whereas BGC-Argo floats and BGC-gliders make measurements from the surface, including the ocean-atmosphere interface, to 2,000 m depth (Figures B2 and B3).

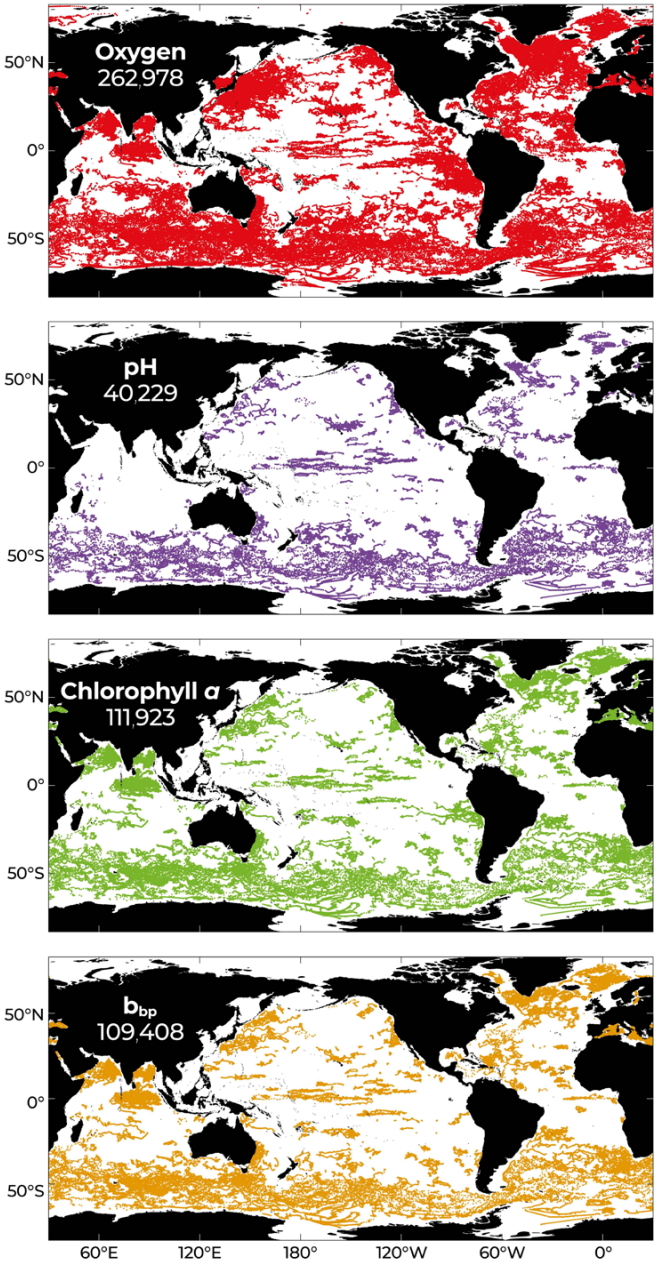

FIGURE 3. Networks of BCG-Argo floats (Figures B1 and B2) will be used for cost-effective acquisition of in situ data required for mCDR monitoring and modeling. The maps show the data for four variables acquired by the present network of floats as of 23 January 2023. The white number on each map indicates the number of profiles available for that variable. Updated versions of these maps are available from the Biogeochemical-Argo website (http://biogeochemical-argo.org/cloud/document/implementation-status/BGC_summary.pdf). *Licensed under CC BY-SA 4.0 by Raphaëlle Sauzède*

DESIGNING AN mCDR MONITORING SYSTEM

Observation System Simulation Experiments (OSSEs) would be used to design the observing system required for the three objectives of mCDR monitoring: detection, attribution, and determination of side effects. OSSEs are powerful tools that provide quantitative assessments of the impacts of observations combined with models to reconstruct the coupled physical and biogeochemical state of the ocean (Figure 4). Using OSSEs, observing systems could be designed to fit the characteristics of long-term mCDR deployments. The observations to be considered in these OSSEs include those from the fundamental GOOS system (satellite and in situ; Figures 2 and 5) and specific new observations in the mCDR regions. Developing such OSSEs is challenging and will require advanced modeling capabilities.

A successful mCDR deployment would shift the perturbed ocean region from its pre-mCDR trajectory to a different, new mCDR trajectory with enhanced carbon sequestration. Measurements prior to mCDR deployments and during the transition period would be especially useful for detection and attribution, and would help identify any initial acute ecological side effects. Measurements during the ongoing mCDR deployment would be used for long-term detection and attribution, and to identify further ecological effects.

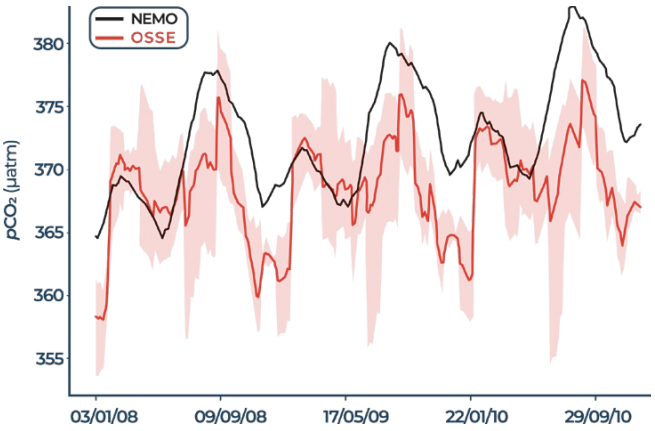

FIGURE 4. Observation System Simulation Experiments (OSSEs) will provide powerful tools for quantitative assessments of the impacts of observations combined with models, to be used to design mCDR monitoring systems. The figure shows the mean of feedforward neural network (FFNN) outputs of pCO_2 in the North and South Atlantic Oceans for corresponding runs of an OSSE and the NEMO/PISCES model. Shading corresponds to the maximum and minimum values from four FFNN outputs for the OSSE. *This figure is a derivative of Figure7a of Denvil-Sommer et al. (2021), used under CC BY 4.0*

Based on present-day observational limitations (e.g., pH is the only variable of the carbonate system measured on BGC-Argo floats; Figure B1) in relation to the anticipated magnitude of mCDR from model projections (Keller et al., 2014), detection, attribution, and detection of side effects will require rapid advances in sensor technology.

MONITORING mCDR DEPLOYMENTS

The monitoring and evaluation of mCDR deployments would use satellites as well as surface and underwater robots to make the following measurements:

Detection. To assess the effectiveness of an mCDR deployment in sequestering CO_2, changes in concentrations of DIC, PIC, TA, DOC, and POC and particle downward fluxes should be measured over the water column based on the design derived from OSSEs. These observations will be used to reconstruct the ocean carbon state together with models (data assimilation). Running OSSEs (with and without mCDR) will also provide ocean carbon state reconstruction errors and the duration of the monitoring required to allow separation of noise from signal. Sensors already exist, or are being developed, for most of these variables. In addition to pH already measured by robots, there are ongoing efforts to adapt sensors to autonomous platforms that measure at least one other parameter of the carbonate system (i.e., TA or pCO_2) to calculate DIC or the air-sea CO_2 flux (Bushinsky et al., 2019). Estimating accurate ocean-atmosphere CO_2 fluxes also requires wind speed, particularly during storms. These values can be derived from BGC-Argo float or BCG-glider passive acoustic measurements, which should be systematically deployed.

Attribution. To understand and deconvolve the processes involved in the cumulative outcome of an mCDR deployment, measurements similar to those used for ocean biological carbon pump studies (e.g., Claustre et al., 2021) would be used. Variables required to validate and run models would likely include environmental forcing (hydrodynamics, light, nutrients), carbon-related processes (net community production, organic matter remineralization), and resulting chemical changes (e.g., DIC and O_2).

Determination of Side Effects. To assess the ecological impacts of an mCDR deployment, both satellite and in situ optical measurements would provide information on changes in plankton size structure and composition. Images and active acoustic-based sensors would provide information on zooplankton and small pelagic organisms (Claustre et al., 2021). In the case of mCDR deployments that purposefully alter the assemblage of suspended particles (e.g., alkalinization), changes in underwater irradiance and associated effects on photosynthesis would also be monitored in situ and remotely, for example, through hyperspectral radiometric measurements.

GOVERNANCE OF AN mCDR MONITORING SYSTEM

Published mCDR studies have mostly considered research aspects for future deployments as explained in the Introduction. Our study represents a departure from these studies as it details an operational system designed to monitor large-scale open-ocean mCDR deployments. For verification to be credible, the monitoring system and the interpretation of measurements in terms of sequestration efficiency must be performed independently of the entities deploying mCDRs. In addition, all monitoring data should promote the FAIR principles of findability, accessibility, interoperability, and reuse.

Meeting these operational characteristics will require governance and best practices fundamentally different from those of curiosity-driven or targeted research (Chapter 9 of NASEM, 2022). Robust governance would be required to implement the following constraints, without which mCDR could not be effectively deployed:

- Confirmation that the principle of additionality is fulfilled, and assessment of evidence of the effectiveness of mCDR in sequestering CO_2 (detection)
- Implementation of pre-deployment periods or control regions (attribution)

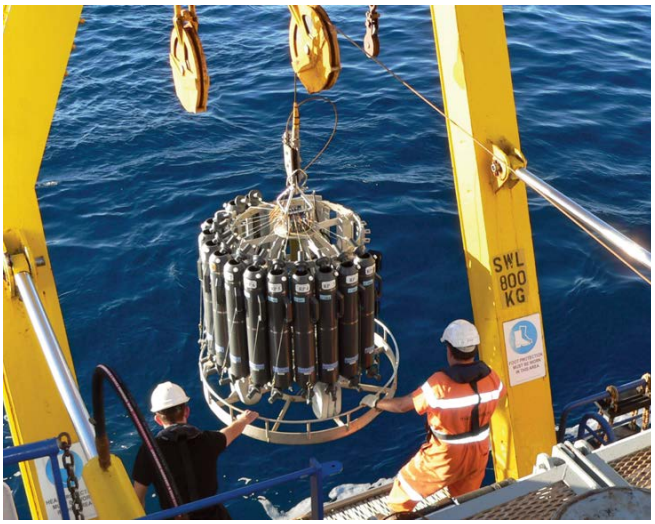

FIGURE 5. A CTD rosette is deployed from an oceanographic ship as part of Global Ocean Observing System (GOOS) sampling. Observations from the GOOS system would be used for designing OSSEs. *https://commons.wikimedia.org/wiki/File:CSIRO_ScienceImage_10807_Deploying_the_CTD_instrument_from_the_RV_Southern_Surveyor.jpg by Bob Beattle, CSIRO, used under CC BY 3.0*

- Implementation of the exclusion principle (i.e., excluding additional mCDR types—and their confounding influences—from any region where there is an ongoing type of mCDR deployment (attribution)
- Assessment of the degree of ecological side effects to decide if their severity should lead to termination of the mCDR deployment (determination of side effects)

Strong governance will be required, as it is highly likely that if a license is granted for a particular mCDR method, then subsequent permissions will be granted for other promising mCDR methods. This is in addition to coastal blue carbon and terrestrial CDR approaches. Achieving efficient monitoring entails two deployment constraints described above: the setting of pre-deployment periods (during which no mCDR could be undertaken in the mCDR-intended region) or control regions (where no mCDR of any type would be deployed), and the exclusion principle whereby the deployment of one type of mCDR in a given ocean region excludes the possibility of deploying other types there. The implementation and effective enforcement of these two constraints would require an ocean governance framework that does not presently exist.

What could be the role(s) of the ocean research community in monitoring forthcoming mCDR deployments? First, prepare plans for mCDR monitoring systems, as outlined above, and contribute to defining governance and best practices of mCDR monitoring. Second, train the scientists and engineers who will run the mCDR monitoring systems and analyze/model the resulting information. Third, contribute to the multi-faceted education of the scientific and other personnel who will staff the oversight authorities for mCDR deployments. Fourth, act as advisors to and watchdogs for the mCDR deployment entities and authorities as knowledge on the influence of mCDR deployments on ocean processes advances.

Until now, the research community has studied the ocean as if it were a pristine environment, despite anthropogenic changes due to factors such as ongoing CO_2 pollution and industrial fishing. With mCDR deployments, this illusion would be dispelled, and we would be faced with a new ocean reality. In order to be ready for (near) future open-ocean mCDR deployments, the entire oceanographic community should investigate without delay the desired characteristics and likely challenges of the operational system(s) needed to monitor a profoundly modified ocean.

REFERENCES

Bushinsky, S.M., Y. Takeshita, and N.L. Williams. 2019. Observing changes in ocean carbonate chemistry: Our autonomous future. *Current Climate Change Reports* 5:207–220, https://doi.org/10.1007/s40641-019-00129-8.

Boyd, P.W., and M. Bressac. 2016. Developing a test-bed for robust research governance of geoengineering: The contribution of ocean iron biogeochemistry. *Philosophical Transactions of the Royal Society A* 374(2081):20150299, https://doi.org/10.1098/rsta.2015.0299.

Chai, F., K.S. Johnson, H. Claustre, X. Xing, Y. Wang, E. Boss, S. Riser, K. Fennel, O. Schofield, and A. Sutton. 2020. Monitoring ocean biogeochemistry with autonomous platforms. *Nature Reviews Earth & Environment* 1:315–326, https://doi.org/10.1038/s43017-020-0053-y.

Claustre, H., L. Legendre, P.W. Boyd, and M. Levy. 2021. The oceans' biological carbon pumps: Framework for a research observational community approach. *Frontiers in Marine Science* 8:780052, https://doi.org/10.3389/fmars.2021.780052.

Denvil-Sommer, A., M. Gehlen, and M. Vrac. 2021. Observation system simulation experiments in the Atlantic Ocean for enhanced surface ocean pCO_2 reconstructions. *Ocean Science* 17(4):1,011–1,030, https://doi.org/10.5194/os-17-1011-2021.

FAO (Food and Agriculture Organization of the United Nations). 2022. *The State of World Fisheries and Aquaculture 2022. Towards Blue Transformation*. FAO, Rome, 266 pp., https://doi.org/10.4060/cc0461en.

GOOS (Global Ocean Observing System). 2021. Essential Ocean Variables, https://www.goosocean.org/index.php?option=com_content&view=article&id=14&Itemid=114.

IPCC (Intergovernmental Panel on Climate Change). 2018. Summary for policymakers. Pp. 1–24 in *Global Warming of 1.5°C. An IPCC Special Report on the Impacts of Global Warming of 1.5°C Above Pre-industrial Levels and Related Global Greenhouse Gas Emission Pathways, in the Context of Strengthening the Global Response to the Threat of Climate Change, Sustainable Development, and Efforts to Eradicate Poverty.* V. Masson-Delmotte, P. Zhai, H.-O. Pörtner, D. Roberts, J. Skea, P.R. Shukla, A. Pirani, W. Moufouma-Okia, C. Péan, R. Pidcock, and others, eds. Cambridge University Press, Cambridge, UK, and New York, NY, USA, https://doi.org/10.1017/9781009157940.001.

IPCC. 2021. Annex VII: Glossary. J.B.R. Matthews, J. S. Fuglestvedt, V. Masson-Delmotte, V. Möller, C. Méndez, R. van Diemen, A. Reisinger, and S. Semenov, eds. Pp. 2,193–2,204 in *Climate Change 2021: The Physical Science Basis. Contribution of Working Group I to the Sixth Assessment Report of the Intergovernmental Panel on Climate Change*. V. Masson-Delmotte, P. Zhai, A. Pirani, S. L. Connors, C. Péan, S. Berger, N. Caud, Y. Chen, L. Goldfarb, M. I. Gomis, and others, eds, Cambridge University Press, Cambridge, UK, and New York, NY, US.

IPCC. 2022. Annex I: Glossary. R. van Diemen, J.B.R. Matthews, V. Möller, J.S. Fuglestvedt, V. Masson-Delmotte, C. Méndez, A. Reisinger, and S. Semenov, eds. In *IPCC, 2022: Climate Change 2022: Mitigation of Climate Change. Contribution of Working Group III to the Sixth Assessment Report of the Intergovernmental Panel on Climate Change*. P.R. Shukla, J. Skea, R. Slade, A. Al Khourdajie, R. van Diemen, D. McCollum, M. Pathak, S. Some, P. Vyas, R. Fradera, and others, eds, Cambridge University Press, Cambridge, UK, and New York, NY, USA.

Keller, D.P., E.Y. Feng, and A. Oschlies. 2014. Potential climate engineering effectiveness and side effects during a high carbon dioxide-emission scenario. *Nature Communications* 5(1):3304, https://doi.org/10.1038/ncomms4304.

NASEM (National Academies of Sciences, Engineering, and Medicine). 2022. *A Research Strategy for Ocean-based Carbon Dioxide Removal and Sequestration*. The National Academies Press, Washington, DC, https://doi.org/10.17226/26278.

Tanhua, T., A. McCurdy, A. Fischer, W. Appeltans, N. Bax, K. Currie, B. DeYoung, D. Dunn, E. Heslop, L.K. Glover, and others. 2019. What we have learned from the framework for ocean observing: Evolution of the global ocean observing system. *Frontiers in Marine Science* 6:471, https://doi.org/10.3389/fmars.2019.00471.

ACKNOWLEDGMENTS

We are grateful to two reviewers for their comments, which were very helpful in revising our manuscript.

ARTICLE DOI. https://doi.org/10.5670/oceanog.2023.s1.2

Assessing Changes in Marine Biogeochemical Processes Leading to Carbon Dioxide Removal with Autonomous Underwater Vehicles

By Catherine Garcia, Benedetto Barone, Sara Ferrón, and David Karl

Biogenic particles originating in the ocean's well-lit, shallow layer help regulate Earth's climate by absorbing carbon dioxide from the atmosphere and subsequently sinking to the ocean's depths. Subtropical gyres, the largest ocean habitats on Earth, are characterized by year-round high light, warm temperatures, and low supplies of nutrients. However, even in these persistently low-nutrient regions, conditions vary on multiple temporal and spatial scales, making low-frequency—even monthly—observations difficult to interpret.

Established in June 1988, the Hawaii Ocean Time-series (HOT) program measures carbon cycling and fluxes at Station ALOHA (A Long-term Oligotrophic Habitat Assessment; 22°45'N, 158°W) in the North Pacific Subtropical Gyre (NPSG). At this site, a predictable peak in particle sinking occurs in late summer, though the scale and magnitude vary annually (Karl et al., 2021). While the peak in primary productivity also occurs in late summer, directly linking primary production to particle export on interannual or intra-seasonal scales remains challenging (Karl et al., 2021).

In addition to the expected increase in carbon export in the summer via sinking biogenic particles, there are also aperiodic phytoplankton blooms that are hard to predict. Summer phytoplankton blooms are vastly undersampled at Station ALOHA, despite 34 years of observations (Dore et al., 2008). As Dore et al. (2008) state: "Unfortunately, it is much more common in practice to observe the result of a bloom (an area of elevated phytoplankton biomass) than the mechanisms that led to its development." As in the Dore et al. study, we define a bloom as a brief period (days to weeks) of rapidly increasing biomass.

Ocean-based carbon dioxide removal (CDR) strategies often involve taking advantage of the marine biological carbon pump (Siegel et al., 2021). Several CDR approaches consist of inputting nutrients near the ocean surface that stimulate photosynthesis and can increase the flux of organic carbon to the ocean interior. To verify the effectiveness of these approaches, open ocean experiments would require methods to estimate productivity and carbon accumulation in near-real time. Here, we propose that monitoring the open ocean ecosystem with autonomous underwater vehicles could provide useful metrics to quantify the stimulation of biogeochemical processes during CDR experiments. These efforts could initially focus on the subtropical gyres, whose vast area suggests a large capacity for carbon sequestration.

The gyre is not a homogeneous ecosystem. There are dynamic swings in productivity as mesoscale and submesoscale circulation features (e.g., eddies, fronts, and internal waves) alter environmental factors (light availability, temperature, and nutrient supply) that control phytoplankton growth. To constrain the environmental factors controlling the magnitude and timing of seasonal features (summer export pulses) and aperiodic events (summertime blooms) requires high-frequency sampling.

As part of this effort, autonomous underwater vehicles (Seagliders) have been deployed from ships in the vicinity of Station ALOHA for more than 16 missions since 2008 (Figure 1a). These Seagliders are equipped with CTD sensors that provide hydrography profiles of temperature, salinity, and pressure along with bio-optical and oxygen sensors that measure sub-daily, depth-resolved changes

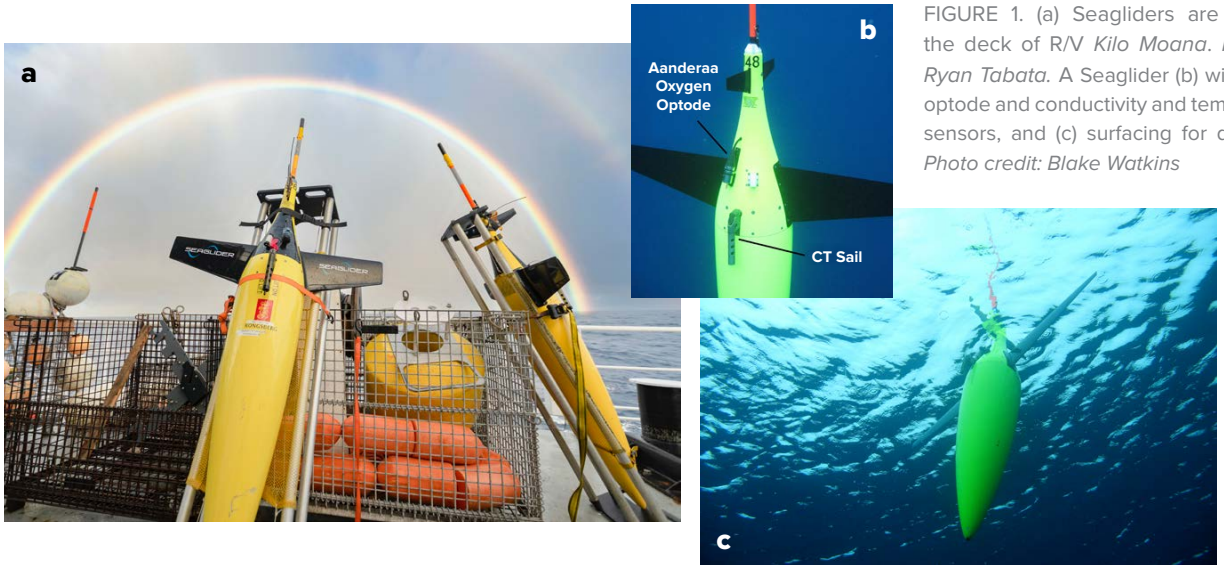

FIGURE 1. (a) Seagliders are secured on the deck of R/V *Kilo Moana*. *Photo credit: Ryan Tabata.* A Seaglider (b) with an oxygen optode and conductivity and temperature (CT) sensors, and (c) surfacing for data retrieval. *Photo credit: Blake Watkins*

in oxygen concentration, chlorophyll *a* concentration, and optical backscatter as a proxy for particle concentration (Figure 1b). The Seagliders surface after each dive to transmit data via satellite and receive updated instructions on sampling location, depth, and frequency (Figure 1c). Thus, Seagliders can be used to characterize the variability of primary production, respiration, and particle dynamics to illuminate their relationship with high-productivity events. These events can serve as a framework for monitoring the short-term evolution of a water patch following "boom" and "bust" phases similar to that predicted during open ocean CDR experiments.

As a case study, we highlight data collected by a Seaglider mission near Station ALOHA in August and September 2008 (Figure 2b–d), when satellite imagery showed patches of elevated chlorophyll *a* concentration (Figure 2a–d). During this mission, the Seaglider measured chlorophyll *a* concentrations well above the climatological seasonal mean, even approaching two standard deviations above the mean (0.145 mg m^{-3}) on August 31 and September 1 (Figure 2e). We define this accumulation of chlorophyll *a* concentrations as a bloom, because the accumulation occurred rapidly over two weeks. Shipboard sampling at Station ALOHA by the HOT program occurred at the end of July, in mid-August, and then in October. These measurements show elevated chlorophyll *a* concentration in August (Figure 2e, yellow stars), but the low sampling frequency of the ship-based observations cannot resolve the summer phytoplankton accumulation evident from Seaglider and satellite observations. Indeed, an oceanographic expedition to the east of Station ALOHA measured a large range of surface chlorophyll *a* concentrations over the course of a few days in August (Figure 2a, cyan diamonds).

On average, the Seaglider collected 16 profiles per day to 200 m, which allowed us to examine both long-term and short-term variability in oxygen concentrations. Seasonally, elevated temperature in late summer leads to outgassing and low surface oxygen (Figure 3a). At the daily scale, oxygen variability is dominated by photosynthesis and respiration, with rates that can be estimated from the shape of the diel oxygen variation (Barone et al., 2019). Using this method, we found that three-day average gross oxygen production (GOP) and community respiration (CR) were higher in late August/early September (Figure 3b). Increased production was linked with elevated particle backscattering and chlorophyll *a* (Figure 3a,c), suggesting particle accumulation and increased productivity during the bloom period.

Linking marine productivity to carbon export remains a challenge because only a small fraction of the carbon fixed by photosynthesis is exported below the euphotic zone (<10%), and there is likely a time lag between carbon fixation and export (Karl et al., 2021). For example, the Ocean Perturbation Experiment (OPEREX1) cruise shown in Figure 2a found evidence of increased particle flux where

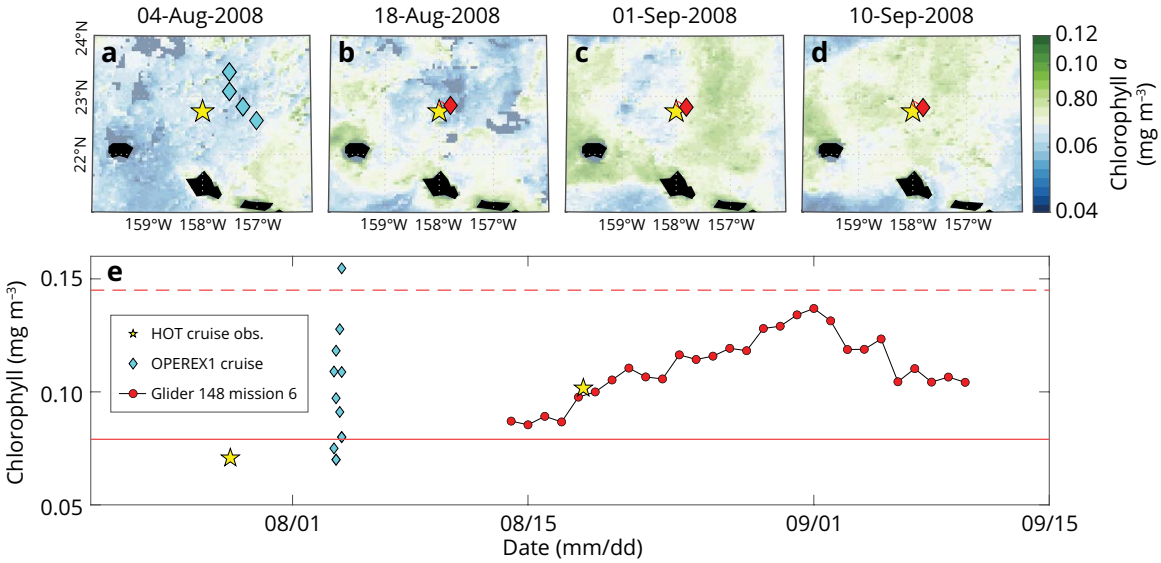

FIGURE 2. Chlorophyll *a* as measured by satellite, Seaglider, and ship-based observations. (a–d) Satellite chlorophyll around Station ALOHA (yellow star). Selected dates are shown when chlorophyll *a* was measured in situ and during the late summer bloom. Cruise tracks for the Ocean Perturbation Experiment (OPEREX1; cyan diamonds) and a Seaglider path (red diamonds) are marked. (e) Chlorophyll *a* concentrations in the surface layer for Station ALOHA (yellow star), OPEREX1 (cyan diamonds), and the Seaglider (red circles). The summertime climatological chlorophyll *a* concentration (0.079 mg m^{-3}) at Station ALOHA in the mixed layer is marked with a solid red line, and two standard deviations above the mean (0.1450 mg m^{-3}) is indicated with a red dashed line. Satellite chlorophyll *a* concentrations were obtained as the Globcolour data product distributed by the Copernicus Marine Service.

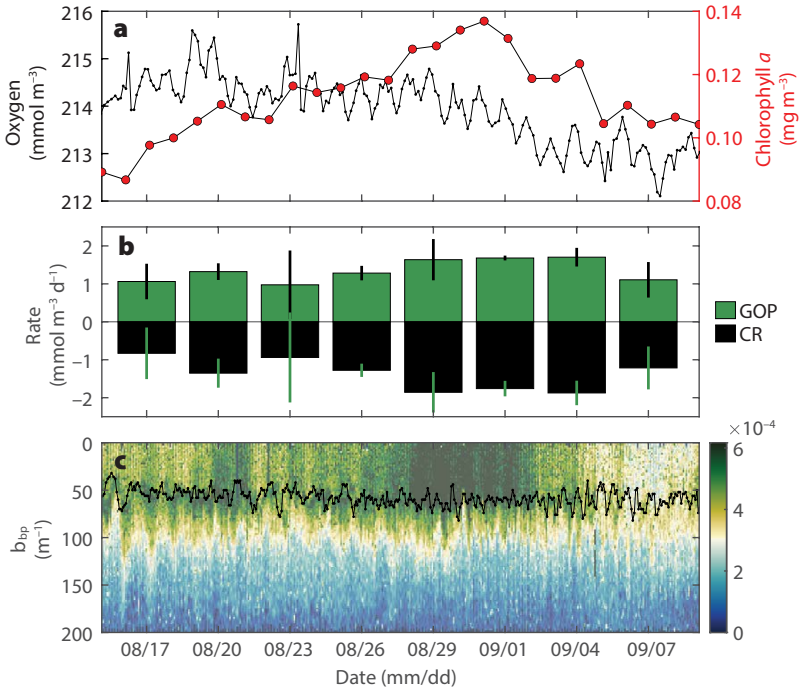

FIGURE 3. Time series of dissolved oxygen, metabolic rates, and suspended particles measured by a Seaglider. (a) Average oxygen (black dots) and chlorophyll *a* (red circles) concentrations in the surface layer (range 30–82 m, defined as in Barone et al., 2019). (b) Mean rates of gross oxygen production (GOP) and community respiration (CR) in three-day intervals. Error bars are the standard errors from the weighted variances. (c) Particle backscattering coefficient in the upper 200 m. Surface layer depths are plotted overlaid as black scatter points.

mixed layer chlorophyll *a* and particle concentrations were higher, but primary production was not enhanced (Guidi et al., 2012). Seagliders are well suited to document periodic changes in production leading up to pulsed export events. While shipboard primary production experiments are time-consuming and unrealistic to maintain beyond several days on station, Seagliders can remain in an area for upward of three months. With these production estimates, there is potential to determine time lags between production and export, and to identify the biological and physical forcings preceding high export events.

Understanding the dynamics that break this coupling and lead to high particle export events can direct future efforts for CDR technologies in nutrient-poor ecosystems. A recent study of CDR timescales suggests carbon exported to depth in the North Pacific Ocean remains sequestered far longer than in other ocean basins (Siegel et al., 2021). Thus, fast-sinking particles that reach the ocean bottom in the Pacific Ocean will more efficiently sequester carbon. Work at Station ALOHA shows that carbon sequestration depends on the species of nitrogen fixers driving new production (Dore et al., 2008; Karl et al., 2021): while fast-sinking endosymbiotic diatoms are detected at 4,000 m depth, more buoyant particles associated with *Trichodesmium* are presumably mineralized before reaching the ocean's abyss.

An exciting development for autonomous underwater vehicles is the ability to attach compact underwater vision profilers to quantify and identify marine particles, including phytoplankton. Combined with novel methods for tracking productivity (Barone et al., 2019), Seagliders are poised to independently track gross oxygen production, community respiration, and particle accumulation that leads to export pulses. Seagliders cannot take discrete water samples; however, when paired with discrete sampling of sinking particle export, they can paint a high-resolution, three-dimensional picture of the water column leading up to enhanced carbon export.

REFERENCES

Barone, B., D. Nicholson, S. Ferrón, E. Firing, and D.M. Karl. 2019. The estimation of gross oxygen production and community respiration from autonomous time-series measurements in the oligotrophic ocean. *Limnology and Oceanography Methods* 17(12):650–664, https://doi.org/10.1002/lom3.10340.

Dore, J.E., R.M. Letelier, M.J. Church, R. Lukas, and D.M. Karl. 2008. Summer phytoplankton blooms in the oligotrophic North Pacific Subtropical Gyre: Historical perspective and recent observations. *Progress in Oceanography* 76:2–38, https://doi.org/10.1016/j.pocean.2007.10.002.

Guidi, L., P.H. Calil, S. Duhamel, K.M. Björkman, S.C. Doney, G.A. Jackson, B. Li, M.J. Church, S. Tozzi, Z.S. Kolber, and others. 2012. Does eddy-eddy interaction control surface phytoplankton distribution and carbon export in the North Pacific Subtropical Gyre? *Journal of Geophysical Research: Biogeosciences* 117(G2), https://doi.org/10.1029/2012JG001984.

Karl, D.M. R.M. Letelier, R.R. Bidigare, K.M. Björkman, M.J. Church, J.E. Dore, and A.E. White. 2021. Seasonal-to-decadal scale variability in primary production and particulate matter export at Station ALOHA. *Progress in Oceanography* 195:102563, https://doi.org/10.1016/j.pocean.2021.102563.

Siegel, D.A., T. DeVries, S.C. Doney, and T. Bell. 2021. Assessing the sequestration time scales of some ocean-based carbon dioxide reduction strategies. *Environmental Research Letters* 16:104003, https://doi.org/10.1088/1748-9326/ac0be0.

ARTICLE DOI. https://doi.org/10.5670/oceanog.2023.s1.3

A Low-Cost Carbon Dioxide Monitoring System for Coastal and Estuarine Sensor Networks

By Philip J. Bresnahan, Elizabeth Farquhar, Daniel Portelli, Michael Tydings, Taylor Wirth, and Todd Martz

As the interest in marine or ocean-based carbon dioxide removal (mCDR) increases, so does the need for more spatially resolved measurement, reporting, and verification (MRV) of the CO_2 sequestered (and for understanding the impacts of these environmental manipulation experiments). The mCDR/MRV community can borrow technology from the past decade's exponential growth of interest in ocean acidification and monitoring. However, available sensors are insufficient to meet the growing demand for spatially resolved mCDR due to technological complexities, availability, and cost. For instance, in a recent review, there were few commercially available autonomous solutions for pH and pCO_2 monitoring and none for total alkalinity or total dissolved inorganic carbon), and the majority of the pH and pCO_2 sensors and analyzers cost well above $10,000. Proper MRV of mCDR requires high spatiotemporal resolution monitoring of the inorganic carbon system. Here we describe our efforts toward a low-cost CO_2 flux or ΔpCO_2 (the difference between air and water partial pressure of CO_2) monitoring system intended for use in distributed sensor arrays in coastal, estuarine, and blue carbon research and in mCDR approaches.

Most aquatic pCO_2 instrumentation is based on either non-dispersive infrared (NDIR) gas analysis or spectrophotometry. These systems typically incorporate expensive NDIR or spectrophotometric instrumentation (>$5,000) and frequently also utilize onboard calibration gas standards, resulting in large and costly solutions. Several recent studies (e.g., Wall, 2014; Hunt et al., 2017) have utilized lower-cost NDIRs that are typically sold for indoor air quality monitoring applications, but these analyzers tend to suffer from sensor drift, as they were not intended to meet climate-quality monitoring objectives. Other biogeochemical instrumentation overcomes limitations in accuracy and stability via the inclusion of onboard standards and/or calibration/validation to well-known values, such as deep dissolved oxygen or pH, or atmospheric oxygen.

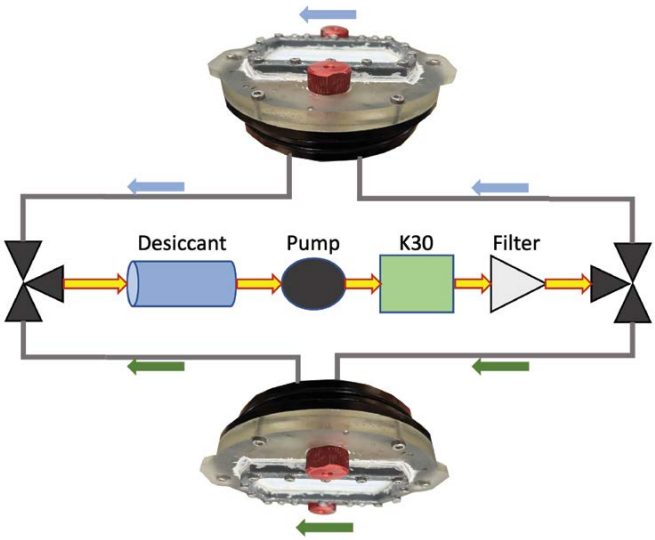

FIGURE 1. SEACOW flow diagram with arrows indicating direction of air flow. Blue arrows = air side. Green arrows = water side. Yellow arrows with red outlines = common.

To meet the need for a lower-cost and sufficiently stable pCO_2 analyzer for deployments in dynamic coastal and estuarine environments and in distributed sensor arrays in mCDR manipulations, we have developed the SEACOW: Sensor for the Exchange of Atmospheric CO_2 with Water. SEACOW replaces more expensive NDIR sensors common in state-of-the-art ΔpCO_2 analyzers (e.g., Friederich et al., 1995) with the $99 Senseair K30 NDIR sensor. Cycling between atmospheric and aquatic pCO_2 measurements enables the calculation of CO_2 flux via the equation

$$F = kK_0(pCO_{2,water} - pCO_{2,air}), \quad (1)$$

where F is the CO_2 flux from air to water, k is the gas transfer velocity, and K_0 is CO_2 solubility (see Wanninkhof et al., 2009, for further details). We note that the estimation of k is itself an active area of research, both in the open ocean and especially in more bathymetrically and hydrodynamically complex water bodies (Ho et al., 2018). Many aquatic pCO_2 analyzers assume an atmospheric CO_2 concentration for flux calculations (often based on Mauna Loa records or a nominal value of 400 µatm). The perfectly mixed atmosphere assumption may suffice in open ocean environments but is insufficient in dynamic wetland and urban environments where atmospheric CO_2 is more variable (Northcott et al., 2019) and needs to be directly measured for accurate CO_2 flux calculation. Furthermore, our focus on ΔpCO_2 allows for drift in sensor offset that is subtracted out of both pCO_2 terms in Equation 1.

SEACOW comprises two semi-independent sampling loops with a single shared K30 CO_2 sensor (Figure 1). When valves select the air-side loop, SEACOW's internal sample air stream flows through a serpentine track in a custom 3D-printed endcap into which CO_2 permeates across a PTFE membrane from the surrounding air. The sample air then circulates through a common air pump, a desiccant tube (intended to minimize interferences due to water vapor in the NDIR), and a custom 3Dl-printed, air-sample housing (containing a K30 CO_2 sensor and a BME 280 pressure/humidity sensor), and then back through the air-side endcap. When the water side is selected, the valves switch so the air sample flows through a submerged endcap with

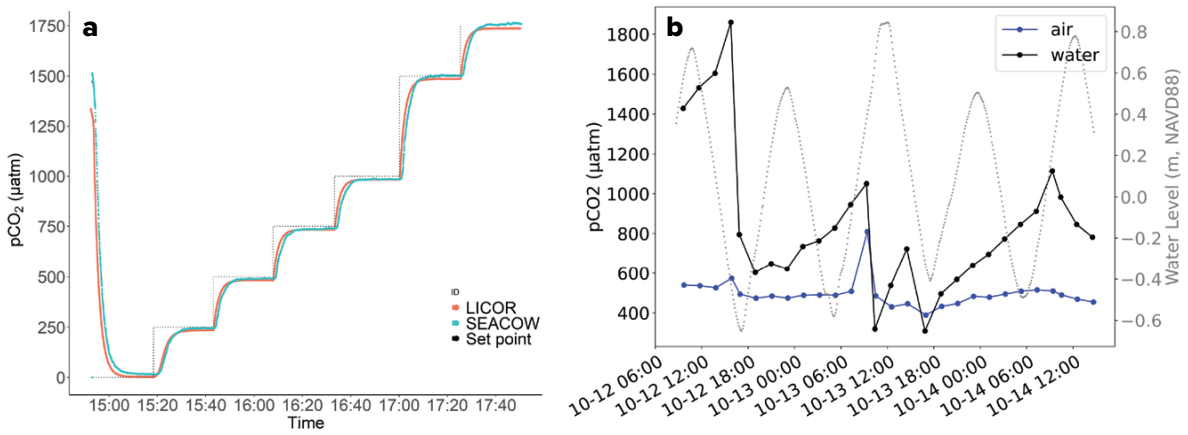

FIGURE 2. (a) SEACOW's gas permeation unit is tested alongside a LI-COR 850 for accuracy and response time evaluation. CO_2 set points are determined with mass flow controllers mixing N_2 and CO_2. (b) Fifty-four hours of SEACOW field data. Blue and black dots represent air- and water-side pCO_2, extrapolated to their steady-state values using Equation 2, and gray dots show collocated water levels from the UNCW Coastal Ocean Research & Monitoring Program (https://CORMP.org).

an identical serpentine track, then through the common pump, desiccant, and sensor housing. SEACOW utilizes a Particle Boron microcontroller with an LTE cellular modem for integration into real-time sensor networks.

Preliminary testing has demonstrated SEACOW's capabilities in laboratory and field settings (Figure 2). A laboratory evaluation of SEACOW's range, accuracy, and response time compares favorably with a LI-COR 850 gas analyzer inside a custom-designed test chamber. Air-side response time (τ_{63}) is 1.6 min while water-side response time is close to an hour. The longer water-side response time is a surmountable issue due to the fact that natural changes in pCO_2 are slow (allowing the instrument to "keep up" with changes) and through fitting the following first-order rate equation to extrapolate to the final value, p_2, following Wall (2014):

$$p(t) = (p_2 - p_1) \times (1 - e^{-t/\tau}) + p_1, \quad (2)$$

where $p(t)$, p_2, and p_1 are partial pressures at arbitrary time t (i.e., instantaneous sensor recordings), at the end of the step change (i.e., the "true" final value), and the beginning of the step change (the initial value), respectively, and τ is the response time. We apply Equation 2 (solving for p_2 to extrapolate to a final value for each measurement) to 54 hours of field data when SEACOW was fixed to the floating dock at the University of North Carolina Wilmington (UNCW) Center for Marine Science in North Carolina, USA. This initial field test demonstrates SEACOW's ability to track tidal/diel fluctuations in ΔpCO_2.

We also acknowledge that there are alternative solutions for monitoring aquatic CO_2 flux beyond the ΔpCO_2 method described here. These include, for example, eddy covariance and chamber techniques (see "Available methods to quantify water-air gas exchange" in Rosentreter, 2022) and can also include low-cost technologies (e.g., Bastviken et al., 2015). However, SEACOW presents a uniquely powerful solution that can be deployed at scale for high-resolution and high-quality monitoring of CO_2 fluxes within sensor networks with minimal operator interaction. A combination of a distributed array of SEACOW instruments with a single, pricier, and perhaps more accurate pCO_2 instrument could yield a valuable spatially resolved air–water CO_2 flux data set at a price point not otherwise currently attainable.

REFERENCES

Bastviken, D., I. Sundgren, S. Natchimuthu, H. Reyier, and M. Gålfalk. 2015. Technical note: Cost-efficient approaches to measure carbon dioxide (CO_2) fluxes and concentrations in terrestrial and aquatic environments using mini loggers. *Biogeosciences* 12(12):3,849–3,859, https://doi.org/10.5194/bg-12-3849-2015.

Friederich, G.E., P.G. Brewer, R. Herlien, and F.P. Chavez. 1995. Measurement of sea surface partial pressure of CO_2 from a moored buoy. *Deep Sea Research Part I* 42(7):1,175–1,186, https://doi.org/10.1016/0967-0637(95)00044-7.

Ho, D.T., V.C. Engel, S. Ferrón, B. Hickman, J. Choi, and J.W. Harvey. 2018. On factors influencing air-water gas exchange in emergent wetlands. *Journal of Geophysical Research: Biogeosciences* 123(1):178–192, https://doi.org/10.1002/2017JG004299.

Hunt, C.W., L. Snyder, J.E. Salisbury, D. Vandemark, and W.H. McDowell. 2017. SIPCO2: A simple, inexpensive surface water pCO_2 sensor. *Limnology and Oceanography: Methods* 15(3):291–301, https://doi.org/10.1002/lom3.10157.

Northcott, D., J. Sevadjian, D.A. Sancho-Gallegos, C. Wahl, J. Friederich, and F.P. Chavez. 2019. Impacts of urban carbon dioxide emissions on sea-air flux and ocean acidification in nearshore waters. *PLoS ONE* 14(3):e0214403, https://doi.org/10.1371/journal.pone.0214403.

Rosentreter, J.A. 2022. Water-air gas exchange of CO_2 and CH_4 in coastal wetlands. Pp. 167–196 in *Carbon Mineralization in Coastal Wetlands*. X. Ouyang, S.Y. Lee, D.Y.F. Lai, and C. Marchand, eds, Elsevier.

Wall, C.M. 2014. *Autonomous in situ Measurements of Estuarine Surface pCO_2: Instrument Development and Initial Estuarine Observations*. Master's Thesis, Oregon State University, 103 pp.

Wanninkhof, R., W.E. Asher, D.T. Ho, C. Sweeney, and W.R. McGillis. 2009. Advances in quantifying air-sea gas exchange and environmental forcing. *Annual Review of Marine Science* 1:213–244, https://doi.org/10.1146/annurev.marine.010908.163742.

ACKNOWLEDGMENTS

We thank UNCW's Department of Earth and Ocean Sciences and Office of Innovation and Commercialization for funding this research. Dave Wells provided support for sensor deployment at the UNCW Center for Marine Science.

ARTICLE DOI. https://doi.org/10.5670/oceanog.2023.s1.4

PERSPECTIVE

The Growing Potential of Antarctic Blue Carbon

By Chester J. Sands, Nadescha Zwerschke, Narissa Bax, David K.A. Barnes, Camille Moreau, Rachel Downey, Bernabé Moreno, Christoph Held, and Maria Paulsen

The removal of carbon from the atmosphere for a long period (sequestration) is an increasingly pressing societal need in order to mitigate the negative effects of climate change. Investment and technology solutions are moving in the direction of industrial carbon capture and storage. To date, this technology is inefficient, expensive, and in some cases, not even net carbon zero. Optimistic estimates suggesting huge investment in infrastructure, which requires resources that include land and fresh water, will only marginally contribute toward the reductions in atmospheric CO_2 required to minimize the impact of climate change over the next 50 years (Hankin et al., 2019).

The ocean is a powerful CO_2 sink, absorbing ~30% of anthropogenic CO_2 output. But, even in the Southern Ocean, the most powerful ocean sink, CO_2 outgassing occurs (Nicholson et al., 2022). Outgassing is particularly associated with storm events, which are suggested to be increasing in frequency and intensity as a result of climate change. Additionally, the ocean's buffering effect is eroding due to climate-associated changes in pH (Iida et al., 2021).

Nature-based CO_2 sequestration associated with the ocean and coastal ecosystems ("blue carbon") is more efficient than commercial carbon capture and storage, and nature does it "for free." Mangrove forests, seagrass beds, and salt marshes are considered the most efficient and are the best studied. Unfortunately, these valuable natural carbon sequestering resources are in rapid decline. Crucially, this means that CO_2 uptake by these coastal ecosystems is much reduced, and they are releasing previously sequestered carbon back into the atmosphere upon their demise.

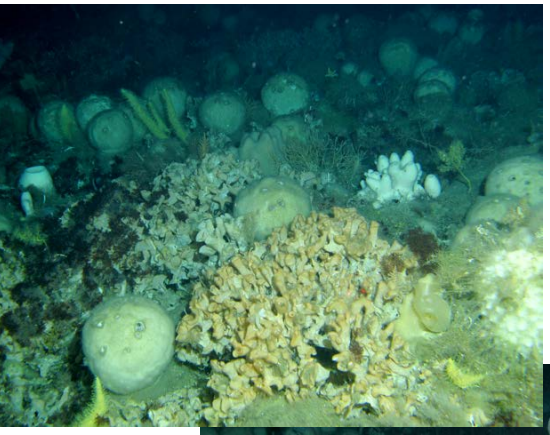

FIGURE 1. Examples of the Antarctic continental shelf benthos.

Among other less well known nature-based pathways to carbon removal and, at least one, Antarctic blue carbon, is growing in response to climate change. Seasonal sea ice extent and duration have been massively reduced in polar regions over recent years, leading to longer-lasting phytoplankton (microalgae) blooms over continental shelf waters (Barnes et al., 2021). As a result, both primary and secondary production (phytoplankton and zooplankton) are in direct contact with the animals living on the seafloor (benthos; Figure 1), providing extended feeding opportunities and demonstrably faster growth (Barnes et al., 2021). Considering the longevity of many polar benthic invertebrates, they are a growing carbon stock if left undisturbed.

Other types of marine ice retreat are also opening up novel habitats for colonization by marine life. Losses from ice shelves create vast new embayments hospitable to primary production and colonization, and the retreat of marine-terminating glaciers along fjords provides new and increasing habitat for benthos (Figure 2). Owing to high sedimentation rates on polar continental shelves and even higher rates in some fjord systems, a proportion of this accumulated carbon will likely be buried in the sediment. Once burial is beyond the oxygenated or active layer, few microbes are available to recycle any carbon back into the carbon cycle.

Recent studies are beginning to add empirical data that suggest the polar pathways are contributing considerably to global carbon sequestration (Pineda-Metz et al., 2020). In particular, Zwerschke et al., (2021) found that the amount of total organic carbon (TOC) in sediments of Antarctic fjords with retreating glaciers (~50 g C m^{-2}) was an order of magnitude greater than that previously estimated based solely on epibenthic fauna. If these findings were to be extrapolated across the entire Antarctic continental shelf (4.4 million km^2), they would represent 220 million tonnes of carbon (t C) storage.

How comparable this TOC value is to other Antarctic open-shelf regions is unknown, as is how much of this carbon is genuinely sequestered. The sedimentary evidence clearly indicates the need for more detailed investigation of the polar shelf regions, fjords in particular, as nature-based carbon removal pathways. This increasing blue carbon around Antarctica is an ecosystem service of considerable societal and economic value that should be taken into

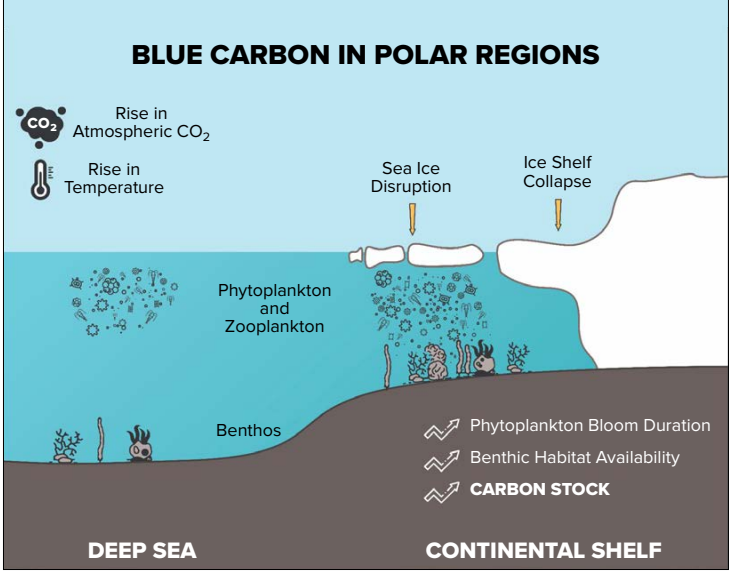

FIGURE 2. A summary of the processes leading to carbon removal on Antarctic continental shelves. Loss of winter sea ice and glacier retreat occur more frequently, resulting in the phytoplankton blooms being in contact with the benthos, thus providing a more efficient carbon capture and storage pathway.

account (Bax et al., 2021). Warming continues to affect sea ice duration and extent. Ice shelves continue to collapse. Marine-terminating glaciers are in retreat. Each year, new shallow sea area is available to phytoplankton populations, and more seafloor opens up as habitat for benthos. Warming is likely to increase metabolic processes and food-web-wide growth, again increasing the rate at which carbon is drawn down, stored, and potentially sequestered in this a rare and powerful negative feedback mechanism to climate change—with lasting benefit to society (Barnes et al., 2021).

At present, the Antarctic is largely protected by conventions and treatises that ban mineral exploitation and limit fishing in an environment that is, as yet, not conducive to commercial exploitation and consequent wide habitat destruction. Adding a further layer of protection to these areas while they are of little commercial value may be advisable in order to safeguard what appears to be a valuable global resource for carbon removal. The UK government currently values CO_2 at £46.40 t^{-1}, which translates into £170 t^{-1} of carbon. A conservative estimate of 1% of primary productivity would be sequestered (Henley et al., 2020), which, on the West Antarctic Peninsula shelf would be 1.9 g C m^{-2} (Barnes, 2017). If this were extrapolated across the entire Antarctic continental shelf, it would equate to 8.36×10^6 t C y^{-1} or £1.4 billion removed from the carbon cycle. If immobilized biological carbon is the focus for marine CO_2 removal (estimated by Henley et al., 2020, at 12% primary productivity, 22.8 g C m^{-2}), then across the Antarctic shelf, 100.32×10^6 t C y^{-1} held in medium term (tens to hundreds of years) storage, is valued at £17.05 billion. These values will continue to grow each year with the increasing value of carbon and the increasing potential of the blue carbon pathway. This may be an attractive carbon offset to be distributed among stakeholders agreeing to lasting and meaningful protection of the area.

Antarctic blue carbon potential is one of many understudied carbon removal pathways. Full understanding of the geography and magnitude of carbon sequestration is required to enable placing an appropriate value on the services nature can provide if adequately safeguarded. Investment in gaining this knowledge (to help prioritize protection and meaningful monitoring) would cost only a fraction of that for commercial carbon capture and sequestration, and a fraction of the ultimate value of the carbon sequestered on the Antarctic continental shelf.

REFERENCES

Barnes, D.K.A. 2017. Iceberg killing fields limit huge potential for benthic blue carbon in Antarctic shallows. *Global Change Biology* 23(7):2,649–2,659, https://doi.org/10.1111/gcb.13523.

Barnes, D.K.A., C.J. Sands, M.L. Paulsen, B. Moreno, C. Moreau, C. Held, R. Downey, N. Bax, J.S. Stark, and N. Zwerschke. 2021. Societal importance of Antarctic negative feedbacks on climate change: Blue carbon gains from sea ice, ice shelf and glacier losses. *The Science of Nature* 108:43, https://doi.org/10.1007/s00114-021-01748-8.

Bax, N., C.J. Sands, B. Gogarty, R.V. Downey, C.V.E. Moreau, B. Moreno, C. Held, M.L. Paulsen, J. McGee, M. Haward, and D.K.A. Barnes. 2021. Perspective: Increasing blue carbon around Antarctica is an ecosystem service of considerable societal and economic value worth protecting. *Global Change Biology* 27(1)5–12, https://doi.org/10.1111/gcb.15392.

Hankin, A., G.G. Guillen, G. Kelsall, N. Mac Dowell, N. Shah, S. Weider, and K. Brophy. 2019. Assessing the economic and environmental value of carbon capture and utilization in the UK. Briefing paper No. 3, Institute for Molecular Science and Engineering, Imperial College London, 12 pp.

Henley, S.F., E.L. Cavan, S.E. Fawcett, R. Kerr, T. Monteiro, R.M. Sherrell, A.R. Bowie, P.W. Boyd, D.K.A. Barnes, I.R. Schloss, and others. 2020. Changing biogeochemistry of the Southern Ocean and its ecosystem implications. *Frontiers in Marine Science* 7:581, https://doi.org/10.3389/fmars.2020.00581.

Iida, Y., Y. Takatani, A. Kojima, and M. Ishii. 2021. Global trends of ocean CO_2 sink and ocean acidification: An observation-based reconstruction of surface ocean inorganic carbon variables. *Journal of Oceanography* 77:323–358, https://doi.org/10.1007/s10872-020-00571-5.

Nicholson, S.-A., D.B. Whitt, I. Fer, M.D. du Plessis, A.D. Lebéhot, S. Swart, A.J. Sutton, and P.M.S. Monteiro. 2022. Storms drive outgassing of CO_2 in the subpolar Southern Ocean. *Nature Communications* 13:158, https://doi.org/10.1038/s41467-021-27780-w.

Pineda-Metz, S.E.A., D. Gerdes, and C. Richter. 2020. Benthic fauna declined on a whitening Antarctic continental shelf. *Nature Communications* 11:2226, https://doi.org/10.1038/s41467-020-16093-z.

Zwerschke, N., C.J. Sands, A. Roman-Gonzalez, D.K.A. Barnes, A. Guzzi, S. Jenkins, C. Muñoz-Ramírez, and J. Scourse. 2021. Quantification of blue carbon pathways contributing to negative feedback on climate change following glacier retreat in West Antarctic fjords. *Global Change Biology* 28(1):8–20, https://doi.org/10.1111/gcb.15898.

ACKNOWLEDGMENTS

We thank Tomas Lundälv for providing the images of the Antarctic continental shelf seafloor from R/V *Polarstern* cruise PS77 and Henrik Christiansen for helpful edit suggestions.

ARTICLE DOI. https://doi.org/10.5670/oceanog.2023.s1.5

Net Zero: Actions for an Ocean-Climate Solution

By Anya M. Waite, Mike Smit, Eric Siegel, Greg Hanna, and Sara Leslie

It has long been understood that stabilizing the global climate requires human carbon emissions to converge toward net zero (Matthews and Caldeira, 2008). Analysis by the Intergovernmental Panel on Climate Change (IPCC) suggests delays in achieving net zero emissions, or a temperature increase of more than 1.5°C, will necessitate even stronger action: net negative emissions. A very large-scale opportunity for carbon sequestration would include yet unproven ocean-based carbon dioxide removal (CDR) technologies (Rogelj et al., 2018).

The ocean is the largest carbon storage depot on Earth (Figure 1). It holds more carbon than the atmosphere and trees combined, thus, achieving net zero within the desired timeframe will not be possible without a better understanding of the ocean and its carbon-absorbing mechanisms. To that end, three actions need to be taken:

1. Create sustained and robust ocean observation systems, including data flows, reanalyses, and modeling that deliver reliable assessments of ocean carbon absorption.
2. Align the multiple international conversations on ocean carbon in key intergovernmental organizations and in the research and observation communities.
3. Engage nations in a comprehensive dialogue regarding support of ocean observation on the high seas, beyond national jurisdiction.

INTERNATIONAL EFFORTS

The IPCC has built a bedrock of climate information based on regular global assessments that rely on the careful compilation of scientific knowledge and an international consensus process to inform governments and other stakeholders of the climate trajectory. Internationally, UN agencies have consolidated the work of many nations to support and inform global action based on IPCC analyses.

The World Meteorological Organization (WMO) recently launched a study group that aims for international consensus on a greenhouse gas monitoring system. The deep ocean remains largely outside the scope of these discussions, but the WMO has harnessed the work of the Global Ocean Observing System (GOOS), under the umbrella of the Intergovernmental Oceanographic Commission (IOC)/UNESCO, to fill this deficit. GOOS has proposed three major programs under the UN Decade of Ocean Science for Sustainable Development (2021–2030), including Ocean Observation Co-Design, which identifies ocean carbon observation as a key focus and seeks a first strategic carbon observing exemplar.

WMO, IPCC, and GOOS activities support the Global Climate Observing System (GCOS) Implementation Plan, which provided critical input to the United Nations Framework Convention on Climate Change (UNFCCC) when accepted by the Parties at COP27 in November 2022.

One of the most important developments in the intergovernmental climate conversation is the formation of a group of experts (GESAMP, undated) to frame ocean CDR technologies such as ocean fertilization and ocean alkalinity enhancement (NASEM, 2022) so researchers and observers can assess the challenges and risks.

However, many actors in these international discussions recognize the deficit in these systems: there are excellent global frameworks that create opportunities for climate action—but in general, do not drive or fund actions that would take advantage of these opportunities. This leaves many in the ocean community with fragile or declining observation systems, short-term funding, and increasingly stretched volunteerism within the ocean observation community (GOOS, 2022).

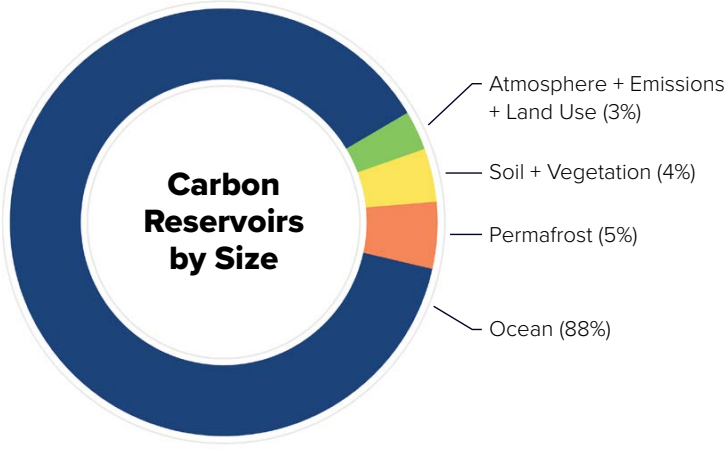

FIGURE 1. The ocean is the world's largest carbon reservoir. The full circle represents global carbon reservoirs that exchange with the atmosphere at a timescale of 1,000 years or less.

THE NEED FOR A STRATEGIC EXEMPLAR

A vision is needed for development of the world's first international climate observatory that would record carbon and heat fluxes from the seafloor to the atmosphere. The observatory could emerge as a first move for a UNFCCC Global Goal for Observation, be nested in the GCOS Implementation Plan (as a Carbon Observatory under Action B6), become a mandated observation system under the WMO, or form a carbon exemplar for the GOOS Ocean Observation Co-Design program.

This initiative would require leading nations to communicate, pool, and coordinate their already substantial investments in observing infrastructure, and their expertise in the areas of science, policy, and innovation, to create information streams that would benefit all participants involved, along with the rest of the world.

OCEAN CARBON

The ocean observation landscape is changing rapidly. More and more, the business community is signaling an eagerness (de Sanctis et al., 2022) to commercialize ocean CDR, and financial markets are indicating their willingness to build an active market in voluntary carbon credits. They realize both the climate urgency and the large economic opportunity at stake. Any such moves require transparency, intense scientific engagement, and a strong and credible framework for validation and certification. An international climate observatory would help to fill the gaps in ocean carbon data so that a baseline could be established for these purposes.

While the GCOS Implementation Plan calls for more traditional shipboard CTD casts and Argo floats (Buontempo et al., 2022), new technologies and exploding private sector interest mean major observations and insights are increasingly generated elsewhere (Brett et al., 2020). Frequently, ocean data flows originate from autonomous vehicles and private sector initiatives concentrated at the surface or in the upper 2,000 m of the ocean, rather than from research vessels that collect high-precision measurements that extend to the seafloor (Brett et al., 2020). A whole new level of siloed data management between private and public sectors hinders mapping and coordination of these data flows into actionable information. Breaking down communication barriers and encouraging data sharing across public and private sectors, and beyond national boundaries, is becoming an urgent task.

To be credible and effective, ocean CDR must be exceptionally well documented and carefully rolled out, and it must scale up quickly enough to impact the global climate. CDR verification requires synthesis of ocean data at multiple scales, from test tube to tank, from bay to continental shelf. Eventually, if ocean CDR is to reach gigatons of carbon removal and millennia of storage, it will have to include the open ocean. It is here, on the high seas, where global risks and carbon opportunities are greatest, that ocean observation and data integration is poorest.

Nations have the funding and resources to support robust ocean observing structures that reach beyond individual countries and outside exclusive economic zones to enable observations, scientific synthesis, and, potentially, safe sequestration of the biggest stores of carbon. It is important they come together to champion and bring to fruition the multiple intergovernmental initiatives under the UN Framework Convention for Climate Change, while maintaining a strong dialogue with the burgeoning private sector.

A new conversation is urgently needed to transform climate action.

REFERENCES

Brett, A., J. Leape, M. Abbott, H. Sakaguchi, L. Cao, K. Chand, Y. Golbuu, T.J. Martin, J. Mayorga, and M. Myksvoll. 2020. Ocean data need a sea change to help navigate the warming world. *Nature* 582:181–183, https://doi.org/10.1038/d41586-020-01668-z.

Buontempo, C., A. Han Dolman, T. Krug, J. Schmetz, S. Speich, P. Thorne, M. Zemp, Q. Chao, A. Han Dolman, M. Herold, and others. 2022. *The 2022 GCOS Implementation Plan*. World Meteorological Organization, Geneva, Switzerland, 85 pp.

de Sanctis, C., P. Lamy, E. Letta, G. Pons, J.-F. Pons, M. Müller, K. Sack, K. Teleki, T. Thiele, and A.M. Waite. 2020. *Delivering a Sea-Change: A G7 Ocean Finance Deal*. Ocean Risk and Resiliance Alliance and Europe Jacques Delors, 7 pp., https://oceanriskalliance.org/wp-content/uploads/G7-Ocean-Finance-Deal-White-Paper-17-May-2022.pdf.

GESAMP (Joint Group of Experts on the Scientific Aspects of Marine Environmental Protection). Undated. "Ocean Interventions for Climate Change Mitigation," http://www.gesamp.org/work/groups/41.

GOOS (Global Ocean Observing System). 2022. *Ocean Observing System Report Card 2022*. 5 pp., https://www.ocean-ops.org/reportcard/reportcard2022.pdf.

Matthews, H.D., and K. Caldeira. 2008. Stabilizing climate requires near-zero emissions. *Geophysical Research Letters* 35(4), https://doi.org/10.1029/2007GL032388.

NASEM (National Academies of Sciences, Engineering, and Medicine). 2022. *A Research Strategy for Ocean-based Carbon Dioxide Removal and Sequestration*. The National Academies Press, Washington, DC, 322 pp., https://doi.org/10.17226/26278.

Rogelj, J., D. Shindell, K. Jiang, S. Fifita, P. Forster, V. Ginzburg, C. Handa, H. Kheshgi, S. Kobayashi, E. Kriegler, and others. 2018. Mitigation pathways compatible with 1.5°C in the context of sustainable development. Chapter 2 in *Global Warming of 1.5°C. An IPCC Special Report on the Impacts of Global Warming of 1.5°C Above Pre-Industrial Levels and Related Global Greenhouse Gas Emission Pathways, in the Context of Strengthening the Global Response to the Threat of Climate Change, Sustainable Development, and Efforts to Eradicate Poverty.* V. Masson-Delmotte, P. Zhai, H.-O. Pörtner, D. Roberts, J. Skea, P.R. Shukla, A. Pirani, W. Moufouma-Okia, C. Péan, R. Pidcock, S. Connors, J.B.R. Matthews, Y. Chen, X. Zhou, M.I. Gomis, E. Lonnoy, T. Maycock, M. Tignor, and T. Waterfield, eds, Cambridge University Press, Cambridge, UK and New York, NY, USA, https://doi.org/10.1017/9781009157940.004.

ARTICLE DOI. https://doi.org/10.5670/oceanog.2023.s1.6

Using Soundscapes to Assess Changes in Coral Reef Social-Ecological Systems

By Tzu-Hao Lin, Frederic Sinniger, Saki Harii, and Tomonari Akamatsu

Coral reefs are among the world's most diversified marine ecosystems. While their rich biodiversity is essential to many social and economic activities, they face unprecedented cumulative impacts from climate change and anthropogenic development. Aligning governance structures with ecological processes has become key to sustaining ecosystem services. Nevertheless, a major obstacle to informing decision-making is the lack of empirical data on interacting ecological and social processes. Therefore, novel methods for facilitating the assessment of coral reef social-ecological systems are necessary.

Sounds are ubiquitous in coral reef ecosystems, where many reef-associated animals intentionally or unintentionally produce sounds (Mooney et al., 2020). In addition, geophysical events (e.g., wind, waves, and rain) and anthropogenic activities (e.g., shipping, fishing, and scuba diving) generate perceptible sounds (Lin et al., 2021; Simmons et al., 2021). Listening to underwater soundscapes—the mixture of biophony, geophony, and anthropophony—opens a new avenue for studying the ecological and human dimensions of coral reef ecosystems (Figure 1).

SOUNDS OF CORAL REEF BIODIVERSITY

In coral reef ecosystems, large aggregations of snapping shrimps produce pervasive broadband snaps dominating frequencies >2 kHz (Figure 2a,b) during territorial behavior, foraging, and social interactions (Anker et al., 2006). Various reef-associated fishes, such as damselfish, surgeonfish, and butterflyfish, also generate pulsed sounds of a few hundred hertz (Figure 2b,c) during agonistic and reproductive behaviors, as well as scraping of reef substrate during feeding behaviors (Tricas and Boyle, 2014). Fish sounds can form acoustic mass phenomena in spawning aggregations when multiple calls coalesce into a long-duration chorus (Erisman and Rowell, 2017), turning a coral reef into a concert hall for soniferous fish (Figure 2d). The diverse arrays of biotic sounds from healthy coral reefs create unique soundscapes that can function as habitat cues for the larvae of coral, crustaceans, and reef-associated fish to settle (Simpson et al., 2005; Duarte et al., 2021). Because of the phonotaxis (the movement of an organism in relation to a sound source) of marine larvae toward these cacophonous reefs, reef sounds have been considered a potentially useful indicator of coral reef health (Lamont et al., 2022b).

Monitoring soundscapes has the advantage of providing a rapid assessment of a coral reef ecosystem. Although there is still much debate about the selection of acoustic analysis methods, there are ongoing efforts to link acoustic indices to trends in marine biodiversity and ecosystem health (Pieretti and Danovaro, 2020). For instance, measurements of soundscape complexity—indicators of biotic sound diversity—can be used to differentiate between healthy and degraded coral reefs (Lamont et al., 2022b). In addition, analyzing the diurnal and seasonal variations of biological choruses can reveal the phenological patterns of coral reef ecosystems (Lin et al., 2021). While more field studies are needed to fully understand the application and limitations of acoustic indices, investigating spatiotemporal changes in soundscapes will help researchers and managers assess ecological processes crucial for coral reef biodiversity.

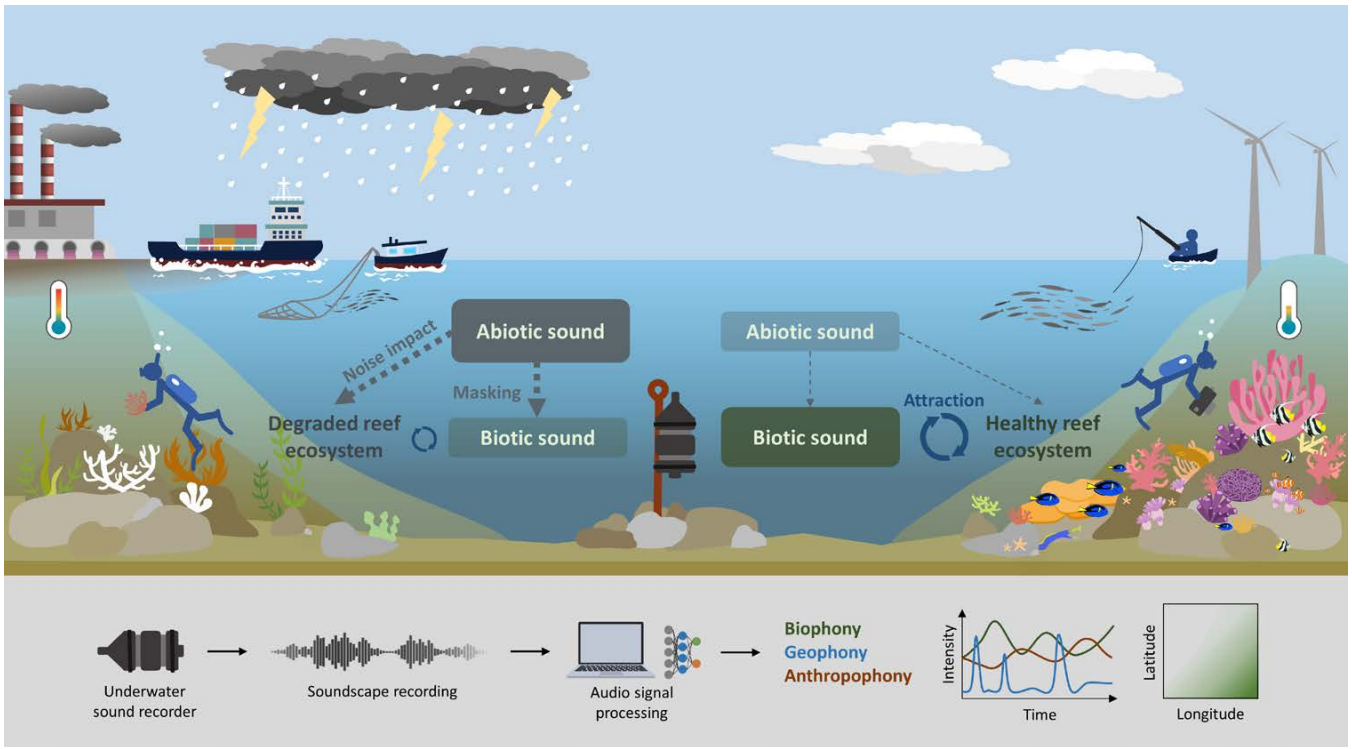

FIGURE 1. Assessing coral reef social-ecological systems using underwater soundscapes. Soundscapes of healthy coral reefs are dominated by intense biotic sounds (biophony), which may acoustically attract reef-associated organisms. Conversely, substantial natural and anthropogenic disturbances produce abiotic sounds (geophony and anthropophony, respectively) that can significantly affect the soundscapes of coral reefs and contribute to their degradation by directly impacting the physiology and behavior of marine animals and reducing the resilience of coral reef ecosystems by masking biotic sounds. Using underwater sound recorders and advanced signal processing techniques, the spatiotemporal dynamics of biotic and abiotic sounds can be monitored, enabling the acoustic observation of social and ecological processes.

SOUNDS OF ENVIRONMENTAL AND ANTHROPOGENIC STRESSORS

Soundscapes also yield information about the effects of environmental and anthropogenic stressors on coral reef ecosystems. Tropical storms can cause severe damage in shallow-water coral reefs through storm-force waves, fast-moving debris, and heavy sediment deposits (Cheal et al., 2017). Estimating storm impact using meteorological data may be less accurate at fine spatial scales, particularly for reefs protected by local topography or those located deeper, such as mesophotic reefs (30–150 m depth). However, underwater sounds recorded on reefs can provide direct observations of environmental disturbance associated with wave action and moving debris (Figure 3a,b), enabling estimation of the extent of physical damage caused by storms. Post-storm changes in biotic sounds may also be useful for assessing the resilience of soniferous animals to changes in benthic habitat and environmental conditions resulting from storm damage (Simmons et al., 2021).

Open-circuit scuba diving, boating, jet skiing, and many other aquatic recreational activities generate high-intensity broadband noise (Ferrier-Pagès et al., 2021). Frequent maritime shipping traffic, particularly in densely populated coastal areas, also produces noise that creates a sort of "acoustic fog" that masks natural soundscapes (Figure 3c,d). Anthropogenic noise can directly influence the physiology and behavior of marine organisms or indirectly weaken ecosystem resilience through acoustic interference with marine larvae dispersion as it masks habitat soundscapes (Duarte et al., 2021). Despite its profound impacts on ocean biodiversity, noise pollution has received little attention in coral reef conservation.

Through the analysis of biotic and abiotic sounds, soundscapes can be transformed into indicators of biodiversity change, environmental perturbation, and anthropogenic interference (Lin et al., 2021). Such indicators represent a promising tool for investigating the interactions between ecological and social processes. In practice, the use of soundscapes in ecosystem assessment is often limited by the need for long-term observations. Moreover, our understanding of soundscape dynamics and associated mechanisms remains highly speculative due to insufficient spatiotemporal coverage and a lack of techniques for identifying distinct sound sources (Mooney et al., 2020; Parsons et al., 2022).

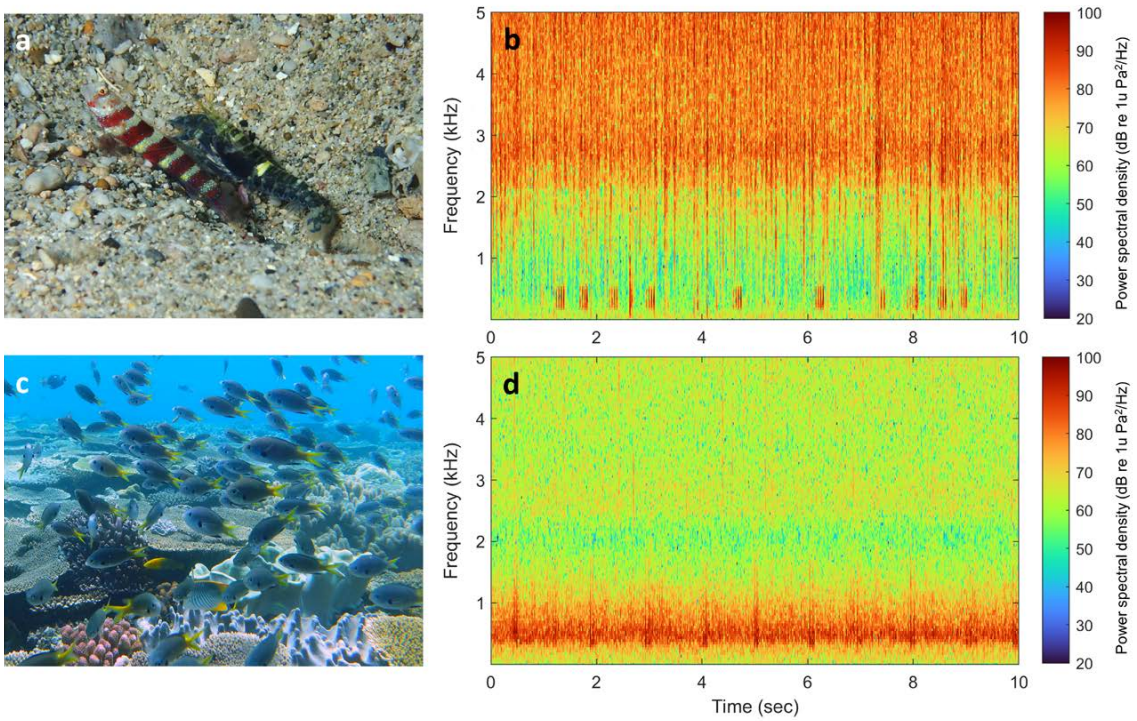

FIGURE 2. Reef-associated animals and their acoustic diversity. (a) A snapping shrimp (*Alpheus djiboutensis*) and a Wheeler's shrimp goby (*Amblyeleotris wheeleri*). (b) A spectrogram of a reef soundscape shows snapping shrimp sounds dominate frequencies >2 kHz, whereas damselfish calls are present between 150 Hz and 600 Hz. The corresponding audio is provided in Supplementary File S1. (c) A group of damselfish on a shallow reef. (d) A spectrogram of the nighttime fish chorus (between 250 Hz and 1 kHz) recorded at a mesophotic coral reef during the spawning season. The corresponding audio is provided in Supplementary File S2.

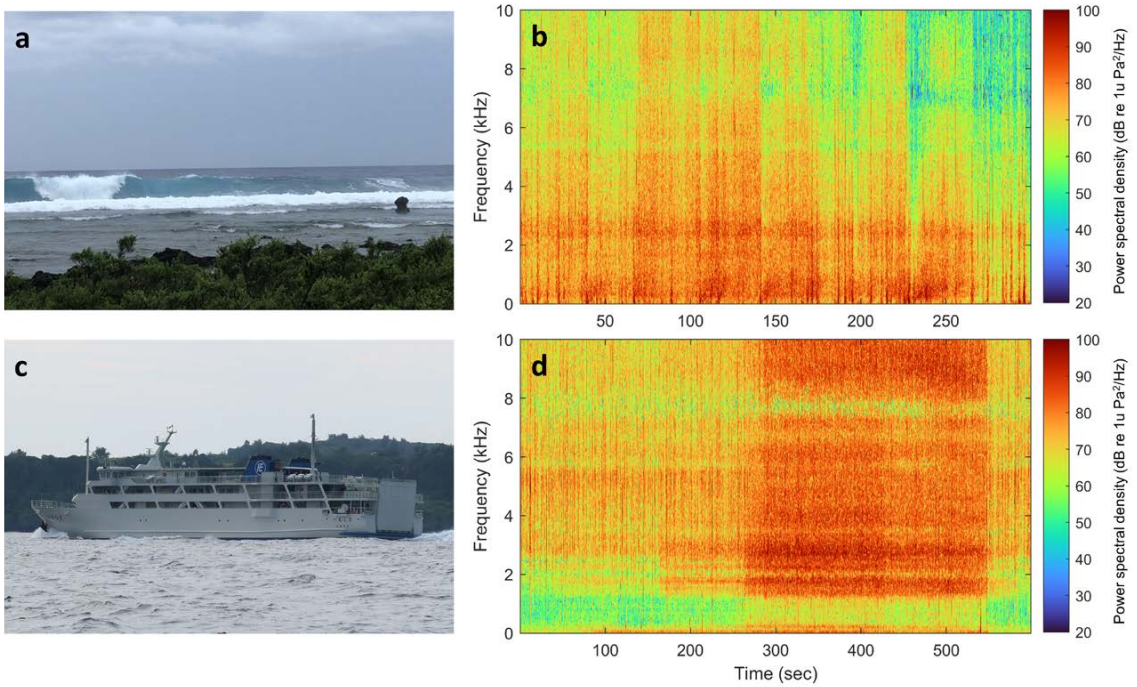

FIGURE 3. Impacts of environmental and anthropogenic stressors on coral reef soundscapes. (a) High waves may physically damage coral reefs in shallow waters. (b) A spectrogram showing the significant wave noise recorded when Typhoon Prapiroon approached Okinawa in 2018. The corresponding audio is provided in Supplementary File S3. (c) A regular ferry between Ie Island and Okinawa Island, Japan. (d) A spectrogram shows the broadband noise of a passing ferry recorded in a shallow-water coral reef. The corresponding audio is provided in Supplementary File S4.

MONITORING CORAL REEF SOUNDSCAPES IN OKINAWA, JAPAN

Recent developments in commercially available audio hardware offer opportunities to monitor soundscapes at scale (Lamont et al., 2022a). While single-channel audio remains the most popular choice for long-term soundscape monitoring, multichannel systems can be used for direction finding (employing stereo recorders with two hydrophones) or source localization (three or more hydrophones), providing spatial information to study the behavior of marine soniferous animals (Figure 4a). The scale of spatial coverage can also be increased by installing audio recording systems on drifting buoys and unmanned surface and underwater vehicles or by towing them behind mobile platforms (Lillis et al., 2018; Luczkovich and Sprague, 2022).

In 2017, a research project focusing on coral reef soundscapes off Sesoko Island in Okinawa, Japan, was initiated for the observation of shallow-water and mesophotic coral ecosystems (Lin et al., 2021). The shallow-water site is on Sesoko Island's southeast shore, where a flat reef dominated by tabular *Acropora* corals is located (Singh et al., 2022). Two other deeper sites are close to a large mesophotic ecosystem located on a flat plateau north of Sesoko Island (Sinniger et al., 2022).

To map the spatial variation of coral reef soundscapes, a Towed Aquafeeler recording system (AquaSound, Kobe, Japan) was towed behind a tandem kayak (Figure 4b). Due to their low-noise characteristic, kayaks provide suitable research platforms for mapping the distribution of soniferous animals such as snapping shrimp and damselfish. In addition, AUSOMS-mini stereo recorders (AquaSound, Kobe, Japan) were used to monitor the soundscape phenology patterns of shallow-water and mesophotic reefs (Figure 4c). After initial success with soundscape monitoring, SoundTrap 300 STD recorders (Ocean Instruments, Auckland, New Zealand) were used for the long-term monitoring of coral reef soundscapes after the summer of 2018 (Figure 4d).

These autonomous recording devices generated a substantial amount of acoustic data that reflect the spatiotemporal dynamics of coral reef soundscapes (approximately one terabyte of audio recordings per year for one recording site using a sampling frequency of 48 kHz and a recording duty cycle of 5 min every 10 min). Because of their long temporal coverage and high-resolution sampling, soundscape recordings can fill observation gaps caused by poor weather conditions, thereby serving as a complementary tool to other survey methods. Monitoring soundscapes also offers a data-driven approach to acoustically observing difficult-to-reach coral reefs at mesophotic depths.

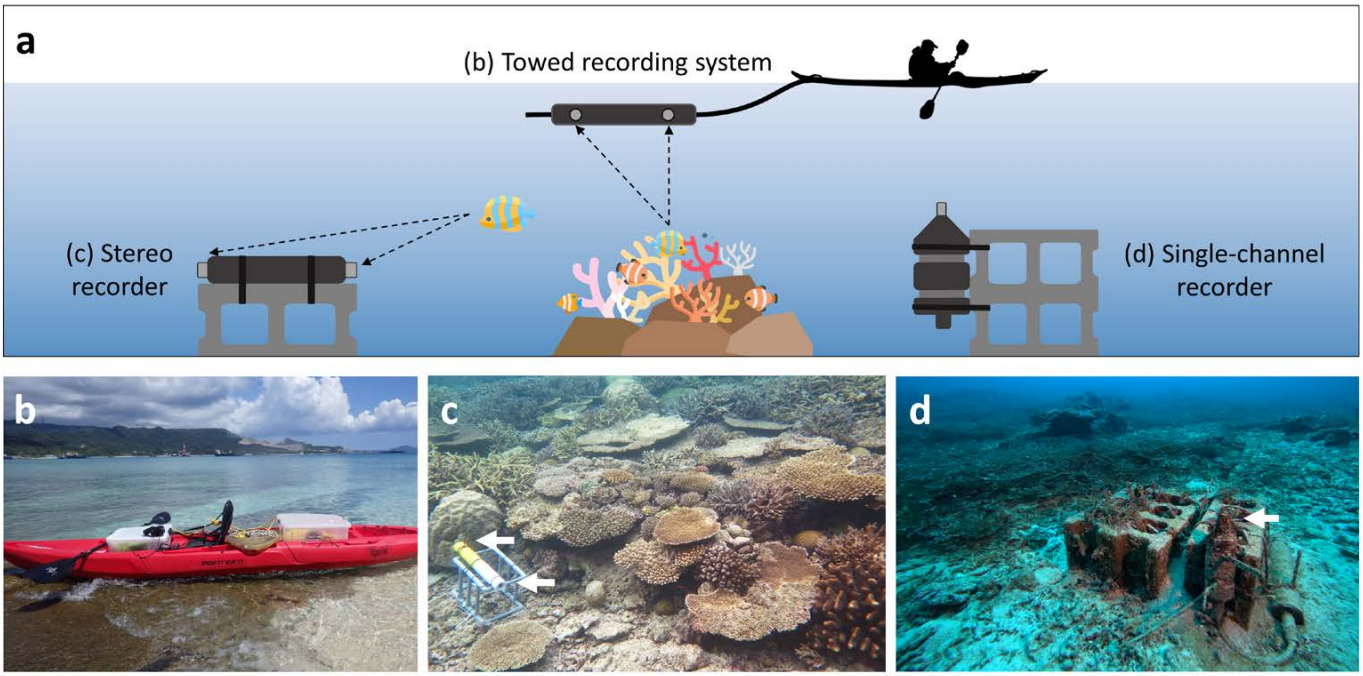

FIGURE 4. Examples of soundscape monitoring methods. (a) An illustration shows the three recording systems used in Sesoko Island waters. While single-channel audio recordings only provide time-series data, stereo recordings can generate additional information about the time difference of arrival between two hydrophones (dashed arrows), allowing the spatial distribution of soniferous animals to be studied. (b) The kayak used for towing an underwater sound recording system. (c) An AUSOMS-mini stereo recorder deployed at the shallow-water site (3 m depth). (d) A SoundTrap ST300 recorder deployed at the mesophotic site (40 m depth). Arrows in the field photos indicate hydrophone positions.

ANALYZING SOUNDSCAPE DYNAMICS

Advances in audio signal processing have enabled the application of long-term spectrograms for visualizing long-duration recordings, so that researchers can inspect soundscape changes in time and frequency domains without listening to the entire audio data set (Lin et al., 2021). This approach provides an intuitive method for comparing soundscapes from different coral reefs or environmental conditions. For example, long-term spectrograms showed that snapping shrimp sounds were predominant at shallow-water reefs (Figure 5a), but fish choruses and shipping noise were the primary contributors to the soundscapes of mesophotic reefs in Sesoko Island waters (Figure 5b).

Identifying the occurrence of biophony, geophony, and anthropophony is essential for using soundscapes to assess ecological and social processes. To analyze soundscape dynamics, we used soundscape_IR, an open-source Python toolbox for soundscape information retrieval (Sun et al., 2022), to perform source separation on long-term spectrograms. Because biological choruses, shipping noise, and wave noise have distinct diurnal and seasonal patterns in long-term spectrograms, a source separation model can effectively learn source-specific temporal activations and calculate their relative intensities. Soundscape recordings can therefore be converted into metrics that describe temporal variations in biophony, geophony, and anthropophony.

Use of soundscapes in marine biodiversity assessment is a rapidly developing field. In addition to the techniques of long-term spectrogram and source separation, there are ongoing efforts to identify marine animal sounds by leveraging artificial intelligence (Mooney et al., 2020). Although acoustics-based species identification remains challenging due to the lack of a comprehensive reference library for marine animal vocalizations (Parsons et al., 2022), digitally stored audio recordings can still be revisited in the future when better techniques are available.

SOUNDSCAPE DYNAMICS REVEAL SOCIAL-ECOLOGICAL CHANGES

Using the techniques of long-term spectrogram and source separation (Lin et al., 2021), we visualized the changes in biological chorus, anthropogenic noise, and environmental noise off Sesoko Island from October 2018 to May 2021 (Figure 6a–c). With the three acoustic dimensions, we observed the broad range of uses of soundscapes to study coral reef social-ecological systems. According to the diurnal and seasonal variations in biological choruses, the activities of soniferous animals were mainly influenced by daylight hours and seasonal environments. In addition, a diverse array of nighttime fish choruses was detected annually from May to August, with intensities that varied with the tide (Figure 6a). These phenological patterns can stimulate new insights into the ecology of reef fauna, such as diel feeding behavior, lunar synchronization in reproduction, and seasonal recruitment—ecological processes that are key to understanding the dynamics of coral reef biodiversity.

During the 2019 Golden Week—one of the busiest Japanese holiday seasons—coral reef soundscapes off Sesoko Island were heavily influenced by shipping noise,

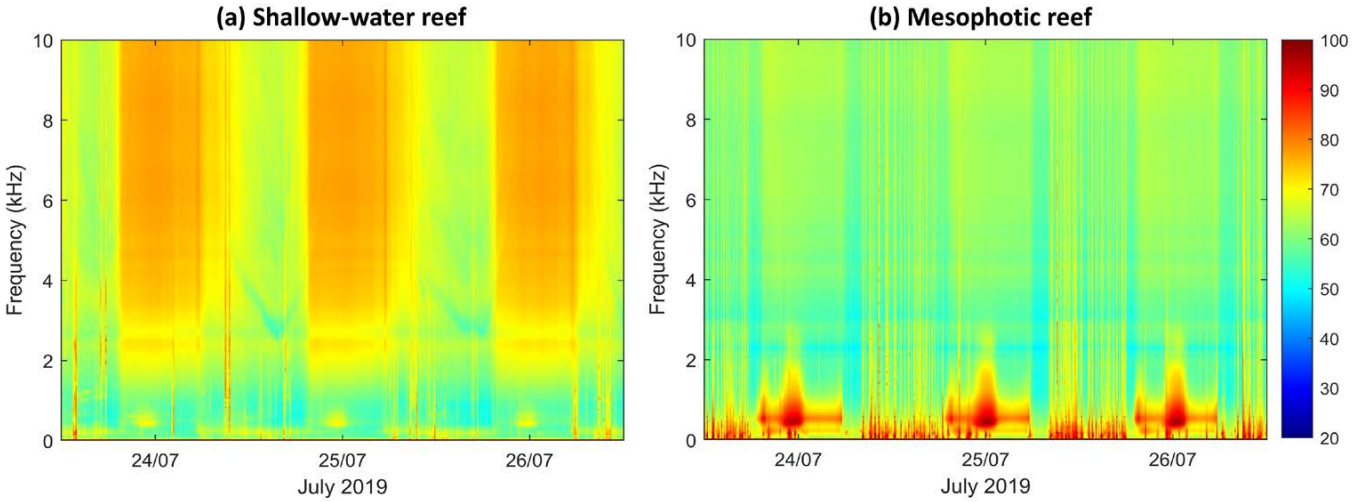

FIGURE 5. Visualization of coral reef soundscapes off Sesoko Island using long-term spectrograms. (a) The soundscapes of shallow-water reefs, such as this one, are dominated by high-frequency snapping sounds produced by crustaceans. (b) In contrast, the soundscapes of mesophotic reefs are characterized by low-frequency fish choruses at night and by shipping noise during the day. Colors of the long-term spectrograms represent the median power spectral densities measured every 10 minutes.

particularly that produced by daytime ferries transporting large numbers of tourists (Figure 6d). In comparison, the noise produced by ferries and fishing vessels was reduced during the 2020 Golden Week when the first nationwide pandemic state of emergency was announced (Figure 6e). The observed change in soundscapes reflects the unprecedented situation faced by local communities due to the COVID-19 pandemic and related lockdown directives. During the COVID-19 anthropause (Rutz et al., 2020), new fish sounds were detected in the nighttime chorus. Although we cannot be sure whether the change was a direct response to reduced noise, the high-resolution acoustic data offer unique opportunities to investigate potential interactions between social and ecological networks.

Coral reefs in subtropical waters are subject to seasonal disturbances. The variation in environmental noise clearly shows that coral reefs in Okinawa waters are affected by two annual periods of higher sea state: the summer typhoon season and the winter monsoon season (Figure 6c). Depending on the intensity and size of a typhoon, high-intensity waves can significantly elevate noise levels (Figure 6f). For typhoons that had severe impacts, biological choruses and anthropogenic noise were reduced in post-typhoon periods, a finding that likely reflects the social-ecological response to deteriorating

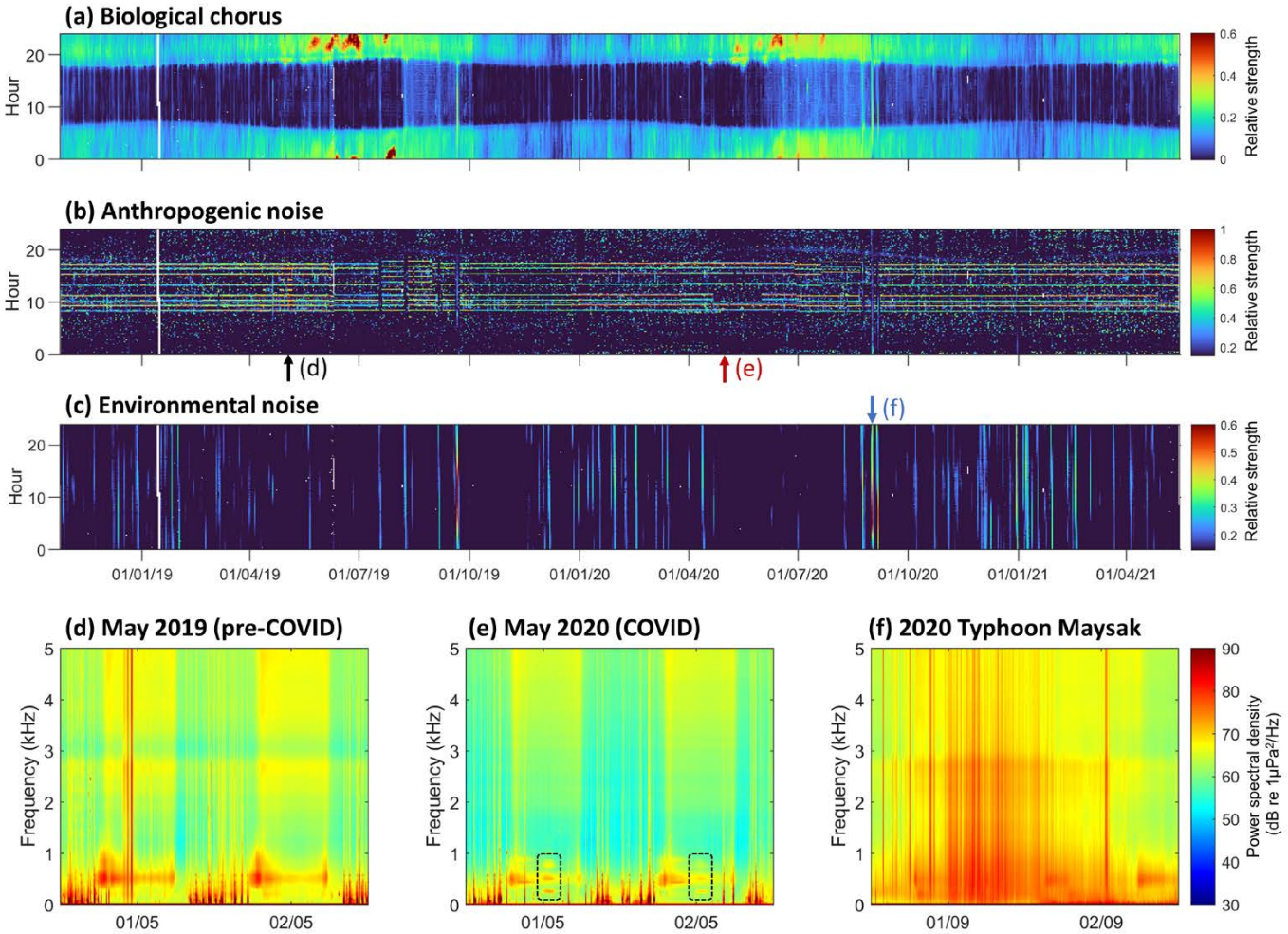

FIGURE 6. Dynamic soundscapes from a coral reef site at 20 m depth off Sesoko Island from October 2018 to May 2021. (a) Biological choruses displayed marked diurnal and seasonal variations. Particularly in warm seasons, more nighttime fish choruses were recorded, and their intensities varied with tidal and lunar phases. (b) Noise events that regularly occurred between 8 a.m. and 6 p.m. were associated with ferries. Other noise events were attributed to fishing vessels, tugboats, and freight ships. (c) Wind and wave noises were mainly produced during typhoon season (June–September) and northeastern monsoon season (December–March). Colors represent the relative strength of each sound source. The arrows indicate the dates corresponding to the long-term spectrograms of (d) the 2019 Golden Week holiday, (e) the first nationwide state of emergency in 2020, and (f) September 1, 2020, when Typhoon Maysak was closest to Okinawa Island. Dashed squares indicate the new type of fish chorus detected during the COVID-19 anthropause. Colors of the long-term spectrograms represent the median power spectral densities measured every 10 min.

ocean conditions. Furthermore, environmental noise during the winters of 2018–2021 showed an annual increase in monsoon-induced wave noise, which is consistent with Okinawa's long-term wind records (Singh et al., 2022). Although monsoon effects on subtropical coral reefs are rarely discussed, information on environmental noise can foster an understanding of regional climate conditions that will support future investigations regarding the adaptation of coral reef biodiversity in response to the changing climate.

LISTENING TO THE OCEAN FOR BETTER CONSERVATION PLANNING

Although current research on coral reef soundscapes is still in its infancy, the emerging potential of acoustic tools for revealing ecological and anthropogenic dynamics in marine ecosystems holds promise for improving the management of coral reef social-ecological systems. One potential method is to use soundscapes as underwater sensing platforms to assess the effects of environmental and anthropogenic stressors on coral reef ecosystems; effects of interest include the decline of biotic sounds in response to increasing fishing and tourist activities, and the recovery of acoustic activity after bleaching events or oil spills (Mooney et al., 2020). Audio recordings alone cannot document every social-ecological process, but they can still provide managers and social actors with acoustic indicators of ecosystem dynamics useful for decision-making. For example, the long-term soundscape monitoring of coral reefs could help identify changes in reef ecosystem health and biodiversity, providing early warning signs of reef degradation to managers, who can then take appropriate action to restrict human activities and plan restoration strategies.

Another method by which conservation management may be improved is tracking changes in coral reef soundscapes over multiple sites (Lin et al., 2021; Lamont et al., 2022b). Under the impact of ocean warming, global shallow-water coral reefs are expected to become substantially degraded. Mapping the spatial heterogeneity of soundscapes could facilitate the identification of coral reefs less susceptible to recurrent bleaching events and those in deeper areas that serve as refuges for shallow-water reef animals. With further work to demonstrate the use of soundscapes in predicting reef degradation and recovery processes, this acoustic technique may provide a more efficient method for assessing climate impacts on global coral reefs and guiding future research and conservation investments.

Using soundscapes to identify the sources of anthropogenic noise and its distribution may also improve marine spatial planning (Williams et al., 2015). For example, if frequent noise from shipping traffic is detected in a marine protected area, it may be necessary to rearrange shipping routes or implement speed limits to reduce noise that interferes with marine fauna within the protected area (Nedelec et al., 2022). In addition, monitoring soundscapes offers opportunities to gather evidence of illegal extraction activities, such as blast fishing. Such information is critical for guiding enforcement decisions, particularly in remote areas where patrolling efforts are limited.

In the Anthropocene, anthropogenic noise has become a global-scale pollutant that may broadly impact marine life at all trophic levels (Duarte et al., 2021). Despite efforts to restore coral reef biodiversity, results may be compounded by pervasive underwater noise (Ferrier-Pagès et al., 2021). Global research on how social development alters coral reef soundscapes and approaches for conserving soundscapes are therefore critical for meeting the Target 14.1 Sustainable Development Goal.

We urge the establishment of a global collaborative monitoring network of soundscapes to develop broader managing strategies for coral reef conservation. This is in line with the scientific need to measure essential ocean variables recently outlined by the Global Ocean Observing System (Howe et al., 2019). Furthermore, such a global soundscape monitoring network will be essential for a more comprehensive understanding of ecosystem dynamics—a critical step toward effective prediction of how climate change and social development impact coral reef social-ecological systems.

SUPPLEMENTARY MATERIALS

The supplementary materials are available online at https://doi.org/10.5670/oceanog.2023.s1.7.

REFERENCES

Anker, A., S.T. Ahyong, P.Y. Noel, and A.R. Palmer. 2006. Morphological phylogeny of Alpheid shrimps: Parallel preadaptation and the origin of a key morphological innovation, the snapping claw. *Evolution* 60(12):2,507–2,528, https://doi.org/10.1111/j.0014-3820.2006.tb01886.x.

Cheal, A.J., M.A. MacNeil, M.J. Emslie, and H. Sweatman. 2017. The threat to coral reefs from more intense cyclones under climate change. *Global Change Biology* 23(4):1,511–1,524, https://doi.org/10.1111/gcb.13593.

Duarte, C.M., L. Chapuis, S.P. Collin, D.P. Costa, R.P. Devassy, V.M. Eguiluz, C. Erbe, T.A.C. Gordon, B.S. Halpern, H.R. Harding, and others. 2021. The soundscape of the Anthropocene ocean. *Science* 371(6529):eaba4658, https://doi.org/10.1126/science.aba4658.

Erisman, B.E., and T.J. Rowell. 2017. A sound worth saving: Acoustic characteristics of a massive fish spawning aggregation. *Biology Letters* 13(12):20170656, https://doi.org/10.1098/rsbl.2017.0656.

Ferrier-Pagès, C., M.C. Leal, R. Calado, D.W. Schmid, F. Bertucci, D. Lecchini, and D. Allemand. 2021. Noise pollution on coral reefs? — A yet underestimated threat to coral reef communities. *Marine Pollution Bulletin* 165:112129, https://doi.org/10.1016/j.marpolbul.2021.112129.

Howe, B.M., J. Miksis-Olds, E. Rehm, H. Sagen, P.F. Worcester, and G. Haralabus. 2019. Observing the oceans acoustically. *Frontiers in Marine Science* 6:426, https://doi.org/10.3389/fmars.2019.00426.

Lamont, T.A.C., L. Chapuis, B. Williams, S. Dines, T. Gridley, G. Frainer, J. Fearey, P.B. Maulana, M.E. Prasetya, J. Jompa, and others. 2022a. HydroMoth: Testing a prototype low-cost acoustic recorder for aquatic environments. *Remote Sensing in Ecology and Conservation* 8(3):362–378, https://doi.org/10.1002/rse2.249.

Lamont, T.A.C., B. Williams, L. Chapuis, M.E. Prasetya, M.J. Seraphim, H.R. Harding, E.B. May, N. Janetski, J. Jompa, D.J. Smith, and others. 2022b. The sound of recovery: Coral reef restoration success is detectable in the soundscape. *Journal of Applied Ecology* 59(3):742–756, https://doi.org/10.1111/1365-2664.14089.

Lillis, A., F. Caruso, T.A. Mooney, J. Llopiz, D. Bohnenstiehl, and D.B. Eggleston. 2018. Drifting hydrophones as an ecologically meaningful approach to underwater soundscape measurement in coastal benthic habitats. *Journal of Ecoacoustics* 2(1):3, https://doi.org/10.22261/JEA.STBDH1.

Lin, T.-H., T. Akamatsu, F. Sinniger, and S. Harii. 2021. Exploring coral reef biodiversity via underwater soundscapes. *Biological Conservation* 253:108901, https://doi.org/10.1016/j.biocon.2020.108901.

Luczkovich, J.J., and M.W. Sprague. 2022. Soundscape maps of sonif-erous fishes observed from a mobile glider. *Frontiers in Marine Science* 9:779540, https://doi.org/10.3389/fmars.2022.779540.

Mooney, T.A., L. Di Iorio, M. Lammers, T.-H. Lin, S.L. Nedelec, M. Parsons, C. Radford, E. Urban, and J. Stanley. 2020. Listening forward: Approaching marine biodiversity assessments using acoustic methods. *Royal Society Open Science* 7(8):201287, https://doi.org/10.1098/rsos.201287.

Nedelec, S.L., A.N. Radford, P. Gatenby, I.K. Davidson, L. Velasquez Jimenez, M. Travis, K.E. Chapman, K.P. McCloskey, T.A.C. Lamont, B. Illing, and others. 2022. Limiting motorboat noise on coral reefs boosts fish reproductive success. *Nature Communications* 13(1):2822, https://doi.org/10.1038/s41467-022-30332-5.

Parsons, M.J.G., T.-H. Lin, T.A. Mooney, C. Erbe, F. Juanes, M. Lammers, S. Li, S. Linke, A. Looby, S.L. Nedelec, and others. 2022. Sounding the call for a global library of underwater biological sounds. *Frontiers in Ecology and Evolution* 10:810156, https://doi.org/10.3389/fevo.2022.810156.

Pieretti, N., and R. Danovaro. 2020. Acoustic indexes for marine biodiversity trends and ecosystem health. *Philosophical Transactions of the Royal Society B: Biological Sciences* 375(1814):20190447, https://doi.org/10.1098/rstb.2019.0447.

Rutz, C., M.-C. Loretto, A.E. Bates, S.C. Davidson, C.M. Duarte, W. Jetz, M. Johnson, A. Kato, R. Kays, T. Mueller, and others. 2020. COVID-19 lockdown allows researchers to quantify the effects of human activity on wildlife. *Nature Ecology & Evolution* 4(9):1,156–1,159, https://doi.org/10.1038/s41559-020-1237-z.

Simmons, K.R., D.B. Eggleston, and D.R. Bohnenstiehl. 2021. Hurricane impacts on a coral reef soundscape. *PLoS ONE* 16(2):e0244599, https://doi.org/10.1371/journal.pone.0244599.

Simpson, S.D., M. Meekan, J. Montgomery, R. McCauley, and A. Jeffs. 2005. Homeward sound. *Science* 308(5719):221–221, https://doi.org/10.1126/science.1107406.

Singh, T., F. Sinniger, Y. Nakano, S. Nakamura, S. Kadena, M. Jinza, H. Fujimura, and S. Harii. 2022. Long-term trends and seasonal variations in environmental conditions in Sesoko Island, Okinawa, Japan. *Galaxea, Journal of Coral Reef Studies* 24(1):121–133, https://doi.org/10.3755/galaxea.G2021_S14O.

Sinniger, F., R.L. Albelda, R. Prasetia, H. Rouzé, E.D. Sitorus, and S. Harii. 2022. Overview of the mesophotic coral ecosystems around Sesoko Island, Okinawa, Japan. *Galaxea, Journal of Coral Reef Studies* 24(1):69–76, https://doi.org/10.3755/galaxea.G2021_S11N.

Sun, Y.-J., S.-C. Yen, and T.-H. Lin. 2022. soundscape_IR: A source separation toolbox for exploring acoustic diversity in soundscapes. *Methods in Ecology and Evolution* 13(11):2,347–2,355, https://doi.org/10.1111/2041-210X.13960.

Tricas, T.C., and K.S. Boyle. 2014. Acoustic behaviors in Hawaiian coral reef fish communities. *Marine Ecology Progress Series* 511:1–16, https://doi.org/10.3354/meps10930.

Williams, R., C. Erbe, E. Ashe, and C.W. Clark. 2015. Quiet(er) marine protected areas. *Marine Pollution Bulletin* 100(1):154–161, https://doi.org/10.1016/j.marpolbul.2015.09.012.

ACKNOWLEDGMENTS

This work was supported by the Japan Society for the Promotion of Science KAKENHI (Grants JP17H00799, JP20K06210 and JP21H04943), the Sesoko CREST field campaign from the Japan Science and Technology Agency, and the National Science and Technology Council, Taiwan (Grants MOST 109-2621-B-001-007-MY3 and NSTC 111-2740-M-001-004). We are grateful to the reviewers for providing constructive comments, which improved an earlier version of this manuscript.

ARTICLE DOI. https://doi.org/10.5670/oceanog.2023.s1.7

Functional Seascapes: Understanding the Consequences of Hypoxia and Spatial Patterning in Pelagic Ecosystems

By Stephen B. Brandt, Sarah E. Kolesar, Cassandra N. Glaspie, Arnaud Laurent, Cynthia E. Sellinger, James J. Pierson, Michael R. Roman, and William C. Boicourt

With greater nutrient loading and seasonal water column stratification, dissolved oxygen has been declining in many of the world's coastal areas, and climate warming is likely to exacerbate this problem (e.g., Roman et al., 2019, and references cited therein). Low dissolved oxygen or hypoxia can profoundly affect a fish's growth, survival, and reproductive success, but tolerances to low dissolved oxygen differ across species. The level of hypoxic stress is also dependent on ambient water temperatures and prey availability. A fundamental challenge to fisheries management is to understand how hypoxia affects fish under different environmental conditions. In this paper, we introduce a new approach to assessing the impacts of hypoxia on fish that can be used to compare impacts among species as well as across other physical, biological, and chemical gradients and in response to environmental change.

FUNCTIONAL SEASCAPES

A seascape shows the spatial patterning of the ocean's physical, chemical, and biological characteristics, regardless of its value to any particular species. Seascapes have been shown to be highly patchy, complex, and dynamic, which has challenged our ability to understand biological impacts. Here, we introduce the concept of a "functional seascape" that maps the spatial patterning of the specific biological responses (e.g., growth rate, survival rate, reproductive success, metabolic rate, activity) of a particular species to observed abiotic and biotic conditions. Functional seascapes must be defined for individual species because biological and ecological rates differ across species. Spatially explicit modeling, that is, modeling where the exact location of a variable (e.g., temperature, salinity, dissolved oxygen) matters to the process being modeled, provides the tools to produce these functional seascapes at the same high resolution as the observed ocean conditions. It also offers a first-order view of habitat quality based on the fundamental responses of a fish species to its environment.

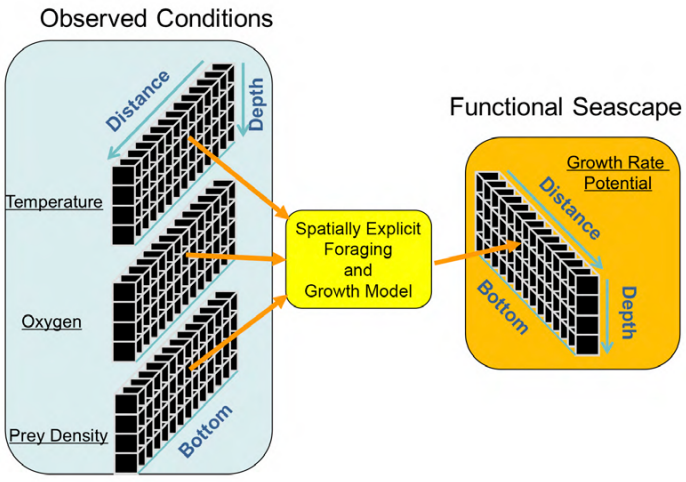

FIGURE 1. Process for deriving a functional seascape (depicted by fish growth rate) based on underlying conditions. Species-specific, spatially explicit models are run in each cell to calculate how well the fish would grow at the observed (or modeled) conditions in each cell.

To illustrate this approach, we use fish growth rate potential (GRP), which calculates how well a particular species of fish would grow based on its bioenergetics capabilities and grown in the prevailing environmental conditions. Growth rate is a critical factor for fish and directly corresponds to survival rates and reproductive success. It is generally considered a valid measure of fish habitat quality. The metabolic processes that regulate growth in fish are often nonlinear responses to physical and biological conditions; thus, growth rates must be assessed at the same spatial and temporal scales as the underlying patterns. Growth rate potential maps are derived using species-specific, spatially explicit modeling driven by spatial patterns in temperature, oxygen, and prey densities (Figure 1).

CASE STUDY: HYPOXIA IN THE NORTHERN GULF OF MEXICO

The Northern Gulf of Mexico (NGOMEX) is one of the largest and most well-known hypoxic regions, characterized by extensive bottom hypoxia driven by nutrient loading from the Mississippi River watershed. We have been using functional seascapes of GRP to better understand how hypoxia affects fish in the region and to predict how proposed reductions in nutrient loading might affect both hypoxia and the lower-level production that fuels fish production.

High-Resolution Spatial Mapping

Seascapes were directly mapped by running a series of ship-based transects across the NGOMEX during summer when hypoxia is most severe (Figure 2a,b). We measured temperature, salinity, oxygen, phytoplankton, zooplankton, and fish prey densities at high spatial resolution throughout the water column. A Scanfish (Figure 2c) that undulated from near surface to near bottom was instrumented with a CTD, an optical dissolved oxygen sensor, a

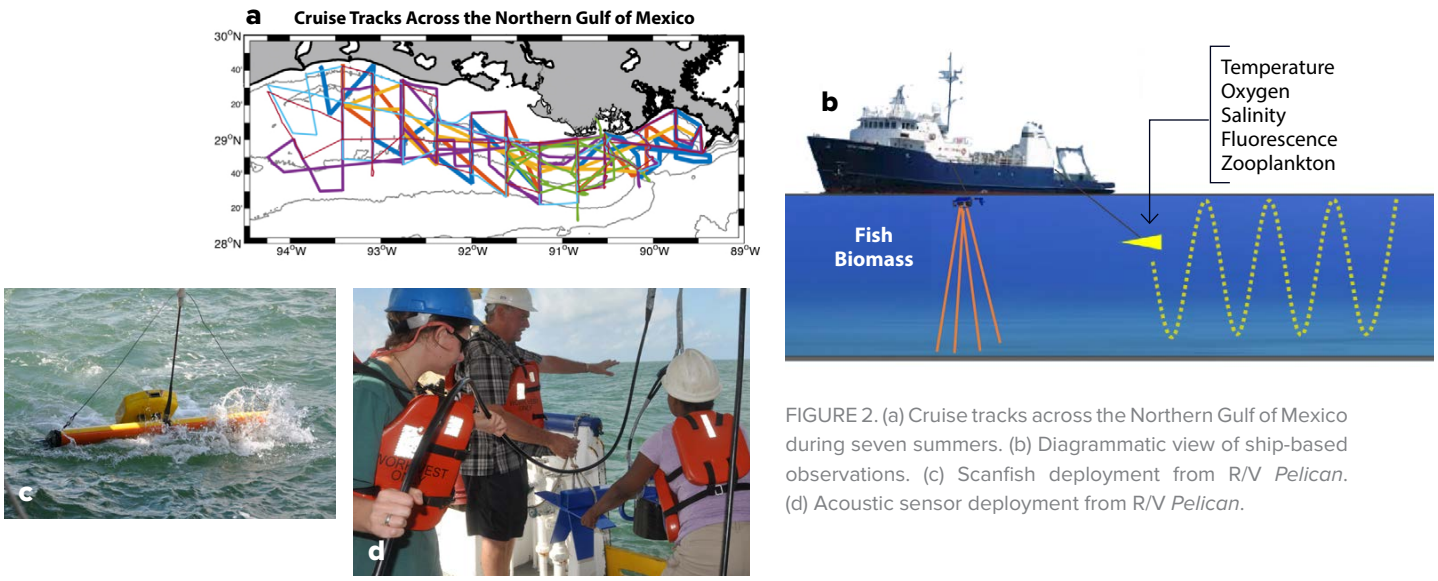

FIGURE 2. (a) Cruise tracks across the Northern Gulf of Mexico during seven summers. (b) Diagrammatic view of ship-based observations. (c) Scanfish deployment from R/V *Pelican*. (d) Acoustic sensor deployment from R/V *Pelican*.

fluorometer, and an optical zooplankton counter. At the same time, prey fish biomass densities and sizes were measured using a calibrated, dual-frequency, split-beam acoustic sensor (Figure 2d) towed near the surface.

We subdivided observed data taken along individual transects into uniform spatial cells and calculated expected growth rate in each cell based on species-specific bioenergetics and foraging models (see Hartman and Brandt, 2011, and Zhang et al., 2014). This spatially explicit modeling approach produces functional seascapes of GRPs for each species along the length of the transect.

Figure 3 is an example taken from a single NGOMEX transect. The high-resolution dissolved oxygen, temperature, and prey density data collected were used to assess the GRP spatial patterns of two piscivores—adult bluefish, *Pomatomus saltatrix*, and striped bass, *Morone saxatilis.* As expected, the GRPs of these species responded quite differently to the same hypoxic conditions due to their different bioenergetics requirements (Hartman and Brandt, 2011) and to their high dependence on prevailing water temperatures and prey densities. Striped bass grew poorly in most conditions because they feed less or not at all under higher temperatures regardless of food availability. These results demonstrate that some differences in underlying structure may have biological significance while others do not. Overall growth responses can be now be summarized in various ways, such as the proportion of water supporting positive growth at different levels of hypoxia.

Hydrodynamic Water Quality Model

Ship-based observations only provide localized snapshots of seascapes during summer. We used a three-dimensional hydrodynamic water quality model to map functional seascapes across the entire NGOMEX region to predict the combined impacts of proposed nutrient reductions and changes in hypoxia. Regional circulation, water temperature, dissolved oxygen, phytoplankton, and zooplankton concentrations were simulated using a high-resolution implementation of the Regional Ocean Modeling System coupled with a biogeochemical model with 10 state variables (Laurent et al., 2017). The model has 163,840 cells and was run daily over 2000–2016, producing nearly a billion cells for each simulation. We predicted daily GRP for different species in each of these cells for each day under current nutrient loadings, and with 20% and 40% reductions in nutrient loadings.

Figure 4 shows the functional seascape on a single day for red snapper, *Lutijanus campechanus*, (with stable food supply) across the bottom during August 2004 and for a pelagic zooplankter, anchovy, *Anchoa mitchilli*, across the surface during June 2014. Red snapper showed some

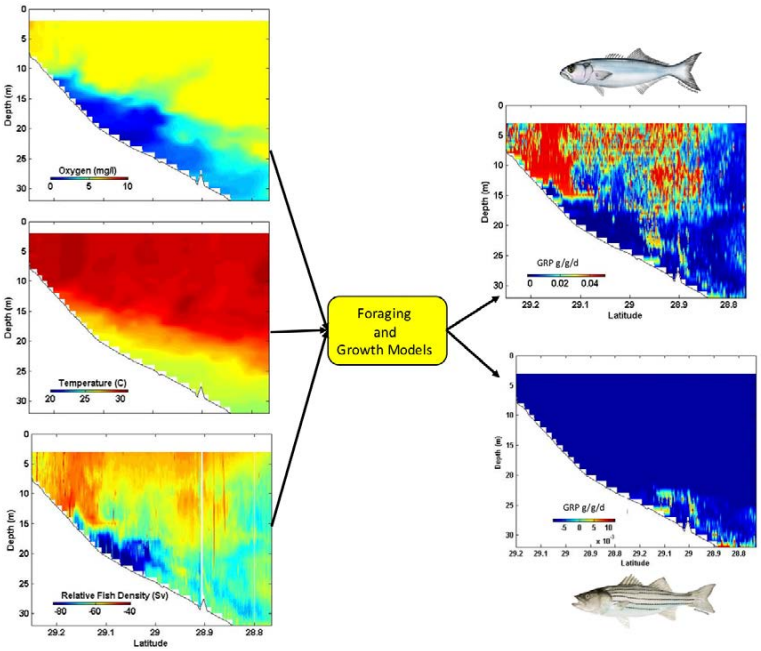

FIGURE 3. Dissolved oxygen, temperature, and fish prey density, along with resultant growth rate potentials for adult bluefish and striped bass across a transect in the Northern Gulf of Mexico.

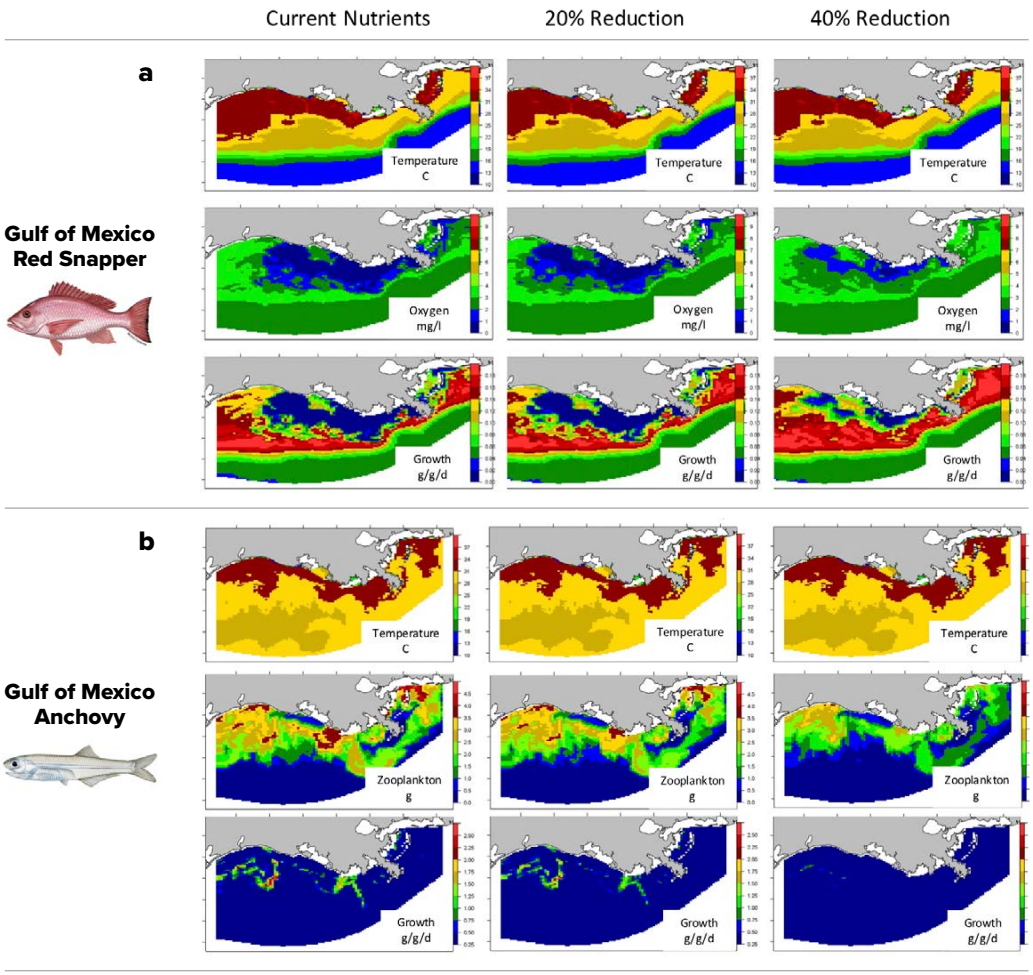

FIGURE 4. Northern Gulf of Mexico regional maps of (a) temperature, oxygen, and growth rate potential of red snapper across the bottom during August 2004, modeled for current nutrient loadings and 20% and 40% reductions in nutrient loadings. (b) Temperature, zooplankton abundance, and growth rate potential of anchovy (see Zhang et al., 2014, for equations) across the surface during June 2014 for current nutrient loadings, and 20% and 40% reduction in nutrient loadings.

improvements in growth in response to reduced bottom hypoxia during summer (Figure 4a). In contrast, anchovy showed poorer growth in spring because prey resources were reduced with lower nutrient inputs (Figure 4b). Overall, results suggest that fish growth responses to improvements in hypoxia may be dampened by lowered trophic level production, but responses were complex, highly variable from year-to-year, and species-specific.

APPLICATIONS AND FUTURE DIRECTIONS

Functional seascapes provide a new framework for viewing and understanding the biological significance of spatial patterning in the ocean by directly linking underwater observations to fishes' vital habitat needs. The approach demonstrated that the same underlying hypoxic conditions can produce consequences that differ dramatically across species and that other factors such as water temperature and food are fundamentally important to these evaluations. The wider use of functional seascapes may help us to (1) better display direct impacts of ocean conditions on fish, (2) identify critical habitats and potential competitors (e.g., overlapping areas of high growth rate potential), (3) better predict how a species might respond to changing environmental conditions such as climate change, and (4) develop more meaningful scaling of spatially complex ocean conditions.

REFERENCES

Hartman, K.J., and S.B. Brandt. 2011. Predatory demand and impact of striped bass, bluefish, and weakfish in the Chesapeake Bay: Applications of bioenergetics models. *Canadian Journal of Fisheries and Aquatic Sciences* 52(8):1,667–1,678, https://doi.org/10.1139/f95-760.

Laurent, A., K. Fennel, W.-J. Cai, W.-J. Huang, L. Barbero, and R. Wanninkhof. 2017. Eutrophication-induced acidification of coastal waters in the northern Gulf of Mexico: Insights into origin and processes from a coupled physical-biogeochemical model. *Geophysical Research Letters* 44:946–956, https://doi.org/10.1002/2016GL071881.

Roman, M.R., S.B. Brandt, E.D. Houde, and J.J. Pierson. 2019. Interactive effects of hypoxia and temperature on coastal pelagic zooplankton and fish. *Frontiers in Marine Science* 6:139, https://doi.org/10.3389/fmars.2019.00139.

Zhang, H., S.A. Ludsin, D.M. Mason, S.B. Brandt, C.A. Stow, A.T. Adamack, X. Zhang, D.G. Kimmel, M.R. Roman, and W.C. Boicourt. 2014. Effects of hypoxia on habitat quality of pelagic planktivorous fishes in the northern Gulf of Mexico. *Marine Ecology Progress Series* 505:209–226, https://doi.org/10.3354/meps10768.

ACKNOWLEDGMENTS

We thank our sponsors NOAA-CSCOR NGOMEX, the National Science Foundation, the National Academy of Sciences, and the numerous colleagues that helped us collect data at sea aboard R/V *Pelican*.

ARTICLE DOI. https://doi.org/10.5670/oceanog.2023.s1.8

Recent Marine Heatwaves Affect Marine Ecosystems from Plankton to Seabirds in the Northern Gulf of Alaska

By Suzanne Strom and the Northern Gulf of Alaska Long-Term Ecosystem Research Team

INTRODUCTION

Several decades of research and monitoring in the northern Gulf of Alaska (NGA) have revealed climate-related shifts in ocean temperature and salinity. Accompanying these shifts have been changes in the abundance and diversity of species, from single-celled plankton to fish, seabirds, and marine mammals. Research is documenting long-term change in the region and revealing the mechanisms by which recent marine heatwaves affect the ability of higher trophic levels to survive in these waters. Heatwaves in the northern Gulf of Alaska are likely to become longer, more frequent, and more intense, making long-term monitoring of ecosystem changes critical to understanding and predicting effects on valuable commercial fisheries and culturally significant native harvesting. In addition, documentation of change is necessary for projecting regional and global future climate scenarios and for informing climate-related policy decisions.

Our multi-decade NGA program (Figure 1) encompasses physics, chemistry, plankton ecology, and seabirds, and links closely to larval and adult fish surveys conducted by NOAA's Alaska Fisheries Science Center. Our program has three primary research goals: (1) document long-term (multi-decadal) change in environmental properties and ecosystem structure, (2) describe ecosystem shifts engendered by disturbance events such as marine heatwaves, and (3) understand the processes by which ecosystem shifts relate to environmental forcing and influence species (including harvestable resources) at higher trophic levels.

BACKGROUND

The region's subarctic latitude and the passage of frequent energetic storms result in an NGA climate that is strongly seasonal and dynamic. Freshwater inputs from rain as well as the snowfields and glaciers that clothe the coastal mountain ranges (Figure 1) heavily influence oceanographic processes. The time- and space-varying intersection of iron-rich, lower salinity coastal waters and iron-limited offshore waters creates a mosaic of community types and productivity regimes. In addition, episodic zones of high production are formed by strong tidal currents interacting with rugged bathymetry, frontal zones associated with alongshore currents and river plumes, and mesoscale eddies that transit the region. Such complexity creates a variety of habitats, increasing system-wide biodiversity across communities from microbes to seabirds and marine mammals. The NGA hosts societally and commercially important fisheries, including finfish (e.g., salmon, pollock, Pacific and black cod) and shellfish (e.g., shrimp, crabs). Accordingly, the relationships among climate, environment, ecosystem-wide species composition, and production are of interest to fishers and management agencies as much as to oceanographers and ecologists.

Regular NGA observation began in 1970 with water column temperature and salinity profiles at a nearshore station (Figure 2). Biological and chemical observations, including nutrients, phytoplankton, zooplankton, and seabirds, commenced in the late 1990s when the program expanded to include a cross-shelf transect (the Seward Line) extending offshore into oceanic waters. In 2018,

FIGURE 1. Sampling the Northern Gulf of Alaska. (a) Bear Glacier and Kenai Mountains are the backdrop for deployment of the "iron fish." (b) Students collect water samples from the CTD. (c) A sediment trap is attached to a cable during mooring deployment. (d) A graduate student displays a giant jelly. (e) A Research Experiences for Undergraduates (REU) participant launches a drifter in the Copper River plume.

the NGA was added to the National Science Foundation's Long-Term Ecosystem Research (LTER) network, an exciting development that enlarges the scope of our observations and increases the potential for ecological insights through comparisons with a variety of ecosystems (https://nga.lternet.edu). The NGA LTER strives for inclusivity at all levels. To this end, we are actively implementing diversity, equity, and inclusion initiatives, including partnering with Alaska Native communities. Increasing the diversity of participants in science influences the range of questions asked and the interpretation of the data collected, and leads to more innovative outcomes (Phillips, 2014).

METHODS

We use a range of approaches to study the NGA, including at-sea sampling; remote observations from moorings, gliders, and satellites; and biophysical modeling. Sampling at sea occurs three times annually (spring, summer, and fall) for ocean physics, carbon cycle parameters including export flux and macro- and micronutrients, lower trophic level production rates and communities, and seabirds. Longer cruises allow for hypothesis testing through shipboard experiments (e.g., iron enrichment). These at-sea observations have been crucial for documenting ecosystem responses to recent marine heatwaves, as they allow detailed examination of community composition shifts and provide ground truth for models that project the effects of future warming.

FINDINGS

As in many biomes worldwide, there is long-term warming in the NGA (Danielson et al., 2022) as well as increased freshening of surface waters (Figure 2). Together, these trends have increased water column stratification. Two recent marine heatwaves (2014–2016 and 2019) tested the resilience of the ecosystem (Litzow et al., 2020; Suryan et al., 2021). Heatwave effects observed by our program include a reduced spring bloom (normally the greatest primary production pulse of the year) and shifts to smaller organisms at both the phytoplankton and microzooplankton trophic levels in spring (Figure 3). This had consequences for the dominant taxa of large-bodied copepods, whose spring lipid storage (which fuels fall-winter survival and reproduction) was reduced and/or required a longer duration of surface feeding. Euphausiids (krill) decreased drastically, and other programs reported similar declines for forage fish such as capelin, sand lance, and herring (Arimitsu et al., 2021).

In contrast, warmer conditions enhanced the survival of southern zooplankton species (including copepods and pyrosomes) that are transported into our region by the Alaska Gyre current system, so fall biodiversity increased at the mesozooplankton trophic level. Seabird responses also revealed "winners" and "losers." There was a huge die-off of common murres, normally one of the most abundant NGA species, in association with the 2015–2016 warm period, likely due to loss of their euphausiid and forage fish prey (Piatt et al., 2020). However, the abundance of planktivorous taxa such as kittiwakes and storm petrels increased over the mid and outer shelf (Cushing et al., in press). The altered food web conditions reduced finfish reproductive success and led to poor body condition in adults of many species. Subsequent recovery has been highly species dependent, indicating that the specifics of diet, reproductive strategy, metabolism, and behavior are crucial to heatwave resilience.

The multi-decadal length of NGA time series observations and records of known relationships among many

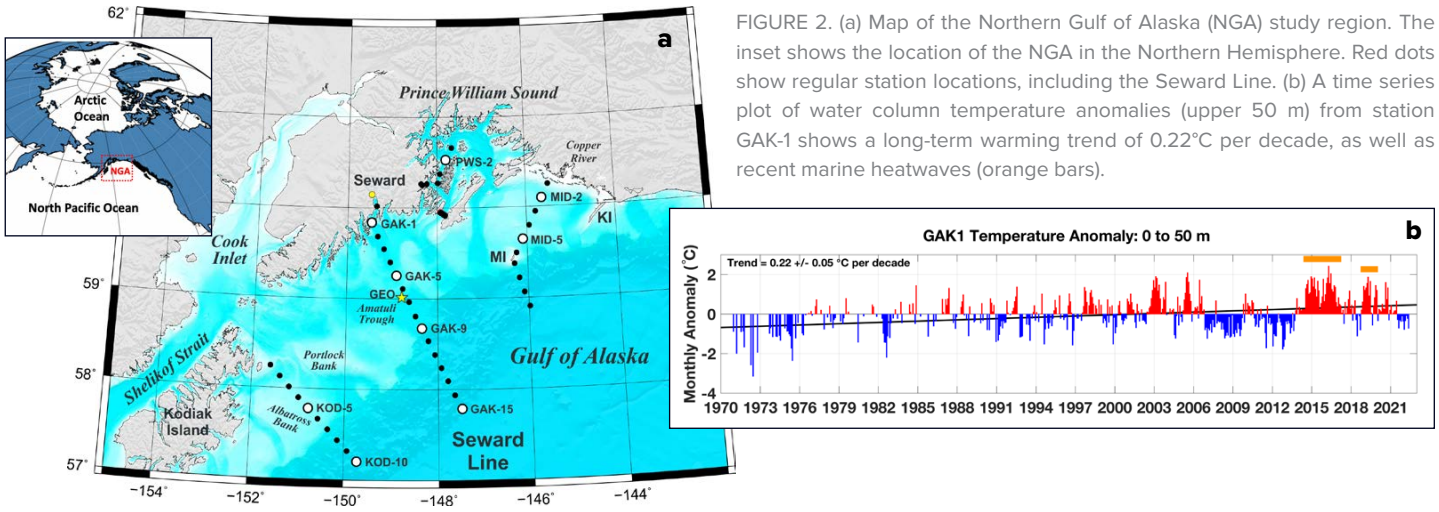

FIGURE 2. (a) Map of the Northern Gulf of Alaska (NGA) study region. The inset shows the location of the NGA in the Northern Hemisphere. Red dots show regular station locations, including the Seward Line. (b) A time series plot of water column temperature anomalies (upper 50 m) from station GAK-1 shows a long-term warming trend of 0.22°C per decade, as well as recent marine heatwaves (orange bars).

ecosystem components, and the occurrences of multiple heatwaves, have allowed development of indices from NGA annual data; these are used in NOAA's annual ecosystem assessment process, which directly informs management of NGA fisheries, including pollock, black and Pacific cod, and salmon (e.g., Ferris and Zador, 2021). As we emerge from our first phase as an LTER site, our burgeoning human resources and ecosystem knowledge should lead to better understanding of connections among environment, biota, and harvested resources.

REFERENCES

Arimitsu, M., J. Piatt, S. Hatch, R. Suryan, S. Batten, M. Bishop, R. Campbell, H. Coletti, D. Cushing, K. Gorman, and others. 2021. Heatwave-induced synchrony within forage fish portfolio disrupts energy flow to top pelagic predators. *Global Change Biology* 27:1,859–1,878, https://doi.org/10.1111/gcb.15556.

Cushing, D.A., K.J. Kuletz, L. Sousa, R.H. Day, S.L. Danielson, E.A. Labunski, and R.R. Hopcroft. In press. Differential response of seabird species to warm- and cold-water events in a heterogeneous cross-shelf environment in the Gulf of Alaska. *Marine Ecology Progress Series*.

Danielson, S.L., T.D. Hennon, D.H. Monson, R.M. Suryan, R.W. Campbell, S.J. Baird, K. Holderied, and T.J. Weingartner. 2022. Temperature variations in the northern Gulf of Alaska across synoptic to century-long time scales. *Deep Sea Research Part II* 203:10515, https://doi.org/10.1016/j.dsr2.2022.105155.

Ferris, B., and S. Zador. 2021. *Ecosystem Status Report 2021: Gulf of Alaska.* Stock Assessment and Fishery Evaluation Report, North Pacific Fishery Management Council, Anchorage, AK, 269 pp.

Litzow, M.A., M.E. Hunsicker, E.J. Ward, S.C. Anderson, J. Gao, S.J. Zador, S.D. Batten, S.C. Dressel, J.T. Duffy-Anderson, E. Fergusson, and others. 2020. Evaluating ecosystem change as Gulf of Alaska temperature exceeds the limits of preindustrial variability. *Progress in Oceanography* 186:102393, https://doi.org/10.1016/j.pocean.2020.102393.

Phillips, K.W. 2014. How diversity works. *Scientific American* 311:42–47, https://doi.org/10.1038/scientificamerican1014-42.

Piatt, J.F., J.K. Parrish, H.M. Renner, S.K. Schoen, T.T. Jones, M.L. Arimitsu, K.J. Kuletz, B. Bodenstein, M. Garcia-Reyes, R.S. Duerr, and others. 2020. Extreme mortality and reproductive failure of common murres resulting from the northeast Pacific marine heatwave of 2014–2016. *PLoS ONE* 15:e0226087, https://doi.org/10.1371/journal.pone.0226087.

Suryan, R.M., M.L. Arimitsu, H.A. Coletti, R.R. Hopcroft, M.R. Lindeberg, S.J. Barbeaux, S.D. Batten, W.J. Burt, M.A. Bishop, J.L. Bodkin, and others. 2021. Ecosystem response persists after a prolonged marine heatwave. *Scientific Reports* 11:6235, https://doi.org/10.1038/s41598-021-83818-5.

ARTICLE DOI. https://doi.org/10.5670/oceanog.2023.s1.9

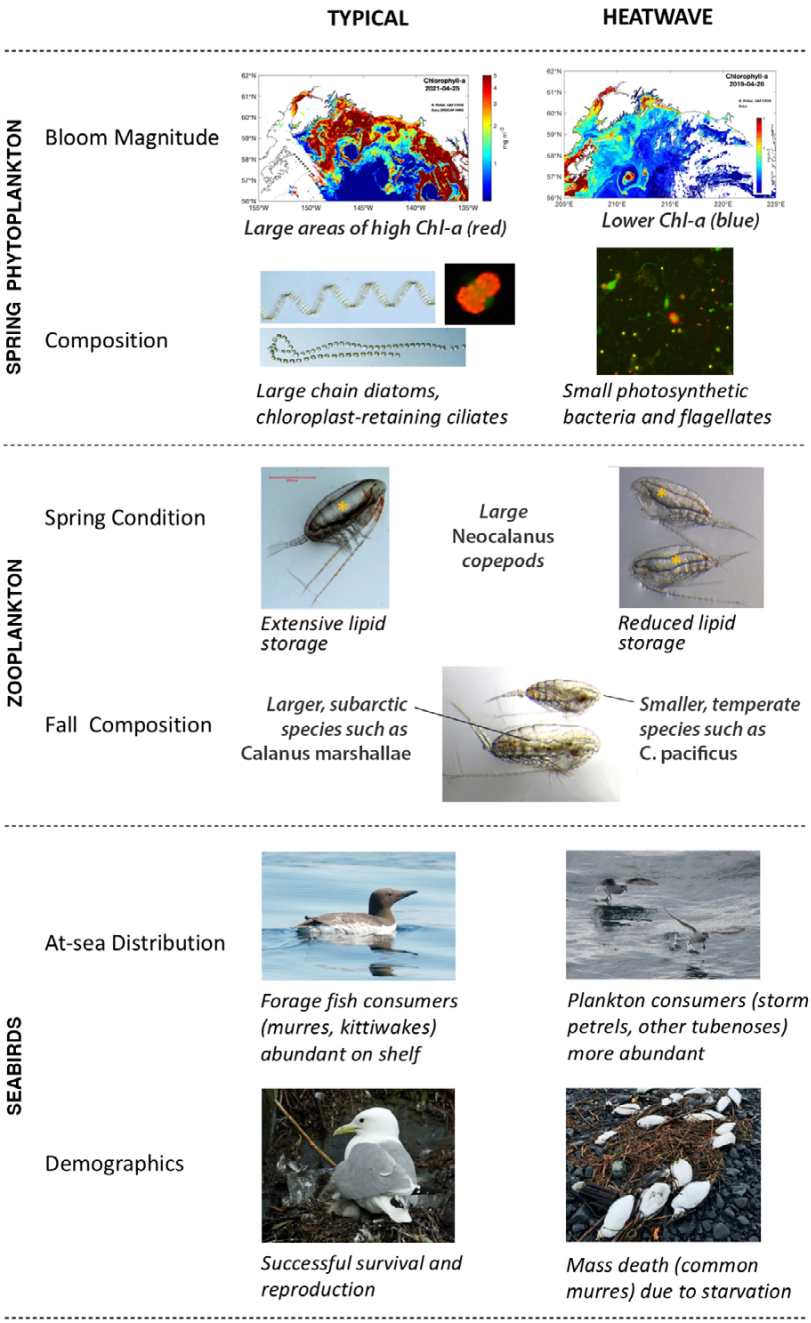

FIGURE 3. Heatwave effects contrasted with non-heatwave conditions for key ecosystem components, including phytoplankton, mesozooplankton, and seabirds. Chl-a = chlorophyl *a*, an indicator of phytoplankton biomass. Yellow asterisks in zooplankton panel indicate lipid storage bodies.

Modeling Aquaculture Suitability in a Climate Change Future

By Amy Leigh Mackintosh, Griffin Goldstein Hill, Mark John Costello, Alexander Jueterbock, and Jorge Assis

INTRODUCTION

Aquaculture has become the primary supplier of fish for human consumption, with production increasing every year since 1990 (FAO, 2020). At the same time, up to 89% of the world's capture fisheries are fully exploited, overexploited, or collapsed. While some fisheries may have increased yields due to climate change in the short term, global fisheries catch is projected to fall by 10% by 2050 (Barange et al., 2014; Ramos Martins et al., 2021). However, the security of aquaculture production will depend on how future climate change affects productive regions as species' optimal climatic conditions shift poleward (Chaudhary et al., 2021). This makes the forecasting of climate impacts on key aquaculture species a top priority in order to facilitate adaptation of this industry.

Simple climate metrics can provide valuable information on the potential impacts of climate change on biodiversity in the future. One such metric, climate velocity, uses an environmental variable, typically temperature, to track the rate and direction of climate change over time (Loarie et al., 2009). This approach can be scaled up to incorporate the dissimilarity in multiple biologically meaningful variables that define species' fundamental niches, from today's climate conditions to those projected under future scenarios of climate change. This enables the identification of the direction and distance a species must relocate to inhabit a climate that is analogous to its current conditions. Climate dissimilarity is a metric that drives the climate analog approach, which identifies other locations with similar climates to a current location across time and geographic space. Climate dissimilarities and their analogs can be determined with or without species distribution data by relying primarily on the selection (and data availability) of the environmental variables most relevant to a location, species, or group of species.

This paper aims to illustrate the potential of climate dissimilarity analyses for projecting future impacts on marine environments, specifically demonstrating how this approach may be used as a tool for managing aquaculture adaptations to climate change.

CLIMATE ANALOGS IN ACTION

In the wild, marine species are moving in pursuit of favorable environmental conditions (Chaudhary et al., 2021). However, aquaculture farms have less freedom, especially across country borders. This makes it important to identify areas where large climatic shifts are likely in order to mitigate losses and to seize emerging opportunities.

Determining where climate analogs favorable to aquaculture will be located under future climate change will enable advance planning of its development (Figure 1). For example, at location A, where example species Atlantic cod *Gadus morhua* is currently farmed, there may be a decrease in production of that species as the environment changes over time. Location B may develop an analogous climate that is similar to the present-day climate at location A. However, the climate suitability for an additional example species, the Atlantic salmon *Salmo salar*, could decline at location B over time, and salmon farms in this region would exhibit a loss in production should they keep farming Atlantic salmon. Location C, which is currently able to support Atlantic salmon aquaculture, although perhaps not at maximum production due to low temperatures, will be analogous to B in the future, resulting in increased production and profitability at that location in the future. However, decreased climate suitability may affect the aquaculture productivity in that region, negatively impacting the long-term profitability of these farms. As Figure 1 illustrates, current favorable climates will shift poleward, leaving polar and equatorial species subject to larger disruptions. Tropical regions already hosting the warmest environments may develop climates that are significantly dissimilar from a production perspective compared to the present day. Opportunities may arise as climate change could facilitate the expansion of tropical aquaculture into the subtropics and cold-temperate aquaculture into polar latitudes.

The reliance of aquaculture species and facilities on climate conditions creates a compelling case for proactive management and adaptation of aquaculture, which requires robust forecasts of climate impacts. To address this need, statistical approaches and metrics must be adaptable to diverse species groups and have regional resolution, while remaining applicable globally. Early identification of areas likely to undergo the biggest swings in aquaculture suitability, for the better or worse, is a critical step toward enabling the maximum adaptive potential of aquaculture as an industry.

CONCLUSION

Estimates of future climate dissimilarities may be a valuable approach for predicting optimal locations for aquaculture under different climate change scenarios. Future exposure to climate change could be estimated for large groups of species on a global scale using group-specific environmental variables with biological relevance, beyond

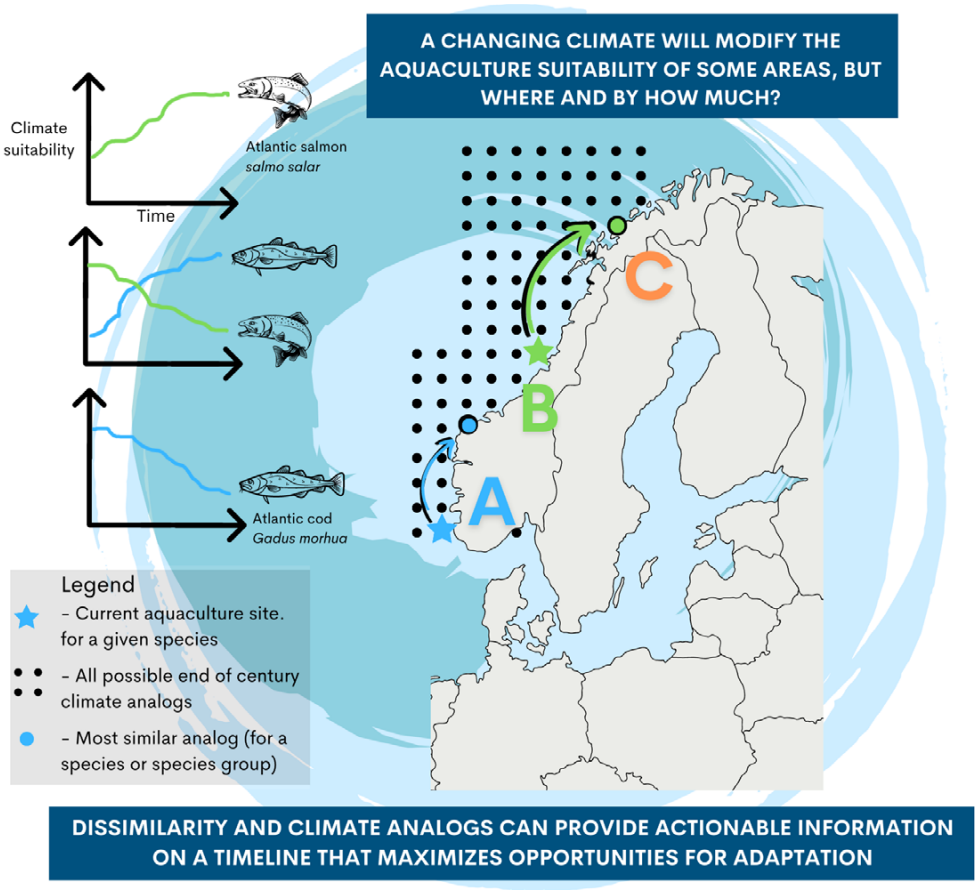

FIGURE 1. A conceptual diagram of how determining climate analogs can be used as a decision-making tool in aquaculture uses Atlantic salmon *Salmo salar* and Atlantic cod *Gadus morhua* along the Norwegian coast as examples.

temperature conditions, in order to improve the accuracy of projections (Ramos Martins et al., 2021). Knowing the distances and directions that aquaculture farms and native populations must travel to track favorable climatic conditions aids planning for the future, as recommended by the Intergovernmental Panel on Climate Change (Pörtner et al., 2022).

Several challenges and unanswered questions exist in the pursuit of accurate global aquaculture suitability models. Global distribution data that describe the native and introduced locations of aquaculture species are readily available, but the global distribution of aquaculture facilities is not. Engineering of aquaculture facilities, farm practices, and selective breeding may moderate the impacts of climatic changes and aid climate adaptation, but it may result in increased costs and decreasing profits, depending on local conditions and market prices.

REFERENCES

Barange, M., G. Merino, J.L. Blanchard, J. Scholtens, J. Harle, E.H. Allison, J.I. Allen, J. Holt, and S. Jennings. 2014. Impacts of climate change on marine ecosystem production in societies dependent on fisheries. *Nature Climate Change* 4:211–216, https://doi.org/10.1038/nclimate2119.

Chaudhary, C., A.J. Richardson, D.S. Schoeman, and M.J. Costello. 2021. Global warming is causing a more pronounced dip in marine species richness around the equator. *Proceedings of the National Academy of Sciences of the United States of America* 118(15):e2015094118, https://doi.org/10.1073/pnas.2015094118.

FAO (Food and Agriculture Organization of the United Nations). 2020. *The State of World Fisheries and Aquaculture 2020*. FAO, 244 pp., https://doi.org/10.4060/ca9229en.

Loarie, S.R., P.B. Duffy, H. Hamilton, G.P. Asner, C.B. Field, and D.D. Ackerly. 2009. The velocity of climate change. *Nature* 462(7276):1,052–1,055, https://doi.org/10.1038/nature08649.

Pörtner, H.-O., D.C. Roberts, H. Adams, I. Adelekan, C. Adler, R. Adrian, P. Aldunce, E. Ali, R. Ara Begum, B. Bednar-Friedl, and others. 2022. Technical summary. Pp. 37–118 in *Climate Change 2022: Impacts, Adaptation and Vulnerability. Contribution of Working Group II to the Sixth Assessment Report of the Intergovernmental Panel on Climate Change*. H.-O. Pörtner, D.C. Roberts, E.S. Poloczanska, K. Mintenbeck, M. Tignor, A. Alegría, and others, eds, Cambridge University Press, Cambridge, UK, and New York, NY, USA.

Ramos Martins, M., J. Assis, and D. Abecasis. 2021. Biologically meaningful distribution models highlight the benefits of the Paris Agreement for demersal fishing targets in the North Atlantic Ocean. *Global Ecology and Biogeography* 30(8):1,643–1,656, https://doi.org/10.1111/geb.13327.

ACKNOWLEDGMENTS

This study was supported by the Foundation for Science and Technology (FCT) of Portugal through projects UID/Multi/04326/2020 and PTDC/BIA-CBI/6515/2020 and the transitional norm DL57/2016/CP1361/CT0035.

ARTICLE DOI. https://doi.org/10.5670/oceanog.2023.s1.10

Monitoring Algal Blooms with Complementary Sensors on Multiple Spatial and Temporal Scales

By David R. Williamson, Glaucia M. Fragoso, Sanna Majaneva, Alberto Dallolio, Daniel Ø. Halvorsen, Oliver Hasler, Adriënne E. Oudijk, Dennis D. Langer, Tor Arne Johansen, Geir Johnsen, Annette Stahl, Martin Ludvigsen, and Joseph L. Garrett

Climate change, and other human-induced impacts, are severely increasing the intensity and occurrences of algal blooms in coastal regions (IPCC, 2022). Ocean warming, marine heatwaves, and eutrophication promote suitable conditions for rapid phytoplankton growth and biomass accumulation. An increase in such primary producers provides food for marine organisms, and phytoplankton play an important global role in fixing atmospheric carbon dioxide and producing much of the oxygen we breathe. But harmful algal blooms (HABs) can also form, and they may adversely affect the ecosystem by reducing oxygen availability in the water, releasing toxic substances, clogging fish gills, and diminishing biodiversity. Understanding, forecasting, and ultimately mitigating HAB events could reduce their impact on wild fish populations, help aquaculture producers avoid losses, and facilitate a healthy ocean.

Phytoplankton respond rapidly to changes in the environment, and measuring the distribution of a bloom and its species composition and abundance is essential for determining its ecological impact and potential for harm. Satellite remote sensing of chlorophyll concentration has been used extensively to observe the development of algal blooms. Although this tool has wide spatial and temporal (nearly daily) coverage, it is limited to surface ocean waters and cloud-free days. Microscopic analyses of water and net samples allow much closer examination of the species present in a bloom and their abundance, but this is a time-consuming process that collects only discrete point samples, sparsely distributed in space and time. Neither of these methods alone captures the rapid evolution of algal blooms, the spatial and temporal patchiness of their distributions, or their high local variability. In situ optical devices and imaging sensors mounted on mobile platforms such as autonomous underwater vehicles (AUVs) and uncrewed surface vehicles (USVs) capture fine-scale temporal trends in plankton communities, while uncrewed aerial vehicles (UAVs) complement satellite remote sensing. Use of such autonomous platforms offers the flexibility to react to local conditions with adaptive sampling techniques in order to examine the marine environments in real time.

Here we present an integrated approach to observing blooms—an "observational pyramid"—that includes both classical and newer, complementary observation methods (Figure 1). We aim to identify trends in phytoplankton blooms in a region with strong aquaculture activity on the Atlantic coast of mid-Norway. Field campaigns were carried out in consecutive springs (2021 and 2022) in Frohavet, an area of sea sheltered by the Froan archipelago (Figure 2). The region is a shallow, highly productive basin with abundant fishing and a growing aquaculture industry. Typically, there are one or more large algal blooms here during the spring months. We use multi-instrumentation from macro- to a microscale perspectives, combined with oceanographic modeling and ground truthing, to provide tools for early algal bloom detection.

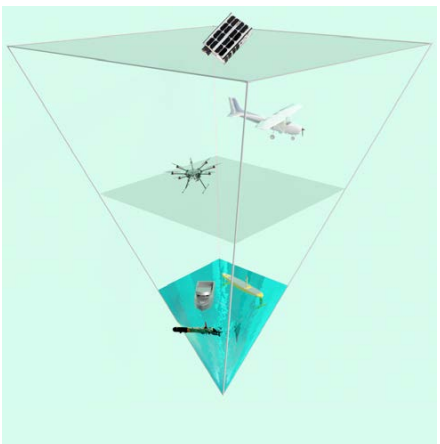

FIGURE 1. The observational pyramid concept offers simultaneous, integrated monitoring of the marine environment from space to seabed and from scales of hundreds of square kilometers to the microscopic. *After Dallolio et al. (2019)*

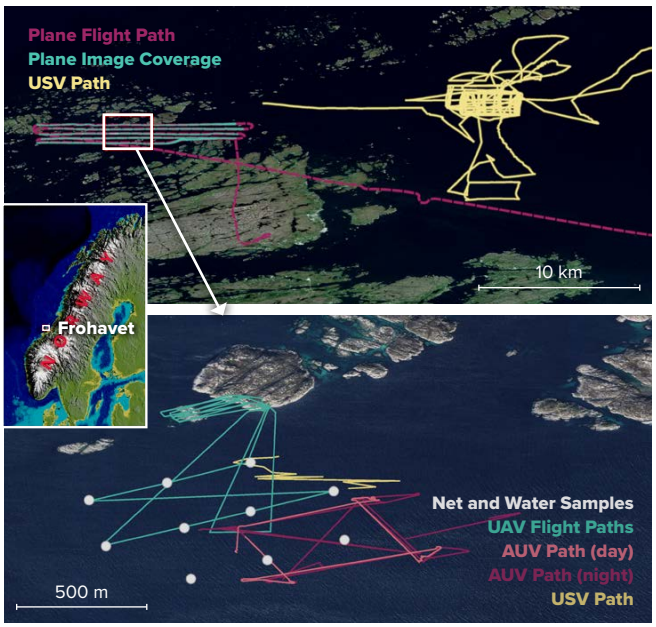

FIGURE 2. (inset) Fieldwork location relative to Norway. (upper panel) The larger Frohavet region is overlain here with the path and coverage of the plane equipped with a hyperspectral camera during 2021 fieldwork, and the path of the long-endurance USV in the weeks around 2022 fieldwork. (lower panel) The locations of net and water samples and the paths of the UAV, AUV, and USV missions in the main sampling area in 2022. *Elevation data from Kartverket, satellite images from Norge i bilder/Kartverket and CNES/Airbus, Landsat/ Copernicus, Maxar Technologies via Google Maps*

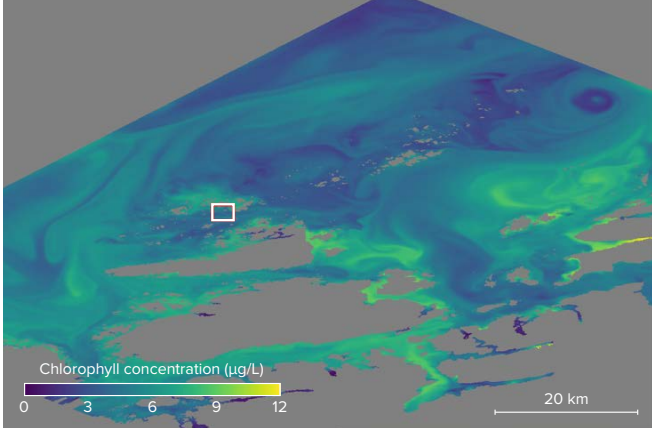

FIGURE 3. A chlorophyll forecast made on April 19 during the 2022 fieldwork using SINMOD, a coupled physical-chemical-biological ocean model (spatial resolution 160 m). The white box shows the fieldwork area.

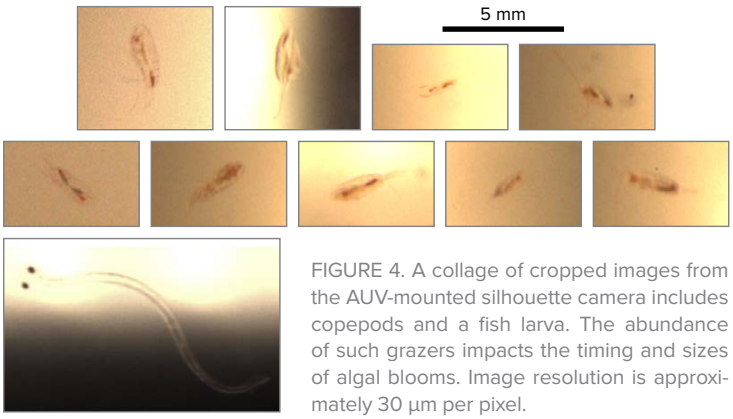

FIGURE 4. A collage of cropped images from the AUV-mounted silhouette camera includes copepods and a fish larva. The abundance of such grazers impacts the timing and sizes of algal blooms. Image resolution is approximately 30 µm per pixel.

At the very largest scale, in 2021 we used multispectral images from the Sentinel-2 and PRISMA satellites, and in 2022 from the Norwegian University of Technical and Natural Sciences Centre's Hypso-1 hyperspectral imaging satellite (Grøtte et al., 2021) to monitor ocean color in the area of interest over several weeks surrounding the main fieldwork. A long-endurance USV, equipped with a payload of ocean sensors including a CTD, an ADCP, an oxygen optode, and a fluorometer also monitored the area before, during, and after the missions. SINMOD, a coupled physical-chemical-biological ocean model, was used to simulate environmental conditions in the area of interest (Figure 3). During the fieldwork, the satellite imagery was supplemented by hyperspectral data collected by cameras mounted on a plane (in 2021) and on a UAV for covering smaller areas at higher resolution; these sensors are also less affected by cloud cover. At the same time, we launched an AUV (Saad et al., 2020) that covered hundreds of cubic meters of ocean while taking high-magnification underwater images (Figure 4) and collecting CTD and chlorophyll data. Finally, we deployed a Niskin water sampler at a number of locations within the AUV and UAV observation area and at several depths for microscopy and eDNA analysis.

The multisensor, multiscale operations will allow us to assess phytoplankton health and divide the growth of their populations into stages: pre-bloom (cells begin to grow), bloom phase (exponential growth), and post-bloom (grazing and decay). While remote sensing provides a broad view of such growth through ocean color, net and water sampling give us insight into the changing species composition within a bloom. Simultaneous AUV imaging provides information on grazers that feed on the phytoplankton—thought to be an important factor in the evolution of algal blooms. Multisensor operations also provide ground truth for remote sensing and help us link hyperspectral observations from novel aerial and satellite sensors with conditions in the water. All of these data sources will be used to validate and improve the SINMOD model of the ocean, allowing it to better predict the occurrence and composition of HABs and other algal blooms. Reliable prediction and automated observation also improve monitoring by telling us where and when expensive fieldwork with small-scale, high-resolution sensors can be most effective.

Observational efforts that combine state-of-the-art ocean monitoring technology, multi- and hyperspectral remote sensing, ecosystem modeling, traditional water sampling, and integrated taxonomy via microscopic and molecular (eDNA) species identification are paramount for a holistic understanding of bloom formation, as well as of marine primary production overall. Our project demonstrates the advantages of this approach and promises to enable more effective ocean monitoring in the future.

REFERENCES

Dallolio, A., L. Bertino, L. Chrpa, T.A. Johansen, M. Ludvigsen, K.A. Orvik, L.H. Smedsrud, J. Sousa, I.B. Utne, P. Johnston, and K. Rajan. 2019. Long-duration autonomy for open ocean exploration: Preliminary results & challenges. RSS 2019 Workshop on Robots in the Wild: Challenges in Deploying Robust Autonomy for Robotic Exploration, June 22–26, 2019, Freiburg, Germany.

Grøtte, M.E., R. Birkeland, E. Honoré-Livermore, S. Bakken, J. Garrett, E.F. Prentice, F. Sigernes, M. Orlandić, J.T. Gravdahl, and T.A. Johansen. 2022. Ocean color hyperspectral remote sensing with high resolution and low latency—The HYPSO-1 CubeSat mission. *IEEE Transactions on Geoscience and Remote Sensing* 60:1–19, https://doi.org/10.1109/TGRS.2021.3080175.

IPCC. 2022. *Climate Change 2022: Impacts, Adaptation and Vulnerability.* Contribution of Working Group II to the Sixth Assessment Report of the Intergovernmental Panel on Climate Change, H.-O. Pörtner, D.C. Roberts, M. Tignor, E.S. Poloczanska, K. Mintenbeck, A. Alegría, M. Craig, S. Langsdorf, S. Löschke, and others, eds, Cambridge University Press, Cambridge, UK, and New York, NY, USA, 3,056 pp.

Saad, A., A. Stahl, A. Våge, E. Davies, T. Nordam, N. Aberle, M. Ludvigsen, G. Johnsen, J. Sousa, and K. Rajan. 2020. Advancing ocean observation with an AI-driven mobile robotic explorer. *Oceanography* 33(3):50–59, https://doi.org/10.5670/oceanog.2020.307.

ACKNOWLEDGMENTS

This work was supported by the Research Council of Norway and industry partners through the Centre of Excellence funding scheme (NTNU AMOS, grant no. 223254), MASSIVE (270959), MoniTare (315514), Nansen Legacy (276730), AILARON (262741), HYPSCI (325961), SeaBee (296478), and the Green-platform project 328674. Figure 1 UAV model by Pablo Sánchez (grabcad.com), workboat model by Lewist123 (thingiverse.com), and plane model from downloadfree3d.com.

ARTICLE DOI. https://doi.org/10.5670/oceanog.2023.s1.11

UAV High-Resolution Imaging and Disease Surveys Combine to Quantify Climate-Related Decline in Seagrass Meadows

By Lillian R. Aoki, Bo Yang, Olivia J. Graham, Carla Gomes, Brendan Rappazzo, Timothy L. Hawthorne, J. Emmett Duffy, and Drew Harvell

Seagrass meadows are essential habitats that support marine biodiversity and coastal communities while sequestering carbon, filtering water, and stabilizing coastal sediments. Warming temperatures stress seagrass meadows and can facilitate seagrass wasting disease, contributing to large-scale diebacks of seagrass meadows. Here, we demonstrate how high-resolution imagery, collected by uncrewed aerial vehicle (UAV) and validated by in situ sampling, can quantify seagrass responses to disease and thermal stress.

Seagrass meadows in the San Juan Islands, Washington, USA, have declined dramatically over the last decade. Shoot densities, measured along permanent monitoring transects, fell over 90% from 2013 to 2021, while wasting disease prevalence (percent infected plants) remained persistently above 40% since the 2016 Northeast Pacific heatwave (Figure 1). Since 2019, we have synchronized UAV surveys with midsummer in situ sampling. The UAV imagery greatly expands the scope of the data, extending beyond the monitoring transects to confirm large-scale loss of seagrass. Because this imagery can achieve 1–3 cm spatial resolution, analysis can connect individual plants (<3 cm) to ecosystem dynamics at the meadow scale (kilometers). The broad picture of seagrass decline detected in the UAV imagery reinforces the need for landscape-scale monitoring.

High-resolution imagery further provides insight into seagrass dynamics under climate change. Wasting disease is sensitive to warming, with infections increasing in warmer years (Groner et al., 2021). In June 2021, there was an unprecedented heating event in the study region (the 2021 Pacific Northwest heat dome). Daily sea surface temperatures exceeded the 90th percentile of long-term temperature records for 10 consecutive days (Figure 2). During this period, low tides occurred in early afternoon and the exposed intertidal meadows reached hourly temperatures as high as 34ºC at some sites, far exceeding the normal temperature range. These high temperatures cause physiological stress in seagrass, and prolonged exposure to high temperatures can cause plant mortality and rapid meadow diebacks. UAV imagery collected immediately following this event highlighted the dramatic loss of seagrass density and coverage for all monitoring sites, including the two sites shown here (Figure 3). At the Beach Haven site, the

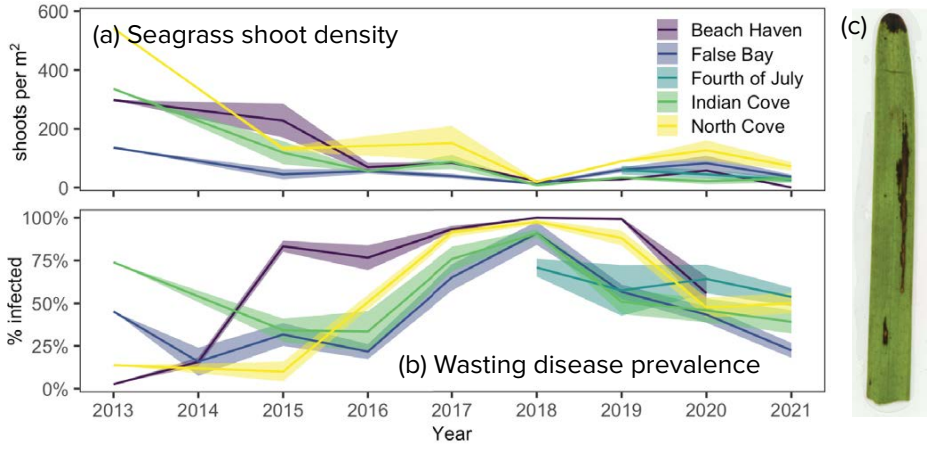

FIGURE 1. Long-term data from in situ surveys show substantial declines in seagrass shoot density over the last decade (a) while seagrass wasting disease infections have increased and remained elevated since the heat wave of 2016 (b). Colors indicate individual eelgrass meadows. Data from 2013 to 2017 redrawn from Groner et al. (2021). (c) An example of an infected eelgrass leaf with a dark wasting disease lesion.

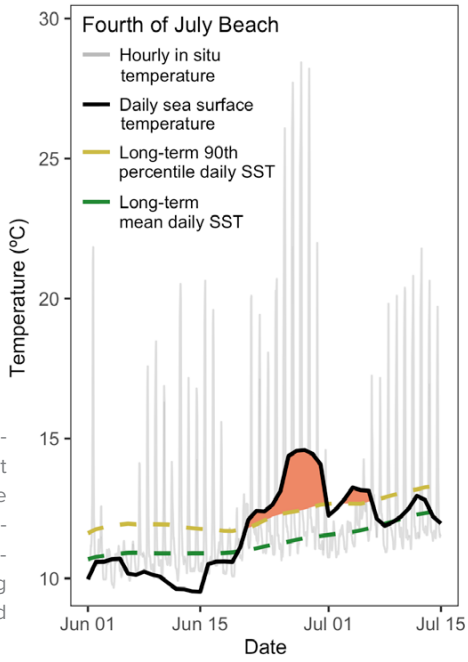

FIGURE 2. During the 2021 Pacific Northwest heat dome, extreme daily sea surface temperatures (black line) above the long-term 90th percentile (gold line) were recorded at study sites, including Fourth of July Beach. Sea surface temperature (SST) records were measured by satellite remote sensing and show the severity of daily temperatures compared to historic baselines, whereas hourly temperatures (gray line) measured with sensors deployed in the seagrass meadow capture the extreme in situ temperatures during mid-afternoon low tides. Maximum hourly temperatures during the heat dome ranged from 28°C to 34ºC across the intertidal seagrass meadows in the study region.

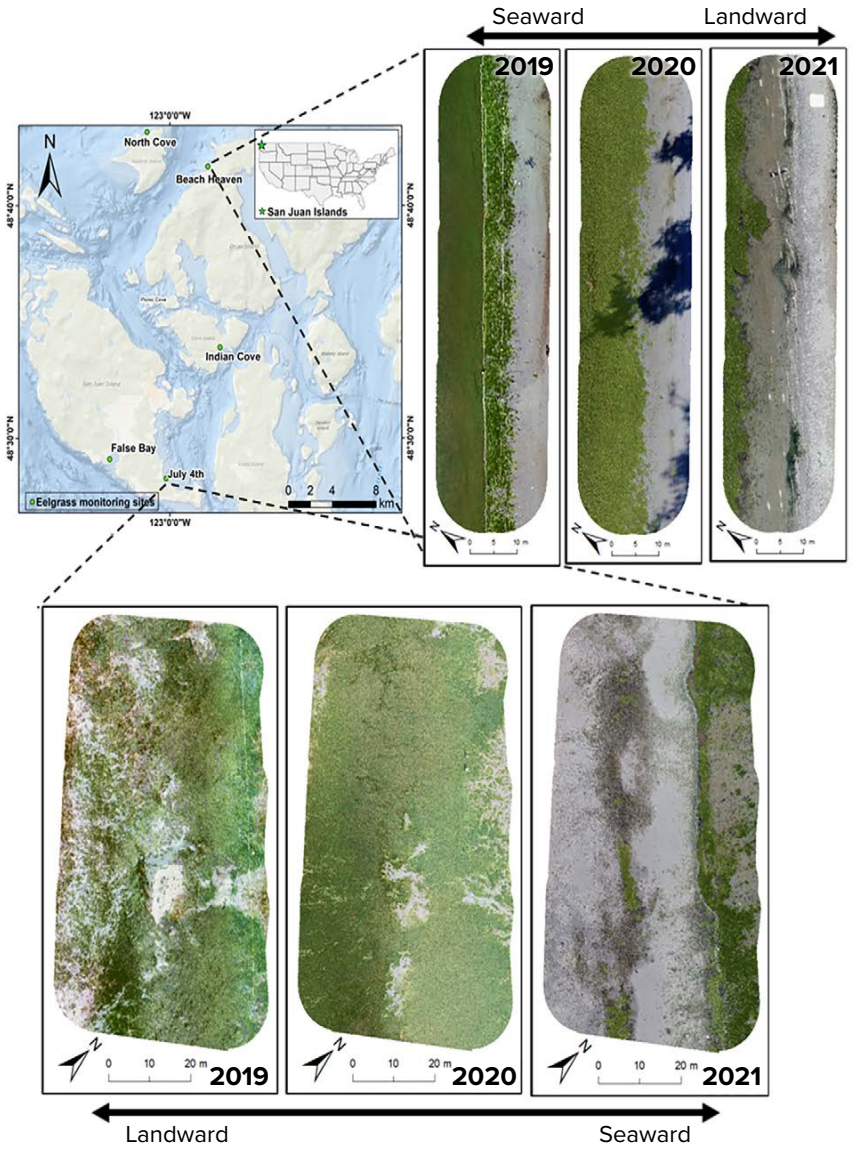

FIGURE 3. Five seagrass meadows in the San Juan Islands were surveyed annually beginning in 2019 using UAVs. Time series of the high-resolution imagery from two representative sites (Beach Haven, upper panels, and July 4, lower panels) show loss of seagrass extent in the 2021 images compared to prior years. At both sites, extensive areas of bare sand had replaced seagrass in the later images (seagrass area is highlighted in green in each image). Other parameters such as green leaf area index, seagrass biomass, and the presence of macroalgae can be derived through classification of the high-resolution images.

UAV imagery showed the nearly complete loss of the upper 10 m of seagrass between 2020 and 2021. This loss of habitat structure will have cascading ecological consequences, including reduced animal abundance, reduced carbon sequestration potential, and reduced shoreline protection. High levels of wasting disease infection in the years prior to this heatwave likely weakened these meadows, increasing their vulnerability to acute thermal stress and contributing to meadow-scale declines (Graham et al., 2021). Further quantification of spatiotemporal trends in patchiness, biomass, and plant health will show how climate-driven disturbance propagates across the landscape. Landscape-scale monitoring using UAV methods is increasingly urgent as the frequency, intensity, and duration of extreme heating events such as the 2021 heat dome increase under climate change.

In the dynamic intertidal zone, the flexibility of UAV methods could revolutionize assessment of disturbance trajectories (Yang et al., 2020). Because UAVs can be deployed rapidly, cross-scale imagery can be collected immediately after disturbance as well as at seasonal or annual intervals. Advanced methods such as deploying UAVs with multispectral, hyperspectral, or thermal sensors, combined with ground-sampled spectral signatures, can provide new insights into indicators of plant health, competition with macroalgae, and the presence of invasive species. The ongoing development of machine learning image processing algorithms will facilitate rapid and high-throughput image analysis and support managers and monitoring programs focused on understanding the real-time status and temporal dynamics of these ecosystems. With worsening wasting disease outbreaks and extreme heating under climate change, synergistic combinations of in situ and UAV methods are needed to understand seagrass meadow dynamics across spatial and temporal scales.

REFERENCES

Graham, O.J., L.R. Aoki, T. Stephens, J. Stokes, S. Dayal, B. Rappazzo, C.P. Gomes, and C.D. Harvell. 2021. Effects of seagrass wasting disease on eelgrass growth and belowground sugar in natural meadows. *Frontiers in Marine Science* 8:768668, https://doi.org/10.3389/fmars.2021.768668.

Groner, M., M. Eisenlord, R. Yoshioka, E. Fiorenza, P. Dawkins, O. Graham, M. Winningham, A. Vompe, N. Rivlin, B. Yang, and others. 2021. Warming sea surface temperatures fuel summer epidemics of eelgrass wasting disease. *Marine Ecology Progress Series* 679:47–58, https://doi.org/10.3354/meps13902.

Yang, B., T.L. Hawthorne, M. Hessing-Lewis, E.J. Duffy, L.Y. Reshitnyk, M. Feinman, and H. Searson. 2020. Developing an introductory UAV/drone mapping training program for seagrass monitoring and research. *Drones* 4:70, https://doi.org/10.3390/drones4040070.

ARTICLE DOI. https://doi.org/10.5670/oceanog.2023.s1.12

Long-Term Observations of Hypoxia off the Yangtze River Estuary: Toward Prediction and Operational Application

By Xiaobo Ni*, Feng Zhou*, Dingyong Zeng, Dewang Li, Tao Zhang, Kui Wang, Yunlong Ma, Qicheng Meng, Xiao Ma, Qianjiang Zhang, Daji Huang, and Jianfang Chen (*equal first authors)

Dissolved oxygen (DO) is essential for the survival of most aquatic organisms. Hypoxia, defined as a DO concentration of less than 2 mg L^{-1}, is a significant issue for ecosystems in estuaries and coastal waters and is one of the top themes of the United Nations Decade of Ocean Science for Sustainable Development (2021–2030). An area off the Yangtze River Estuary (YRE), China, annually develops one of the world ocean's largest hypoxic areas. Observations collected by ship since 1999, and by long-term sensors since 2009, show that DO concentration in this region has been both declining and greatly fluctuating.

The best marine fishing grounds in China are located in the YRE. Prior to 2009, no continuous observations of hypoxia were collected off the YRE because fishing trawls routinely tear up instruments placed on and above the seafloor. Since 2009, we have experimented with placing sensors in a trawl-resistant bottom mount (TRBM) designed to work in this region of heavy sedimentation and energetic tides, along with a buoy to monitor hypoxia structure and processes. In 2019, our hypoxia observatory was upgraded to an integrated marine field station of the Ministry of Natural Resources in China, the Observation and Research Station of Yangtze River Delta Marine Ecosystems (MORSE; Figure 1), in which numerical modeling based on the Regional Ocean Modeling Systems (ROMS) coupled with the Carbon, Silicate, and Nitrogen Ecosystem (CoSiNE) model is integrated into the observation network.

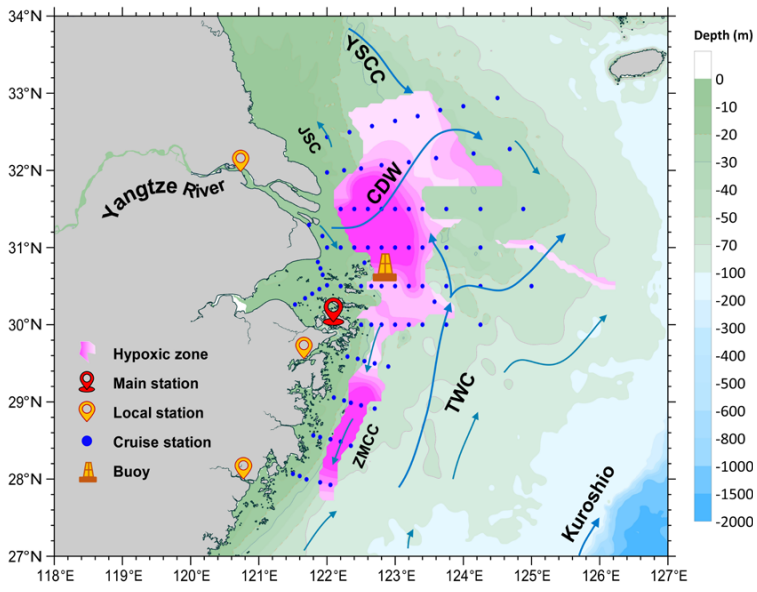

FIGURE 1. Map of the components of the Chinese Ministry of Natural Resources' Observation and Research Station of Yangtze River Delta Marine Ecosystems (MORSE). Historic hypoxia zones off the Yangtze River Estuary are indicated with pink shading, and blue arrows show summer water circulation. CDW = Changjiang (Yangtze River) Diluted Water. YSCC = Yellow Sea Coastal Current. TWC = Taiwan Warm Current. JSC = Jiangsu Shoal Current. ZMCC = Zhe-Min Coastal Current.

TRBM

To enable collection of long-term observations, we modified DeepWater Buoyancy AL200 TRBMs for use in the YRE region (Figure 2). First, we moved the acoustic releases and sensors to the upper half of the buoyant pod to reduce the risk of sediment burial, although that slightly weakens the anti-trawling performance. Second, we added a time-release function to the acoustic releases to improve the chance of recovery if the TRBM is buried. Third, we designed a barb device that springs out of the buoyant pod after release, increasing the chance of the TRBM being dragged out of sediment by a fishing trawler should it become buried, thus reducing the probability of loss.

Since 2009, our TRBM has been deployed more than 20 times to acquire continuous DO, temperature, salinity, turbidity, and depth information in the hypoxic area off the YRE. From the 104-day time series data for bottom DO collected by the TRBM in 2009, summer formation, maintenance, and disappearance of hypoxia off the YRE is evident for the first time (Figure 2; Ni et al., 2016). We found this hypoxia to be severe, sometimes close to anoxic conditions, during summer. The turbidity data suggest that hypoxic conditions were more likely to appear or were enhanced after passage of a typhoon.

BUOY

Ocean stratification and high biological productivity are essential factors for hypoxia formation. Hypoxia generally occurs at the sea bottom, while the pycnocline and photosynthesis are located in the upper ocean. To understand the mechanism of hypoxia formation, we developed a real-time buoy system to observe the entire water column.

A surface buoy, moored to the seafloor, supports instruments that monitor temperature, salinity, DO, turbidity, chlorophyll *a*, nutrients, and current in four layers: the surface layer and three layers within the pycnocline (Figure 3). A TRBM acquires the same data types at the seafloor. Coupled inductive and acoustic communication technologies are used to transmit the underwater data to the

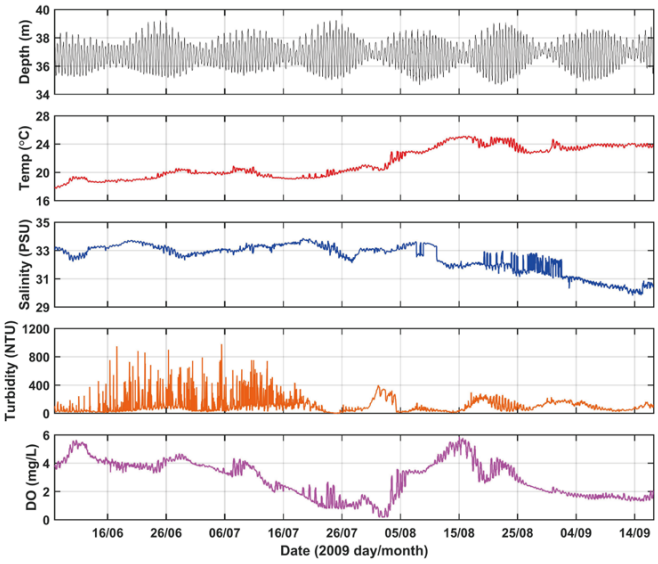

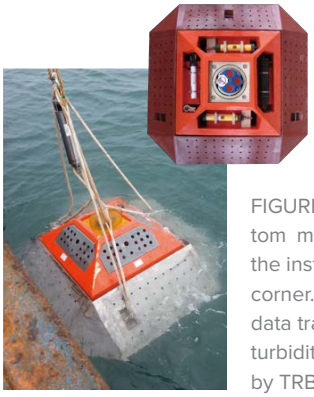

FIGURE 2. (right) Photo of trawl-resistant bottom mount (TRBM) deployment at sea, with the instrument layout shown in the upper right corner. (left) Plots of the 104-day time-series data track bottom depth, temperature, salinity, turbidity, and dissolved oxygen (DO) collected by TRBM sensors in summer 2009.

surface buoy, and then the surface buoy data logger sends all the data to the shore station via satellite and cellphone.

Our buoy system has monitored hypoxia in the YRE area for more than 12 successive summers. Sensors in the TRBM have provided information while hypoxic conditions were developing, while they were sustained, and while they were dispersing. The data collected by the buoy sensors provided information about the thickness of the hypoxic layer. After nutrient sensors were added to the surface buoy in 2013, the steps toward hypoxia formation in the YRE were revealed, from eutrophication to algal blooms to hypoxia.

HYPOXIA SIMULATION AND PREDICTION

Due to complex circulation and mixing, DO off the YRE exhibits a highly variable, three-dimensional structure, which may not be well resolved by data from the one deployed buoy system combined with ship survey data collected in summer and/or fall (blue dots in Figure 1). A physical-biogeochemical model was run by customizing ROMS and coupling it with CoSiNE (Zhou et al., 2017). We used MORSE data (including time-series data) to improve parameterization of both physical and biological processes.

FIGURE 3. (left) A drone photo shows deployment of the surface buoy. (right) Time series of temperature, salinity, density, chlorophyll *a* (Chl-a), and dissolved oxygen (DO) at five depths in summer 2015. Some data in the pycnocline and at the seafloor are missing because of sensor malfunctions or sabotage by fishing activities.

Since 2020, the model has contributed to the National Marine Environmental Forecasting Center of China's experimental forecasts (up to 120 hours) for nutrients, DO, chlorophyll *a*, currents, salinity, and temperature off the YRE.

OUTLOOK

Although usually a seasonal phenomenon at the seabed, coastal hypoxia is characterized by variability at multiple temporal and spatial scales. Physical-biogeochemical models need additional observational data to support hypoxia prediction and operational application off the YRE. New observing methods soon to be implemented include a benthic chamber and uncrewed survey vessels that will measure oxygen consumption in the sediment and automatically survey the entire hypoxic area within one or two days.

REFERENCES

Ni, X.B., D.J. Huang, D.Y. Zeng, T. Zhang, H.L. Li, and J.F. Chen. 2016. The impact of wind mixing on variation of bottom dissolved oxygen off the Changjiang Estuary in summer. *Journal of Marine Systems* 154:122–130, https://doi.org/10.1016/j.jmarsys.2014.11.010.

Zhou, F., F. Chai, D.J. Huang, H.J. Xue, J.F. Chen, P. Xiu, J.L. Xuan, J. Li, D.Y. Zeng, X.B. Ni, and K. Wang. 2017. Investigation of hypoxia off the Changjiang Estuary using a coupled model of ROMS-CoSiNE. *Progress in Oceanography* 159:237–254, https://doi.org/10.1016/j.pocean.2017.10.008.

ARTICLE DOI. https://doi.org/10.5670/oceanog.2023.s1.13

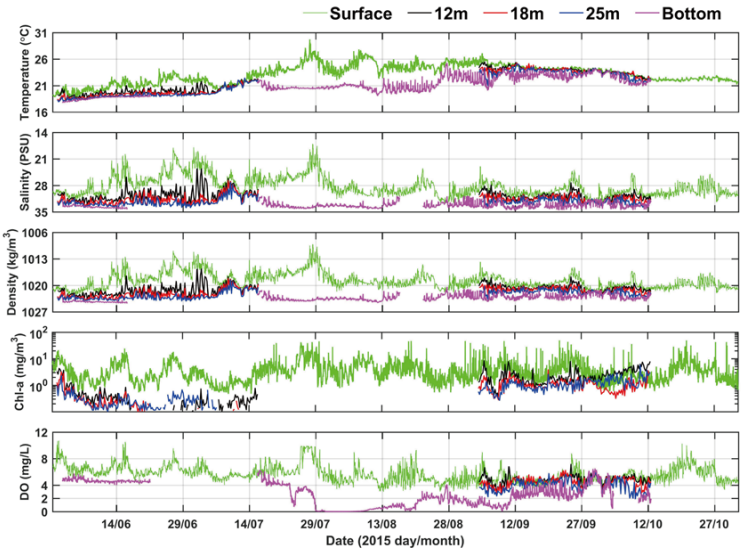

Exploring Methods for Understanding and Quantifying Plastic-Derived Dissolved Organic Matter

By Lixin Zhu*, Nicola Gaggelli*, Amedeo Boldrini, Aron Stubbins, and Steven Arthur Loiselle (*equal first authors)

PLASTIC-DERIVED DISSOLVED ORGANIC MATTER

Plastics have accumulated in the environment to become a globally significant pool of organic carbon (Stubbins et al., 2021) and a contaminant of ecological concern (McLeod et al., 2021). Most studies still report plastics in terms of counts (i.e., pieces of plastics) though some report masses of plastics, and even fewer report plastic carbon. In a recent review, we assumed plastics to be 83% carbon by mass based on data for oceanic microplastics (Zhu et al., 2020; Stubbins et al., 2021). This overly simplistic conversion allows plastics to be placed in a carbon cycle context, a context critical to plastic-derived dissolved organic carbon (DOC; Figure 1). However, this conversion should be improved to account for variations in the carbon content of different polymers. To make these improvements, studies should report data for sizes, masses, and types of base polymer of plastics collected. These data would allow comparison among studies and facilitate improved accounting for plastics and their fates in the environment. Reporting masses of specific polymers would make conversion from plastics to carbon more accurate and provide a common chemical unit for comparison among plastic polymer types (i.e., we could use carbon as we do biomass).

From a geochemical perspective, plastics are ultrahigh molecular weight organic geomaterials that also carry other organics into aquatic ecosystems (e.g., additives and other lower molecular weight organics adsorbed to the plastics). Once plastics enter aquatic ecosystems, they can leach organic substances that include additives such as plasticizers (e.g., phthalates), colorants, and flame retardants (Gewert et al., 2015) as well as adsorbed chemicals such as organic pollutants and natural organic matter. If these molecules are leached from plastics into water, they enter the pool of dissolved organic matter (DOM, defined as organic matter that passes through a filter of 0.2–0.7 µm; Bracchini et al., 2010; Dittmar and Stubbins 2014). In addition to leaching from passenger molecules, DOM can derive directly from plastic polymers that are degraded in natural waters via photo-dissolution by sunlight (Romera-Castillo et al., 2018; Zhu et al., 2020). Photo-dissolution, which results from this scission (photochemical "cutting" of bonds in the polymer) and oxidation reactions, produces a suite of soluble low molecular weight products (Eyheraguibel et al., 2017). Sunlight can completely dissolve microplastics floating at sea in 0.3 to 50 years, depending on polymer type, and the kinetics employed in modeling suggests all floating microplastics at sea would dissolve within decades if inputs ceased (Zhu et al., 2020).

The mass of microplastics floating at or near the sea surface amounts to 93–236 thousand metric tons (Van Sebille et al., 2015) or 0.07–0.20 Tg plastic-C (Stubbins et al., 2021). If all this plastic were to dissolve, it would constitute a tiny fraction of total ocean DOC stocks (662,000 Tg-C; Hansell et al., 2009). However, because plastic-derived DOM is produced in sunlit surface waters, the addition of DOM could impact the ecology and biogeochemical functioning of surface waters. Photoproduced plastic-derived DOM contains transphilic products such as carboxylic acids that may fractionate into the marine microlayer and impact trace gas and aerosol exchange with the atmosphere and with surface ocean ecology and biogeochemistry (Boldrini et al., 2021; Galgani and Loiselle, 2021). In most cases, the DOM produced as plastics photo-dissolve is highly biolabile and utilized by bacteria, thus causing no obvious adverse effects (Romera-Castillo et al., 2018; Zhu et al., 2020). However, dissolved photoproducts from one sample of polyethylene inhibited microbial growth (Zhu et al., 2020), indicating some plastic-derived DOM may be cytotoxic. Whether this

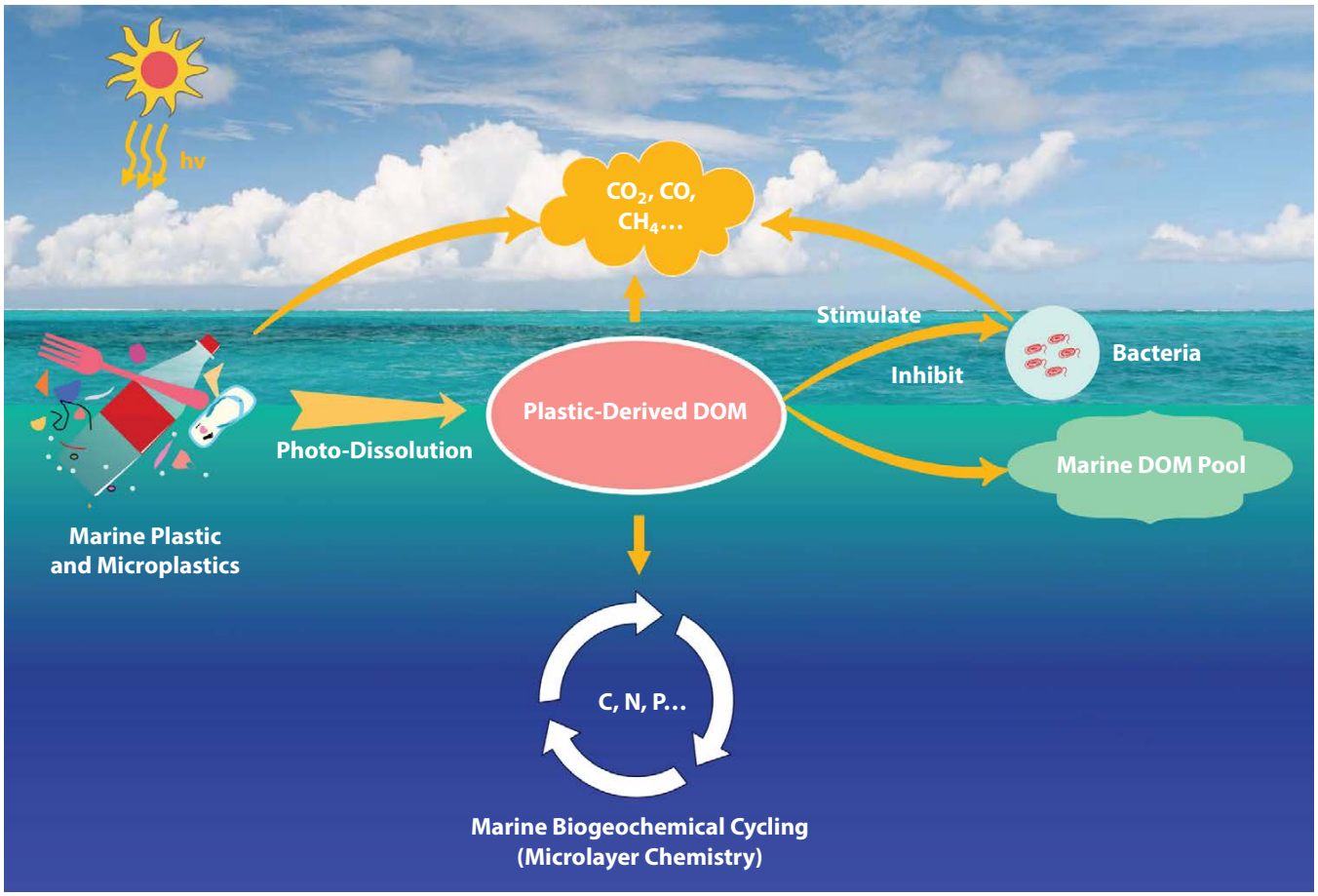

FIGURE 1. Schematic illustrating the production of plastic-derived dissolved organic matter (DOM) and its potential impacts on marine biogeochemistry.

is true for other types of plastic-derived DOM or at environmentally relevant concentrations remains unclear.

Although there is broad concern about the impacts of microplastics in natural waters (Macleod et al., 2021), there is limited understanding about the production and impacts of plastic-derived DOM. To aid efforts to gain greater understanding, we present some of the tools used to study DOM, including their applications to plastic-derived DOM.

LABORATORY STUDIES OF PLASTIC-DERIVED DOM PHOTOPRODUCTION

Because direct measurement of environmental photochemical rates in natural waters is challenging, rates are usually determined in more controlled settings and then extrapolated to the field (e.g., Mopper et al., 2015). To reduce the number of variables, but still maintain the functionality of key drivers, photochemical microcosm and mesocosm studies are employed, with irradiation times varying from hours to years. For all types of experiments discussed below, plastics should be thoroughly cleaned, and low DOM background water should be used. In studies seeking to assess abiotic photochemical rates, bacterial abundance should be monitored to ensure samples remain sterile and DOM is not altered or consumed prior to analysis. Studies seeking to understand the coupling of photochemical and biological processes do not need to be sterile.

Microcosms

Microcosm experiments explore a limited number of variables under controlled conditions (Table 1). The photodissolution of plastics is assessed in quartzware, as quartz allows environmentally relevant wavelengths of ultraviolet (UV) light (>280 nm) to enter. This wavelength range is responsible for most environmental photochemical reactions (Loiselle et al., 2009a; Mopper et al., 2015). One common microcosm is a lab-based solar simulator (Figure 2a), equipped with calibrated commercial lamps (e.g., Q-Panel UVA-340 bulbs) that provide light with a spectral quality and flux approximating the UV radiation in natural sunlight. Integrated irradiance can be quantified via spectroradiometers (e.g., OL 756, Optronic Laboratories), and temperature can be maintained by side mounted fans or water baths.

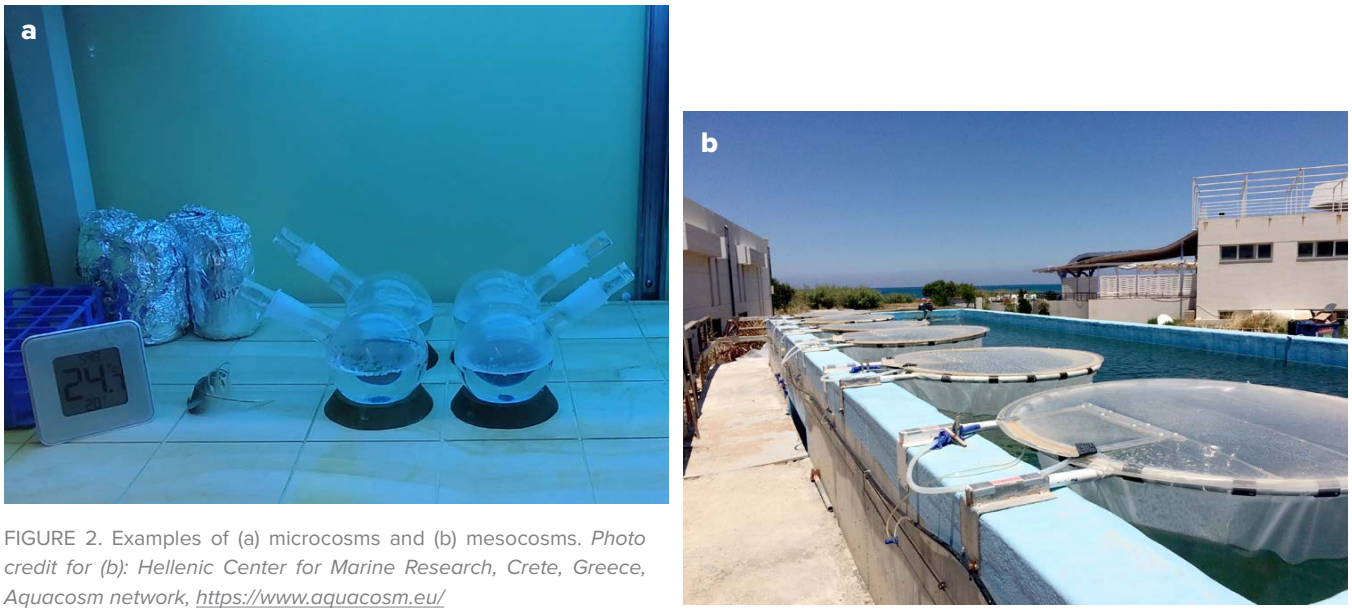

FIGURE 2. Examples of (a) microcosms and (b) mesocosms. *Photo credit for (b): Hellenic Center for Marine Research, Crete, Greece, Aquacosm network, https://www.aquacosm.eu/*

Microcosms can also use natural sunlight and quartz flasks in a water bath (e.g., on a rooftop), thus allowing exposure to the natural diurnal dynamics of sunlight. Sunlight irradiance can be measured using UV spectroradiometers (e.g., SKR, 1850; SKR 420, 430; Skye Instruments LTD, UK). The spectral incident irradiance (E_o (λ, t), kW m^{-2} nm^{-1}) is calculated by considering total solar irradiance on the circular mesocosm surface and the spectral transmission of the quartz (Loiselle et al., 2012). For example, DOM production from the degradation of different plastic bags was assessed by cutting them into 10 cm^2 squares, weighing and analyzing the plastic via Fourier transform infrared spectroscopy (FTIR), then floating them in quartz microcosms. Temperatures over a summer averaged 30°C, and light exposures matched those of unshaded local waters.

DOM samples should be collected through time to assess the kinetics of plastic-derived DOM accumulation. Extended periods of irradiation outdoors increase the possibility of complications due to extreme weather events and biofouling of the external quartz surface. Whether in the lab or outside, it is important to define, a priori, whether samples are to remain sterile or exposed to typical microbial conditions, as biolabile DOM will be modified by both photodegradation and microbial degradation and production processes (Galgani et al., 2018).

Mesocosms for Photochemistry

Larger-scale mesocosm (usually 1–10,000 L) experimental systems are set up in natural environments and provide a link between field and microcosm experiments. While still controlled, they are more exposed to environmental influences (Table 1, Figure 2b). Irradiance, temperature, and other factors are monitored using sensors, while regular sampling at different depths allows improved understanding of the processes mediating production, loss, and transformation of plastic-derived DOM in natural conditions. Mesocosms were used to determine the impact of microplastics on microbial DOM production by enhancing the production and accumulation of two important classes of marine gels in the sea surface microlayer (Galgani et al., 2023) and in bulk waters.

For mesocosm experiments, contamination with DOM from external sources should be avoided. In Galgani et al. (2019), mesocosms were filled with 3 m^3 of coastal oligotrophic seawater pumped directly from the Sea of Crete. The mesocosms were constructed of transparent polyethylene that was previously tested to ensure they did not release DOM. These mesocosms were housed in a concrete tank (150 m^3) with circulating seawater to maintain temperature (20° ± 1°C). After 24 hours, homogeneity between mesocosms was assessed. Transparent polystyrene microbeads (Sigma-Aldrich, nr. 84135; density of 1.05 g cm^{-3}) were added to three mesocosms (430 beads L^{-1}); polystyrene beads were chosen to reduce the possibility of attraction to the polyethylene walls of the mesocosm (Beneš and Paulenová, 1973). A centralized airlift system (Pitta et al., 2016) assured homogeneous distribution of the microplastics. Following Carlson (1982), the surface microlayer was sampled every other day using acid washed and Milli-Q rinsed glass plates, collection bottles, and wipes for phytoplankton sampling in the microlayer. Bulk water

TABLE 1. Summary of differences between experimental systems for quantification of plastic-derived dissolved organic matter.

	IRRADIATION SOURCE	IRRADIATION TIME	SIZE/SCALE	ADVANTAGES	DISADVANTAGES
Microcosms (Controlled lab experiments)	Commercial lamps that simulate sunlight	Up to 24 hours per day	Small (10 mL to 5 L)	• Highly controlled • Avoid external factors • Small space • Accelerated degradation	• Imitates the natural environment less
Microcosms (Natural environment)	Natural sunlight	Determined by local sunlight	Small (100 mL to 1 L)	• Small space	• Longer experimental time • Exposed to external elements • Variability in spectral quality and dose
Mesocosms	Natural sunlight	Determined by local sunlight	Medium to large (1–10,000 L)	• Incorporate natural variations • Key variables are controlled to some extent	• Large space • Longer experimental time

was sampled from 0.5 m depth using acid-washed and Milli-Q rinsed tubes. To avoid cross-contamination, different sampling equipment (glass plates, funnels, collection bottles, wipes) was used for the control mesocosms and the microplastic-treated mesocosms. Mesocosms containing microplastics showed increased production of DOM in both bulk waters and surface microlayers and an increase in the production of carbohydrate-like and proteinaceous marine gel compounds in the surface water (Galgani et al., 2019). Implications of this increased layer of organic material at the sea surface concern the transport of microplastics out of the photic zone and gas exchange across the sea surface.

EXPERIMENTAL CONSIDERATIONS FOR PLASTIC-DERIVED DOM INTERACTIONS

Experiments have been conducted using standards, commercial products, and environmentally collected plastic debris. All plastics should be cleaned and dried to avoid contamination. Cleaned plastics can be cut into various sizes or shapes. The cleanness of the plastics can be checked under a microscope. Prior to transferring to mesocosms or microcosms, all plastic samples should be identified for polymer type, weight, dimension, and number.

Plastics are added to water to assess DOM production and leaching. Natural seawater, artificial seawater, freshwater, or ultraclean water (e.g., Milli-Q) can be used. The amount of photochemically active background DOM in natural waters can be lowered by irradiating under germicidal ultraviolet-C light (Zhu et al., 2020). Milli-Q water has a near-zero DOM background, making it easier to quantify DOM production from plastics. However, the mechanisms of DOM release in Milli-Q do not reflect those of natural waters. Natural water contains DOM and other photo-active solutes (e.g., chloride, bromide), as well as microbes that can colonize plastic surfaces as biofilm and transform released DOM. Both light and dark controls are recommended. Light control samples are irradiated in the same way as the experimental samples that do not contain plastics. Two types of dark controls should be included. The first includes plastics, while the second should have no plastics, and both should be kept in the dark (e.g., foil wrapped but otherwise in the same location and condition as the light samples).

The amount of plastic sample used depends on the objective. To best mimic natural processes, the concentration and surface area of the plastic should be comparable to that found in the environment. For example, 240 particles per liter were used in Zhu et al. (2020). However, to obtain enough plastic-derived DOM for further analyses or experiments, or to explore kinetics and mechanisms, higher concentrations of plastics can be used. In microcosms, flasks can be repositioned daily to average out potential spatial variation in the light flux. Throughout the irradiation period, liquid samples can be drawn from the flasks using pre-combusted glass Pasteur pipettes at regular intervals. Duplicates or triplicates are advised. At the end of the experiments, plastic fragments can be dried, weighed, and further analyzed for carbon content using an elemental analyzer. Changes in surface properties can be accessed via optical and electron microscopy, as well as FTIR. All sample handling and experimental procedures should follow trace clean protocols for natural DOC analysis (Stubbins and Dittmar, 2012). All plasticware should be cleaned by triple rinsing with Milli-Q water, soaked overnight in ~pH 2 water, triple rinsed with Milli-Q, and then dried. Glassware and quartzware should be cleaned in the same way and then combusted at 450°C for 6 hours to remove any trace organics. Ideally, the bacterial abundance throughout the experiments should be monitored. Numerous techniques exist for this, including flow cytometry (Zhu et al., 2020).

DOM QUANTIFICATION AND PROPERTIES

Plastic-derived DOM generated during incubation in microcosms or mesocosms can be qualified and quantified in the following ways.

Dissolved Organic Carbon

DOM is generally quantified as dissolved organic carbon (Dittmar and Stubbins, 2014). Samples are filtered and then acidified to pH <2 using hydrochloric acid before analysis using a TOC analyzer (e.g., Shimadzu). For marine work, certified DOC Consensus Reference Materials (CRM, University of Miami; https://hansell-lab.earth.miami.edu/_assets/pdf/lc-table-1-consensus-values-for-doc-and-tdn_2021.pdf) should be used to confirm accuracy and consistency with the international marine DOC community. Routine minimum DOC detection limits are 0.034 mg C L^{-1}, and standard errors are typically 1.7 ± 0.5% of the DOC concentration. The accumulation of plastic-derived DOC can be normalized to the initial plastic weight, initial plastic carbon weight, or initial plastic surface area.

Optical Properties of DOM

The optical properties of DOM are measured via absorption or fluorescence spectrophotometry (Dittmar and Stubbins, 2014). Samples are filtered and stored in the dark, but not acidified or frozen, and are ideally measured within a day of sampling.

Absorbance spectra (typically from 230 nm to 750 nm), including the spectral slope, provide information about the chemistry (e.g., aromaticity, molecular weight), origin, and degradation of DOM in the environment (Helms et al., 2008; Loiselle et al., 2009b). Fluorescent excitation-emission matrix spectra (EEMs) give information about DOM quality, including signatures that may correspond to DOM photo- and biolability (Coble, 1996; Dittmar and Stubbins, 2014; Fellman et al., 2010).

When sealed quartz cuvettes (10 cm path length, Hellma 120-QS, Quartz SUPRASIL, Helma Analytics) are used as microcosms, absorption can be analyzed without invasive sampling by positioning the cuvettes in a spectrophotometer and then returning them to the experimental conditions (Galgani et al., 2018). Plastics used in these circumstances should have densities sufficiently different from water so the plastics do not remain in the light path of the cuvettes. As biofilms may form on the cuvette surface, cells should be cleaned prior to analysis. Monitoring changes in CDOM absorbance in this way is a low cost, low impact method for assessing the impacts of plastics on aquatic DOM.

Ultrahigh-Resolution Mass Spectrometry

Ultrahigh-resolution mass spectrometry resolves the molecular complexity of DOM. Fourier-transform ion cyclotron resonance mass spectrometry (FT-ICRMS) coupled with soft ionization techniques such as electrospray ionization (ESI) is used to simultaneously detect the exact mass of tens of thousands of molecular ions within DOM samples. Molecular formulas are then assigned to the exact masses. Each identified molecular formula can have numerous structural isomers (Dittmar and Stubbins, 2014).

Nuclear Magnetic Resonance Spectroscopy

To obtain information about the molecular structures present in DOM, solid and liquid state nuclear magnetic resonance spectroscopy (NMR) can be applied (for reviews see Mopper et al., 2007; Dittmar and Stubbins, 2014). The NMR approach depends upon what information is desired and the NMR available. For most NMR methods, isolates or concentrates of DOM are required to increase signal strength or separate the DOM from inorganics that degrade signal quality. For seawater samples, low salt isolates are generated via solid phase extraction or reverse osmosis coupled to electrodialysis (Green et al., 2014). Cryoprobes (Kovacs et al., 2005; Bruker 500 MHz spectrometer, equipped with cryoprobe) with water suppression pulse sequences now allow simple, one-dimensional ^{1}H-NMR spectra to be determined directly from seawater samples (McKay, 2011). Plastic-derived DOM is a complex mixture of thousands of molecules that approach natural DOM in complexity. Thus, structural signatures observed by NMR are average structural properties for the suite of molecules present and are not easily resolved to the molecular level (Mopper et al., 2007; Dittmar and Stubbins, 2014).

Support Technologies

The degradation of plastic and the release of plastic-DOM impacts natural waters and the plastics themselves. For waters, continuous measurement of dissolved oxygen can provide important information on microbial activity and oxygen use during plastic-photooxidation. Oxygen content can be measured in gas-tight micro- and mesocosms using self-adhesive sensor spots (e.g., PyroScience, Aachen, Germany) with oxygen probes, or, for high precision, the Winkler method.

Changes in the surface conditions of plastic samples can be determined using scanning electron microscopy (SEM), FTIR, and time-of-flight secondary ion mass spectrometry (ToF-SIMS). SEM provides detailed surface texture information for plastic fragments, while FTIR and ToF-SIMS provide information on the formation of new organic structures (e.g., carbonyl groups) and the incorporation of inorganic

elements onto the plastic surface. ToF-SIMS provides spatially resolved chemical composition (Carretti et al., 2022). Simple gravimetric approaches provide an overall indication of material lost during degradation, whereas thermogravimetry can evaluate changes in polymer structure caused by photodegradation (Pashaei et al., 2021).

CONCLUSIONS

Plastics are an emergent organic geomaterial with unknown consequences for the Earth system. As plastics photodegrade in natural waters, they release DOM that may impact marine ecology and biogeochemistry, particularly in the surface microlayer. In this brief review, we introduce some experimental and analytical methods for studying this phenomenon. Some potential impacts of plastic-derived DOM on marine ecosystems are also noted. However, much is unknown about the photochemical processes that dissolve plastics and the chemical products formed. Fortunately, oceanographers have studied DOM for a century and have a mature toolbox of methods for monitoring and modeling these changes. Those wishing to study plastic-derived DOM should become familiar with the broader DOM literature (e.g., Hansell and Carlson, 2014) as well as the environmental photodegradation literature. We provide links to some gateway reviews into the DOM literature that may assist readers who wish to expand the field.

REFERENCES

Beneš, P., and M. Paulenová. 1973. Surface charge and adsorption properties of polyethylene in aqueous solutions of inorganic electrolytes. *Kolloid-Zeitschrift und Zeitschrift für Polymere* 251(10):766–771, https://doi.org/10.1007/BF01499104.

Boldrini, A., L. Galgani, M. Consumi, and S.A. Loiselle. 2021. Microplastics contamination versus inorganic particles: Effects on the dynamics of marine dissolved organic matter. *Environments* 8(3):21, https://doi.org/10.3390/environments8030021.

Bracchini, L., A. Tognazzi, A.M. Dattilo, F. Decembrini, C. Rossi, and S.A. Loiselle. 2010. Sensitivity analysis of CDOM spectral slope in artificial and natural samples: An application in the central eastern Mediterranean Basin. *Aquatic Sciences* 72:485–498, https://doi.org/10.1007/s00027-010-0150-y.

Carlson, D.J. 1982. Phytoplankton in marine surface microlayers. *Canadian Journal of Microbiology* 28:1,226–1,234, https://doi.org/10.1139/m82-183.

Carretti, E., G. Poggi, E. Ghelardi, F. Porpora, A. Magnani, E. Fratini, L. Dei, and M. Consumi. 2022. Nanostructured fluids confined into Highly Viscous Polymeric Dispersions as cleaning tools for artifacts: A rheological, SAXS, DSC and TOF-SIMS study. *Colloids and Surfaces A: Physicochemical and Engineering Aspects* 646:128968, https://doi.org/10.1016/j.colsurfa.2022.128968.

Coble, P.G. 1996. Characterization of marine and terrestrial DOM in seawater using excitation-emission matrix spectroscopy. *Marine Chemistry* 51(4):325–346, https://doi.org/10.1016/0304-4203(95)00062-3.

Dittmar, T., and A. Stubbins. 2014. Dissolved organic matter in aquatic systems. Pp. 125–156 in *Treatise on Geochemistry,* 2nd ed. Elsevier, Oxford, UK.

Eyheraguibel, B., M. Traikia, S. Fontanella, M. Sancelme, S. Bonhomme, D. Fromageot, J. Lemaire, G. Lauranson, J. Lacoste, and A.M. Delort. 2017. Characterization of oxidized oligomers from polyethylene films by mass spectrometry and NMR spectroscopy before and after biodegradation by a *Rhodococcus rhodochrous* strain. *Chemosphere* 184:366–374, https://doi.org/10.1016/j.chemosphere.2017.05.137.

Fellman, J.B., E. Hood, and R.G.M. Spencer. 2010. Fluorescence spectroscopy opens new windows into dissolved organic matter dynamics in freshwater ecosystems: A review. *Limnology and Oceanography* 55(6):2,452–2,462, https://doi.org/10.4319/lo.2010.55.6.2452.

Galgani, L., A. Engel, C. Rossi, A. Donati, and S.A. Loiselle. 2018. Polystyrene microplastics increase microbial release of marine chromophoric dissolved organic matter in microcosm experiments. *Scientific Reports* 8(1):14635, https://doi.org/10.1038/s41598-018-32805-4.

Galgani, L., M. Tsapakis, P. Pitta, A. Tsiola, E. Tzempelikou, I. Kalantzi, C. Esposito, A. Loiselle, A. Tsotskou, S. Zivanovic, and E. Dafnomili. 2019. Microplastics increase the marine production of particulate forms of organic matter. *Environmental Research Letters* 14(12):124085, https://doi.org/10.1088/1748-9326/ab59ca.

Galgani, L., and S.A. Loiselle. 2021. Plastic pollution impacts on marine carbon biogeochemistry. *Environmental Pollution* 268:115598, https://doi.org/10.1016/j.envpol.2020.115598.

Galgani, L., E. Tzempelikou, I. Kalantzi, A. Tsiola, M. Tsapakis, P. Pitta, C. Esposito, A. Tsotskou, I. Magiopoulos, R. Benavides, and T. Steinhoff. 2023. Marine plastics alter the organic matter composition of the air-sea boundary layer, with influences on CO_2 exchange: A large-scale analysis method to explore future ocean scenarios. *Science of the Total Environment* 857:159624, https://doi.org/10.1016/j.scitotenv.2022.159624.

Gewert, B., M.M. Plassmann, and M. MacLeod. 2015. Pathways for degradation of plastic polymers floating in the marine environment. *Environmental Science: Processes & Impacts* 17(9):1,513–1,521, https://doi.org/10.1039/C5EM00207A.

Green, N.W., E.M. Perdue, G.R. Aiken, K.D. Butler, H. Chen, T. Dittmar, J. Niggemann, and A. Stubbins. 2014. An intercomparison of three methods for the large-scale isolation of oceanic dissolved organic matter. *Marine Chemistry* 161:14–19, https://doi.org/10.1016/j.marchem.2014.01.012.

Hansell, D., C. Carlson, D. Repeta, and R. Schlitzer. 2009. Dissolved organic matter in the ocean: A controversy stimulates new insights. *Oceanography* 22(4):202–211, https://doi.org/10.5670/oceanog.2009.109.

Hansell, D., and C. Carlson, eds. 2014. *Biogeochemistry of Marine Dissolved Organic Matter.* Academic Press, 712 pp.

Helms, J.R., A. Stubbins, J.D. Ritchie, and E.C. Minor. 2008. Absorption spectral slopes and slope ratios as indicators of molecular weight, source, and photobleaching of chromophoric dissolved organic matter. *Limnology and Oceanography* 54(3):955–969, https://doi.org/10.4319/lo.2009.54.3.1023.

Kovacs, H., D. Moskau, and M. Spraul. 2005. Cryogenically cooled probes—A leap in NMR technology. *Progress in Nuclear Magnetic Resonance Spectroscopy* 46(2–3):131–155, https://doi.org/10.1016/j.pnmrs.2005.03.001.

Loiselle, S.A., L. Bracchini, A. Cózar, A.M. Dattilo, A. Tognazzi, and C. Rossi. 2009a. Variability in photobleaching yields and their related impacts on optical conditions in subtropical lakes. *Journal of Photochemistry and Photobiology B: Biology* 95(2):129–137, https://doi.org/10.1016/j.jphotobiol.2009.02.002.

Loiselle, S.A., L. Bracchini, A.M. Dattilo, M. Ricci, A. Tognazzi, A. Cózar, and C. Rossi. 2009b. The optical characterization of chromophoric dissolved organic matter using wavelength distribution of absorption spectral slopes. *Limnology and Oceanography* 54(2):590–597, https://doi.org/10.4319/lo.2009.54.2.0590.

Loiselle, S., D. Vione, C. Minero, V. Maurino, A. Tognazzi, A.M. Dattilo, C. Rossi, and L. Bracchini. 2012. Chemical and optical phototransformation of dissolved organic matter. *Water Research* 46(10):3,197–3,207, https://doi.org/10.1016/j.watres.2012.02.047.

MacLeod, M., H.P.H. Arp, M.B. Tekman, and A. Jahnke. 2021. The global threat from plastic pollution. *Science* 373(6550):61–65, https://doi.org/10.1126/science.abg5433.

McKay, R.T. 2011. How the 1D-NOESY suppresses solvent signal in metabonomics NMR spectroscopy: An examination of the pulse sequence components and evolution. *Concepts in Magnetic Resonance Part A* 38A(5):197–220, https://doi.org/10.1002/cmr.a.20223.

Mopper, K., A. Stubbins, J.D. Ritchie, H.M., Bialk, and P.G. Hatcher. 2007. Advanced instrumental approaches for characterization of marine dissolved organic matter: Extraction techniques, mass spectrometry, and nuclear magnetic resonance spectroscopy. *Chemical Reviews* 107(2):419–442, https://doi.org/10.1021/cr050359b.

Mopper, K., D.J. Kieber, and A. Stubbins. 2015. Marine photochemistry of organic matter: Processes and impacts. Pp. 389–450 in *Biogeochemistry of Marine Dissolved Organic Matter,* vol. 2. D. Hansell and C. Carlson, eds, Academic Press, https://doi.org/10.1016/B978-0-12-405940-5.00008-X.

Pashaei, R., S.A. Loiselle, G. Leone, G. Tamasi, R. Dzingelevičienė, T. Kowalkowski, M. Gholizadeh, M. Consumi, S. Abbasi, V. Sabaliauskaitė, and B. Buszewski. 2021. Determination of nano and microplastic particles in hypersaline lakes by multiple methods. *Environmental Monitoring and Assessment* 193(10):1–15, https://doi.org/10.1007/s10661-021-09470-8.

Pitta, P., J.C. Nejstgaard, T.M. Tsagaraki, S. Zervoudaki, J.K. Egge, C. Frangoulis, A. Lagaria, I. Magiopoulos, S. Psarra, R.A. Sandaa, and E.F. Skjoldal. 2016. Confirming the "rapid phosphorus transfer from microorganisms to mesozooplankton in the Eastern Mediterranean Sea" scenario through a mesocosm experiment. *Journal of Plankton Research* 38(3):502–521, https://doi.org/10.1093/plankt/fbw010.

Romera-Castillo, C., M. Pinto, T.M. Langer, X.A. Álvarez-Salgado, and G.J. Herndl. 2018. Dissolved organic carbon leaching from plastics stimulates microbial activity in the ocean. *Nature Communications* 9:1430, https://doi.org/10.1038/s41467-018-03798-5.

Stubbins, A., and T. Dittmar. 2012. Low volume quantification of dissolved organic carbon and dissolved nitrogen. *Limnology and Oceanography: Methods* 10(5):347–352, https://doi.org/10.4319/lom.2012.10.347.

Stubbins, A., K.L. Law, S.E. Munoz, T.S. Bianchi, and L. Zhu. 2021. Plastics in the Earth system. *Science* 373:51–55, https://doi.org/10.1126/science.abb0354.

Van Sebille, E., C. Wilcox, L. Lebreton, N. Maximenko, B.D. Hardesty, J.A. Van Franeker, M. Eriksen, D. Siegel, F. Galgani, and K.L. Law. 2015. A global inventory of small floating plastic debris. *Environmental Research Letters* 10(12):124006, https://doi.org/10.1088/1748-9326/10/12/124006.

Zhu, L., S. Zhao, T.B. Bittar, A. Stubbins, and D. Li. 2020. Photochemical dissolution of buoyant microplastics to dissolved organic carbon: Rates and microbial impacts. *Journal of Hazardous Materials* 383:121065, https://doi.org/10.1016/j.jhazmat.2019.121065.

ARTICLE DOI. https://doi.org/10.5670/oceanog.2023.s1.14

On the Potential for Optical Detection of Microplastics in the Ocean

By Daniel Koestner, Robert Foster, and Ahmed El-Habashi

Since the advent of industrial manufacturing of petroleum-based plastics, their use in everyday products has become ubiquitous due to their durability, moldability, low weight, and affordability. Consequently, plastics have quickly become one of the largest components of solid waste pollution on the planet and can now be found in marine sediment, coastal waters, surface waters of oceanic gyres, and marine organisms. However, the extent of this problem has yet to be fully understood, in part due to the challenges associated with discrete water sampling in the vast global ocean. Optical detection of microplastics is one promising approach with the potential to circumnavigate the temporal and spatial limitations of discrete water sampling, though methodological techniques are still in their infancy and libraries of inherent optical properties (IOPs) of microplastics are sparse.

The IOPs of any particle suspended in seawater describe the amount of absorption (loss) and scattering (redirection) of light per unit distance. Scattering events also involve changes in the polarization state of light, which describes the orientation of electromagnetic field oscillations. These optical properties are functions of material properties such as particle concentration, size, shape, and composition. Measurements of the IOPs are key to unlocking the potential for remote detection of any specific particle type from satellite or above-water observations. Furthermore, knowledge of the IOPs is useful for interpreting underwater measurements that are not accessible by above-water observations but that can be collected by profiling or autonomous platforms surveying subsurface waters.

The current state of our understanding of the abundance and distribution of marine plastic pollution using above-water optical measurements is limited to positively buoyant macroplastics (Hu, 2021; Zhou et al., 2021) that are large enough to be detected by satellite sensors or other above-water observations. However, marine microplastics are of particular concern given their higher concentrations and strong potential for bioaccumulation through ingestion by smaller organisms near the bottom of marine food webs. Microplastics are typically defined as >1 μm and <5 mm in size; however, the microplastics that can be ingested by zooplankton and other small filter feeders are typically missed by the standard 333 μm sampling mesh used in many field studies (Cole et al., 2013; Brandon et al., 2020). Because detection and quantification of small phytoplankton from optical observations is possible, it is reasonable to believe that microplastics can be detectable as well, despite challenges related to concentration and particle variability. If we are to overcome these challenges, we need to advance our knowledge of the IOPs of microplastics.

We have begun to address this knowledge gap by making a comprehensive suite of optical measurements on virgin microplastic samples (Figure 1). These measurements can be utilized to identify optical fingerprints of microplastics and aid in the development of detection approaches. We present some results from this research, including measurements of six microplastic samples. These include four samples generated from industrial-grade sheets of commonly utilized plastic (i.e., glycol-modified polyethylene terephthalate [PETG], polystyrene [PS], polyvinyl chloride [PVC], and polypropylene [PP]), and two samples of other common plastic pollutants derived from washing of synthetic fabrics and clothing (i.e., dryer lint [DL] and polyester fibers [PEF]).

To generate a size-spectrum of relatively small microplastic particles that generally remain suspended in water,

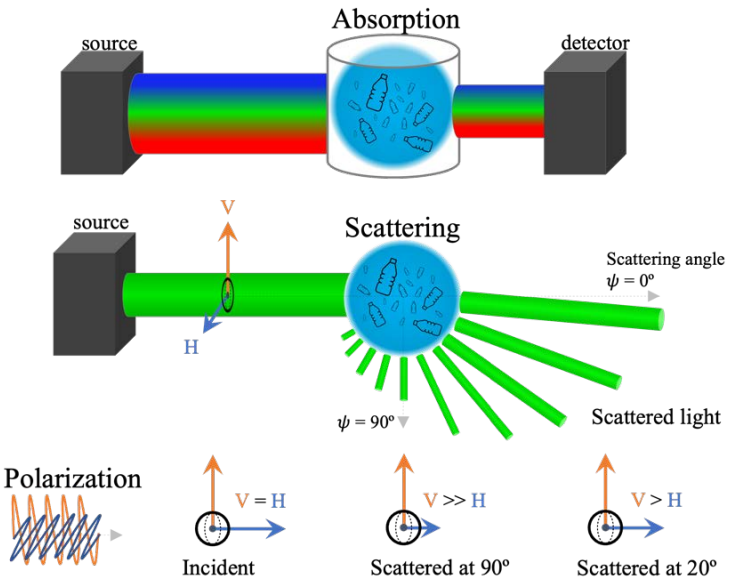

FIGURE 1. Schematic describing absorption and scattering measurements of microplastic samples. The size of each light beam is proportional to the intensity of the light. All scattered and transmitted light is collected by the detector for the absorption measurement, whereas the scattered light, 15°–150° in 1° increments, is measured to derive scattering and polarization properties. The intensity of light oscillating in the vertical (V) and horizontal (H) orientations is measured using polarizing filters placed before the detector. Note that light is considered randomly polarized when V = H.

the original samples were shaved into small pieces and blended using a typical kitchen blender with ice cubes made from deionized and 0.2 µm filtered water. The blended and concentrated samples were then further subsampled for optical characterization. Figure 2 shows example images of particles from the six plastic samples. These microplastic samples contained particles of many sizes and irregular shapes, with some notable differences between plastic types. The particles generated from the sheet-based samples are irregularly shaped with lots of rough edges. The PS particles have some unique dimensionality with visible folding, while PETG, PP, and PVC appear more solid and rigid. The DL particles tend to have fibers with rough surfaces, while PEF have soft and round edges (Figure 2).

Figure 3 depicts measurement results of the inherent optical properties for the microplastic samples. For comparison, Figure 3 also includes measurement results from a selection of contrasting natural seawater samples from Southern California and Northern Alaska (Koestner et al., 2021). The seawater samples represent a large range of conditions, from turbid and inorganic-dominated to phytoplankton and organic-dominated particle assemblages. Generally, microplastic particles have several unique optical features in comparison with typical seawater samples. First, the microplastic samples tend to have spectrally flat absorption and relatively low absorption of blue and green light (λ = 400–550 nm; Figure 3a). Second, the microplastic samples have relatively high scattering in the backwards angles (ψ = 90°–180°; Figure 3b). A signal observed by a satellite or above-water sensor becomes stronger with increased backscattering and decreased absorption, two areas where microplastics exhibit noteworthy differences from natural seawater samples. Finally, microplastic samples generally have low values of the degree of linear polarization, which indicate that these particles depolarize light more effectively than typical marine particles (Figure 3c). In this sense, the use of polarizing filters may provide an additional advantage in terms of detectability.

These results are quite promising, though more work is needed to develop specific algorithms or instrumentation capable of detecting and quantifying microplastic particles suspended in seawater. For example, the optical properties of microplastics are expected to change after photodegradation and pigmentation, and when bacteria or phytoplankton live on the surface in biofilms; therefore, measurement results of virgin microplastic samples may have some limitations (Garaba and Dierssen, 2018). Our results also suggest that differentiating between polymer types may be challenging using optical measurements

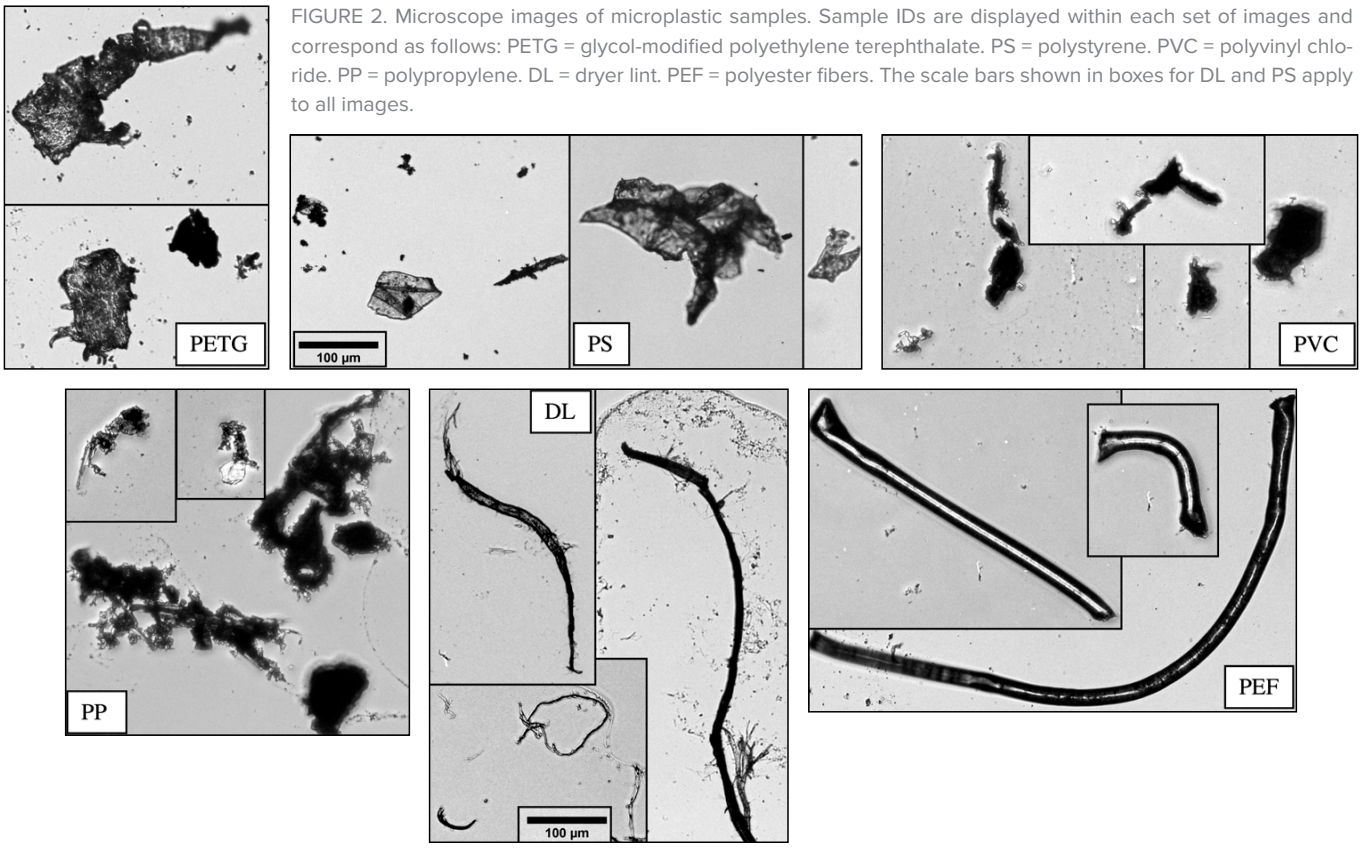

FIGURE 2. Microscope images of microplastic samples. Sample IDs are displayed within each set of images and correspond as follows: PETG = glycol-modified polyethylene terephthalate. PS = polystyrene. PVC = polyvinyl chloride. PP = polypropylene. DL = dryer lint. PEF = polyester fibers. The scale bars shown in boxes for DL and PS apply to all images.

with visible light (note both similarities and differences in optical properties of different microplastics in Figure 3). Nonetheless, these measurements are extremely useful for further development of optical detection techniques and understanding of limitations because they can be used in modeling simulations of the ocean light field. In particular, the measurements we present are more representative of the types of microplastics (smaller than about 333 µm in diameter) that are likely entering marine food webs (Cole et al. 2013; Brandon et al., 2020), as opposed to microplastics greater than about 333 µm, which have been examined in other studies (e.g., Garaba and Dierssen, 2018; Hu, 2021).

REFERENCES

Hu, C. 2021. Remote detection of marine debris using satellite observations in the visible and near infrared spectral range: Challenges and potentials. *Remote Sensing of Environment* 259:112414, https://doi.org/10.1016/j.rse.2021.112414.

Cole, M., P. Lindeque, E. Fileman, C. Halsband, R. Goodhead, J. Moger, and T.S. Galloway. 2013. Microplastic ingestion by zooplankton. *Environmental Science & Technology* 47:6,646–6,655, https://doi.org/10.1021/es400663f.

Brandon, J.A., A. Freibott, and L.M. Sala. 2020. Patterns of suspended and salp-ingested microplastic debris in the North Pacific investigated with epifluorescence microscopy. *Limnology and Oceanography Letters* 5:46–53, https://doi.org/10.1002/lol2.10127.

Garaba, S.P., and H.M. Dierssen. 2018. An airborne remote sensing case study of synthetic hydrocarbon detection using short wave infrared absorption features identified from marine-harvested macro- and microplastics. *Remote Sensing of Environment* 205:224–235, https://doi.org/10.1016/j.rse.2017.11.023.

Koestner, D., D. Stramski, and R.A. Reynolds. 2021. Characterization of suspended particulate matter in contrasting coastal marine environments with angle-resolved polarized light scattering measurements. *Applied Optics* 60:11,161–11,179, https://doi.org/10.1364/AO.441226.

Zhou, S., T. Kuester, M. Bochow, N. Bohn, M. Brell, and H. Kaufmann. 2021. A knowledge-based, validated classifier for the identification of aliphatic and aromatic plastics by WorldView-3 satellite data. *Remote Sensing of Environment* 264:112596, https://doi.org/10.1016/j.rse.2021.112598.

ACKNOWLEDGMENTS

This research was funded by the US National Aeronautics and Space Administration (80HQTR21T0051) and the Office of Naval Research. It was initiated while the first author (DK) held an NRC Research Associateship award at the Naval Research Laboratory in Washington, DC, and completed with support from the European Union's Horizon 2020 Framework Programme for Research and Innovation under the Marie Skłodowska-Curie grant agreement No. 101034309. We would like to express our gratitude to Shungu Garaba, The Ocean Cleanup, and the European Space Agency for supplying the plastic standard samples and to Dariusz Stramski for loaning the light scattering meter.

ARTICLE DOI. https://doi.org/10.5670/oceanog.2023.s1.15

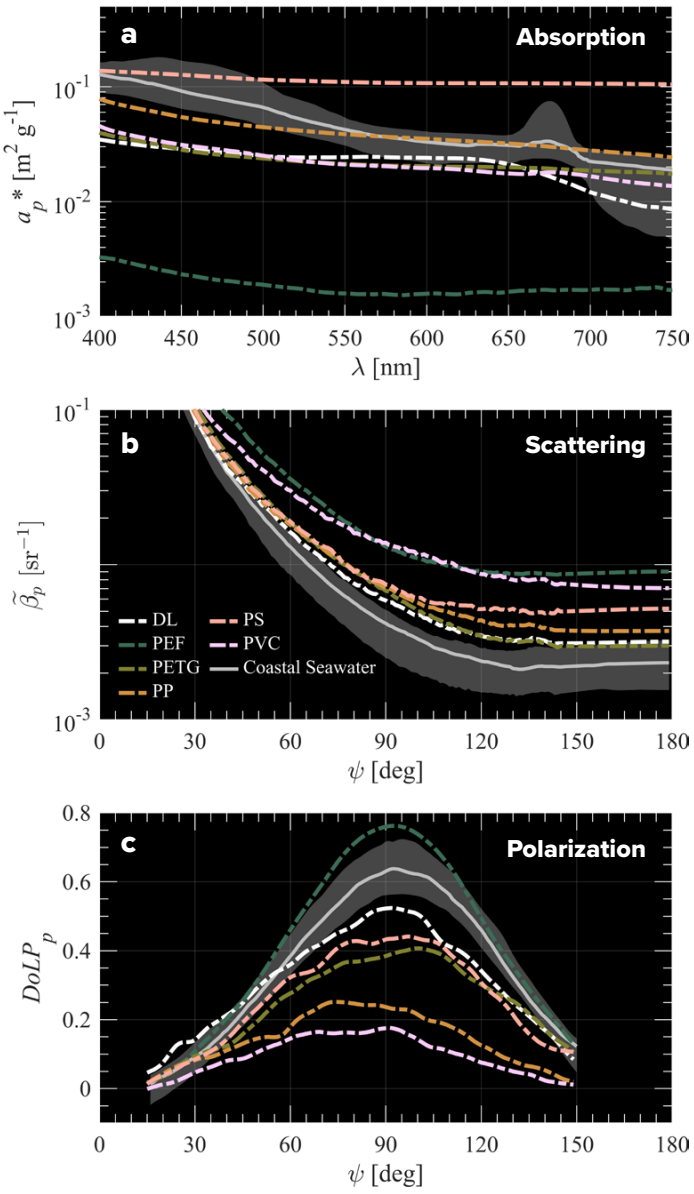

FIGURE 3. (a) Absorption, (b) scattering, and (c) polarization properties of six microplastic samples in comparison with coastal seawater samples from Southern California and Northern Alaska. Microplastic samples are plotted with dash-dotted lines. Solid gray lines represent median data and gray shaded regions represent 10th and 90th percentile data from 52 natural seawater samples from nearshore oceanic and coastal waters. Panel (a) shows the particulate absorption spectra normalized by particle mass concentration for each of the six samples, (b) shows the particulate phase function $\tilde{\beta}_p$ (the normalized intensity of the scattered light as a function of angle), and (c) shows the particulate degree of linear polarization $DoLP_p$ (the fraction of scattered light that is linearly polarized in the vertical orientation as a function of angle). Note that these results refer to absorption and scattering properties of particles only, with contributions of molecular water and dissolved salts removed. Data shown in (b) and (c) utilize only green light of wavelength λ = 532 nm.

Sediment Traps: A Renowned Tool in Oceanography Applied to New Marine Pollutants

By Luisa Galgani, Helmke Hepach, Kevin W. Becker, and Anja Engel

Particles afloat in the ocean are important components of marine element cycles. Most of this particulate matter is suspended in the sunlit surface layer and is mainly composed of microscopic living and dead organisms and fecal pellets. Aggregation of small, suspended particles into large, rapidly sinking aggregates can transport surface-derived material to the deep ocean and the seafloor, contributing to the so-called biological pump. The comprehensive analysis of these sinking particles has increased our understanding of important biogeochemical ocean processes, such as the relationship between the rate of primary production and downward flux of particulate organic matter, the biological control of the removal of abiogenic particles from the surface ocean, and seasonal or interannual variations in downward particle fluxes. Sediment traps have been widely used since the late 1970s to capture the downward flux of particles for study (e.g., Staresinic et al., 1978; Knauer et al., 1979).

While helping us to understand how fast "natural" elements such as carbon and nutrients (i.e., nitrogen, phosphorus, and iron) are exported from the surface to the deep ocean on various timescales, sediment traps can also provide important information on fluxes and removal rates of anthropogenic pollutants such as plastic particles. Although plastic is very resistant to (bio-)degradation and can remain in the marine environment for hundreds of years, physical, chemical, and biological stressors break down larger plastic debris into micro- and nanoplastics that threaten marine life.

The fate of marine plastic is little understood. Flux estimates of plastic input into the ocean and actual concentrations observed suggest an unidentified sink. The interaction of plastic with sinking biological material in the ocean might explain a large fraction of the missing plastic mass inventory (van Sebille et al., 2020).

TRAPPING SINKING PLASTIC PARTICLES

Plastic is transported both horizontally and vertically in the ocean. To look for the missing plastic, we deployed multi-level, surface-tethered drifting sediment traps in the summer of 2019 during a cruise to the North Atlantic Gyre, one of the hotspots of plastic debris accumulation (Galgani et al., 2022; Figure 1). Surface-tethered sediment traps can drift along the paths of ocean currents and enable identification of areas of high plastic concentration.

The trap setup consisted of eight PVC cross-shaped arrays hooked to a main line to collect sinking material at depths of 50 m, 100 m, 150 m, 200 m, 300 m, 400 m, 500 m, and 600 m. Each array contained 12 tubular Particle Interceptor Traps (PITs; Figure 2), with an aspect ratio of 7.5 and a collection area of 0.0038 m^2. The main line carried a ground weight and various floats as well as a yellow buoy at the top with two GPS beacons (Argos and Iridium), and a flashing light to allow continuous tracking and recovery of the traps at the end of the drift period (Figure 2).

PIT preparation and sample recovery followed Engel et al. (2017). The traps were left to drift in the water for four to five days to ensure collection of sufficient material for later analysis. After recovery, the collected material was pre-screened (500 µm) to remove swimmers and visible plastic particles for later identification, and the remaining material was then split into aliquots for different analyses.

More recently, we deployed a similar setup in the southwestern Baltic Sea as part of the Boknis Eck Marine Time Series Station in Eckernförde Bay (Germany) (Figure 3; for more information, see https://www.bokniseck.de/). The sediment trap array is moored in a restricted area close to the time-series station, where the water depth is about 17 m (Figure 1). Sinking material is collected at about 5 m and 9 m depth. The whole system is moored with a ~600 kg weight. Each array contains four PITs with one lid-sealed PIT per array providing a blank. The sediment traps are exchanged every one to two months. Surface water

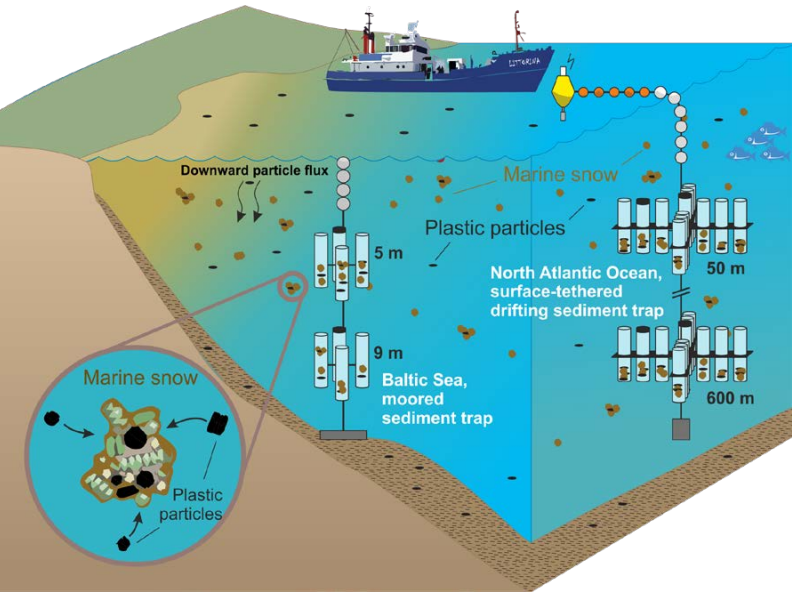

FIGURE 1. Different types of sediment traps are geared for use in coastal waters (Baltic Sea, moored system) and the open ocean (North Atlantic Ocean, surface-tethered, free-drifting system).

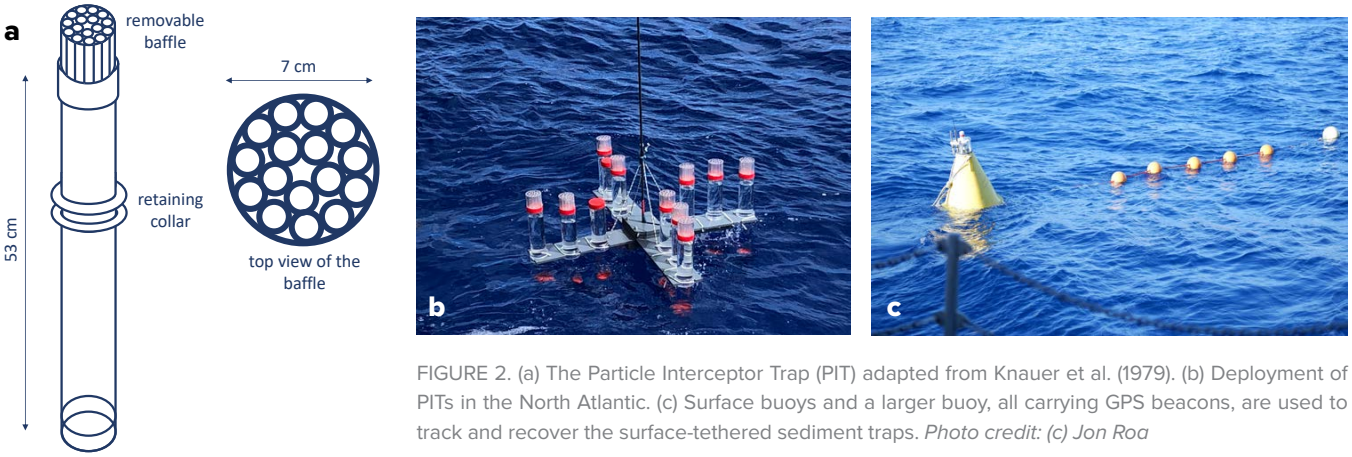

FIGURE 2. (a) The Particle Interceptor Trap (PIT) adapted from Knauer et al. (1979). (b) Deployment of PITs in the North Atlantic. (c) Surface buoys and a larger buoy, all carrying GPS beacons, are used to track and recover the surface-tethered sediment traps. *Photo credit: (c) Jon Roa*

samples are obtained by filtering ~2 L of the brine solution onto 300 µm, 125 µm, 50 µm, and 1 mm sieves.

In contrast to the surface-tethered drifting array, which permits estimations of downward particle fluxes in open waters, the year-round coastal array serves as an in situ particle collector that allows us to study how plastic particles correlate with organic particle abundance over seasonal cycles. This long-term monitoring strategy will enable us to track changes in the marine ecosystem and in plastic concentrations, and will potentially provide information on plastic interaction with biogeochemical and physical processes that drive long-term ecosystem changes.

BLANKS AND CONTAMINATION CONTROL

Sediment trap equipment, including that used for our studies, is usually made from plastics. Therefore, each array (for every depth and every deployment) contains at least one or two PITs serving as blank controls. These PITs are filled with filtered brine and filtered seawater but sealed immediately before deployment, allowing us to account for any potential source of contamination from the system itself at any step of the process. The blanks are successively pooled and treated like the regular samples. As an additional measure, we take particular care to work in 100% cotton clothes while preparing the setup and handling the samples, and we use all glass materials when possible. Moreover, a laboratory blank control is always run to account for possible contamination in the lab during the analysis.

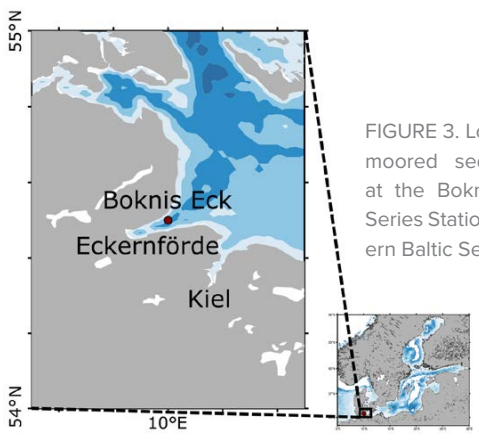

FIGURE 3. Location of the moored sediment traps at the Boknis Eck Time Series Station, southwestern Baltic Sea, Germany.

Sediment traps are a reliable method for studying plastic fluxes and their interactions with biogenic components. Although this approach requires specific platforms for deployment, planned ship time, and ship crews for deployment and recovery, because sediment traps are widely used tools in oceanographic research, they offer a combined opportunity to obtain more data on plastic fluxes and on particle distributions.

REFERENCES

Engel, A., H. Wagner, F.A.C. Le Moigne, and S.T. Wilson. 2017. Particle export fluxes to the oxygen minimum zone of the eastern tropical North Atlantic. *Biogeosciences* 14(7):1,825–1,838, https://doi.org/10.5194/bg-14-1825-2017.

Galgani, L., I. Goßmann, B. Scholz-Böttcher, X. Jiang, Z. Liu, L. Scheidemann, C. Schlundt, and A. Engel. 2022. Hitchhiking into the deep: How microplastic particles are exported through the biological carbon pump in the North Atlantic Ocean. *Environmental Science and Technology*, https://doi.org/10.1021/acs.est.2c04712.

Knauer, G.A., J.H. Martin, and K.W. Bruland. 1979. Fluxes of particulate carbon, nitrogen, and phosphorus in the upper water column of the northeast Pacific. *Deep Sea Research Part A.* 26(1):97–108, https://doi.org/10.1016/0198-0149(79)90089-X.

Staresinic, N., G.T. Rowe, D. Shaughnessey, and A.J. Williams III. 1978. Measurement of the vertical flux of particulate organic matter with a free-drifting sediment trap. *Limnology and Oceanography* 23(3):559–563, https://doi.org/10.4319/lo.1978.23.3.0559.

van Sebille, E., S. Aliani, K. Lavender Law, N. Maximenko, J.M. Alsina, A. Bagaev, M. Bergmann, B. Chapron, I. Chubarenko, A. Cózar, and others. 2020. The physical oceanography of the transport of floating marine debris. *Environmental Research Letters* 15(2):023003, https://doi.org/10.1088/1748-9326/ab6d7d.

ACKNOWLEDGMENTS

Jon Roa, Lindsay Scheidemann, Sandra Golde, Cathleen Schlundt, and the Technology & Logistic Centre at GEOMAR are gratefully acknowledged for their continuous help in the deployment and recovery of the sediment traps over the seas and years. The deployments of the sediment traps are made possible thanks to funding from the Helmholtz Association (GEOMAR) and the Bundesministerium für Bildung und Forschung, BMBF, under the joint research project FACTS ID 03F0849B, JPI-Oceans. LG is funded by the European Union's Horizon 2020 research and innovation programme under the Marie Skłodowska-Curie grant agreement No 882682.

ARTICLE DOI. https://doi.org/10.5670/oceanog.2023.s1.16

Developing Realistic Models for Assessing Marine Plastic Pollution in Semi-Enclosed Seas

By Jun She, Asbjørn Christensen, Francesca Garaventa, Urmas Lips, Jens Murawski, Manolis Ntoumas, and Kostas Tsiaras

INTRODUCTION

The accumulation of plastic debris in the ocean is now recognized as a major environmental problem, with consequences directly affecting not only marine ecosystems but also human well-being. Human activities create plastic litter, much of which is either directly discharged into the ocean or transported to the sea via inland pathways (e.g., rivers, lakes, wastewater treatment plants). Once in the ocean, plastics are further transported and transformed by processes such as ocean currents, winds and waves, water dispersion, fragmentation, biofouling, sinking, and beaching (Figure 1).

Assessing the particle size, concentration, and distribution of plastic pollution in the ocean is a prerequisite for managing and protecting marine ecosystems. The sizes of plastic litter in the sea vary widely, from nanometers to meters, posing great challenges for monitoring and modeling. Because it is costly and complex to monitor seaborne plastics, there are large spatial and temporal gaps in monitoring data that hamper modeling of their distribution and the processes acting upon them.

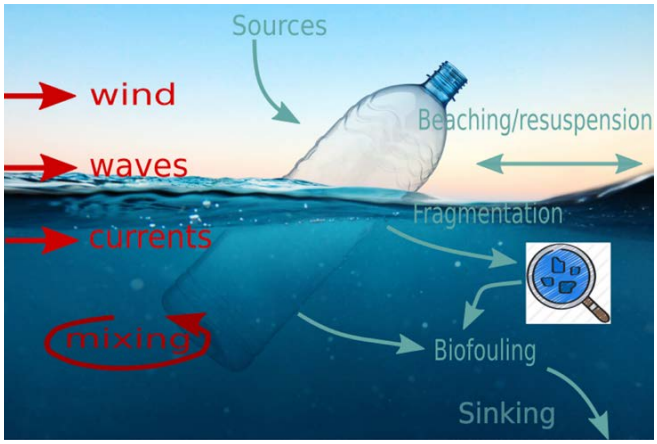

FIGURE 1. An illustration on key marine processes in the transport and transformation of plastic litter in the sea. "Sources" represents plastic litter discharged to the sea from either land or oversea sources. All plastic litter in the sea is forced by physical processes such as ocean currents and wave-induced turbulence mixing, mainly in the upper layer. Macroplastics floating at the sea surface are also affected by winds. "Beaching" is the process whereby plastic litter is retained on the coast. Large plastic litter in the sea can be fragmented into smaller pieces due to degradation. Plastics heavier than seawater will sink to the seabed; lighter plastics can also sink due to biofouling. The plastics reaching the seabed can be resuspended due to waves and currents.

In this paper, we discuss recent progress in developing realistic marine plastic modeling capacity, including mapping plastic sources from land, cost-effective microplastic monitoring, and advanced micro- and macroplastic basin-scale models and their validation for the semi-enclosed Baltic and Mediterranean Seas (Figure 2). Most of the progress is attributed to the plastic modeling team in EU H2020 project CLAIM (Cleaning Litter by Developing and Applying Innovative Methods in European Seas).

MARINE PLASTIC SOURCE MAPPING

The dominant sources of plastics emissions are land-based, such as those emitted from tire wear, painting, laundry (microplastics with particle size <5 mm), and mismanaged bags and bottles (macroplastics). Global plastic litter riverine inputs to the sea have been derived from a regression model based on river mouth plastic concentration measurements and an estimate of mismanaged plastics (Lebreton et al., 2017). This data set, however, has higher uncertainty in regional seas where few river mouth plastic measurements are available, for example, the Baltic Sea. The CLAIM team developed specific methods for mapping microplastic discharges from tire wear and household microplastics from laundry and personal care and cosmetic products. Microplastic emissions on land and discharges to the sea were estimated using socioeconomic

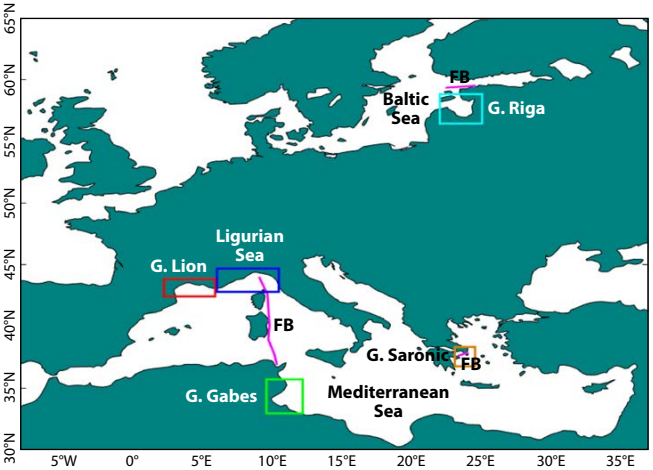

FIGURE 2. Study region of CLAIM (Cleaning Litter by Developing and Applying Innovative Methods in European Seas) covers the Baltic and Mediterranean Seas. The areas that have been modeled at high resolution are the Saronic Gulf (orange), Ligurian Sea (blue), Gulf of Lion (red), Gulf of Gabes (green), and Gulf of Riga (cyan). The FerryBox (FB, magenta) transects are also highlighted.

statistics in European countries, including population density, the number of motor vehicles per country, the distribution and purification capacity of sewage systems and wastewater treatment plants, and geological data (catchment and river distribution and linkages).

MICROPLASTIC OBSERVATIONS IN THE SEA

Marine plastic models require reliable and consistent observations for calibration. Current plastic observations in the sea are measured with different methods that are usually not comparable due to the lack of common monitoring standards. The CLAIM team analyzed 27 microplastic observation data sets to quantify data uncertainties and check consistency among different Baltic Sea data sets (She et al., 2022). It was found that even replicated samples have uncertainties around 40%–56%. In addition, fewer existing data sets contain particle sizes <100 µm.

Recent developments show that the FerryBox system used for ocean physical and biogeochemical monitoring can provide cost-effective and autonomous microplastic measurements. In addition, FerryBox systems can provide measurements for multiple particle size ranges. To avoid contamination from plastic parts in the filtering system, the CLAIM team developed a stainless steel passive seawater flow-through filtering system for sampling plastic particles using FerryBox systems on ships of opportunity (Figure 3).

The instruments were deployed from the ferry C/F *Carthage* during a trip from Tunis to Genoa, the research vessel *Salme* in the Baltic Sea, and the sailing vessel *Marie Galante* in the Saronic Gulf. These test deployments resulted in collection of 65 samples and proved that the system can be configured to sample effectively both in open seas and coastal areas.

MARINE PLASTIC MODELING AND ASSESSMENT

After they reach the sea, plastics are dispersed by winds, ocean currents, and waves. Plastics heavier than seawater sink to the seabed, while lighter ones float. The movement of plastic litter in the sea can be simulated by using numerical models; however, successful modeling of the transport of microplastics in a three-dimensional ocean has only been recently reported (Mountford and Morales Maqueda, 2019).

A major challenge in microplastic modeling is simulating the removal of lighter particles from the water column in order to maintain the observed microplastic concentration in the ocean. A major mechanism for removing plastic from the surface ocean is biofouling. In this process, marine organisms grow on the plastic particles, making them heavier so that they gradually sink. Earlier modeling (Mountford and Morales Maqueda, 2019; Schernewski et al., 2020) did not resolve this process but rather led to excessive unrealistic estimates of microplastic concentrations in the water column. The CLAIM team explicitly parameterized biofouling-induced sinking in its models. Biofilm growth was calculated as a function of ecological and environmental parameters, derived from biogeochemical models. For the Baltic Sea, chlorophyll *a* concentration was used to calculate biofilm growth (Murawski et al., 2022), while for the Mediterranean Sea, algae concentration was used (Tsiaras et al., 2021).

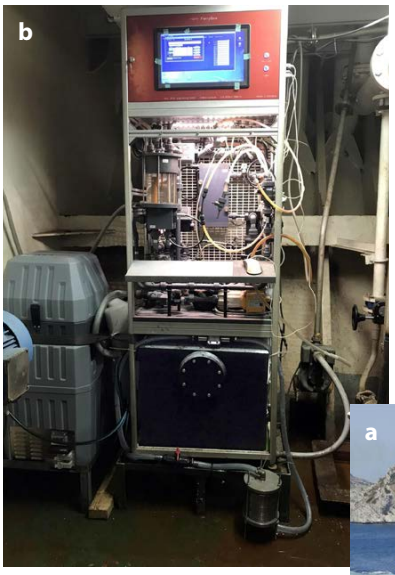

FIGURE 3. (a) The CLAIM project's filtering system was installed in a FerryBox system aboard the ferry C/F *Carthage*. (b) The system's stainless steel mesh filters are housed in the cylinder in the lower part of the framework. *Left photo © Institut National des Sciences et Technologies de la Mer*

Another modeling challenge is to resolve plastic transport in the riverine-estuarine-coastal sea continuum. Inland rivers, lakes, and coastal lagoons play a significant role in the accumulation of plastic litter, and they act as a buffer zone in the pathway of plastic litter to the sea. High-resolution models are needed to resolve the dynamics in the estuarine-coastal continuum. In the Baltic, key areas were modeled with resolutions up to 90 m (Figure 4) to simulate the transition of microplastics from inland waters to the open sea, while also accounting for retention in rivers/lakes (Frishfelds et al., 2022). In the Mediterranean, high-resolution (~800 m) models were implemented in four coastal areas (Figure 1; Tsiaras et al., 2022). The fine-resolution models produced better results than the basin-scale models (Figure 5).

The models developed by the CLAIM team have been applied to simulate microplastics of varying sizes in the Baltic (5, 42, and 300 µm) and in the Mediterranean (50, 200, 350, 500, 1,000, and 2,000 µm). Multiple categories of objects (e.g., bottles, bags, foam) were also included in macroplastic transport models, where wind drag is

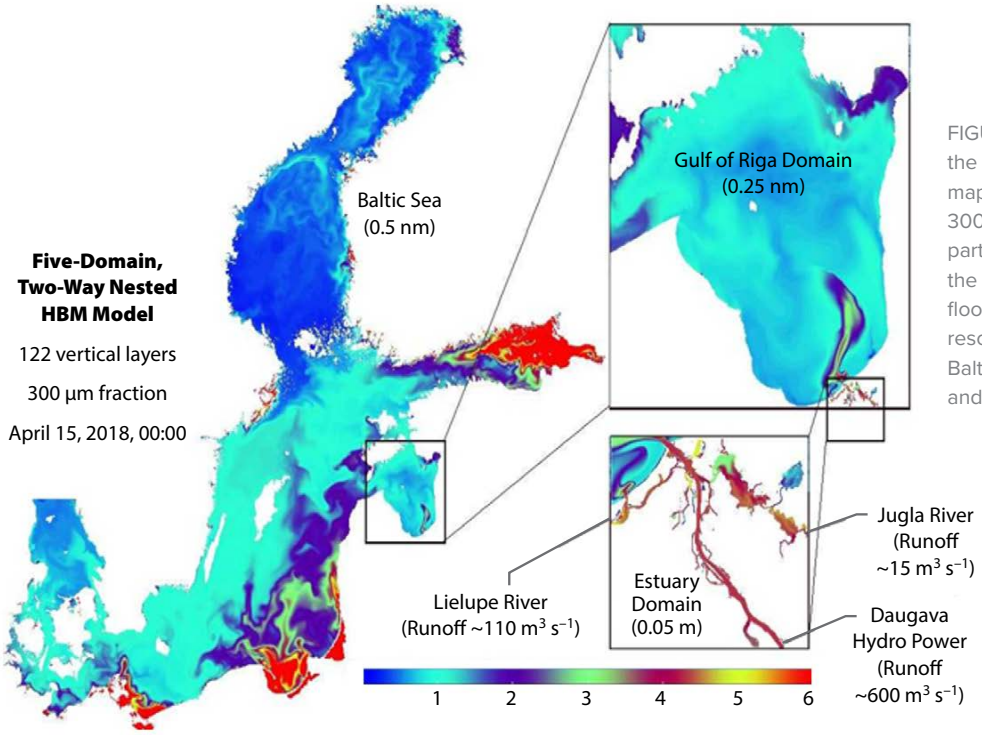

FIGURE 4. High-resolution domains inside the Baltic Sea model domain. The color map represents a surface concentration of 300 µm microplastic particles (number of particles per m^3) on April 15, 2018, within the Daugava River plume after a spring flood (Frishfelds et al., 2022). The model resolution in subregions is 0.5 nm for the Baltic Sea, 0.25 nm for the Gulf of Riga, and 0.05 nm for Latvian inland waters.

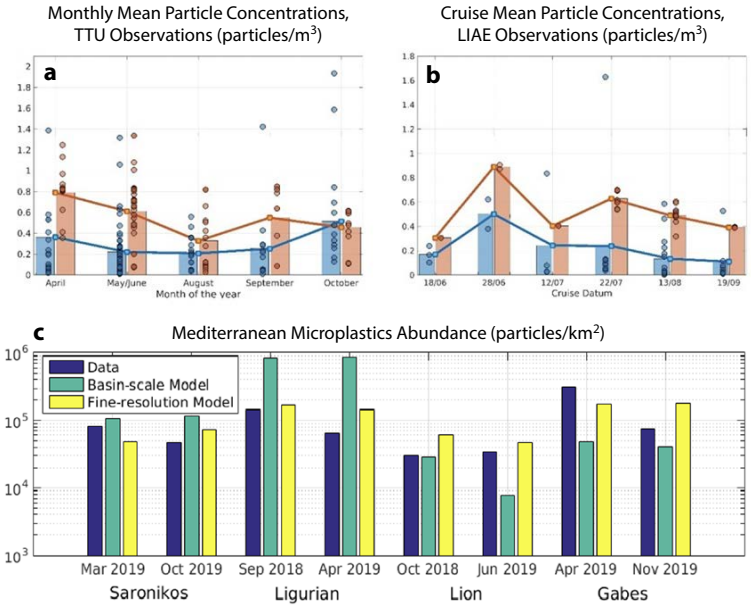

FIGURE 5. Basin-scale validation of simulated microplastic concentrations against in situ observations for >300 µm particles in the Baltic Sea (upper panels) and the Mediterranean Sea (lower panel). (a) In Estonian waters, observations were collected by Tallinn Technical University during 2016–2020 in the Gulf of Finland, the Gulf of Riga, and the Northern Baltic Proper. Spatially averaged monthly mean values are displayed. (b) Latvian waters: observations were collected from five cruises during 2018–2019 by the Latvian Institute of Aquaculture and Ecology, covering the Latvian part of the Gulf of Riga and the eastern Baltic Sea. Cruise mean values are displayed. In (a) and (b), mean values are shown as solid lines and bars, and individual data points are presented in dots (red for observations, blue for model data; Murawski et al., 2022). (c) In situ data (blue bars) from two sampling campaigns (Tsiaras et al., 2022) are plotted along with simulated microplastics mean concentrations from basin-scale (green bars) and fine-resolution (yellow bars) models for four key study areas, Saronic Gulf, Ligurian Sea, Gulf of Lion, and Gulf of Gabes (see Figure 2)

a significant transport mechanism. When calibrated and validated against available observations, all the models exhibited reasonable skill in reconstructing major climatological spatial patterns for both micro- and macroplastics in the Baltic and Mediterranean Seas, although simulated concentrations in some subregions were still under- or overestimated. Correlations between model data and observations were statistically significant. Figure 5 provides one example.

Model outputs can be used to identify ecologically or commercially important areas that are potentially threatened by plastic pollution (e.g., Hatzonikolakis et al., 2022), and modeling tools can be used, by means of scenario simulations, to evaluate the impacts of cleanup activities and management plans for mitigating plastic pollution. An important observation is that pollution plumes from many sources contribute to the streams of plastics that are transported by oceanographic processes. Therefore, mapping of plumes of different plastic fractions is a central task when planning cleanup efforts (Christensen et al., 2021). We concluded from our investigations that pollution plumes are highly variable and directional and cannot be described by a simple distance relationship. Figure 6 shows simulated macroplastic pollution plumes in the Mediterranean.

RECOMMENDATIONS FOR FUTURE RESEARCH

Successful development of realistic marine plastic modeling capacity requires accurate plastic source mapping; sufficient, reliable, and consistent observations; and improved parameterizations.

For monitoring microplastics, common technical standards are needed for sampling and analysis methods to make the data intercomparable, with standards established for mesh size, sampling error, false-zero samples, lack of representativity, and clogging. Cost-effective monitoring capabilities for a wide range of particle sizes and macroplastics are needed. The FerryBox monitoring instrument has been effectively operated for the CLAIM project on several cruises in the Baltic and Mediterranean Seas, as well as during a six-month monitoring period on board a Kiel-Oslo Ferry (van Bavel et al., 2020). It is one of the proven technical solutions and is therefore recommended for wider applications. Better field sampling analysis technology is needed to improve cost effectiveness and timeliness. Large observational gaps exist, especially at the mouths of rivers. Observations related to vertical dynamics, for example, biofouling and resulting sinking and macroplastic fragmentation, are essential for improving the models, but are currently scarce.

For source mapping, we recommend considering individual wastewater treatment plants' cleanup capacity. The size spectrum of microplastic particles needs updating, and improved river retention estimates are needed. Extreme events such as flooding have large impacts on transport of land litter to the sea, but are currently not included in source mapping.

To improve microplastic modeling, major knowledge gaps need to be filled, such as quantifying the processes related to biofouling, resuspension of plastics in the seabed, and macroplastic fragmentation into small particles. For macroplastic modeling, principal uncertainties are the varying wind drag coefficients for different plastic objects, the seasonal dynamics of sinking/breakdown, and beaching/resuspension processes, including fragmentation. Dedicated field experiments may provide new knowledge needed for improving the models. For future model validation and calibration, more coordinated and sustained observation programs are required as well as experiments targeting key processes listed above. Although submesoscale eddies may play an important role in transport of plastics (e.g., Mishra et al., 2022), they are not well resolved in current models.

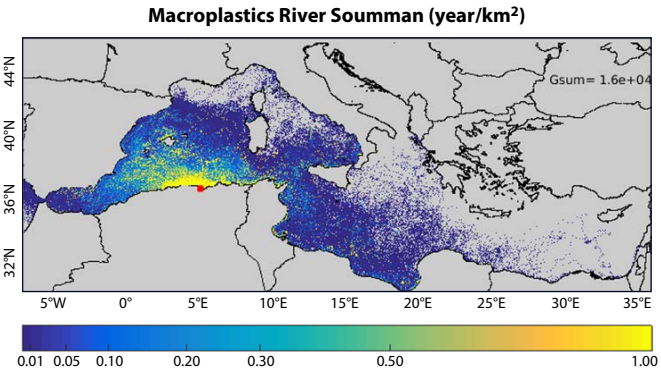

FIGURE 6. Examples of macroplastic plumes for the river Soumman (red dot) in the Mediterranean. The unit of the plume function is yr km^{-2} because the actual pollution (kg km^{-2}) is obtained by multiplying the plume function with the pollution source input rate (kg yr^{-1}).

REFERENCES

Christensen A., K. Tsiaras, J. Murawski, Y. Hatzonikolakis, J. She, M. St. John, U. Lips, and R. Brouwer. 2021. A cross disciplinary framework for cost-benefit optimization of marine litter cleanup at regional scale. *Frontiers in Marine Science* 8:744208, https://doi.org/10.3389/fmars.2021.744208.

Frishfelds, V., J. Murawski, and J. She. 2022. Transport of microplastics from the Daugava Estuary to the open sea. *Frontiers in Marine Science* 9:886775, https://doi.org/10.3389/fmars.2022.886775.

Hatzonikolakis, Y., S. Giakoumi, D.E. Raitsos, K. Tsiaras, S. Kalaroni, G. Triantaphyllidis, and G. Triantafyllou. 2022. Quantifying transboundary plastic pollution in marine protected areas across the Mediterranean Sea. *Frontiers in Marine Science* 8:762235, https://doi.org/10.3389/fmars.2021.762235.

Lebreton, L.C.M., J. van der Zwet, J.-W. Damsteeg, B. Slat, A. Andrady, and J. Reisser. 2017. River plastic emissions to the world's oceans. *Nature Communications* 8:15611, https://doi.org/10.1038/ncomms15611.

Mishra, A., N. Buhhalko, K. Lind, I. Lips, T. Liblik, G. Väli, and U. Lips. 2022. Spatiotemporal variability of microplastics in the eastern Baltic Sea. *Frontiers in Marine Science* 9:875984, https://doi.org/10.3389/fmars.2022.875984.

Mountford, A.S., and M.A. Morales Maqueda. 2019. Eulerian modeling of the three-dimensional distribution of seven popular microplastic types in the global ocean. *Journal of Geophysical Research: Oceans* 124(12):8,558–8,573, https://doi.org/10.1029/2019JC015050.

Murawski, J., J. She, and V. Frishfelds. 2022. Modeling drift and fate of microplastics in the Baltic Sea. *Frontiers in Marine Science* 9:886295, https://doi.org/10.3389/fmars.2022.886295.

Schernewski, G., H. Radtke, R. Hauk, C. Baresel, M. Olshammar, R. Osinski, and S. Oberbeckmann. 2020. Transport and behavior of microplastics emissions from urban sources in the Baltic Sea. *Frontiers in Environmental Science* 8:579361, https://doi.org/10.3389/fenvs.2020.579361.

She, J., N. Buhhalko, K. Lind, A. Mishra, V. Kikas, E. Costa, C. Gambardella, A. Montarsolo, M. Faimali, F. Garaventa, and I. Lips. 2022. Uncertainty and consistency assessment in multiple microplastic observation datasets in the Baltic Sea. *Frontiers in Marine Science* 9:886357, https://doi.org/10.3389/fmars.2022.886357.

Tsiaras, K., Y. Hatzonikolakis, S. Kalaroni, A. Pollani, and G. Triantafyllou. 2021. Modeling the pathways and accumulation patterns of micro- and macro-plastics in the Mediterranean. *Frontiers in Marine Science* 8:743117, https://doi.org/10.3389/fmars.2021.743117.

Tsiaras, K., E. Costa, S. Morgana, C. Gambardella, V. Piazza, M. Faimali, R. Minetti, C. Zeri, M. Thyssen, S. Ben Ismail, and others. 2022. Microplastics in the Mediterranean: Variability from observations and model analysis. *Frontiers in Marine Science* 9:784937, https://doi.org/10.3389/fmars.2022.784937.

van Bavel, B., A.L. Lusher, P.F. Jaccard, S. Pakhomova, C. Singdahl-Larsen, J.H. Andersen, and C. Murray. 2020. *Monitoring of Microplastics in Danish Marine Waters Using the Oslo-Kiel Ferry as a Ship-of-Opportunity.* NIVA-Denmark Report Serial Number 7524-2020, Copenhagen, 35 pp.

ARTICLE DOI. https://doi.org/10.5670/oceanog.2023.s1.17

Ocean Monitoring and Prediction Network for the Sustainable Development of the Gulf of Mexico and the Caribbean

By Juan Carlos Herguera, Edward M. Peters, Julio Sheinbaum, Paula Pérez-Brunius, Vanesa Magar, Enric Pallàs-Sanz, Sheila Estrada Allis, M. Leopoldina Aguirre-Macedo, Victor Manuel Vidal-Martinez, Cecilia Enriquez, Ismael Mariño Tapia, Hector García Nava, Xavier Flores Vidal, Tomas Salgado, Rosario Romero-Centeno, Jorge Zavala-Hidalgo, Eduardo Amir Cuevas Flores, Abigail Uribe Martínez, and Laura Carrillo

The need to understand and forecast disasters driven by anthropogenic and natural forces in the Gulf of Mexico and to support management responses to hazardous events led policymakers, scientists, and industry representatives in Mexico to launch an ocean observation and modeling project (2015–2023) aimed at collecting multi-layered baseline information and continuous monitoring of the ocean environment across the southern Gulf of Mexico. The observational network and modeling efforts, led by the Research Consortium for the Gulf of Mexico (CIGoM), include developing a marine hazard warning system to investigate multiple stressors that are altering the state and health of this large marine ecosystem and its coastal communities. This warning system is intended to aid in the establishment of national contingency plans and mitigate the impacts of extreme events and long-term ocean trends. Stressors include hydrocarbon spills, tropical cyclones, marine heatwaves, long-term ocean surface warming, harmful algal blooms, and massive *Sargassum* landings.

OCEAN OBSERVATIONAL NETWORK

Over the past eight years, CIGoM implemented an extensive observational and modeling effort concerning the deep-sea waters of the southern Gulf of Mexico (GoM; see oceanographic collections at https://atlascigom.cicese.mx/). The collaborative project, which brought together more than 300 researchers from more than two dozen institutions in Mexico and abroad, developed a system of ocean data collection and satellite imagery analysis to continuously observe surface ocean circulation, marine meteorology, ocean waves, and several essential ocean variables, including temperature, salinity, oxygen content, and chlorophyll. The system consists of a network of coastal oceanographic buoys and open-ocean oceanographic and meteorology buoys that were partially developed, designed, and built at the Center for Scientific Research and Higher Education at Ensenada (CICESE; Figure 1 and Table 1). This buoy network transmits continuous hydrographic, oceanographic, and meteorological observations collected from the coastal and oceanic regions of the GoM in real time to CICESE as well as to the Servicios de Manejo Integral de Datos (Comprehensive Data Management Services, SMID; https://smid.cigom.org), a web-based system also developed by CIGoM. A fleet of eight underwater gliders samples the water column continuously from the surface to 1,000 m depth at very high spatial resolution (Figures 1 and 2). A network of high-frequency radars (HFR) on the coast (the only one in Latin America) between Tampico and the Yucatán Peninsula provide continuous measurements of the surface currents up to 170 km offshore over the entire Mexican exclusive economic zone using the Hawai'i line-array approach (Flament et al., 2016; Figure 3). Data from these assets are complemented by analysis of different types of satellite images, ranging from passive (ocean color) sensors that collect information on sea surface temperature and chlorophyll *a* to active (synthetic aperture radars) sensors that allow us to analyze wind and wave fields at the ocean surface. All of these observations—from buoys, gliders, drifters, HFR network stations, and satellite imagery—are integrated in the SMID data management and distribution web platform that can simultaneously display these diverse data in different layers for the user.

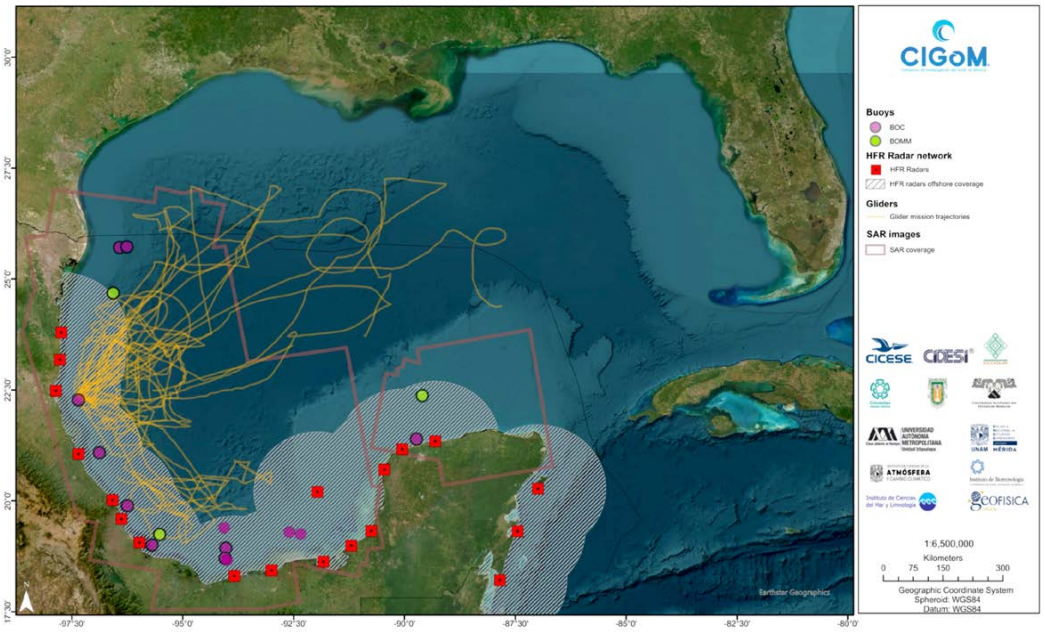

FIGURE 1. Map of observation platforms deployed by the Research Consortium for the Gulf of Mexico (CIGoM). Solid purple and green circles mark the locations of buoys positioned during 2017–2021. Solid red squares show the locations of 19 coastal high-frequency radar (HFR) stations, and the hatched region indicates open-ocean HFR coverage. Yellow lines trace the trajectories of glider missions, and transparent polygons mark synthetic aperture radar (SAR) satellite imagery coverage.

TABLE 1. Observational assets of the Consortium for the Gulf of Mexico (CIGoM).

Buoys: Coastal Ocean Buoys (COB) and Oceanographic and Marine Meteorological Buoys (OMMB)
- INSTRUMENTS. 5 COB, 1 OMMB
- VARIABLES MEASURED. Wind direction and magnitude, atmospheric pressure, relative humidity, precipitation, surface layer temperature, salinity, dissolved oxygen, atmospheric CO_2, pH, waves (amplitude and direction), wave directional spectrum, surface current direction and speed
- LOCATION. Located in the southern Gulf of Mexico platform and upper slope environments (Figure 1)
- COORDINATOR. Vanesa Magar-Brunner (CICESE)

High-Frequency Radio Scatterometers
- INSTRUMENTS. 18 radars
- VARIABLES MEASURED. Shallow surface ocean currents
- LOCATION. Around the Mexican coast of the Gulf of Mexico and the Caribbean (Figure 1)
- COORDINATOR. Xavier Flores Vidal (IIO-UABC)

Gliders
- INSTRUMENTS. 8 Seagliders diving to 1,000 m; 2 deployed at all times
- VARIABLES MEASURED. Salinity, temperature, fluorescence-chlorophyll, CDOM, dissolved oxygen; 2 equipped with AD2CPs
- LOCATION. Followed zonal trajectories in the central Gulf of Mexico between 23°N and 25°N and in the southern Gulf of Mexico between 18°N and 21°N (Figure 1, continuous yellow lines)
- COORDINATORS. Enric Pallás and Miguel Tenreiro (CICESE)

Satellite Synthetic Aperture Radar Images
- INSTRUMENTS. Sentinel-1A and -1B, TerraSAR-X, and TanDEM-X
- VARIABLES MEASURED. Wind and wave fields
- LOCATION. Covering the central and southern region of the Gulf of Mexico
- COORDINATOR. Guillermo Diaz (CICESE)

Satellite Color Images
- INSTRUMENTS. Moderate Resolution Imaging Spectroradiometer (MODIS) on Aqua and Terra satellites
- VARIABLES MEASURED. Chlorophyll, sea surface temperature, surface water hydrocarbon detection, *Sargassum*
- LOCATION. Covering the central and southern region of the Gulf of Mexico
- COORDINATORS. Gabriela Reséndiz Colorado (CICESE) and Abigail Uribe (Instituo de Ingenieria Sisal-UNAM)

Web Platform for Visualization and Integration (SMID)
- INSTRUMENTS. Standardized data base (NETCDF-CF-ACDD), 2 data servers (THREDDS and ERDDAP), a metadata server (CKAN), and a visualization server (Terria)
- VARIABLES MEASURED. Visualization of all the above variables in space and time
- COORDINATOR. Favio Medrano (CICESE)

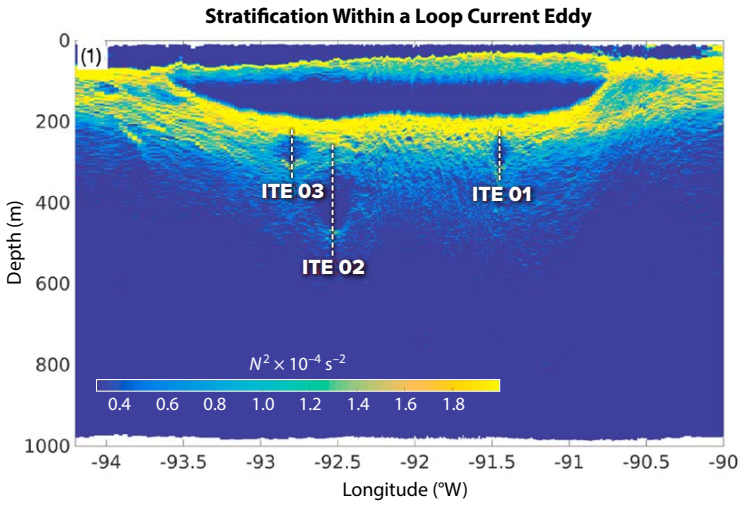

FIGURE 2. Spatial distribution patterns collected by ocean gliders showing buoyancy frequency (N^2) across the anticyclonic eddy Poseidon shed from the Gulf of Mexico Loop Current. Yellow colors mark the domains where water densities increase rapidly, and blue colors highlight domains that exhibit densities similar to one another. Blue features below the yellow domain mark the locations of small-scale anticyclonic eddies revolving around the larger Poseidon eddy. *Modified after Figure 1b in Meunier et al. (2018)*

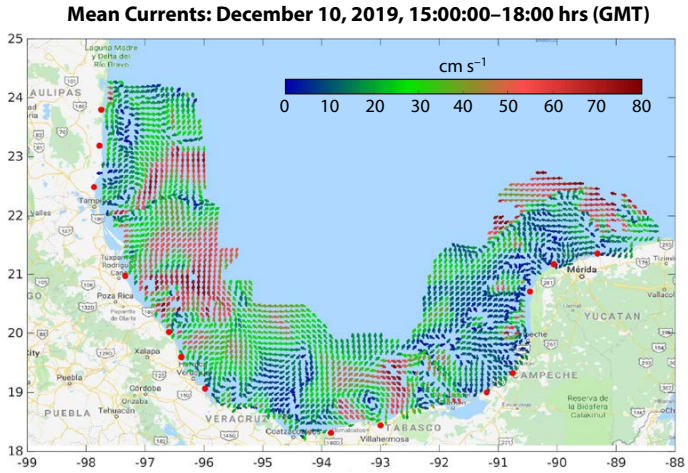

FIGURE 3. Mean currents are plotted for December 10, 2019, 15:00–18:00, derived from the coastal HFR network. Solid red circles mark the HFR station locations.

Here, we provide a few examples of how our instrument network and modeling efforts are being used for hazard warning in the southern Gulf of Mexico.

HAZARD WARNING

Hydrocarbon Spills

CIGoM has been working on two strategic capacities, one of them based on satellite observations and the other on models for forecasting oil spill trajectories.

In collaboration with the US National Oceanic and Atmospheric Administration (NOAA) and Mexico's El Colegio de la Frontera Sur (ECOSUR), CIGoM is developing an oil spill early warning system that covers the southern domain of the GoM, a region characterized by continuous major hydrocarbon industry operations and natural hydrocarbon seeps (Figure 4). To maximize the temporal coverage and spatial detection of large to small spatial scale slicks, we use a combination of three different types of publicly available satellite imagery: the Landsat-Operational Land Imager that measures in the visible, near infrared, and shortwave infrared portions of the spectrum; the Sentinel-1 synthetic aperture radar instrument; and the Sentinel-2 Multispectral Instrument that measures Earth's reflected radiance.

The integrated numerical modeling system developed by CIGoM has provided some interesting results on complex problems related to predicting the dispersion and probable fate of oil during large-scale hydrocarbon spills in the GoM. To forecast and visualize the evolution and fate of different oil spill scenarios at pre-defined locations, we employ several international operational models: the HYbrid Coordinate Ocean Model (HYCOM), the Regional Ocean Modeling System (ROMS), the Nucleus for European Modelling of the Ocean (NEMO), the Navy Coastal Ocean Model (NCOM), the Global Forecasting System model (GFS, NCEI-NOAA), and the Weather Research and Forecasting (WRF) and WRF-Chem for the atmosphere and WAVEWATCHIII for waves. An analysis of the differences and similarities among the modeling results has helped us understand their capabilities and guided their use for development of an ensemble-based system to generate oil spill scenarios and a probabilistic forecast system (Meza-Padilla et al., 2019; Duteil et al., 2019; Gómez-Valdivia and Parés-Sierra, 2020; Mazlo et al., 2020; Moreles et al., 2020; Guerrero et al., 2020; Damien et al., 2021). These ensembles are coupled to three oil spill models of different complexity: OilSpill and PetroTrans (both two-dimensional models) and CIC-OIL (a three-dimensional model) with which we have implemented innovative routines, modifications, and couplings, as well as stochastic parameterizations or models. The CIC-OIL couples the Texas A&M Oil Spill Calculator, a near-field model that simulates "blowout," and OpenDrift, a far-field software package for modeling the trajectories and fates of objects or substances drifting in the ocean. OpenDrift incorporates features recently developed at CICESE (weathering processes) to simulate the plume produced by the explosion of a well and its evolution (Figure 5). Because the three-dimensional CIC-OIL model simulates many processes (e.g., entrainment and dispersion) with different properties, such as hydrocarbon composition and droplet size, its results can be compared

to other models that do not include or parameterize some of these processes (Pares-Sierra et al., 2018; Anguiano-García et al., 2019; Duteil et al., 2019) or models with similar complexity (Meza-Padilla et al., 2021). We are using these models to generate different scenarios, incorporating the impacts of model and initial condition errors (ensemble forecasts) and testing, for example, the use of dispersants either on the surface or at depth, that affect oil characteristics and the fate of oil downstream (see Kotzakoulakis and George, 2021).

As part of this project, we also developed a novel weather forecasting system for the GoM that consists of two tools that are necessary for reliably predicting the evolution and impact on the atmosphere of a large oil spill event. The first estimates air quality and the second calculates the downstream evolution of polluting plumes associated with the volatilization and burning of hydrocarbons from large-scale spills at the sea surface (see CIGoM air-quality forecast at http://132.248.8.198/CIGOM_PM.php). This meteorological forecast system, in addition to providing information on atmospheric circulation, is essential for planning daily activities at sea such as fishing and marine operations. It is important for executing prevention and mitigation procedures, because knowledge of air quality and the trajectory of gas emissions associated with hydrocarbon spills helps to safeguard public health.

We are currently combining observations from our southern GoM network and modeling efforts to provide an Early Response Protocol for Hydrocarbon Spills that will systematize the role and function of science panels within regional and local coordination agencies. These agencies are responsible for early responses to hydrocarbon and other hazardous spills under the leadership of the Mexican naval command. In the past two years, CIGoM has participated in oil spill drills organized by the Mexican Navy in several major GoM port cities (including Tampico, Veracruz, Ciudad del Carmen, and Campeche),

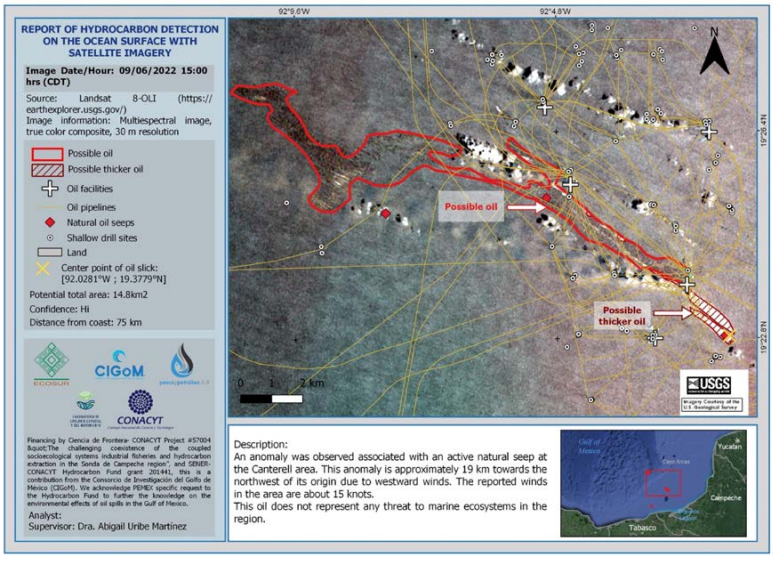

FIGURE 4. Web alert for a hydrocarbon slick associated with a natural seep in the southeastern Gulf of Mexico. The map at lower right shows the location of the image.

Oil Spill Probabilistic Forecast Showing Results from One of the Ensemble Members

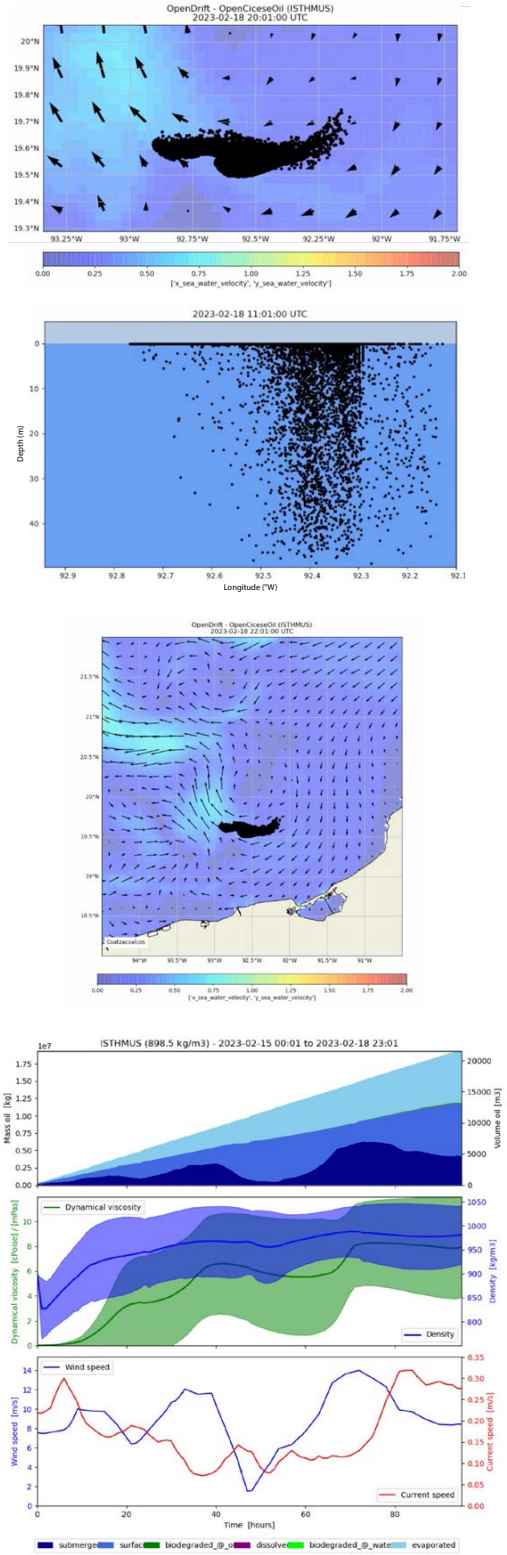

FIGURE 5. CIGoM web portal for oil spill forecast simulations at pre-determined locations. Each day, a five- to 10-day ensemble forecast is generated. Ensemble members include results from simulations using different wind factors and/or ocean circulation forecasts from different models.

where we provided the Unified Command with different scenarios based on real-time observations and forecasting models and tried to estimate the impacts of alternative actions for mitigating and containing the oil spills.

Tropical Cyclones

Growing coastal populations and rising sea levels magnify vulnerability to tropical storms, increasing the need for more accurate storm intensity and tracking forecasts. Advances in forecasting capability include remarkable improvements in atmospheric forecasts and the use of gliders, which have proven to be reliable observing systems for gathering critical real-time ocean data in regions of potential rapid storm intensification such as the Caribbean and the eastern Gulf of Mexico. Gliders' ability to obtain upper ocean salinity and temperature profiles and transmit them to shore in real time even under the most severe storm conditions is improving the accuracy of hurricane intensity forecasts (NOAA, 2020). The CIGoM glider group is collaborating with the US Integrated Ocean Observing System to provide data to reduce uncertainties in global forecasting models through improved estimation of ocean heat content. A better understanding of ocean-storm prediction will help to advise stakeholders and prepare coastal populations to react to and mitigate destructive storm impacts. During the 2022 hurricane season, from July to November, three glider missions provided real-time data during the passages of Tropical Storm Karl and Hurricane Lisa over Campeche Bay, demonstrating the importance of the monitoring efforts implemented by CIGoM.

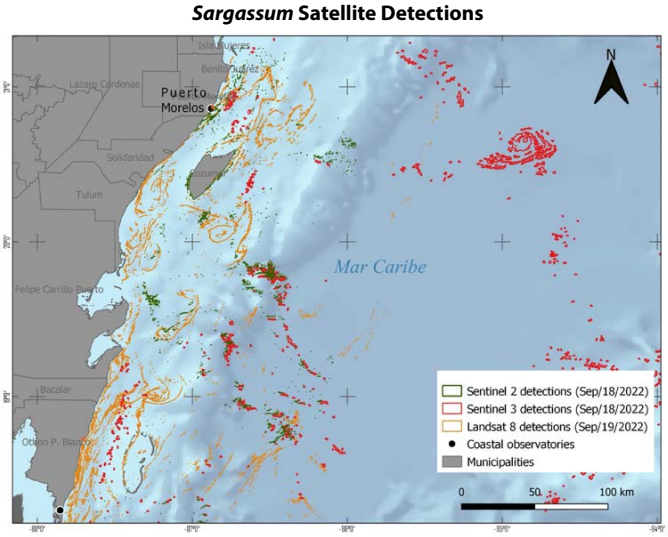

FIGURE 6. Composite of *Sargassum* detection in the northwestern Caribbean close to the eastern Yucatán Peninsula. Red dots mark Sentinel-2 and -3 derived *Sargassum* detections. Orange dots mark Landsat 8 detections, and black dots mark coastal observations in Puerto Morelos and Xcalak in the south.

Sargassum Inundations

To mitigate the effects of excessive *Sargassum* deposition on coastal populations, tourism, fishing activities, and coastal marine ecosystems, CIGoM members are implementing an early detection, monitoring, and forecasting system for massive *Sargassum* landings on the Mexican Caribbean coast. The goal of the project is to provide information to end users about *Sargassum* distribution at different temporal and spatial scales (from days to weeks and regional to local; Figure 6), and the probability of the timing and approximate locations of landings (also with different scales and scopes). This information will be made available through a dedicated website where observations and forecasts will be publicly available to end users for planning and managing logistics during these events. This multidisciplinary and multi-institutional effort is being constructed along four thematic lines: (1) operational modeling of *Sargassum* transport and the probability of its landing in a coastal region, (2) detection in the open ocean as well as close to shore, (3) local observations of environmental conditions along the coast during *Sargassum* inundations, and (4) data dissemination and communication to end users. This system monitors *Sargassum* biomass landings at two coastal observatories (Puerto Morelos and Xcalak), analyzes their biogeochemical compositions, and assesses their impacts on coastal environments. The system also monitors brown tides in reef lagoon environments.

CONCLUSIONS

The data generated by the CIGoM oceanographic observation system allows characterization of surface and deep-water ocean circulation and biogeochemical processes in the southern Gulf of Mexico. The continuous collection of key oceanographic variables in real time and the knowledge generated from oceanographic cruises and fieldwork, together with the computational modeling efforts, are critical inputs to decision-making regarding mitigation procedures during extreme events originating from natural causes or of anthropogenic origin and for setting the appropriate public policy to maintain the resilience of this large marine ecosystem to natural and anthropogenic disturbances.

In 2022, the UN Ocean Decade of Ocean Science for Sustainable Development (2021–2030) endorsed CIGoM's Ocean Decade project ID 37, "Ocean Monitoring and Prediction Network for the Sustainable Development of the Gulf of Mexico and the Caribbean." This project provides large spatial and long-term baseline observations from the network we developed, together with modeling/forecasting capabilities to inform end users and coastal communities that have not so far been able to obtain such

information, which is vital for their safety. Our objectives include the maintenance, optimization, and expansion of the metoceanic, hydrographic, biogeochemical, and ecological observations we have been collecting for the past eight years to help us understand, in combination with our numerical modeling efforts, the emerging long-term environmental trends that threaten the habitats and key species of Gulf of Mexico and Caribbean Sea ecosystems.

The communication and use of this information is of great value for implementing safer ways to operate in the ocean, preventing loss of lives during extreme weather events, and conducting mitigation procedures during oil spills, harmful algal blooms, massive *Sargassum* influxes, and other anthropogenic sources of perturbation to GoM marine life. The observing system for the southern Gulf of Mexico and the western Caribbean that we are attempting to keep functional can become the basic infrastructure for monitoring the emerging trends in sea surface temperatures, ocean acidification, biodiversity loss, and sea level rise, among other processes related to climate change, and to other anthropogenic pressures introduced by plastics and metals pollution and deoxygenation of coastal regions in the area. These accessible data sets and the knowledge generated will further advance the local, national, and international capacities needed for the sustainable development of the ocean resources in this region. Making the system part of global observing and forecasting efforts would further enhance capacity building and inspire the next generation of scientists, policymakers, and stakeholders in the greater Caribbean for the sustainable development of this large ocean region.

REFERENCES

Anguiano-García, A., O. Zavala-Romero, J. Zavala-Hidalgo, J.A. Lara-Hernández, and R. Romero-Centeno. 2019. High performance open source Lagrangian oil spill model. Pp. 118–128 in *Communications in Computer and Information Science*, vol. 948. M. Torres, J. Klapp, I. Gitler, and A. Tchernykh, eds, International Conference on Supercomputing in Mexico: Supercomputing, Springer, Cham, https://doi.org/10.1007/978-3-030-10448-1_11.

Damien, P., J. Sheinbaum, O. Pasqueron de Frommervault, J. Jouanno, L. Linacre, and O. Duteil. 2021. Do Loop Current eddies stimulate productivity in the Gulf of Mexico? *Biogeosciences* 18(14):4,281–4,303, https://doi.org/10.5194/bg-18-4281-2021.

Duteil, O., P. Damien, J. Sheinbaum, and M. Spinner. 2019. Ocean currents and coastal exposure to offshore releases of passively transported material in the Gulf of Mexico. *Environmental Research Communications* 1:081006, https://doi.org/10.1088/2515-7620/ab3aad.

Flament, P.J., D. Harris, M. Flament, I.Q. Fernandez, R. Hlivak, X. Flores-Vidal, and L. Marié. 2016. A compact high frequency Doppler radio scatterometer for coastal oceanography. Paper presented at the fall meeting of the American Geophysical Union, December 12–16, 2016, San Francisco, California, abstract #OS11C-06.

Gómez-Valdivia, F., and A. Parés-Sierra. 2020. Seasonal upper shelf circulation along the central western Gulf of Mexico: A preferential upcoast flow reinforced by the recurrent arrival of loop current eddies. *Journal of Geophysical Research: Oceans* 125(1), e2019JC015596, https://doi.org/10.1029/2019JC015596.

Guerrero, L., J. Sheinbaum, I. Mariño-Tapia, J.J. González-Rejón, and P. Pérez-Brunius. 2020. Influence of mesoscale eddies on cross-shelf exchange in the western Gulf of Mexico. *Continental Shelf Research* 209:104243, https://doi.org/10.1016/j.csr.2020.104243.

Kotzakoulakis, K., and S.C. George. 2021. Advanced oil spill modeling and simulation techniques. Chapter 8 in *Oil Spill Occurrence, Simulation, and Behavior*, 1st ed. M.R. Riazi, ed., CRC Press.

Maslo, A., J.M. Azevedo Correia de Souza, and J. Sheinbaum Pardo. 2020. Energetics of the deep Gulf of Mexico. *Journal of Physical Oceanography* 50(6):1,655–1,675, https://doi.org/10.1175/JPO-D-19-0308.1.

Meunier, T., M. Tenreiro, E. Pallàs-Sanz, J. Ochoa, A. Ruiz-Angulo, E. Portela, S. Cusí, P. Damien, and X. Carton. 2018. Intrathermocline eddies embedded within an anticyclonic vortex ring. *Geophysical Research Letters* 45(15):7,624–7,633, https://doi.org/10.1029/2018GL077527.

Meza-Padilla, R., C. Enriquez, Y. Liu, and C.M. Appendini. 2019. Ocean circulation in the western Gulf of Mexico using self-organizing maps. *Journal of Geophysical Research: Oceans* 124(5):4,152–4,167, https://doi.org/10.1029/2018JC014377.

Meza-Padilla, R., C. Enriquez, and C.M. Appendini. 2021. Rapid assessment tool for oil spill planning and contingencies. *Marine Pollution Bulletin* 166:112196, https://doi.org/10.1016/j.marpolbul.2021.112196.

Moreles, E., J. Zavala-Hidalgo, B. Martínez-López, and A. Ruiz-Angulo. 2020. Influence of stratification and Yucatan Current transport on the Loop Current eddy shedding process. *Journal of Geophysical Research: Oceans* 126:e2020JC016315, https://doi.org/10.1029/2020JC016315.

NOAA (National Oceanic and Atmospheric Administration). 2020. "Ocean gliders head to sea to improve hurricane forecasts: NOAA and partners expect 50-percent boost in ocean data." July 15, 2020, https://research.noaa.gov/article/ArtMID/587/ArticleID/2647/Unmanned-ocean-gliders-heading-to-sea-to-improve-hurricane-prediction.

Parés-Sierra, A., A.L. Flores-Morales, and F. Gómez-Valdivia. 2018. An efficient Markovian algorithm for the analysis of ocean currents. *Environmental Modelling & Software* 103:158–168, https://doi.org/10.1016/j.envsoft.2018.02.014.

ACKNOWLEDGMENTS

The Research Consortium for the Gulf of Mexico (CIGoM) includes the Center for Scientific Research and Higher Education at Ensenada as the lead institution; the National Autonomous University of Mexico with four participating institutes, the Institute for Atmospheric Sciences and Climate Change, the Institute of Biotechnology, the Institute of Marine Sciences and Limnology, and the Institute of Geophysics; the Center for Research and Advanced Studies of the National Polytechnic Institute in Mérida; the Autonomous University of Baja California and the Center for Engineering and Industrial Development. These are presently joined by the Escuela Nacional de Educación Superior in Mérida and the School of Engineering at Sisal from UNAM, El Colegio de la Frontera Sur, Autonomous University of the State of Morelos, and Autonomous Metropolitan University.

This study is a contribution of Project No 201441 "Implementation of oceanographic observation networks (physical, geochemical, ecological) for the generation of scenarios in the case of possible contingencies related to the exploration and production of hydrocarbons in deep waters of the Gulf of Mexico," funded by the Hydrocarbon Fund SENER-CONACyT and CONACYT. This is a contribution of CIGoM. We acknowledge a PEMEX request to the Hydrocarbon Fund to further knowledge about the environmental effects of oil spills in the Gulf of Mexico. We further acknowledge all the participants in this project, the crews of BO *Justo Sierra* and BO *Alpha Helix* for their help during the cruises, and all the administrative staff at CIGOM who greatly aided the success of this project.

ARTICLE DOI. https://doi.org/10.5670/oceanog.2023.s1.18

An Experimental Platform to Study Wind, Hydrodynamic, and Biochemical Conditions in the Littoral Zone During Extreme Coastal Storms

By Brian M. Phillips, Forrest J. Masters, Britt Raubenheimer, Maitane Olabarrieta, Elise S. Morrison, Pedro L. Fernández-Cabán, Christopher C. Ferraro, Justin R. Davis, Taylor A. Rawlinson, and Michael B. Rodgers

Tropical cyclones and other extreme coastal storms cause widespread interruption and damage to meteorological and hydrological measurement stations exactly when researchers need them most. There is a longstanding need to collect collocated and synchronized measurements in areas where storms severely damage civil/coastal infrastructure. To fill this observational gap, researchers led by author Masters developed a state-of-the-art monitoring station called a "Sentinel." Sentinels are intended for temporary installation on the beach between the mean tidal datum and the sand dunes and are engineered to operate in and measure extreme wind, storm surge, wave, and hazardous water quality conditions. They are envisioned as a shared-use resource—a hardened Internet of Things platform set up in the right place at the right time to study wind and wave loads, coastal erosion and morphology changes, water quality, and other processes during extreme coastal storms.

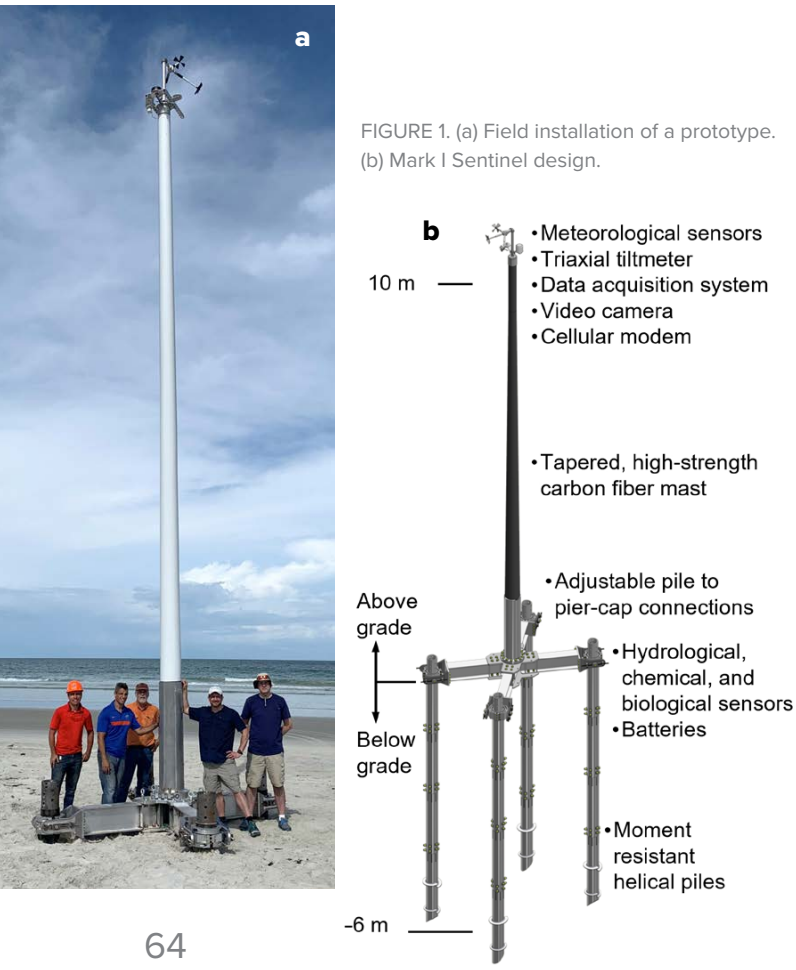

FIGURE 1. (a) Field installation of a prototype. (b) Mark I Sentinel design.

In 2021, a fully functional prototype Sentinel (Mark I) was designed and built through internal support and industry contributions. The structure is engineered to survive a design wind load of 90 m s^{-1} (3 sec gust measured at 10 m above ground level) in marine exposure, 5 m breaking waves in 5 m still water with a wave celerity (the propagation speed of a wave crest or trough) of 6.7 m s^{-1}, and 1 m of combined erosion and pile scour. The structure anchors to the beach using four 200 mm diameter steel helical piles driven by a hydraulic auger. The piles are segmented such that four sections can reach an embedment depth of 6 m for the worst-case design load. The piles support an adjustable aluminum alloy "crossbeam" pier cap that in turn supports a 10 m tall carbon fiber mast. Three-dimensional wind velocity, mast tilt, atmospheric pressure, temperature, and humidity data are collected at 10 Hz at the top of the mast, along with video. The upper instrumentation package makes up the "nerve center" for the system and includes a data logger and cell modem. The base houses batteries and a wave/water depth, temperature, and salinity sensor (sampled at up to 5 Hz) that connects to the upper instrumentation package. Figure 1b shows the Mark I design. A field test was completed in October 2021 (Figure 1a) to identify logistical challenges and areas for improvement in future Sentinel versions.

In 2022, authors Phillips, Masters, Raubenheimer, Olabarrieta, Morrison (co-PI), Ferraro, and Davis received a National Science Foundation (NSF) Major Research Instrumentation (MRI) award to support the design of a Mark II Sentinel and the commissioning of a fleet of six Mark II Sentinels. Mark II will improve on Mark I in several key areas: (1) the deployment conditions will expand beyond tropical cyclones, (2) the pile installation system will accommodate non-cohesive and cohesive soils as well as layers of harder geomaterial, (3) the structural loads will be revisited through field and laboratory studies, (4) the structural design will be further optimized to reduce weight and installation time, and (5) additional sensor packages will be explored for measuring erosion, water current, and a suite of water quality parameters. Design work on the Mark II is underway.

As tropical cyclones approach, Sentinels will be installed one to three days before landfall. The project is supported by the SHared Operational REsearch Logistics

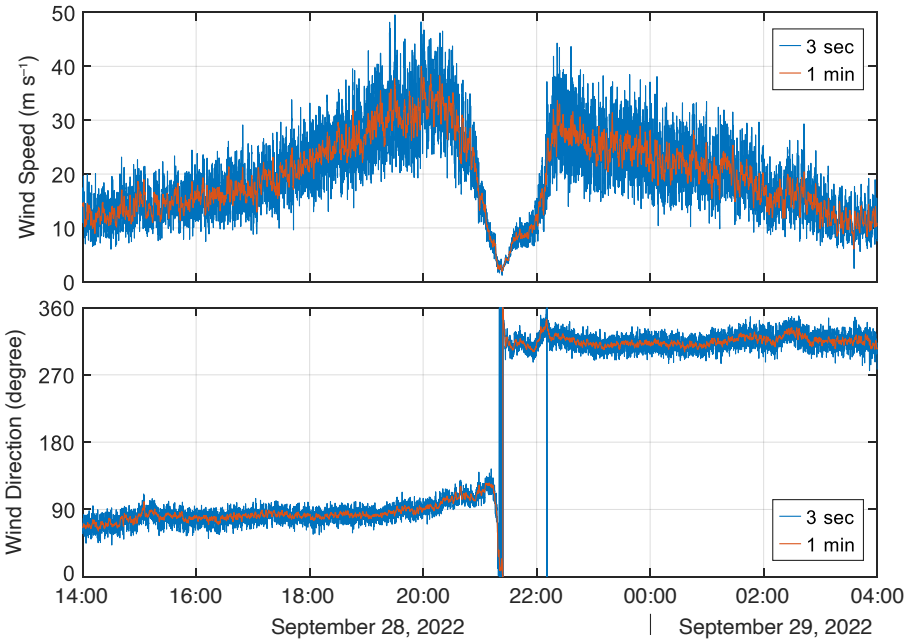

FIGURE 2. Example 10 m (above ground level) wind velocity data collected during Hurricane Ian (2022) by a Florida Coastal Monitoring Program (FCMP) weather station. Data are filtered using 3 sec and 1 min moving averages. FCMP stations have the same wind and atmospheric sensors as Sentinels.

In the Nearshore Environment (SHORELINE) Network, a national collaboration represented by universities in hurricane-prone states. Through SHORELINE, an array of pre-selected sites and permits are maintained along the Gulf of Mexico and the Atlantic coasts. Ad hoc site approvals are also pursued based on expected landfall locations. Selected sites are locally surveyed using a radiodetection meter and a ground penetrating radar to avoid installation of piles in bearing strata containing underground objects. With input from conservationists, the team avoids selecting sites near nesting grounds for sea turtles, shorebirds, and other species. Installation time is anticipated to be several hours based on field tests, and the installation process takes into account deteriorating weather conditions. Sentinels will be removed after the team can safely return to the deployment sites.

Sentinels are designed to continuously transmit live data and video feeds over cellular networks. During an event, data and video are intended to be shared with a broad spectrum of research, operational, and commercial partners as well as interests supporting local response and recovery (e.g., emergency management and state departments of environmental protection or natural resources). Post-event data sets will be made publicly available through NSF's DesignSafe Data Depot (https://www.designsafe-ci.org/data/browser/public/; Rathje et al., 2017). These stations will support fundamental research that includes but is not limited to numerical weather prediction, storm surge and shallow wave modeling, coastal erosion, boundary layer meteorology, air-sea interaction, biogeochemistry, aircraft- and satellite-based remote sensing of surface wind and wave fields, and hydrodynamic loading of coastal structures.

The Sentinel Project is a culmination of more than two decades of conducting field data collection in landfalling tropical cyclones (Fernández-Cabán et al., 2019). The University of Florida, through the Florida Coastal Monitoring Program (FCMP), has continuously conducted field experiments in landfalling storms since the late 1990s (40 storms to date, including more than 10 major hurricanes). Example data from an FCMP weather station is shown in Figure 2. Sentinel weather stations are complementary to FCMP with a focus on beach deployments. The team anticipates deploying three Sentinels in 2023 and several more in the 2024 hurricane season.

REFERENCES

Fernández-Cabán, P.L., A.A. Alford, M.J. Bell, M.I. Biggerstaff, G.D. Carrie, B. Hirth, K. Kosiba, B.M. Phillips, J.L. Schroeder, S.M. Waugh, and others. 2019. Observing Hurricane Harvey's eyewall at landfall. *Bulletin of the American Meteorological Society* 100(5):759–775, https://doi.org/10.1175/BAMS-D-17-0237.1.

Rathje, E.M., C. Dawson, J.E. Padgett, J.P. Pinelli, D. Stanzione, A. Adair, P. Arduino, S.J. Brandenberg, T. Cockerill, C. Dey, and others. 2017. DesignSafe: New cyberinfrastructure for natural hazards engineering. *Natural Hazards Review* 18(3):06017001, https://doi.org/10.1061/(ASCE)NH.1527-6996.0000246.

ACKNOWLEDGMENTS

This material is based upon work supported by the National Science Foundation under grant nos. 2215297, 1848650, and 1939275.

ARTICLE DOI. https://doi.org/10.5670/oceanog.2023.s1.19

Probabilistic Approaches to Coastal Risk Decision-Making Under Future Sea Level Projections

By Tom Spencer, Mike Dobson, Elizabeth Christie, Richard Eyres, Sue Manson, Steve Downie, and Angela Hibbert

Coastal communities are increasingly threatened by flooding from climate change-induced sea level rise and potential increases in storminess. Informed decisions on risk and resilience related to flood risk need to be made, but the assessment process is complex. It is difficult to bring all of the climate science and sea level rise projections to decision-making, and as a result, decisions are made without a real understanding of the uncertainties involved, a problem magnified the further projections go into the future (Figure 1).

Comprehensive modeling approaches (see ideal option in Figure 2) that allow the impact of a range of potential future conditions to be assessed are not resource efficient. Therefore, the conventional approach (see current option in Figure 2) involves selecting a narrow range of future sea level rise scenarios for further interrogation—typically the median estimate (solid lines in Figure 1). In addition, the uncertainties implicit in future climate scenarios are rarely taken through the hazard-to-impact framework, resulting in poorly defined predictions and likely limited trust in outputs and low levels of uptake. The research described here (proposed option in Figure 2) uses a source-pathway-receptor model of flood risk for the city of Hull, Humber Estuary, eastern England to address these problems and develops a new streamlined approach to modeling the interactions between sea level hazards, economic activity, and risk. The purpose of this research was to examine the boundaries of the full range of climate predictions to inform judgment on where to focus attention for detailed study of and planning for future urban flood risk at the large scale and over the long term. Modeling results are not intended for more detailed design or planning activities for Hull at present (where model accuracy would become much more critical).

Situated on the northern bank of the Humber estuary, with a population of 258,000, Hull has the highest number of UK properties at risk of flooding (140,000) in a single urban area outside of London (Figure 3). England's Environment Agency has warned that, with changing climate, water levels in the Humber Estuary could rise by

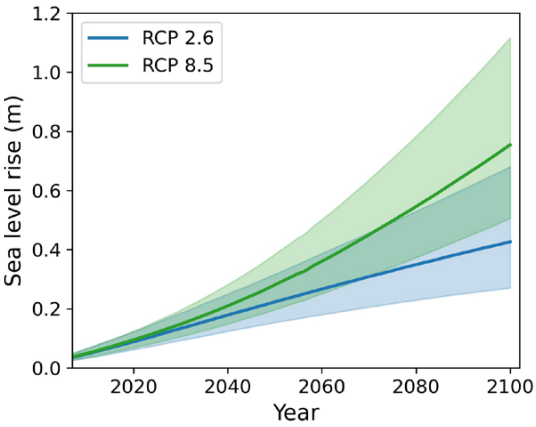

FIGURE 1. Sea level rise projections for the River Humber for a low (RCP2.6) and high emission scenario (RCP8.5), showing 5th, 50th (solid line), and 95th percentiles. Underlying data are from UKCP18 (Palmer et al., 2018). The RCP numbers refer to the projected radiative forcing at 2100 under different climate change scenarios, for example, 2.6 W m^{-2} and 8.5 W m^{-2}.

FIGURE 3. Study area location. (left) Humber estuary, Hull, UK. Content licensed under the CC BY-SA 3.0. Contains Ordnance Survey data © Crown copyright and database right. (right) Outer Humber estuary areas at risk of flooding—nearly 90% of the city of Hull lies below the high-tide level. Contains public sector information licensed under the Open Government License v2.0, https://flood-warning-information.service.gov.uk/long-term-flood-risk/map.

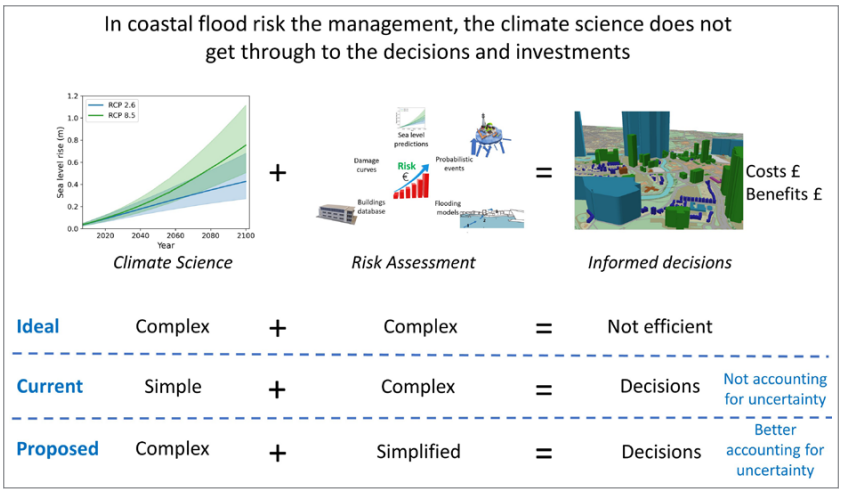

FIGURE 2. Problem specification of flood risk for Hull, Humber Estuary, eastern England.

over 1 m in the next century. The city thus offers a prime case study location for testing our approach. The estuarine margins are extremely low lying; a major storm surge on December 5, 2013, inundated 7,000 hectares of low-lying ground, significantly impacting infrastructure of national importance for energy generation, industry, and agriculture. In addition, Hull is at risk from flooding by the River Hull, which flows through the city center, as well as surface water flooding. The city is currently protected by a tidal surge barrier and by flood defenses that run along the Humber frontage and the river banks. Though many of these defense structures are being strengthened and upgraded, studies predict a continuing risk of breach. Furthermore, "mid-range" sea level rise will reduce the Standard of Protection (SoP) of most of the existing tidal defenses structures to less than 1:5 (20% annual chance of flooding) by around 2040. The SoP will continue to decline between 2040 and 2115 as sea level rises further. These issues clearly illustrate the need for better informed flood risk management options for the city.

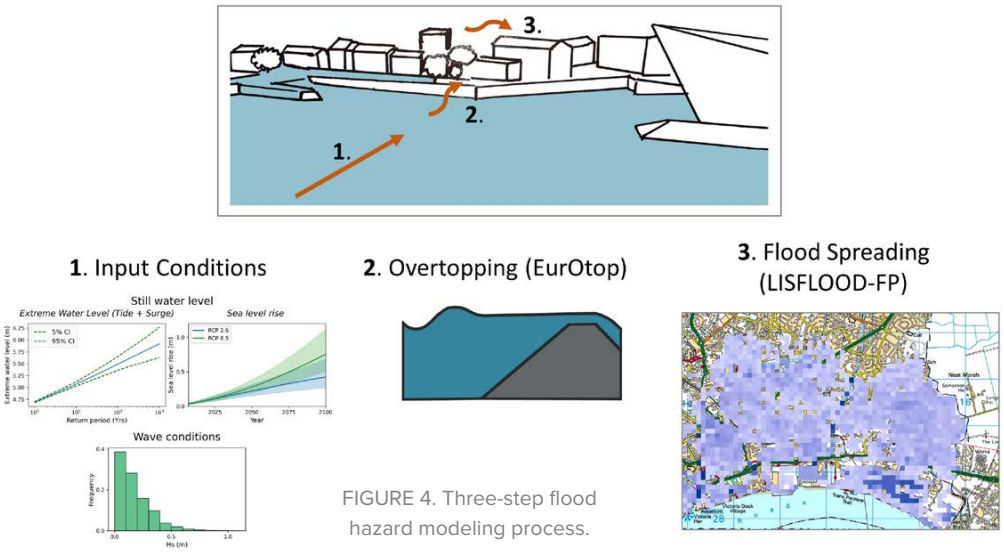

FIGURE 4. Three-step flood hazard modeling process.

The modeling of the physical flood hazard takes a three-step approach (Figure 4). It involves: (1) collating the range of potential nearshore hydrodynamics, (2) calculating the pathway of water onto the land through overflow and wave overtopping of the defense line, and (3) determining how the flood water spreads behind the defense.

A matrix of input conditions covered (1) the full range of sea level rise scenarios from the marine UK Climate Projections 2018 (Palmer et al., 2018), including variation between emissions scenarios and uncertainty over predicted rise for each scenario; (2) transient augmentation of the still water level due to storm surges; and (3) a range of wave conditions. The input hydrodynamics were then used to calculate overtopping discharge at representative transects on the coastal defenses of the Humber using the EurOTop manual (Van der Meer et al., 2018). The overtopping discharge time series was then used to drive a LISFLOOD-FP flood model (Bates and De Roo, 2000). A raster topographic grid file was created from lidar digital terrain map (DTM) data with a spatial resolution of 100 m to allow a fast model run time (< 1 second). Maximum water level by grid cells were then spatial averaged onto a planning viewer grid over the city of 1,000 virtual hexagons (400 m resolution). A sensitivity analysis of different grid sizes was undertaken to balance model resolution versus model run time. A qualitative assessment of model outputs (city-wide water depths) against earlier (2016) comprehensive modeling for the Hull Humber Frontage flood defense business case (https://consult.environment-agency.gov.uk/yorkshire/humber-hull-frontages/) by members of the author team showed generally good agreement between the two exercises.

In total, 21,350 model runs were completed, comprising 122 sea level rise increments (0.06–1.115 m in 0.005 m increments), seven extreme water level (including surge events) return periods (1-, 10-, 50-, 100-, 200-, 500-, and 1,000-year return periods), and 25 wave conditions (H_S 0.05–0.85 m; T 0.90–2.85 sec). Wave conditions differed depending on distance to four locations within the Humber estuary (Salt End, Alexandra Dock, Albert Bridge Dock, Hessle Haven). The wave conditions were obtained from a joint probability analysis report with wave height and direction fitted to a probability distribution function and 25 conditions chosen at random, based on probability. Wave period was selected based on a linear regression with wave height. Model runs were completed in a few hours on a standard PC laptop.

In order to generate economic impacts from flood model outputs, a simple risk model was produced, including depth damages. This model combined receptor data (houses, businesses, supplied by the Environment Agency) and depth damage data (receptor types, damages per type for varying depth, from the UK Multi-Coloured Manual produced by the Flood Hazard Research Centre with the modeled flood depths to calculate economic damages. The annual chance of each flood depth was then used to produce an annualized economic risk, converted into a present value equivalent over the duration of the analysis.

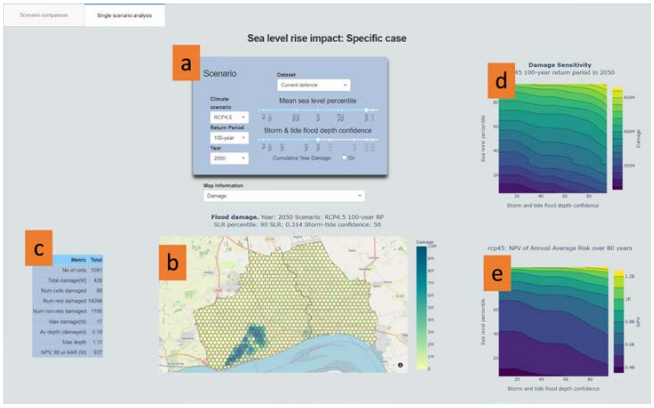

FIGURE 5. A screenshot of the visualization prototype for a single scenario, in this case sea level model RCP4.5 at the 90th percentile with the best estimate (50%) storm and tide flood depth confidence at a 100-year return period in 2050. (a) The user sets the scenario. (b) A map of the region provides a visual representation of the data for the selected scenario. The user can choose to show flood depth, economic damage, elevation, and population density. In addition, the cursor hover-over functionality provides further information, including: number of buildings affected (residential and non-residential) and socioeconomic descriptor for the region. (c) A summary table shows key metrics for the whole region and (if selected) sub-region. (d) A contour plot indicates the effect of the sea level rise and storm-tide uncertainties on resulting total damage across the region for the chosen scenario. (e) A contour plot shows the effect of the sea level rise and storm-tide uncertainties on the net present value (NPV) of the average annual risk across the region for the chosen scenario.

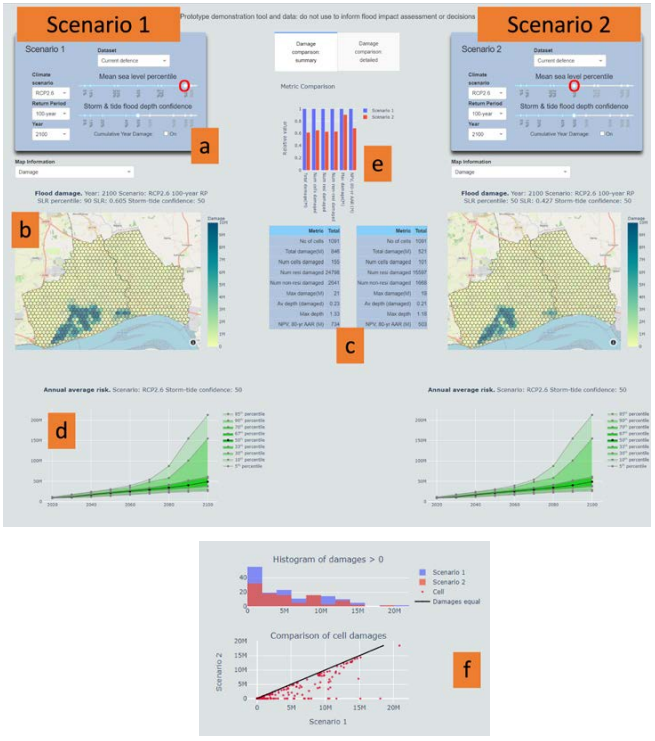

FIGURE 6. A screenshot of the visualization prototype comparing two scenarios, in this case sea level model RCP2.6 at the 90th percentile on the left with the 50th percentile on the right (highlighted as a red ring). Orange boxes a–d as with the single scenario in Figure 5. (e) A bar chart compares the key metrics between the two scenarios. (f) A more detailed analysis of the differences between the scenarios at the hexagonal region level offers a histogram of damages to highlight trends in economic damages, and a scatter plot of the damages for each scenario, plotted against each other for each hexagonal region to show whether the different scenarios are creating more regions of damage and/or making the existing damaged regions better or worse.

A web-based visualization prototype was then created to promote discussion with stakeholders. There are two main methods of display and interrogation:

- **Single scenario** allows the user to look at one scenario and provides detailed metrics associated with that scenario. The user can easily change the scenario and view updated metrics (Figure 5).
- **Two-scenario comparison** allows the user to directly compare two scenarios for the same data set or compare two different data sets. Again, the user can rapidly switch between scenarios to gauge the sensitivities (Figure 6).

Feedback from stakeholder meetings, including live demonstration of the visualization prototype online, confirmed that there is value in this approach: visualization explains uncertainty well and helps users to better understand their appetites for risk; it informs the planning horizons associated with adaptation to future coastal changes resulting from sea level rise; and, at smaller spatial scales, allows the spatial distribution of expected damage to be examined between scenarios and along timelines, with and without changes to local defense heights. This innovative approach brings more science through the risk assessment process and results in better-informed decision-making and investment planning.

REFERENCES

Bates, P.D., and A.P.J. De Roo. 2000. A simple raster-based model for flood inundation simulation. *Journal of Hydrology* 236:54–77, https://doi.org/10.1016/S0022-1694(00)00278-X.

Palmer, M., T. Howard, J. Tinker, J. Lowe, L. Bricheno, D. Calvert, T. Edwards, J. Gregory, G. Harris, J. Krijnen, and M. Pickering. 2018. UKCP18 Marine Report. Met Office Hadley Centre, Exeter, UK, 133 pp, https://www.metoffice.gov.uk/binaries/content/assets/metofficegovuk/pdf/research/ukcp/ukcp18-marine-report-updated.pdf.

Van der Meer, J.W., N.W.H. Allsop, T. Bruce, J. De Rouck, A. Kortenhaus, T. Pullen, H. Schüttrumpf, P. Troch, and B. Zanuttigh, 2018. EurOtop: Manual on Wave Overtopping of Sea Defences and Related Structures: An Overtopping Manual Largely Based on European Research, but for Worldwide Application, 2nd ed. 320 pp., http://www.overtopping-manual.com/assets/downloads/EurOtop_II_2018_Final_version.pdf.

ACKNOWLEDGMENTS

This research was funded by the EuroSea project, which received funding from the European Union's Horizon 2020 research and innovation programme under grant agreement No 862626.

ARTICLE DOI. https://doi.org/10.5670/oceanog.2023.s1.20

The Texas A&M – University of Haifa Eastern Mediterranean Observatory: Monitoring the Eastern Mediterranean Sea

By Gianna Milton, Steven F. DiMarco, Anthony H. Knap, John Walpert, and Roee Diamant

The need for sustained long-term measurements of the ocean has increased due to climate variability and societal desire to mitigate the impact of natural disasters on coastal communities. Knowledge about key ocean variables is essential for monitoring and predicting long-term ocean variability, and real-time capability is needed to inform short-term forecasting systems to assist coastal managers and response teams. Ocean observatories collect oceanographic data for scientific and societal reasons, and open access to these data enables their use by the general public, decision-makers, and stakeholders.

Established in 2014, THEMO is a partnership between Texas A&M University and the University of Haifa to service the eastern Mediterranean Sea nexus of economic, environmental, industry, and scientific interests. The observatory is based on the Texas Automated Buoy System (TABS), which provides near-real-time MetOcean information to regional coastal managers and decision-makers in the context of offshore energy operations (Walpert et al., 2021). TABS data are used to guide emergency response in the event of accidental environmental releases (oil/gas leaks, spills, contamination) and environmental hazards, (severe weather and harmful algal blooms), and to advance scientific understanding of MetOcean processes. THEMO is standing watch in the eastern Mediterranean to provide the same community service.

THEMO is comprised of two real-time reporting 2.25 m diameter surface discus buoys (Diamant et al., 2018; Figure 1). The deep-water (1,500 m depth) buoy, deployed November 2018, is 80 km from the Israeli coast in the Levant Basin (32.79°N, 34.38°E). The shallow (124 m depth) buoy, deployed in June 2017, is 8 km from the northern Israeli coast (33.04°N, 34.95°E). Both buoys are equipped with MetOcean sensors that collect atmospheric (temperature, pressure, wind, humidity) and sea surface (temperature, fluorometer, velocity) observations. Data are relayed in near-real time to the University of Haifa for processing and dissemination via HF radio communication. A McLane profiler (MMP) at the deep location, deployed in August 2019, provides subsurface oceanographic data: conductivity, and temperature measurements and bottom-mounted acoustic Doppler current profiler (ADCP) data. A standalone McLane sediment trap (MK8-13) collects particulate material at monthly intervals.

Data analysis has revealed the temporal evolution of the hydrographic vertical structure and surface mixed layer of the region, surface gravity wave climatology, vertical current structure, and the presence of particle deep resuspension and transport events 200–400 m above bottom.

All data from the mooring sites are processed with internationally recognized quality-assurance and quality-control protocols (Diamant et al. 2020). Increases in oil and gas exploration in the basin will increase the value of THEMO's data to the general coastal population to mitigate potential damage from natural and accidental hazards.

REFERENCES

Diamant, R., A. Knap, S. Dahan, I. Mardix, J. Walpert, and S.F. DiMarco. 2018. THEMO: The Texas A&M – University of Haifa – Eastern Mediterranean Observatory. Paper presented at 2018 OCEANS–MTS/IEEE Kobe Techno-Oceans (OTO), May 28–30, 2018, https://doi.org/10.1109/OCEANSKOBE.2018.8558873.

Diamant, R., I. Shachar, Y. Makovsky, B.M. Ferreira, and N.A. Cruz. 2020. Cross-sensor quality assurance for marine observatories. *Remote Sensing* 12:3470, https://doi.org/10.3390/rs12213470.

Walpert, J., A.H. Knap, S.F. DiMarco, and S.G. Buschang. 2020. Texas Automated Buoy System (TABS): 25 years providing data for spill response, modeling and research. Paper presented at Global Oceans 2020: Singapore–US Gulf Coast, October 5–30, 2020, Biloxi, MS, https://doi.org/10.1109/IEEECONF38699.2020.9389429.

ACKNOWLEDGMENTS

THEMO is a collaboration between the University of Haifa, Texas A&M University, and Texas A&M University System. THEMO data are accessible at: https://themo.haifa.ac.il/. TABS data are accessible at http://tabs.gerg.tamu.edu.

ARTICLE DOI. https://doi.org/10.5670/oceanog.2023.s1.21

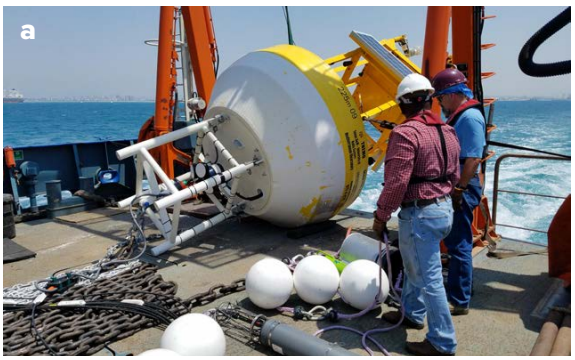

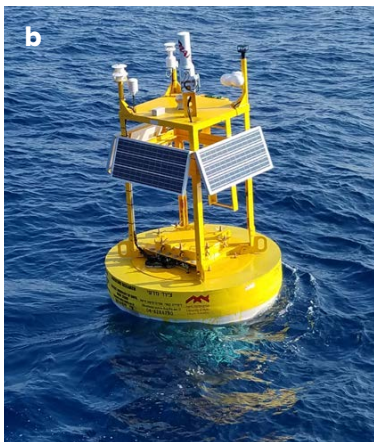

FIGURE 1. (a) A THEMO buoy is prepared for deployment in the eastern Mediterranean Sea off the coast of northern Israel. (b) The THEMO Shallow Buoy is a 2.25 m discuss buoy equipped for near-real-time reporting of MetOcean parameters and with downward-looking ADCP.

Subsea Cables as Enablers of a Next Generation Global Ocean Sensing System

By Eduardo Pereira, Marcos Tieppo, João Faria, Douglas Hart, Pierre Lermusiaux, and the K2D Project Team

The ocean is vast, complex, and increasingly threatened by human activities. There is an urgent need to find complementary ways to gather information and promote the comprehensive understanding and management of the ocean. The global network of subsea cables provides an opportunity to support a holistic ocean observation system. Data gathered from this system can be employed to anticipate and provide warning about hazardous events. Large-scale and widespread ocean monitoring may also enable the oversight and tracing of global phenomena that have local impacts.

The Knowledge and Data from the Deep to Space (K2D) project aims to develop the critical components that will enable the large-scale coupling of autonomous underwater vehicles (AUVs) and subsea cables for global ocean environmental monitoring and multi-hazard warning. Funded by the Fundação para a Ciência e Tecnologia/ Massachusetts Institute of Technology Portugal Program and involving teams from Portugal and the United States, the project started in 2021 with a global budget of 1.4 M€ and an estimated duration of three years. Sustained ocean observation systems are scarce, especially those that focus on or near the seafloor (Figure 1). The combination of subsea cables and marine robotics is promising not only because it allows access to remote locations and provides an extensive network (deep sea, open ocean; Figure 2), but also because it combines a large set of capabilities in a highly resource-efficient way, unmatched by any other ocean observation approach. These assets may initiate the first global ocean "nervous system" in the near future.

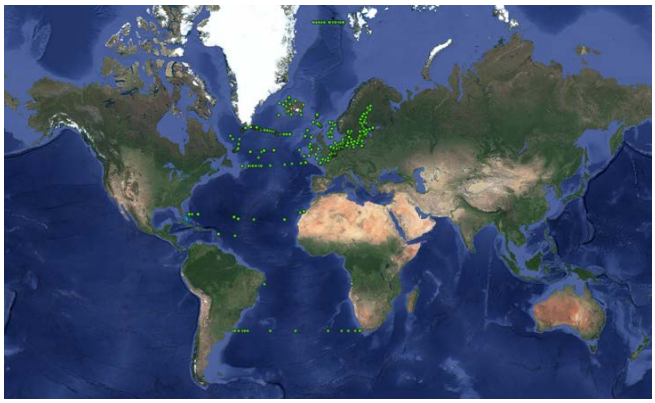

FIGURE 1. Green dots mark the global locations of all fixed monitoring stations that cover the full water column and include seafloor.

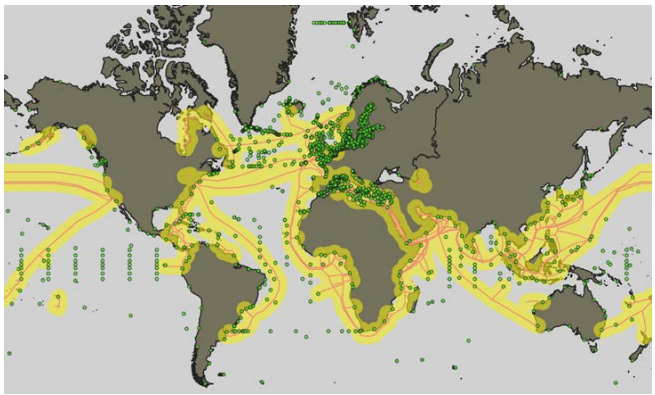

FIGURE 2. Areas marked in yellow indicate regions that could be covered by autonomous underwater vehicles if they were supported by current telecommunications cables and those expected to be laid in the next three years (red lines), assuming 1,000 km of autonomy. Green dots show all existing fixed monitoring stations.

SMART CABLES

Over the past two decades, several pioneering research teams in Japan, Canada, the United States, China, and Europe, among others (see Howe et al., 2022, and references therein), have demonstrated the use of Science Monitoring And Reliable Telecommunications (SMART) cables to collect Earth and ocean information. These fiber-optic telecommunications cables, which combine power and high bandwidth, have been used to support permanent cabled observatories that integrate a variety of sensors and show great potential for supporting multi-hazard warning systems. SMART cables could contribute in a major way to monitoring Essential Ocean Variables (EOVs) globally, including seafloor pressure and temperature, pH, sea surface height, and biological variables and many others. The greatest challenge to widespread implementation of SMART cables is perhaps the funding model, as well as the perceived added value, which is yet to be fully recognized.

INTEGRATION WITH AUVs

AUVs and subsea cables perfectly complement one another to provide monitoring infrastructure. Cable nodes, in addition to hosting sensors that provide sustained measurements of EOVs at fixed locations, they may serve as beacons for AUV co-registration and give vehicles access to power and data. AUVs can serve as mobile sensor platforms as well as data and energy mules that connect the cabled nodes with distant autonomous stations. Additionally, interoperable cables may serve as open ocean highways, allowing increased AUV mobility.

FIGURE 3. The N2ODE prototype is shown ready for deployment near the Troia peninsula south of Lisbon, Portugal.

In the K2D project, the AUVs integrate four fundamental components (Martins et al., 2022): multi-range navigation, communications, wireless power transfer, and payload capability. For communications, long-range acoustic, short-range high-speed acoustic, and very short ultra-high-speed optical devices are implemented. The long-range acoustic sensors use low frequencies and high-power acoustic sources for distances up to 25 km, guaranteeing connection with an AUV as it travels between nodes at the seafloor. The short-range (up to 200 m) high-speed acoustic sensors use frequencies up to 1 MHz, allowing data exchange and AUV control in real time. The very short ultra-high-speed optical communication system is used for ranges up to 10 m for docking and for intensive data exchange.

PROJECT DEVELOPMENT

The project includes lab testing of components and pilot deployment of a system that replicates, at a smaller scale, the functions and critical parts needed for a large, oceanic-scale system. Lab testing was mostly focused on the development of a modular multifunctional node, called N2ODE, that establishes the connection between the telecommunications cable and the system of environmental sensors, the external AUVs, and the charging docking station. N2ODE also includes essential devices to support localization and communications with the AUVs.

Currently, the project's focus is on the deployment of an in situ pilot that includes four N2ODEs installed in a 2 km-long cable at depths between 100 m and 1,000 m. Figure 3 shows the prototype recently deployed in the Portuguese Navy's Technological Free Zone near the Troia peninsula south of Lisbon and aimed at testing the essential set of N2ODE components. Previous measurements identified sounds of marine mammals and other organisms as well as human activities; these will be combined with environmental DNA-based information and deep learning models to better understand the ocean soundscape. Other sound sources will also be included in the study, such as those generated by underwater landslides and seismic activity, along with variables such as temperature, conductivity, pressure, and currents, to derive key indicators useful for monitoring ocean health and multi-hazard warnings.

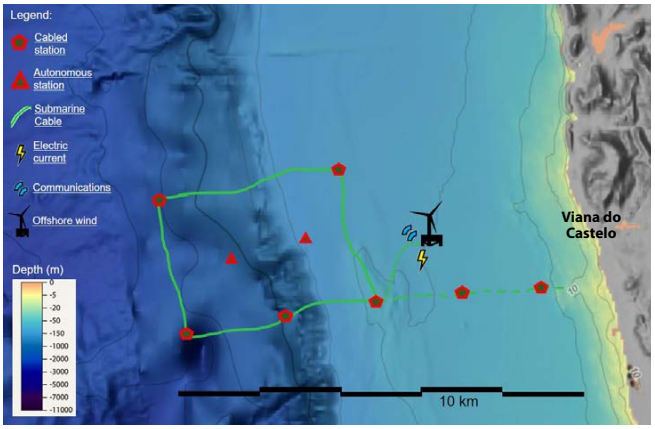

FIGURE 4. Schematic shows the area planned for the final pilot test of a modular multifunctional node, called N2ODE, off the coast of Viana do Castelo, Portugal, in an offshore renewable energy zone.

After successful validation of N2ODE, the final pilot test is planned for the coastal area off Viana do Castelo, Portugal (Figure 4). In addition to geological and ecological richness, the area hosts abundant and diverse marine fauna and flora, including large soniferous species such as whales and dolphins. Anthropogenic pressure in the area includes intense fishing and shipping traffic as well as offshore renewable energy (wind farms) and port activity. Uses of N2ODE related to hazard warning include avoiding clashes between large mammals and vessels or floating platforms, a need exhibited by the increasing frequency of aggressive encounters. Storm surges and assessment of their impacts on human-made structures in the ocean are also targeted. Tracing of the migratory behaviors of soniferous species such as whales will also be used as global ocean health and warning indicators (Tieppo et al., 2022). The integration of data and modeling will contribute to the building of a digital twin of the area. All results will be updated at the K2D project websites, http://www.k2d.pt/ and http://mseas.mit.edu/Research/K2D/.

REFERENCES

Howe, B.M., M. Angove, J. Aucan, C.R. Barnes, J.S. Barros, N. Bayliff, N.C. Becker, F. Carrilho, M.J. Fouch, B. Fry, and others. 2022. SMART subsea cables for observing the Earth and ocean, mitigating environmental hazards, and supporting the blue economy. *Frontiers in Earth Science* 9:775544, https://doi.org/10.3389/feart.2021.775544.

Tieppo, M., E. Pereira, L. González Garcia, M. Rolim, E. Castanho, A. Matos, A. Silva, B. Ferreira, M. Pascoal, E. Almeida, and others. 2022. Submarine cables as precursors of persistent systems for large scale ocean monitoring and autonomous underwater vehicles operation. Paper presented at *OCEANS 2022, Hampton Roads*, October 17–20, 2022, Hampton Roads, Virginia, https://doi.org/10.1109/OCEANS47191.2022.9977360.

Martins, M.S., N.A. Cruz, A. Silva, B. Ferreira, F. Zabel, T. Matos, S.M. Jesus, A. Pinto, E. Pereira, A. Matos, and others. 2022. Network nodes for ocean data exchange through submarine fiber optic cable repeaters. Paper presented at *OCEANS 2022, Hampton Roads*, October 17–20, 2022, Hampton Roads, Virginia, https://doi.org/10.1109/OCEANS47191.2022.9977361.

ARTICLE DOI. https://doi.org/10.5670/oceanog.2023.s1.22

Integrating Topographic and Bathymetric Data for High-Resolution Digital Elevation Modeling to Support Tsunami Hazard Mapping

By Cassandra Bosma, Adrienne Shumlich, Mark Rankin, Soroush Kouhi, and Reza Amouzgar

Tsunamis pose a threat to coastal communities. Flooding from tsunami-generated waves can cause extensive damage to infrastructure, and in some cases may even lead to loss of human life. Sea level rise due to climate change is expected to exacerbate the risk of flooding hazards. In British Columbia (BC), coastal communities are particularly vulnerable to tsunamis because of their proximity to the Alaska-Aleutian and Cascadia subduction zones.

To mitigate risks, it is imperative to understand how tsunami events could impact coastal communities. One method for understanding tsunami hazards is to generate inundation and risk models to determine areas that will be impacted by flooding. These tsunami models require a continuous bathymetric and topographic Earth surface model to determine tsunami behavior and flood patterns. This article focuses on the creation of three-dimensional digital elevation models (DEMs) of Earth's surface to support tsunami modeling, inundation mapping, and risk assessment.

METHODOLOGY

Multiple nested DEM grids of varying scales and resolutions are necessary to accurately model tsunami behavior. Generating these seamless bathymetric-topographic DEMs requires collecting, compiling, converting, processing, and integrating large volumes of data.

First, topographic (elevation) data and bathymetric (depth) data are acquired from numerous sources at varying levels of processing. Some source data are obtained in raw formats with virtually no previous processing or quality control, while other data sets may be provided already appropriately classified and quality checked.

Once data have been collected, it is necessary to evaluate the vertical and horizontal datums, the coordinate systems, data type, data resolution, and level of previous processing. Each data set then needs to be converted to a consistent vertical and horizontal datum with coordinates represented in decimal degrees. If lidar data are available, the topographic and bathymetric data need to be classified and only the bare-earth points retained because bare-earth surfaces are required to create DEMs suitable for tsunami modeling (NTHMP, 2010).

Data sources are checked for potential errors. For example, in certain cases, the lidar files contained docks, bridges, buildings, water features, and vegetation erroneously classified as bare-earth. Because these structures would impact tsunami wave propagation in the model, they need to be removed before being integrated into the DEM (Figure 1).

After data sources have been checked and processed into consistent formats, the final step before integration is to convert each file into a format where each point has a longitude, latitude, and elevation/depth. After several additional data preparation steps, a weighting structure is applied to the data sets that gives the highest priority to higher resolution and more reliable input to ensure these data have the most influence in the grid cell values of the resulting DEM. Finally, MB-Grid, a software tool, is used to create a DEM with a specified resolution and bounding box coordinates. Figure 2 shows a completed high-resolution DEM for a large area of the lower mainland in southwest BC.

Integrating the differing data sources, especially in remote coastal areas lacking high-resolution data, can lead to abrupt transitions in the DEM at the boundaries of the data sets. This may cause instability and unphysical waves during the tsunami modeling process. This effect can be reduced by applying a Gaussian blur smoothing algorithm to the bathymetry portions of the DEM (Figure 3).

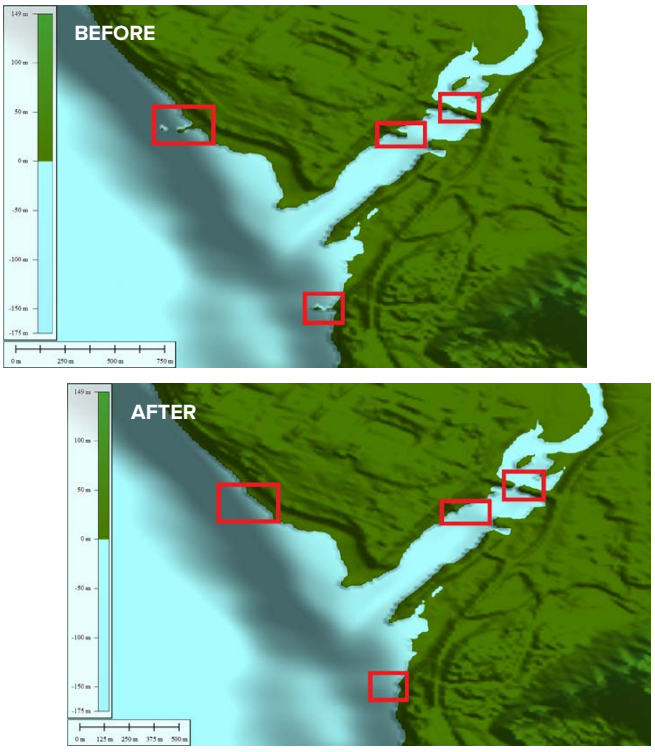

FIGURE 1. Before (top) and after (bottom) erroneous lidar structure removal for a 10 m digital elevation model (DEM) at Masset Inlet created for a project in Haida Gwaii, BC.

FIGURE 2. Canadian Safety and Security Program 3 m horizontal resolution DEM for the lower mainland, southwest British Columbia.

MODEL ASSESSMENT

A number of methods are used to evaluate the accuracy of the final DEM models. Comparisons with satellite imagery, ground control points, and established map and nautical chart contours are some of the main tools used to assess the models. When a model deviates significantly from reality, the source data are examined, and any remaining outliers are removed. DEM grids are then re-run until a suitable surface is achieved.

It should be noted that while DEMs are extremely useful for studies of Earth's surface, they are only a representation of reality, and caution should be taken when using DEMs outside of their intended purpose. DEMs generated using this method contain data from numerous sources of varying reliability and can result in areas with significant interpolation due to sparse high-resolution data in remote areas. Furthermore, these DEMs cover very large swaths of Earth's surface, and it is impossible to ground truth the entire modeled area. It is also possible that outliers have not been identified and remain in the model. However, with that said, the highest-quality products possible are assured through internal expertise and training through NOAA and its National Centers for Environmental Information, as well as review from internal and external partners and collaborators.

CONCLUSION

Developing bathymetric-topographic DEMs is a time-consuming and complex process that involves preparing numerous large volume data sets from various sources and integrating them into a seamless product. This process is significantly more challenging for remote areas because data can be sparse. However, with detailed analysis, a high-quality product can be created that reasonably reflects reality and can significantly aid in improving coastal community safety.

Ocean Networks Canada has contributed DEMs to a number of projects in support of coastal community emergency preparedness, including for communities in Haida Gwaii, for northwest Vancouver Island (Kouhi et al., 2022), and through a cross-border collaborative effort as part of the Canadian Safety and Security Program for the lower mainland of southwestern British Columbia. Ocean Networks Canada looks forward to fostering collaborations and supporting future emergency preparedness efforts.

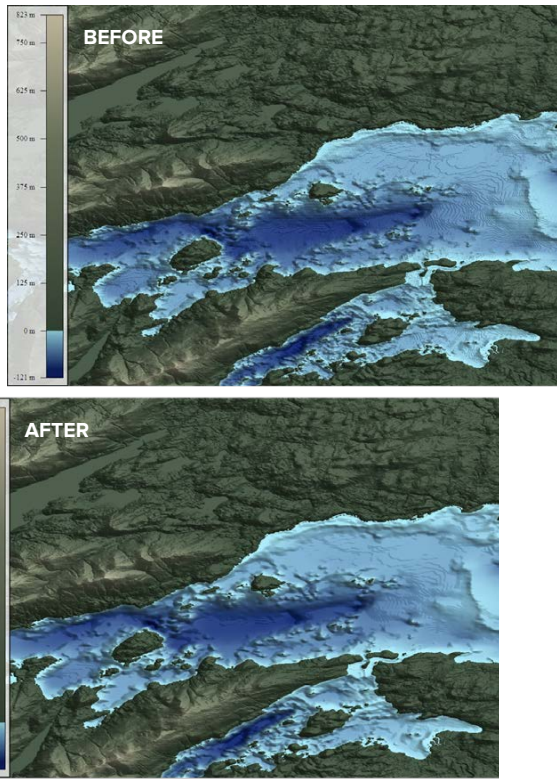

FIGURE 3. Comparison of a 10 m horizontal resolution DEM before (top) and after (bottom) a smoothing script with a smoothing factor of 20 was applied to the bathymetry.

REFERENCES

Kouhi, S., R. Amouzgar, M. Rankin, and C. Bosma. 2022. Assessment of tsunami coastal hazard along the Northwest Vancouver Island from coseismic sources in Cascadia and Alaska subduction zones. Paper presented at OCEANS 2022 Hampton Roads, October 17–22, 2022, IEEE/MTS.

NTHMP (National Tsunami Hazard Mitigation Program). 2010. *Tsunami Modeling and Mapping: Guidelines and Best Practices, Part I: Tsunami Inundation Modeling*. National Tsunami Hazard Mitigation Program, Mapping and Modeling Subcommittee, 4 pp.

ACKNOWLEDGMENTS

This work would not have been possible without collaboration with NOAA, NOAA's National Centers for Environmental Information, Northwest Hydraulic Consultants Ltd., Northwest Seismic Consultants Ltd., Natural Resources Canada, Fisheries and Oceans Canada, Defence Research and Development Canada's Centre for Security Science, Indigenous Services Canada, Emergency Management BC, and the University of Victoria. We would like to thank our funders and the communities we have worked with, including the North Coast Regional District, the Village of Daajing Giids, the Village of Masset, the village of Port Clements, Strathcona Regional District (SRD), Ka:'yu:'k't'h'/Che:k:tles7et'h' First Nations, Nuchatlaht First Nation, and Semiahmoo First Nation.

ARTICLE DOI. https://doi.org/10.5670/oceanog.2023.s1.23

Assessment of Tsunami Hazard Along British Columbia Coastlines from Coseismic Sources

By Soroush Kouhi, Reza Amouzgar, Mark Rankin, Cassandra Bosma, and Adrienne Shumlich

Recent major tsunamis have demonstrated their potential for widespread destruction and associated danger to human populations. Tsunamis generated from local and distant sources in the Pacific Ocean have impacted the western coast of Canada over time, and destructive tsunamis are expected to affect west coast communities in the future. Ocean Networks Canada (ONC) has undertaken several collaborative tsunami hazard assessment projects along the west coast of Canada (Figure 1) with the goals of (1) identifying and assessing tsunami hazards and risks using tsunami modeling, mapping, community engagement, and Indigenous knowledge; and (2) raising public awareness by producing a documentary film, offering educational programs to K–12 students, and developing tsunami signage and online story maps. This article focuses on tsunami hazard identification through modeling and drawing upon Indigenous knowledge.

MODELING METHODOLOGY

Modeling the generation and propagation of tsunami waves requires three essential elements: (1) ocean floor (bathymetry) and land (topography) elevation data, (2) seismic source data from local and distant earthquakes, and (3) a suitable numerical model.

Multiple bathymetric and topographic data sets were integrated to develop the high-resolution digital elevation models (DEMs) required for tsunami modeling, including lidar and single beam and multibeam bathymetric data. For the local tsunami source, the Cascadia subduction zone, Natural Resources Canada (NRCan) provided a recent rupture model corresponding to a magnitude 9 earthquake (Gao et al., 2018). This source resembles great megathrust earthquakes that occur roughly once every 300–500 years in this region, with the latest in 1700. While there is no written record of the impact of this earthquake along the eastern Pacific, it has been recorded in oral history as well as in the coastal and offshore stratigraphy from northern California to Vancouver Island. The distant tsunami source, the Alaska-Aleutian subduction zone, was the origin site for numerous significant earthquakes of magnitude 8 and more in the twentieth century. The largest of recent earthquakes, the 1964 Alaska earthquake, produced the largest instrumentally recorded tsunami waves to date on the British Columbia coast; this event provides a realistic proxy for similar large events that may be generated by the Alaska-Aleutian subduction zone. The numerical simulation of the 1964 tsunami in Figure 1 was based on recent earthquake information acquired from the University of Alaska Fairbanks (Suleimani and Freymueller, 2020).

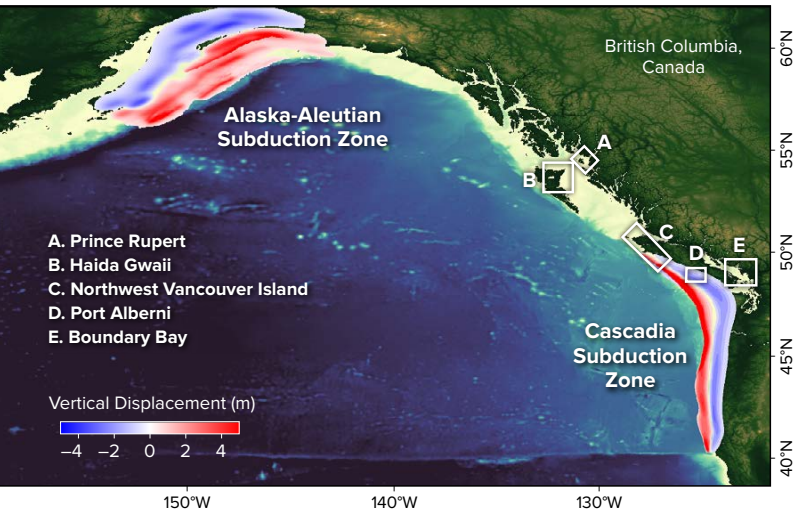

FIGURE 1. Several study areas along the coastlines of British Columbia, Canada, where tsunami risk assessment was performed by Ocean Networks Canada. Seismic source data are shown as seafloor vertical displacement (m) for the Alaska-Aleutian and Cascadia subduction zones. Blue indicates the seafloor/topography subsidence and red indicates seafloor/topography uplift.

We modeled the propagation and inundation of tsunamis induced by seismic events using FUNWAVE-TVD (Shi et al., 2012). The first step was to set up a series of nested grids to enable the model to resolve the complex physics as a tsunami propagates from the deep ocean into shoaling coastal regions. The nested grids increase resolution from the outer grid (2 arc-minutes) to the inner grid (~10 m). The wave elevations and horizontal water velocities are transferred from the coarser resolution to finer resolution grids at the model boundaries. Several parameters were also adjusted in the model based on the geographic location of each study area.

The next step was to establish tsunami model scenarios based on current-day sea level and projected future sea level rise (SLR). Recently, James et al. (2021) studied several averaged and enhanced SLR scenarios for the water bodies surrounding Canada, based on different pathways of greenhouse gas emissions through the twenty-first century. The worst-case scenario for 2100 predicts a maximum of up to 1.5 m of SLR for the Enhance Scenario at 2100 along British Columbia coasts. For our tsunami simulations, we lowered the underlying DEM by the local projected SLR value as a way to account for SLR.

FIGURE 2. This image of a silkscreen print created in 1977 by artist A-nii-sa-put (Tim Paul) from Mowachaht-Muchalaht First Nation depicts the earthquake foot legend. Along with other stories, this one highlights the knowledge and teachings that exist regarding earthquakes and tsunamis.

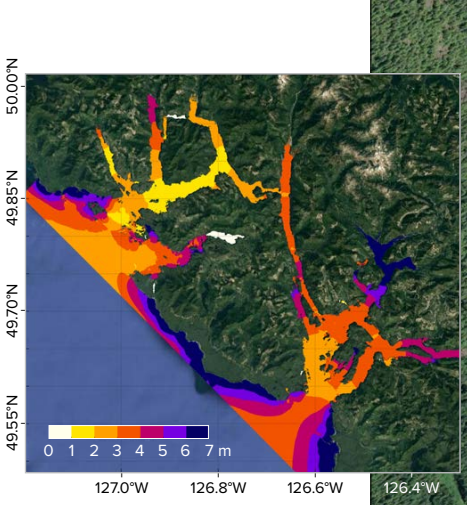

FIGURE 3. Maximum wave amplitudes are shown for a Cascadia-generated tsunami in Esperanza Inlet and Nootka Sound, as determined by the Northwest Vancouver Island Tsunami Risk Assessment Study.

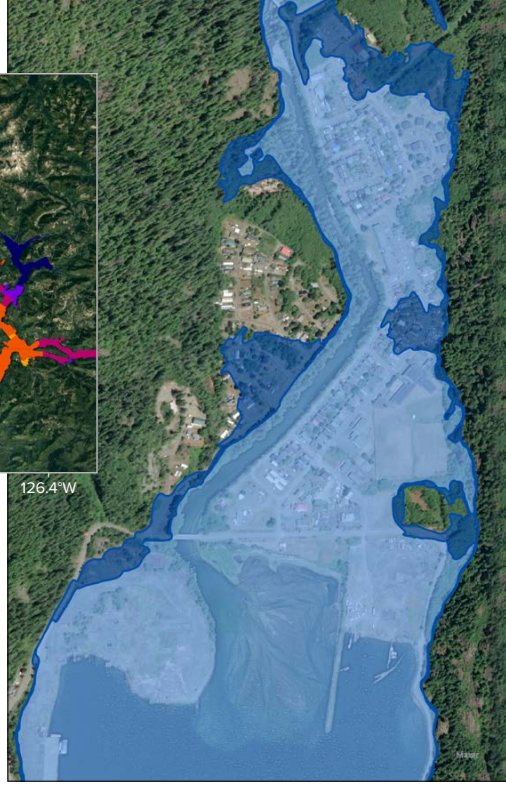

FIGURE 4. Inundation extent map for a Cascadia Tsunami in Tahsis, BC, Canada, were produced by the Northwest Hydraulic Consultant Ltd. in collaboration with Ocean Networks Canada for the Northwest Vancouver Island Tsunami Risk Assessment Project.

COMMUNITY AND INDIGENOUS ENGAGEMENT

Indigenous communities living where tsunami risk is high have fostered disaster resilience for millennia. Highlighting the knowledge and experience of the Indigenous community is critical for understanding current and future risks and implementing mitigation plans. Using a framework of "two-eyed seeing," where different ways of knowing are used simultaneously for the benefit of all, helps to improve the science by learning from community stories. For the Northwest Vancouver Island tsunami risk assessment study, through both research and interviews conducted with Elders and community members, multiple stories, teachings, and oral histories of past tsunamis, including but not limited to the 1700 and 1964 tsunamis, were collected and used to authenticate modeling results (Figure 2).

RESULTS

The modeling results demonstrate that tsunami waves generated by both local and distant earthquakes would considerably impact British Columbia coastal communities. The impact of the locally generated tsunami is more significant in Boundary Bay, Port Alberni, and Northwest Vancouver Island, while a tsunami originating in Alaska would have greater impacts in Prince Rupert and Haida Gwaii. Tsunami arrival times to the outer coast of Northwest Vancouver Island and Boundary Bay were estimated at about 20 minutes and 3 hours, respectively, after an earthquake in the Cascadia subduction zone. The Alaska tsunami, however, reaches Haida Gwaii and Prince Rupert about 2.5 and 3.5 hours, respectively, after the earthquake occurs.

Results also suggest that SLR does not significantly influence the tsunami wave amplitude offshore. However, propagation of these waves over land will lead to a greater extent of flooding as a result of SLR. Several overwater hazard graphics (Figure 3) and inundation maps (Figure 4) were created to represent the tsunami hazard information in each study area, including the tsunami wave amplitudes, current velocities, tsunami arrival times, and extent of flooding.

REFERENCES

Gao, D., K. Wang, T.L. Insua, M. Sypus, M. Riedel, and T. Sun. 2018. Defining megathrust tsunami source scenarios for northernmost Cascadia. *Natural Hazards* 94:445–469, https://doi.org/10.1007/s11069-018-3397-6.

James, T.S., C. Robin, J.A. Henton, and M. Craymer. 2021. Relative sea-level projections for Canada based on the IPCC Fifth Assessment Report and the NAD83v70VG national crustal velocity model. Geological Survey of Canada, Open File 8764, 1 .zip file, https://doi.org/10.4095/327878.

Shi, F., J.T. Kirby, J.C. Harris, J.D. Geiman, and S.T. Grilli. 2012. A high-order adaptive time-stepping TVD solver for Boussinesq modelling of breaking waves and coastal inundation. *Ocean Modelling* 43–44:36–51, https://doi.org/10.1016/j.ocemod.2011.12.004.

Suleimani, E., and J.T. Freymueller. 2020. Near-field modeling of the 1964 Alaska tsunami: The role of splay faults and horizontal displacements. *Journal of Geophysical Research: Solid Earth* 125(7), e2020JB019620, https://doi.org/10.1029/2020JB019620.

ACKNOWLEDGMENTS

The authors would like to thank Northwest Hydraulic Consultants Ltd., Ocean Networks Canada partner at tsunami risk assessment projects for Prince Rupert, Northwest Vancouver Island, and Haida Gwaii. The authors would also like to thank the funders and involved communities, including the North Coast Regional District, the city of Prince Rupert, the village of Daajing Giids, the village of Masset, the village of Port Clements, Strathcona Regional District, Ka:'yu:'k't'h'/Che:k:tles7et'h' First Nations, Nuchatlaht First Nation, Ehattesaht/Chinehkint First Nations, Quatsino First Nations, Mowachaht/Muchalaht First Nations, and Semiahmoo First Nation.

ARTICLE DOI. https://doi.org/10.5670/oceanog.2023.s1.24

Detection of Landslides and Tsunamis in Douglas Channel and Gardner Canal, British Columbia

By Fatemeh Nemati, Lucinda Leonard, Gwyn Lintern, Camille Brillon, Andrew Schaeffer, and Richard Thomson

In 1975, an underwater landslide in Kitimat Arm at the northern end of Douglas Channel, British Columbia (Figure 1a), triggered tsunami waves that were observed to reach a height of over 8 m at the head of the inlet, destroying a dock and a newly built barge terminal (Bornhold, 1983). Elsewhere in the Douglas Channel region, seafloor deposits attest to previous submarine landslide events (Conway et al., 2012; Stacey et al., 2019), and subaerial landslides of various sizes regularly occur (Maynard et al., 2017). Landslide-generated tsunamis are increasingly recognized as a substantial hazard worldwide, with the potential for extreme wave runup and localized damage, particularly in narrow, steep-sided bays and inlets. In most cases it is not possible to prevent landslides from occurring; however, mitigation efforts can include early landslide detection and the development of tsunami early warning systems using real-time data.

The Douglas Channel region provides an ideal location for developing and testing a landslide and tsunami detection system. Douglas Channel and Gardner Canal, a side inlet, are located in a complex coastal area with a history of landslide-generated tsunamis. The district of Kitimat, the villages of Kitamaat and Hartley Bay, the traditional territories of the Haisla and Gitga'at Nations, and various sites of infrastructure, including ports and the Rio Tinto Generating Station docks near Kemano, are all at risk of damage from landslide-generated tsunamis.

Throughout the steep-sided Douglas Channel and Gardner Canal region there are many potential source locations for both subaerial and underwater failures that may be triggered by heavy rainfall, tidal loading, earthquake shaking, erosion, or changes in groundwater pressure (Lintern et al., 2019; Stacey et al., 2019). The 8 m 1975 tsunami was caused by a submarine failure of delta sediments (e.g., Skvortsov and Bornhold, 2007), and there is ongoing potential for large rigid subaerial landslides. Figure 1b,c shows two examples of landslides that occurred in Gardner Canal in 2017, triggered by heavy rain.

A SYSTEM FOR EARLY DETECTION OF LANDSLIDES AND TSUNAMIS

The Douglas Channel and Gardner Canal landslide and tsunami detection system is based on a network of land-based seismometers, underwater hydrophones, and bottom pressure sensors (Figure 1a). The seismometers and hydrophones will be used to detect and locate landslides, with water level observations provided by the bottom pressure sensors.

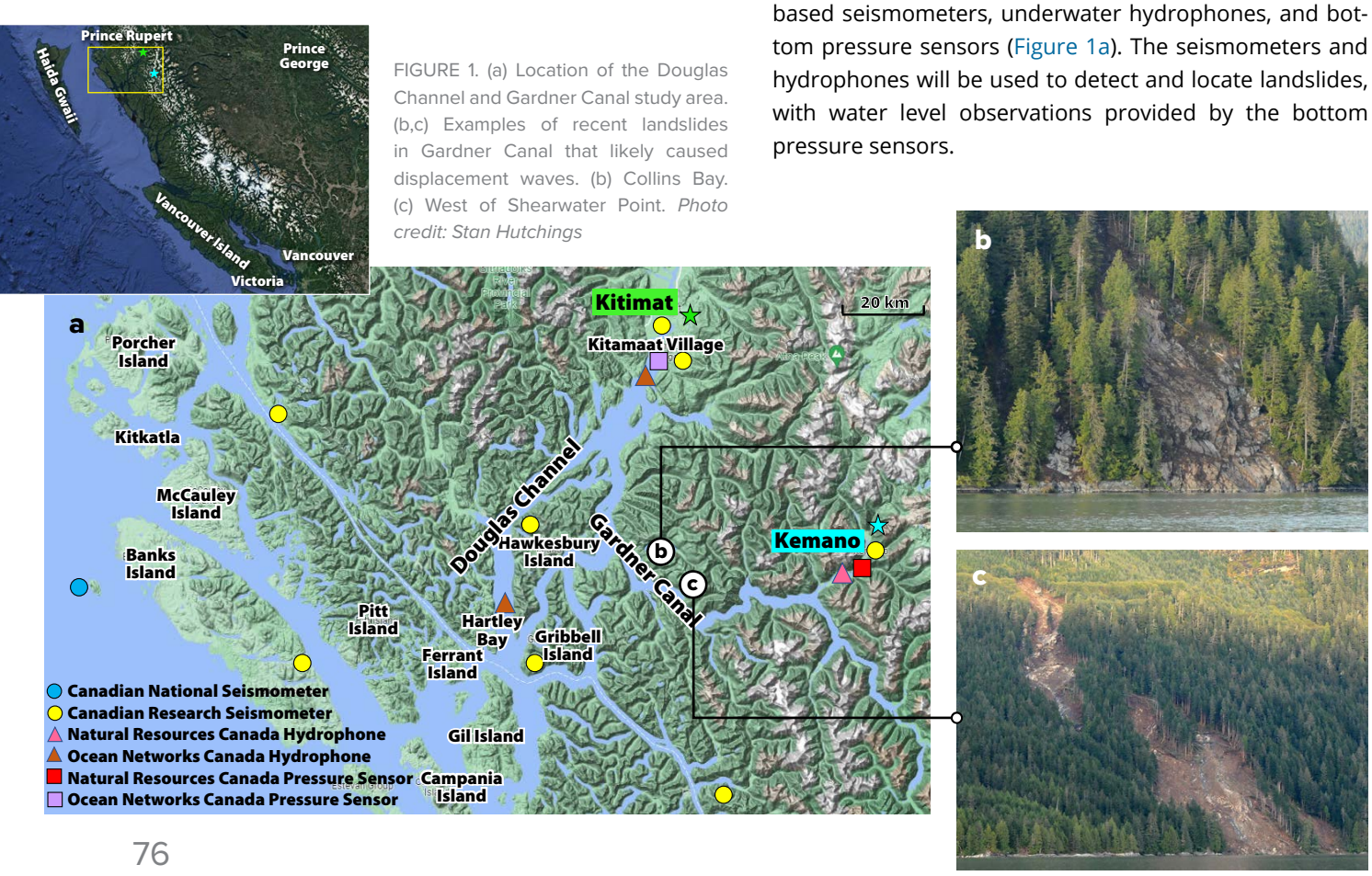

FIGURE 1. (a) Location of the Douglas Channel and Gardner Canal study area. (b,c) Examples of recent landslides in Gardner Canal that likely caused displacement waves. (b) Collins Bay. (c) West of Shearwater Point. *Photo credit: Stan Hutchings*

Seismometers are the principal tool for measuring earthquake energy; three-component instruments record a time series of ground motion in three orthogonal spatial orientations. Landslides produce high-energy, low-frequency signals that can also be captured by broadband seismometers located at large distances from the source region (dependent on landslide volume). Recorded landslide signals are distinct from those produced by earthquakes, which contain higher frequency energy, are more impulsive, and have shorter source durations (Figure 2). Because of major differences between a landslide and a typical tectonic earthquake-generated waveform, traditional approaches for (near) real-time seismic detection and epicenter location need to be adjusted for landslides in order to detect and locate them rapidly.

Submarine and subaerial landslides release energy as hydroacoustic waves as they enter a body of water. Low-frequency hydrophones, which record hydroacoustic signals, are cost-efficient and time-saving instruments that supplement land-based broadband seismometer networks to detect and locate landslides.

Bottom pressure sensors record a time series of the bottom pressure of the water above the sensor, which is directly related to water depth. Thus, the time series provides a record of both gradual changes in water level due to tides as well as sudden changes due to tsunami waves, which have very different characteristics than wind-generated surface gravity waves.

The tsunami detection system consists of eight pre-existing seismic stations (including two outside the map area), mostly installed since 2014 for the purpose of recording earthquakes; two hydrophones located at Hartley Bay and near Kitamaat Village; and one bottom pressure sensor near Kitamaat Village (Figure 1). In November 2022, we installed an additional seismic station, a hydrophone, and a bottom pressure sensor near the Kemano dock in Gardner Canal. These new instruments will improve the detection and location capability of the seismic-hydrophone network, particularly for landslides within Gardner Canal, which typically occur several times a year. The new bottom pressure sensor will enable the observation of any significant landslide-generated tsunami waves in Gardner Canal.

Preliminary work will involve the identification of past landslide events in seismic and hydrophone data with ground-truth observations, and potential tsunami wave events in bottom pressure data. For each data type, detection algorithms will focus on signals unique to landslides/tsunamis, with processing steps involving bandpass filtering and spectral analysis. When a landslide occurs, the seismometers and hydrophones may detect the associated seismic waves and acoustic emissions as an early warning method. The goal is for landslide detection to provide early tsunami warning before waves reach the pressure sensors and the communities and infrastructure that are at risk. The features of possible landslide-generated tsunamis can be predicted using numerical modeling. A combination of numerically simulated tsunamigenic events and instrumentally recorded waves will enable us to optimize the positioning of the instrumental array for the real-time tsunami warning system and to better estimate the effects of the waves within the study region.

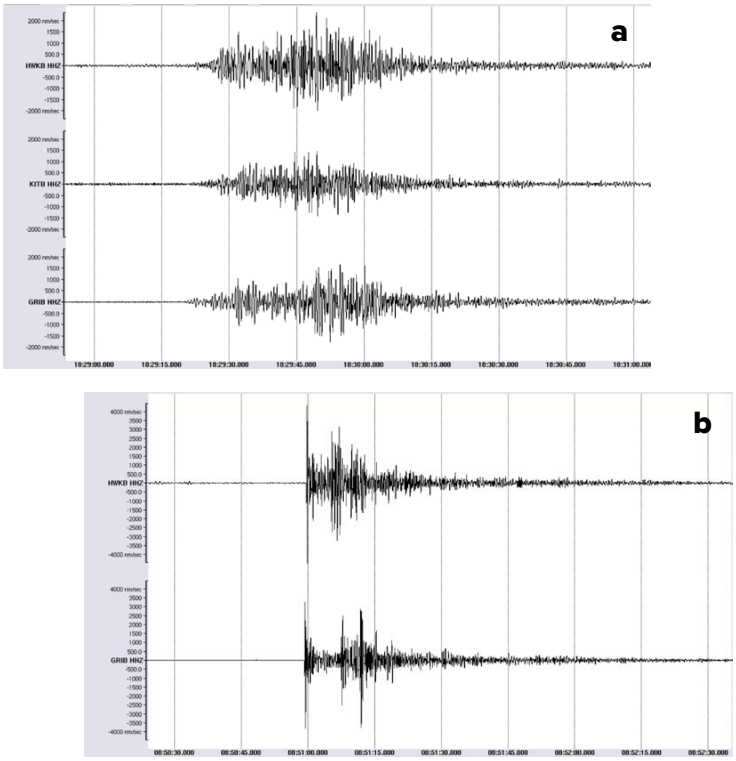

FIGURE 2. Example vertical component recordings at seismic stations in the network, bandpass filtered to 1–5 Hz. Recording of (a) a landslide near Ecstall River, BC, on September 1, 2022, and (b) a local M3.1 earthquake on September 29, 2022.

REFERENCES

Bornhold, B.D. 1983. Fiords. *GEOS* 12(1):1–4.

Conway, K.W., J.V. Barrie, and R.E. Thomson. 2012. *Submarine Slope Failures and Tsunami Hazard in Coastal British Columbia: Douglas Channel and Kitimat Arm.* Geological Survey of Canada, Current Research, 2012-10, 17 pp., https://doi.org/10.4095/291732.

Maynard, D.E., I.C. Weiland, A. Blais-Stevens, and M. Geertsema. 2017. Surficial geology, North Kitimat Arm, Douglas Channel area. Canadian Geoscience Map 300 (Preliminary Edition), Geological Survey of Canada, 1:25,000 scale map area, https://doi.org/10.4095/300850.

Stacey, C.D., D.G. Lintern, J. Shaw, and K.W. Conway. 2020. Slope stability hazard in a fjord environment: Douglas Channel, Canada. *Geological Society, London, Special Publications* 500(1):427–451, https://doi.org/10.1144/SP500-2019-191.

Skvortsov, A., and B. Bornhold. 2007. Numerical simulation of the landslide-generated tsunami in Kitimat Arm, British Columbia, Canada, 27 April 1975. *Journal of Geophysical Research* 112(F2), https://doi.org/10.1029/2006JF000499.

ARTICLE DOI. https://doi.org/10.5670/oceanog.2023.s1.25

EASTMOC: Environmental Alert System for Timely Maintenance of the Coastal Zone

By Vitalijus Kondrat, Ilona Šakurova, Eglė Baltranaitė, and Loreta Kelpšaitė-Rimkienė

Healthy beaches are essential for managing the coastal zone, including growing coastal tourism, maintaining seaside property values, developing infrastructure, and sustaining coastal ecosystems and communities. Beaches worldwide face problems such as erosion and shoreline recession caused by both natural factors and anthropogenic pressures. Beach erosion is caused by short-term fluctuations such as storms or by longer-term processes related to sediment budget deficits, rising sea levels, and wave regime changes. Responsible beach management requires precise knowledge of the short-term fluctuations and long-term processes involved in coastal evolution in order to assess the risks to infrastructure and to identify acceptable weaknesses in future development or in coastal management. Knowledge of short- and long-term shoreline changes could also contribute to the design of beach nourishment plans so that human activities can be conducted consistent with natural processes rather than in conflict with them.

This study focuses on the need for an Environmental Alert System for Timely Maintenance of the Coastal Zone (EASTMOC) along Lithuania's Baltic Sea coast. It is based on coastal research conducted in the Port of Klaipeda. Because this area is affected by constant dredging of the port, intensive shipping, recreational zones, and continuous reconstruction of jetties, it is important to create an environmental alert system for timely port maintenance.

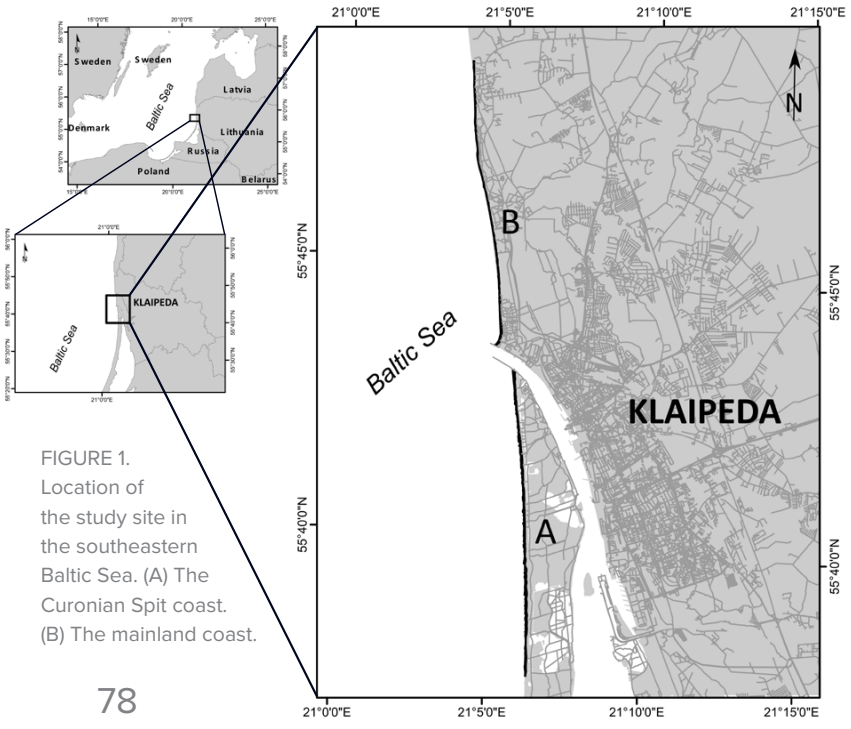

FIGURE 1. Location of the study site in the southeastern Baltic Sea. (A) The Curonian Spit coast. (B) The mainland coast.

THE KLAIPEDA PORT IMPACT ZONE

The Lithuanian Baltic Sea coast is affected by wind and waves from a wide range of directions. The study site was chosen based on its (1) broad spectrum of recreational uses, (2) high risk of coastal erosion, and (3) possibility of direct and indirect anthropogenic impacts.

The Port of Klaipeda is located at the Klaipeda Strait and divides the Lithuanian coast into two morphologically and geologically diverse parts: the Curonian Spit coast to the south and the mainland coast to the north (Figure 1; Bitinas et al., 2005). The port's jetties disturb the main sediment transport path (from south to north) along the Lithuanian coast and significantly influence its northern sector.

Analysis of long-term trends in shoreline change show that shoreline formation processes, which determine and form the balance of shoreline change, have intensified due to port reconstruction. Net shoreline movement analysis for the entire 1993–2022 study period (Figure 2) shows that 39.05% of the shoreline was erosive, 34.04% was accumulative, and 26.53% was stable or within the range of uncertainty (±5.02 m). A comparison of shoreline changes for the periods 1993–2003 and 2003–2022 shows that the area of eroded coast increased 4.4 times, from 2.73 km to 11.90 km. Significant coastal erosion (−51.95 m) extends north from the port jetties of Klaipeda. Shoreline positions were determined from sets of aerial photo charts, orthophotos, and GPS survey data. Measurements of coastline position were collected in the middle of the swash zone using Leica 900 dual-band GPS receivers. Historical coastline positions were measured every 25 m along the coastline. Three coastline positioning and detection errors were calculated (see Crowell et al., 1993), and shoreline position changes were analyzed with the ArcGIS extension DSAS v. 5.0 (Digital Shoreline Analysis System) package developed by the US Geological Survey.

Coastal geomorphology and underwater elevation changes calculated from bathymetry data using Global Mapper software helped to identify that reconstruction and continuous dredging of the Port of Klaipeda influence the sediment budget along the study area. In the period 2003–2022, about 2.5 km north of the port jetties, a bottom sediment deficit was observed, with the coastal elevation reduced by about 5–7 m (Figure 2).

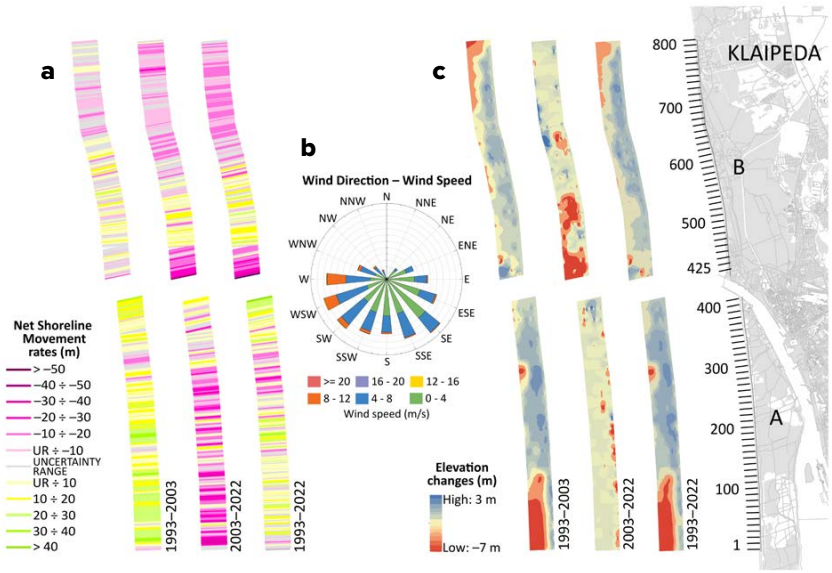

FIGURE 2. (a) Net shoreline movement rate tendencies on the (A) Curonian Spit coast, and (B) mainland coast. (b) Wind direction and speed (m s^{-1}) during 1993–2022. (c) Coastal zone elevation changes (m) on the (A) Curonian Spit coast, and (B) mainland coast.

FIGURE 3. Essential inputs to EASTMOC.

EASTMOC

EASTMOC combines research and monitoring of coastal morphological features, hydrometeorological conditions, and human activities, which are critical inputs to an environmental warning system (Figure 3). In order to ensure that EASTMOC addresses stakeholders' needs, interviews with stakeholders helped to identify the data they use in day-to-day operations (e.g., wind speed and direction, wave direction and height, water and air temperatures, atmospheric pressure), data gaps, and data sharing practices, as well as to determine the relevant thresholds for various industries. Stakeholders are interested in hydrometeorological thresholds because they limit the activities of port authorities, passenger ferries, and commercial fishermen. For example, strong winds (≥15 m s^{-1}) limit local passenger ferry traffic, interrupting transportation links to the Curonian Spit. They also disrupt port activities, sometimes resulting in port closures to ship traffic for several hours or days. In addition, the long-term effects of local hydrometeorological conditions can lead to adjustments in municipal to national-level strategic plans.

Bayesian networks are well suited for explicitly integrating both prior knowledge and information obtained from daily environmental observations. As determined in previous studies based on Bayesian networks, there is a correlation between socioeconomic and natural factors, such as air and water temperature, the presence of dunes and sandy beaches, and tourists' recreational needs (Baltranaitė et al., 2021). EASTMOC will include quantitative assessment and prediction modeling based on the Bayesian networks to ensure sustainable planning and operation of all parties active in the study area. The current stage of development of EASTMOC includes creating a network of data sources to ensure data availability and accessibility among stakeholders. These sources are essential to the alert system concept, as the thresholds will be set based on these data.

The database compiled in EASTMOC will be directed to the stakeholders and end users. Stakeholders involved in the development of EASTMOC will receive tailored alerts generated according to the thresholds that are relevant to their specific activities. While some end users require simple wind speed and direction warnings, others need more complex correlation of several data sets. However, EASTMOC may become relevant to the general population and further adapted on a smaller scale. For instance, beachgoers and extreme watersport enthusiasts may benefit from strong wind warnings while planning a day out, as strong winds may not be favorable for sunbathing but beneficial for extreme sports.

EASTMOC has the potential to fill the gap in access to current data, serve as a hub for knowledge sharing, and provide early warning to stakeholders in accordance with the thresholds set up in line with the specifics of their activities. Though our study area is significant on a regional scale, our research methodology can be adapted to assess similar coasts worldwide.

REFERENCES

Crowell, M., S.P. Leatherman, and M.K. Buckley. 1993. Shoreline change rate analysis: Long term versus short term data. *Shore & Beach* 61:13–20.

Baltranaitė, E., L. Kelpšaitė-Rimkienė, R. Povilanskas, I. Šakurova, and V. Kondrat. 2021. Measuring the impact of physical geographical factors on the use of coastal zones based on Bayesian networks. *Sustainability* 13:7173, https://doi.org/10.3390/su13137173.

Bitinas, A., R. Žaromskis, S. Gulbinskas, A. Damušyte, G. Žilinskas, and D. Jarmalavičius. 2005. The results of integrated investigations of the Lithuanian coast of the Baltic Sea: Geology, geomorphology, dynamics and human impact. *Geological Quarterly* 49:355–362.

ARTICLE DOI. https://doi.org/10.5670/oceanog.2023.s1.26

Advances in Environmental DNA Sampling for Observing Ocean Twilight Zone Animal Diversity

By Annette F. Govindarajan, Allan Adams, Elizabeth Allan, Santiago Herrera, Andone Lavery, Joel Llopiz, Luke McCartin, Dana R. Yoerger, and Weifeng Zhang

THE OCEAN TWILIGHT ZONE

The ocean's vast twilight, or mesopelagic, zone (200–1,000 m depth) harbors immense biomass consisting of myriad poorly known and unique animal species whose quantity and diversity are likely considerably underestimated. As they facilitate the movement of carbon from surface waters to the deep sea through feeding and migratory behaviors, ocean twilight zone (OTZ) animals are vital to regulating Earth's climate (Ducklow et al., 2001). However, anthropogenic threats, such as climate change, ocean acidification, pollution, and overfishing pose an imminent threat to OTZ animals. Long-term spatially and temporally intensive observations are essential to our understanding of biodiversity in the OTZ, to resolving global carbon cycles, and to monitoring ocean health. Environmental DNA (eDNA) analysis, which involves studying the trace genetic signatures of organisms (Figure 1), is a promising approach to filling this urgent need. eDNA can be sampled and diagnostic genetic markers ("barcodes") can be sequenced in order to detect the animals inhabiting a given water parcel. Other laboratory protocols (e.g., quantitative PCR, or "qPCR" and "digital droplet PCR") can be applied to facilitate quantitative assessments of specific target species (Eble et al., 2020). In seagoing oceanographic research, eDNA assessment is transitioning from being considered an experimental approach to becoming an established routine that can be scaled up to match ocean observing needs.

TECHNOLOGICAL NEEDS FOR OTZ eDNA ANALYSES

As eDNA analyses are incorporated into mid- and deep-water oceanographic research and observing platforms, new technologies and an improved understanding of eDNA distributions and their relationships to animal distributions and sampling methods are required. Each step of the eDNA analysis process, from experimental design and sample collection to data analysis, impacts the final result (Figure 2). Of the different steps that could introduce bias (Eble et al., 2020; Shelton et al., 2022), sampling approaches and strategies are particularly underexplored (Govindarajan et al., 2022).

FIGURE 1. The ocean twilight zone (OTZ) is home to a diverse faunal assemblage, including fish, crustaceans, and gelatinous animals, all of which leave behind genetic traces (eDNA, conceptualized as particle clouds in the background) as they move through the water. eDNA can originate from sloughed cells and scales, fecal pellets, gametes, tissue fragments from sloppy feeding, and other processes. Animal images are not to scale. *Photo credits: Paul Caiger (WHOI) and Laurence Madin (WHOI)*

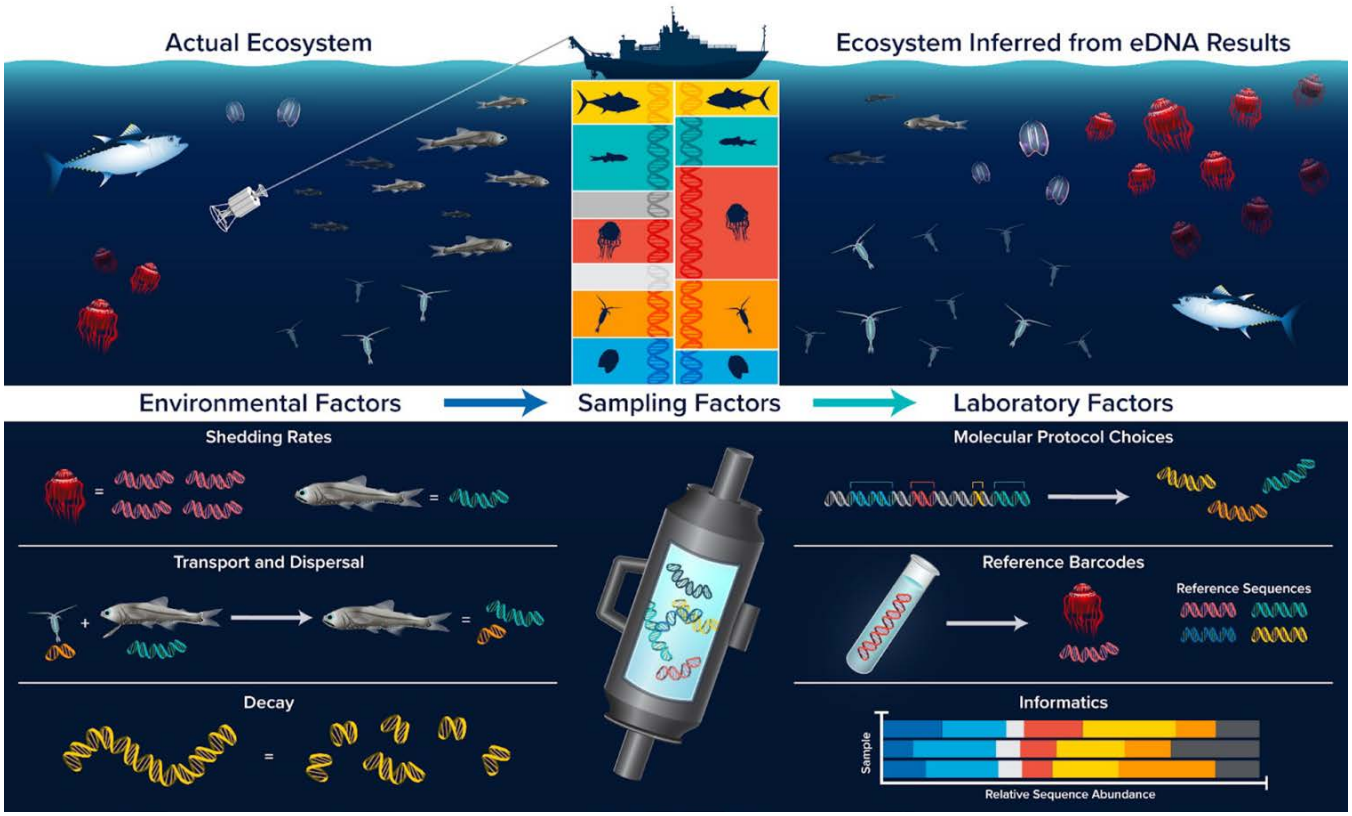

FIGURE 2. A schematic of the eDNA analysis process and the different environmental, sampling, and laboratory factors that may cause the results to differ from the true biodiversity landscape.

The OTZ has unique attributes requiring special considerations for sampling. This habitat is massive in size, difficult to access, and has heterogeneously distributed biomass. Traditional sampling requires extensive seagoing effort and expensive instrumentation. Notably, a substantial fraction of OTZ animal biota undertakes daily vertical migrations—moving up to surface waters to feed at night and back down to depth during the day. This process, considered the largest migration of biomass on our planet, greatly facilitates carbon transfer to the deep sea. Understanding the relationships between diel vertical migration, the biological carbon pump, and Earth's climate requires OTZ biodiversity observations at a scale and scope beyond what traditional methods like net tows can offer.

For eDNA analyses to fill this critical need, the following questions must be addressed. How do we effectively and representatively sample such a vast environment? What sampling strategies and spatiotemporal scales best represent mesopelagic biodiversity distributions and phenomena? In a setting where both the animals and the surrounding water move horizontally and vertically, how can we know if eDNA signals represent biodiversity signatures of the sampling location or elsewhere? Answers to these questions are vital to guiding the development of technologies that will fulfill ocean observing needs.

NISKIN BOTTLE eDNA SAMPLING

A primary impediment to the expansion of eDNA biodiversity assessments into mid- and deep-ocean observing programs is the lack of adequate sampling capability. Most seawater samples are collected via Niskin bottles mounted to oceanographic instruments. Niskin bottles are most commonly deployed on CTD rosettes, although they can also be deployed on submersibles. eDNA sample volumes are typically between 1 liter and 5 liters and are often limited by the size of the Niskin bottle and by other competing needs for seawater (e.g., nutrient and biogeochemical analyses). There are only a modest number of bottles per deployment (typically between 8 and 24), limiting the number of target depths sampled during a given deployment. The number of independent samples becomes smaller if two- or three-fold sample replicates are taken. Water collected by the bottles is filtered onboard the ship to capture the eDNA once the CTD rosette is recovered, usually with peristaltic or vacuum pumps (Figure 3). The filtration process is labor intensive. For example, peristaltic pumps connected to commonly used encapsulated Sterivex filters (Millipore Sigma) have a flow rate of around 100 milliliters per minute (manufacturer's documentation) resulting in about 50 minutes of filtering time for a 5-liter water sample. Multiple bottles must be filtered simultaneously, potentially providing opportunities for handling errors and contamination.

FIGURE 3. Typical oceanographic eDNA collection strategy. Seawater in Niskin bottles on a CTD rosette is filtered for eDNA collection. In this example, tubing connects the Niskin bottle spigots directly to filters with submicron pore sizes. Seawater is pumped with multi-head peristaltic pumps so that several samples can be filtered simultaneously. The filtering outflow is collected in carboys to determine the exact volume of water filtered. *Photo credit: Erin Frates (WHOI)*

AUTONOMOUS eDNA SAMPLERS AND SAMPLING PLATFORMS

Autonomous sampling with in situ filtration is an alternative approach for sample collection. In situ filtration offers numerous advantages, including reduced labor, fewer opportunities for contamination, larger sample volumes, and fewer experimental design constraints (Yamahara et al., 2019; Govindarajan et al., 2022; Truelove et al., 2022). Autonomous samplers must be mounted on platforms that access the target environment, such as autonomous underwater vehicles (AUVs), remotely operated vehicles (ROVs), or towed instruments. For example, the Environmental Sample Processor (ESP) has been incorporated into a long-range AUV (Yamahara et al., 2019; Truelove et al., 2022) and can take up to 50 eDNA samples, filtering seawater at a rate of about 1 liter per hour. In a different approach, a large-volume eDNA sampler that could take 12 samples was mounted on the midwater robot *Mesobot* to filter seawater at a rate of about 2 liters per minute (Govindarajan et al., 2022). A newer version of the large-volume sampler can take up to 16 samples and can be daisy-chained with additional sampler units for greater collection capacity (recent work by authors Adams, Govindarajan, and Yoerger, and Lui Kawasumi of Oceanic Labs) and deployed on both *Mesobot* (Box 1) and the towed acoustic and imaging instrument Deep-See (Box 2).

SAMPLING STRATEGIES

Standard CTD-mounted Niskin bottle sampling strategies typically involve a vertical profile with samples collected at targeted depths. Water is collected instantaneously at a point when the designated bottle is triggered. Animals are patchily distributed and often found in layers, and real-time acoustic backscatter data from an echosounder can be used to guide the selection of sampling depths by identifying concentrations of biomass (Govindarajan et al., 2021). Niskin bottles may be mounted on other platforms, such as ROVs or AUVs, permitting greater sampling flexibility (Everett and Park, 2018).

In contrast to instantaneous Niskin bottle sampling, samplers with in situ filtration filter continuously over a

BOX 1. LARGE-VOLUME eDNA SAMPLING ON *MESOBOT*

We coupled large-volume eDNA sampling with the robot *Mesobot*, a recently developed autonomous underwater vehicle designed for studying midwater regions (Yoerger et al., 2021). *Mesobot* carries a wide variety of sensors, can track and image small animals and particles, and can carry eDNA samplers in its payload section. Figure B1 shows three 16-sample modules integrated into *Mesobot*'s payload section. The unit on the far right is loaded with cartridges (dark blue) containing collection filters. The sampler has a high filtration rate (approximately 2 liters/minute) and uses large-area filters to accommodate large sample volumes. By sampling larger volumes, more animal taxa can be detected, making this approach well suited for environments where the eDNA signal is dilute and when it is important to detect rare species (Govindarajan et al., 2022). We took advantage of *Mesobot's* Lagrangian motion capabilities and our large-volume samplers to collect several time series of eDNA samples at a constant depth from the same water parcel to determine the timing of ocean twilight zone animal migrations. Our time-series experiments consisted of continuous, consecutive collection of ~30-liter samples before, during, and after the evening migration period. We conducted these experiments during cruises on E/V *Nautilus* in the Santa Monica Basin in September 2021 and on R/V *Endeavor* in the Slope Sea in the Northwest Atlantic Ocean in August 2022. Analysis of both data sets is in progress.

FIGURE B1. The autonomous midwater vehicle *Mesobot* is loaded with a variety of sensors and samplers. *Photo credit: Lui Kawasumi (Oceanic Labs)*

period of time (Figure 4). Sampling is "Lagrangian" if the sampler collects samples as it moves along with the water parcel. *Mesobot*, designed to track organisms and particles (Yoerger et al., 2021), can act as a Lagrangian sampling platform (Box 1). In contrast, non-Lagrangian sampling is integrative. For example, "Eulerian" sampling is a type of non-Lagrangian, integrative sampling where the sampler is at a fixed location (e.g., from a mooring or a stationary vessel), filtering as the water flows past. Sampling is also integrative if the sampler is mounted on non-Lagrangian mobile platforms, such as some AUVs and towed instruments like Deep-See (Box 2). These platforms may traverse water parcels over the duration of sampling, resulting in "crosscutting" spatially and temporally integrated samples. This is the case with powered autonomous vehicles that must maintain forward motion to stay in control while surveying. These often move in a "sawtooth" pattern (e.g., Govindarajan et al., 2015), although the integration can be minimized by containing the vehicle movements within the moving flow. For example, the vehicle can travel forward while turning continuously in tight circles (Truelove et al., 2022). As a result, the vehicle remains with a water mass of known size, rendering it effectively Lagrangian. Integrative sampling also occurs with Deep-See, which, as a towed instrument, moves with the ship, potentially against the prevailing flow and traversing water parcels (Box 2). It is important to recognize that as these approaches (instantaneous, Lagrangian, and non-Lagrangian) may be sampling different entities, they may not be directly comparable.

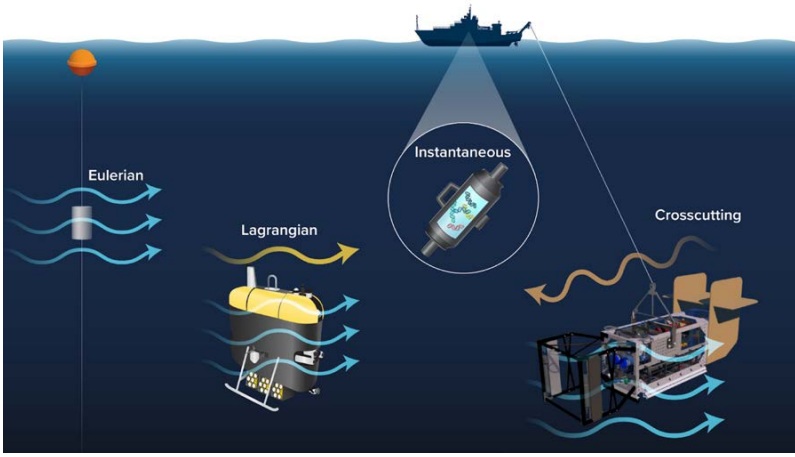

FIGURE 4. Sampling can be instantaneous (at a point in time and space), Lagrangian (over time moving with the water parcel), Eulerian (integrative over time from a fixed point with water moving by), or crosscutting (integrative over time from a moving non-Lagrangian platform). The wavy blue lines indicate ambient water movement during sampling for the non-instantaneous approaches. The yellow arrow shows *Mesobot* moving with the ambient water parcel and the brown arrow shows *Deep-See* moving against the ambient flow.

FILTRATION TIME AND SAMPLE VOLUME

The OTZ environment is immense, and the animals that live there (and their eDNA traces) are patchily distributed. Current eDNA sampling strategies may not yield representative results as they may not match the appropriate temporal and spatial scales of eDNA variation. Field observations have demonstrated that eDNA concentrations decrease with depth and that there can be high variability in the types and proportions of taxa found in sampling replicates (Easson et al., 2020; Govindarajan et al., 2022). These observations indicate that typical sample volumes (1 to 5 liters) are not aligned with eDNA distributions and that sampling strategies used in shallow and coastal environments may need to be increased for mid- and deep-ocean waters. Autonomous sampling can facilitate the filtration of larger sample volumes. To obtain these larger volumes while minimizing unwanted spatial and temporal sample integration, higher sampler filtration rates are needed (Govindarajan et al., 2022). Ideally, a sample should be taken within the confines of the target water parcel. However, the size of the target parcel is usually undefined or unknown, given the lack of knowledge about eDNA distributions. Determining optimal sample volume, the number of replicates, and the spatial and temporal sampling frequencies will require further advances in sampling technology, including developing low-cost samplers that can be intensively deployed over large areas.

CO-COLLECTION OF eDNA WITH NET TOW AND ACOUSTIC SENSOR DATA

eDNA sampling is complementary to other sampling and sensing methods. Traditional net tows and trawls collect physical specimens, which can provide insights into life histories and ecology (e.g., life stage-specific distributions and dietary analyses) of OTZ animals. The Multiple Opening/Closing Environmental Sensing System (MOCNESS) is composed of a series of nets that can take vertically discrete samples (generally integrative over tens or hundreds of meters) and is useful for assessing phenomena such as diel vertical migration. As eDNA-based biodiversity assessments are adopted, several studies have compared eDNA-based biodiversity estimates with those from net or trawls, including the MOCNESS (e.g., Govindarajan et al., 2021). These studies typically find that both methods recover many of the same animal taxa, while also recovering taxa unique to each method. It is important to note that these are "apples to oranges" comparisons that fundamentally measure different entities (organisms vs eDNA) and the volume of water parcels that they are sampling. Net tows are integrative over time and space (i.e., integrative sampling from a mobile, non-Lagrangian platform)—but

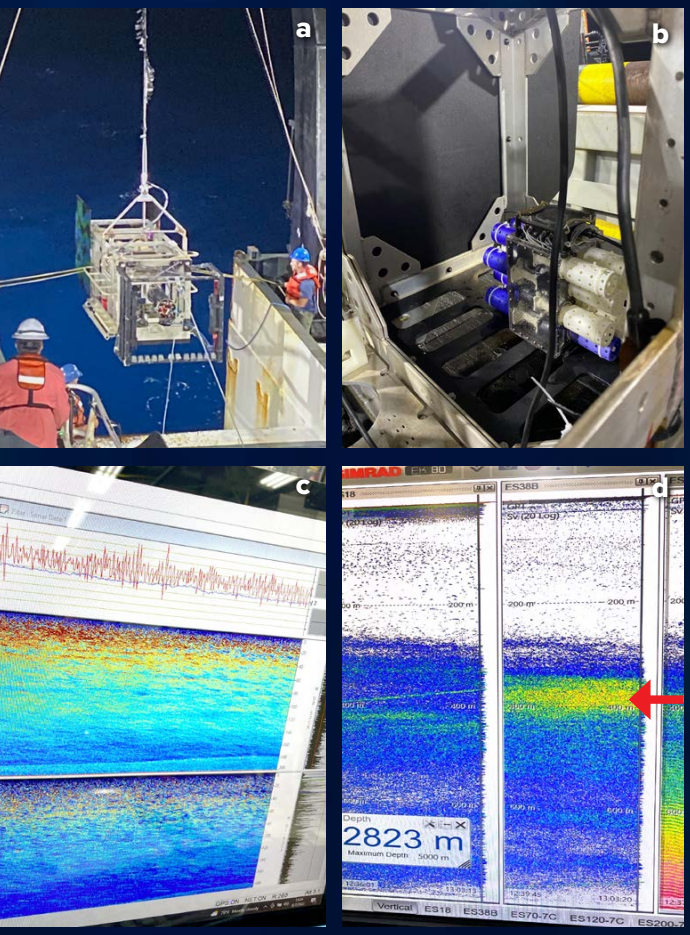

BOX 2. ADAPTIVE eDNA SAMPLING AND ACOUSTICS WITH DEEP-SEE

We paired autonomous eDNA sampling with the towed instrument Deep-See (Figure B2a) to enable the co-collection of eDNA, acoustics, and imaging data (Lavery et al., 2019). Deep-See combines wide-band, split-beam acoustics (1–500 kHz) with optical and environmental sensors and enables acoustic and image data collection from mesopelagic depths. We mounted one 16-filter large-volume sampler unit on the tail section of Deep-See (Figure B2b). During an August 2022 cruise on NOAA Ship *Henry B. Bigelow* to study the ocean twilight zone in the Slope Sea in the Northwest Atlantic, we conducted adaptive eDNA sampling by triggering sampling from a shipboard computer in response to observed acoustic backscatter from both Deep-See (Figure B2c) and the shipboard echosounder (Figure B2d). Unlike the narrowband signals used with shipboard echosounders, the wide-band capabilities of Deep-See allow the spectral responses of individual animals to be measured. To identify eDNA signatures associated with these unique spectral signatures, we are analyzing samples collected inside and outside observed biomass patches. The ability to take eDNA samples adaptively in response to real-time acoustic backscatter will allow us to better target patchily distributed biomass and transient phenomena such as vertical migration behavior. Sampling inside and outside of biomass patches could also potentially facilitate understanding of the relationship between eDNA metabarcoding results and biomass.

FIGURE B2. (a) The towed instrument Deep-See. (b) A large-volume sampler unit attached to Deep-See's tail section allows triggering of eDNA sampling in response to (c) acoustic backscatter from Deep-See instrumentation and (d) the ship's echosounder. The red arrow in (d) indicates an adaptively sampled biomass patch. *Photo credits: Annette Govindarajan (WHOI)*

at a much larger scale than integrative eDNA sampling. Net tows sample very large volumes, covering hundreds or thousands of meters over the course of an hour or more, and sampling orders of magnitude more water (Govindarajan et al., 2021). As such, eDNA and net tow comparisons should be viewed as complementary, not as "calibrations" of each other.

Data collected with echosounders, which measure acoustic backscattering from OTZ animals, can be used to estimate distribution and biomass and are also complementary to eDNA sampling. Both data types are especially valuable for the OTZ, where migrating biomass can be identified from the movements of sound-scattering layers. Typically, shipboard echosounders for OTZ studies operate at frequencies of 18 kHz and 38 kHz. Real-time observations of acoustic backscatter can be used to guide eDNA sampling (Zhang et al., 2020; Govindarajan et al., 2021; Box 2). Conversely, eDNA data can potentially provide taxonomic resolution for interpretation of acoustic signals, which at these frequencies are typically dominated by animals with gas-bearing structures such as fish with swim bladders and siphonophores (Lavery et al., 2007), and may identify the broader animal communities associated with these signals. Traditionally, depth-stratified net tows have been used for this purpose. However, net tows may integrate across acoustic layers, and animals such as active swimmers and delicate gelatinous species are undersampled. eDNA can potentially provide more spatially precise information about species occurrence relative to the observed acoustic backscatter.

INTERPRETING eDNA SIGNALS

An essential issue for eDNA observing is the ability to interpret a signal appropriately. eDNA is collected from a dynamic fluid medium, and it is important to understand whether the resulting genetic signatures reflect the biodiversity from the sampling location or elsewhere. This is critical for stand-alone assessments and when the eDNA data are meant to inform co-collected data (e.g., acoustics). Laboratory studies on eDNA persistence are especially valuable for understanding the fate of eDNA and, consequently, the origin of eDNA signals. The rate at which eDNA decays (which affects how long the signal can be detected) is primarily controlled by temperature (Allan et al., 2020; McCartin et al., 2022). Thus, the cold temperatures of the OTZ and deeper waters likely result in greater

eDNA persistence and signal transport than do the warmer waters of coastal systems. However, further investigation is needed into other factors that may influence eDNA persistence, such as the state of the eDNA (i.e., intracellular vs. disassociated), the rate of microbial degradation, interactive effects among the microbial community, and abiotic conditions (e.g., Jo and Minamoto, 2021).

A particular challenge for interpreting eDNA results from the OTZ is the vertical migration behavior of many mesopelagic species. The regular, daily transit of these animals between surface waters and depth may result in their genetic traces being left throughout the water column, making it difficult to ascertain their sources. Allan et al. (2021) conducted a modeling study using realistic parameters for a temperate system to address this issue. They found that eDNA signatures remain close to their depth of origin despite the potential for movement. This finding supports the use of eDNA to study vertical phenomena in the mesopelagic, including identifying which taxa migrate (Canals et al., 2021) and the timing of their migrations. Because vertical variation of eDNA signals induced by diel vertical migration persists over time (Allan et al., 2021), eDNA measured along a vertical profile could also be used to estimate the percentage of mesopelagic species that undergo diel vertical migration. A related challenge for interpreting eDNA results stems from the ocean's heterogeneous flow field, which could differentially impact the transport of eDNA. Understanding the spatial distribution of the source animals in areas of strong flow variations would require robust knowledge of temporal and spatial variability in the region (e.g., Andruszkiewicz et al., 2019, in a coastal environment).

FUTURE DIRECTIONS AND NEXT STEPS

Environmental DNA analyses are ushering in a new era for biodiversity observations and ecological research in the OTZ. Developing and adopting new sampling technologies is crucial to documenting the impacts of climate change and other anthropogenic stressors. Sampling is fundamental for biodiversity assessments, and sampling technologies must expand from ship-based approaches to routine sampling that employs underwater vehicles and instrumentation ranging from AUVs to ROVs and towed instruments tailored to specific goals. We expect development of eDNA sampler types with different advantages and constraints, integrated into diverse platforms with a variety of sensors and geared toward specific analyses and research questions (Figure 5).

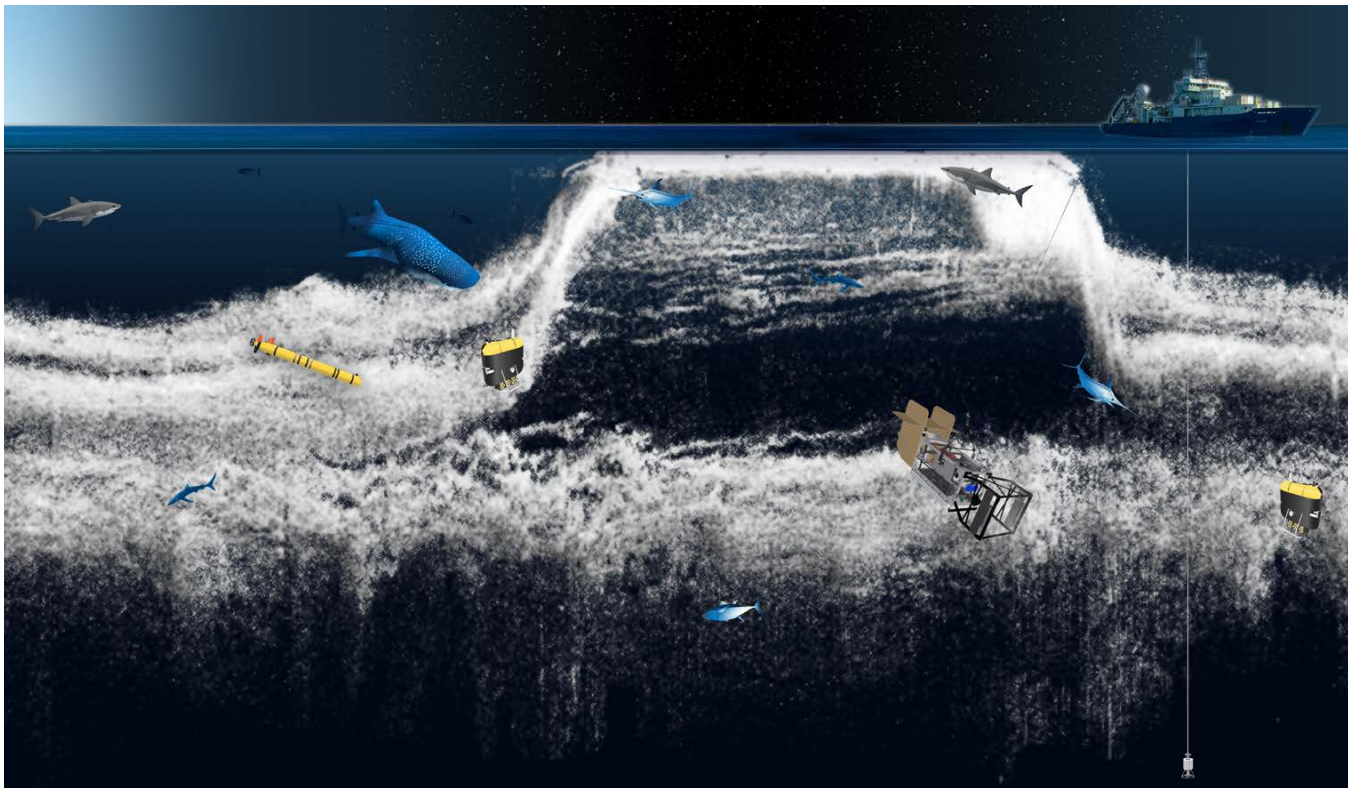

FIGURE 5. A vision for incorporating eDNA into ocean observing in the twilight zone. High-resolution sampling with a suite of samplers and diverse platforms is superimposed on 38 kHz acoustic backscatter data obtained over a 24-hour period (data credit: Andone Lavery, WHOI). The acoustic backscatter data demonstrate diel vertical migration of a significant portion of the OTZ biomass. At dusk, a portion of the biomass is seen transiting from mesopelagic to shallow depths. The biomass moves back to mesopelagic depths at dawn. Diverse approaches to eDNA sampling will help to determine the depth distributions and migratory behaviors of different species.

As sampling technologies develop, it is important to simultaneously pursue a better understanding of how eDNA is distributed in the ocean. This understanding is necessary both to guide the development of sampling technologies and to shape sample collection strategies. Computational modeling studies that consider the influence of oceanographic environments (e.g., temperature and flows) and incorporate eDNA shedding, persistence, transport, and dispersal are critical for linking measured eDNA signatures with their sources and for inferring species distributions and biomasses. They should be coupled with lab and field experiments for calibration, data analysis, and designing representative and effective field sampling strategies. For inferring biomass of multiple species (e.g., quantitative metabarcoding), incorporating an understanding of PCR dynamics into overall data interpretation will be especially important (Shelton et al., 2022). More research is needed to determine appropriate spatial and temporal sampling scales, which may depend on regional ocean currents; the biology of the target organisms; and specific research questions. In most, if not all, cases, we will need to vastly scale up our sampling efforts to enable spatiotemporally resolved data and obtain the replication required for statistical analyses. These steps are crucial for drawing scientific conclusions and translating eDNA observations into actionable conservation and policy insights.

REFERENCES

Allan, E., W.G. Zhang, A.C. Lavery, and A.F. Govindarajan. 2020. Environmental DNA shedding and decay rates from diverse animal forms and thermal regimes. *Environmental DNA* 3(2):492–514, https://doi.org/10.1002/edn3.141.

Allan, E.A., M.H. DiBenedetto, A.C. Lavery, A.F. Govindarajan, and W.G. Zhang. 2021. Modeling characterization of the vertical and temporal variability of environmental DNA in the mesopelagic ocean. *Scientific Reports* 11:21273, https://doi.org/10.1038/s41598-021-00288-5.

Andruszkiewicz, E.A., J.R. Koseff, O.B. Fringer, N.T. Ouellette, A.B. Lowe, C.A. Edwards, and A.B. Boehm. 2019. Modeling environmental DNA transport in the coastal ocean using Lagrangian particle tracking. *Frontiers in Marine Science* 6:477, https://doi.org/10.3389/fmars.2019.00477.

Canals, O., I. Mendibil, M. Santos, X. Irigoien, and N. Rodríguez-Ezpeleta. 2021. Vertical stratification of environmental DNA in the open ocean captures ecological patterns and behavior of deep-sea fishes. *Limnology and Oceanography Letters* 6(6):339–347, https://doi.org/10.1002/lol2.10213.

Ducklow, H.W., D.K. Steinberg, and K. Buesseler. 2001. Upper ocean carbon export and the biological pump. *Oceanography* 14(4):50–58, https://doi.org/10.5670/oceanog.2001.06.

Easson, C.G., K.M. Boswell, N. Tucker, J.D. Warren, and J.V. Lopez. 2020. Combined eDNA and acoustic analysis reflects diel vertical migration of mixed consortia in the Gulf of Mexico. *Frontiers in Marine Science* 7:552, https://doi.org/10.3389/fmars.2020.00552.

Eble, J.A., T.S. Daly-Engel, J.D. DiBattista, A. Koziol, and M.R. Gaither. 2020. Marine environmental DNA: Approaches, applications, and opportunities. Pp. 141–169 in *Advances in Marine Biology*, vol. 86, no. 1. C. Sheppard, ed., Academic Press, https://doi.org/10.1016/bs.amb.2020.01.001.

Everett, M.V., and L.K. Park. 2018. Exploring deep-water coral communities using environmental DNA. *Deep Sea Research Part II* 150:229–241, https://doi.org/10.1016/j.dsr2.2017.09.008.

Govindarajan, A.F., J. Pineda, M. Purcell, and J.A. Breier. 2015. Species- and stage-specific barnacle larval distributions obtained from AUV sampling and genetic analysis in Buzzards Bay, Massachusetts, USA. *Journal of Experimental Marine Biology and Ecology* 472:158–165, https://doi.org/10.1016/j.jembe.2015.07.012.

Govindarajan, A.F., R.D. Francolini, J.M. Jech, A.C. Lavery, J.K. Llopiz, P.H. Wiebe, and W. Zhang. 2021. Exploring the use of environmental DNA (eDNA) to detect animal taxa in the mesopelagic zone. *Frontiers in Ecology and Evolution* 9:574877, https://doi.org/10.3389/fevo.2021.574877.

Govindarajan, A.F., L. McCartin, A. Adams, E. Allan, A. Belani, R. Francolini, J. Fujii, D. Gomez-Ibanez, A. Kukulya, F. Marin, and others. 2022. Improved biodiversity detection using a large-volume environmental DNA sampler with in situ filtration and implications for marine eDNA sampling strategies. *Deep Sea Research Part I* 189:103871, https://doi.org/10.1016/j.dsr.2022.103871.

Jo, T., and T. Minamoto. 2021. Complex interactions between environmental DNA (eDNA) state and water chemistries on eDNA persistence suggested by meta-analyses. *Molecular Ecology Resources* 21(5):1,490–1,503, https://doi.org/10.1111/1755-0998.13354.

Lavery, A.C., P.H. Wiebe, T.K. Stanton, G.L. Lawson, M.C. Benfield, and N. Copley. 2007. Determining dominant scatterers of sound in mixed zooplankton populations. *The Journal of the Acoustical Society of America* 122(6):3,304–3,326, https://doi.org/10.1121/1.2793613.

Lavery, A.C., T.K. Stanton, J.M. Jech, and P. Wiebe. 2019. An advanced sensor platform for acoustic quantification of the ocean twilight zone. *The Journal of the Acoustical Society of America* 145(3):1,653–1,653, https://doi.org/10.1121/1.5101063.

McCartin, L.J., S.A. Vohsen, S.W. Ambrose, M. Layden, C.S. McFadden, E.E. Cordes, J.M. McDermott, and S. Herrera. 2022. Temperature controls eDNA persistence across physicochemical conditions in seawater. *Environmental Science & Technology* 56(12):8,629–8,639, https://doi.org/10.1021/acs.est.2c01672.

Shelton, A.O., Z.J. Gold, A.J. Jensen, E. D'Agnese, E.A. Andruszkiewicz, A. Van Cise, R. Gallego, A. Ramón-Laca, M. Garber-Yonts, K. Parsons, and R.P. Kelly. 2022. Toward quantitative metabarcoding. *Ecology* e3906, https://doi.org/10.1002/ecy.3906.

Truelove, N.K., N.V. Patin, M. Min, K.J. Pitz, C.M. Preston, K.M. Yamahara, Y. Zhang, B.Y. Raanan, B. Kieft, B. Hobson, and L.R. Thompson. 2022. Expanding the temporal and spatial scales of environmental DNA research with autonomous sampling. *Environmental DNA* 4(4):972–984, https://doi.org/10.1002/edn3.299.

Yamahara, K.M., C.M. Preston, J. Birch, K. Walz, R. Marin III, S. Jensen, D. Pargett, B. Roman, W. Ussler III, Y. Zhang, and J. Ryan. 2019. In situ autonomous acquisition and preservation of marine environmental DNA using an autonomous underwater vehicle. *Frontiers in Marine Science* 6:373, https://doi.org/10.3389/fmars.2019.00373.

Yoerger, D.R., A.F. Govindarajan, J.C. Howland, J.K. Llopiz, P.H. Wiebe, M. Curran, J. Fujii, D. Gomez-Ibanez, K. Katija, B.H. Robison, and B.W. Hobson. 2021. A hybrid underwater robot for multidisciplinary investigation of the ocean twilight zone. *Science Robotics* 6(55):eabe1901, https://doi.org/10.1126/scirobotics.abe1901.

Zhang, Y., B. Kieft, B.W. Hobson, B.Y. Raanan, S.S. Urmy, K.J. Pitz, C.M. Preston, B. Roman, K.J. Benoit-Bird, J.M. Birch, and F.P. Chavez. 2020. Persistent sampling of vertically migrating biological layers by an autonomous underwater vehicle within the beam of a seabed-mounted echosounder. *IEEE Journal of Oceanic Engineering* 46(2):497–508, https://doi.org/10.1109/JOE.2020.2982811.

ACKNOWLEDGMENTS

This research is part of the Woods Hole Oceanographic Institution's Ocean Twilight Zone Project, funded as part of The Audacious Project housed at TED, and a result of research funded by the National Oceanic and Atmospheric Administration's (NOAA's) Ocean Exploration Cooperative Institute under award NA19OAR4320072 to the University of Rhode Island (subaward number is 0007525/102212019 to WHOI), and NOAA's Office of Ocean Exploration and Research under award NA18OAR0110289 to Lehigh University.

ARTICLE DOI. https://doi.org/10.5670/oceanog.2023.s1.27

Detecting Mediterranean White Sharks with Environmental DNA

Jeremy F. Jenrette, Jennifer L. Jenrette, N. Kobun Truelove, Stefano Moro, Nick I. Dunn, Taylor K. Chapple, Austin J. Gallagher, Chiara Gambardella, Robert Schallert, Brendan D. Shea, David J. Curnick, Barbara A. Block, and Francesco Ferretti

The white shark (*Carcharodon carcharias*) is a globally distributed, ecologically important top predator whose biology and population dynamics are challenging to study. Basic biological parameters remain virtually unknown in the Mediterranean Sea due to its historically low population density, dwindling population size, and lack of substantial sightings. White sharks are considered Critically Endangered in the Mediterranean Sea, and recent analyses suggest that the population has declined by 52% to 96% from historical levels in different Mediterranean sectors (Moro et al., 2020). Thus, white shark sightings dating back to 1860 are being used to estimate population trajectories throughout the entire region. Though the population size is unknown, remaining individuals are thought to be primarily restricted to a handful of hotspots deemed important for their reproduction and foraging. One of these hypothesized hotspots is the Sicilian Channel, which accounts for 19% of total historical sightings.

White sharks shed genetic material (skin and feces) into their environment. Non-invasive molecular methods for determining the presence of organisms in nature, such as detecting environmental DNA (eDNA) from water samples, offer a developing but powerful technique for studying cryptic or rare species. In the Mediterranean Sea, where white shark catches and sightings are limited and unpredictable, the analysis of genetic material shed from white sharks provides novel insights into their distribution and abundance, thus aiding traditional surveying methods based on encountering individuals.

Here, we describe a survey conducted in the Sicilian Channel to test and refine methods for detecting white shark eDNA and combine historical aggregations with movement simulations of eDNA molecules in seawater to interpret white shark distributions and set goals for future monitoring efforts.

WHITE SHARK eDNA SURVEY

In June 2021, we collected environmental water samples from 16 sites within the Sicilian Channel (Figures 1 and 2). We filtered the samples to capture any cells and free-flowing eDNA that may be present. We amplified a unique cytochrome B gene fragment (CYTB) found in the mitochondria of white shark cells (Lafferty et al., 2018). We then observed the CYTB gene fragment on gel electrophoresis to confirm that the sample contained white shark DNA.

From this survey, four samples (out of 69) exhibited the unique gene fragment. These samples were selected for DNA sequencing that revealed the similarities between eDNA and the white shark reference sequence for the CYTB gene (Truelove et al., 2019). To understand the likelihood of a false-positive detection, we compared our samples to the CYTB genes of the white shark and its closest relative in the region, the shortfin mako (*Isurus oxyrinchus*). The four samples were significantly more similar to white shark than mako. Positive white shark detections (>95% similarity) were identified at the Pantelleria Banks and Lampedusa sites, and a third site at the Egadi Islands, indicating recent white shark presence (see online Supplementary Materials).

Using historical white shark sightings, we developed relative abundance distributions for May and June to guide our selection of survey sites (Figure 3a). By detecting the DNA of possible multiple white shark individuals, we completed an important step for confirming their presence in hypothesized hotspots. Our goal, once white shark DNA was detected, was to predict where the animal shed its genetic material by considering the movement of eDNA molecules in seawater (Figure 3b–d).

DNA molecules are subjected to environmental factors such as water currents and chemistry, tides, temperature, and sunlight once they are shed by white sharks. By modeling the trajectory of detected eDNA molecules,

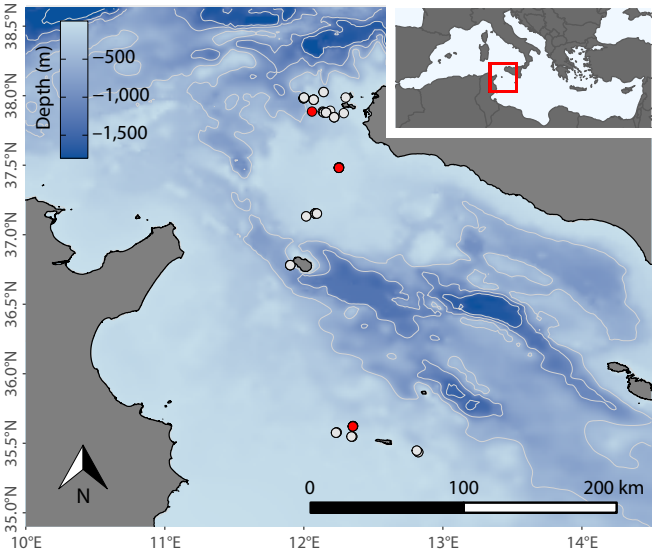

FIGURE 1. Locations of 16 sampling sites within the Sicilian Channel. Red indicates detection of white shark eDNA, and white represents no detection.

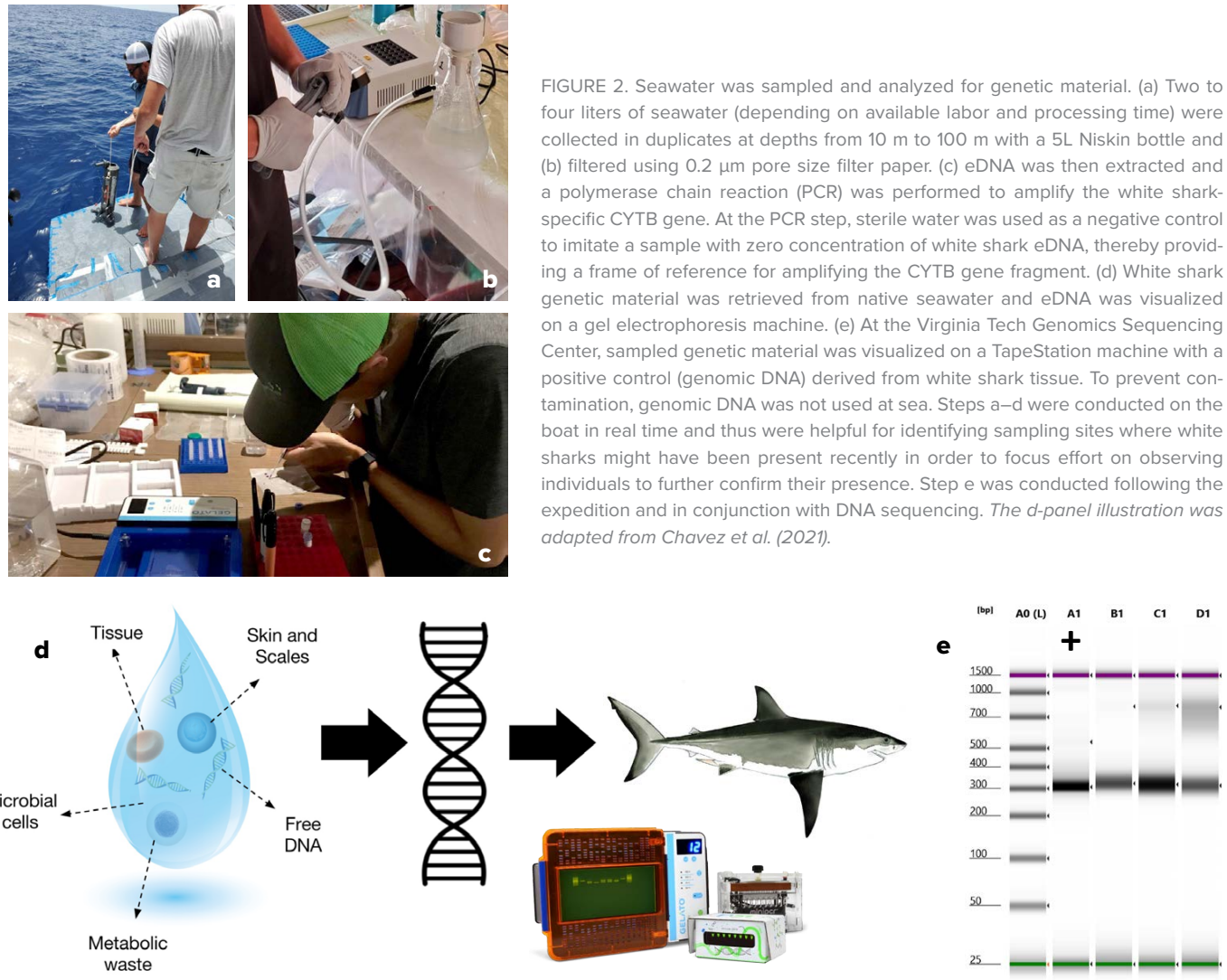

FIGURE 2. Seawater was sampled and analyzed for genetic material. (a) Two to four liters of seawater (depending on available labor and processing time) were collected in duplicates at depths from 10 m to 100 m with a 5L Niskin bottle and (b) filtered using 0.2 µm pore size filter paper. (c) eDNA was then extracted and a polymerase chain reaction (PCR) was performed to amplify the white shark-specific CYTB gene. At the PCR step, sterile water was used as a negative control to imitate a sample with zero concentration of white shark eDNA, thereby providing a frame of reference for amplifying the CYTB gene fragment. (d) White shark genetic material was retrieved from native seawater and eDNA was visualized on a gel electrophoresis machine. (e) At the Virginia Tech Genomics Sequencing Center, sampled genetic material was visualized on a TapeStation machine with a positive control (genomic DNA) derived from white shark tissue. To prevent contamination, genomic DNA was not used at sea. Steps a–d were conducted on the boat in real time and thus were helpful for identifying sampling sites where white sharks might have been present recently in order to focus effort on observing individuals to further confirm their presence. Step e was conducted following the expedition and in conjunction with DNA sequencing. *The d-panel illustration was adapted from Chavez et al. (2021).*

it is possible to predict their drifting pattern in space and time in the ocean (Andruszkiewicz et al., 2019). We ran a computer simulation to track these molecules backward in time to estimate where and when they originated. This procedure allowed us to predict the origin of eDNA from positive detections up to 128 hours prior to detection, which largely bounds the maximum time eDNA can persist in the marine realm without completely degrading to the point that it can no longer be detected (see Supplementary Materials). Hence, molecule tracking can provide insight into the locations of white shark individuals and facilitate real-time tracking of the animal to increase the chance of observing them.

These findings are congruent with our expectations to find white sharks in this specific Mediterranean sector during this season. Seasonality is known to affect not only water temperature and eDNA movement but also white shark behavior due to reproductive strategies and variation in prey abundance. Because one or multiple individuals were detected in the suspected area, these conditions were presumably favorable for white sharks. The survey produced baseline results and expectations for future monitoring of white sharks with eDNA techniques. Importantly, to construct population landscapes in the Mediterranean, there should be seasonal eDNA surveys across multiple regions.

INVOLVING THE PUBLIC IN OUR WORK

Our approach is effective and scalable for clarifying spatio-temporal patterns in white shark distribution. To increase sampling effort and reduce ship-time costs, citizen scientists should be incorporated into eDNA surveys, as it is relatively straightforward for fishermen, tourists, and other ocean-goers to collect and filter seawater without training or prior knowledge. Expeditions are important for establishing and refining techniques, but financial and logistic constraints challenge the implementation of multiple, simultaneous sampling surveys. Therefore, public scientists are a valuable untapped resource for consistently sampling selected regions of the Mediterranean and offer the possibility for a low-cost and persistent monitoring network in parallel with scientific expeditions.

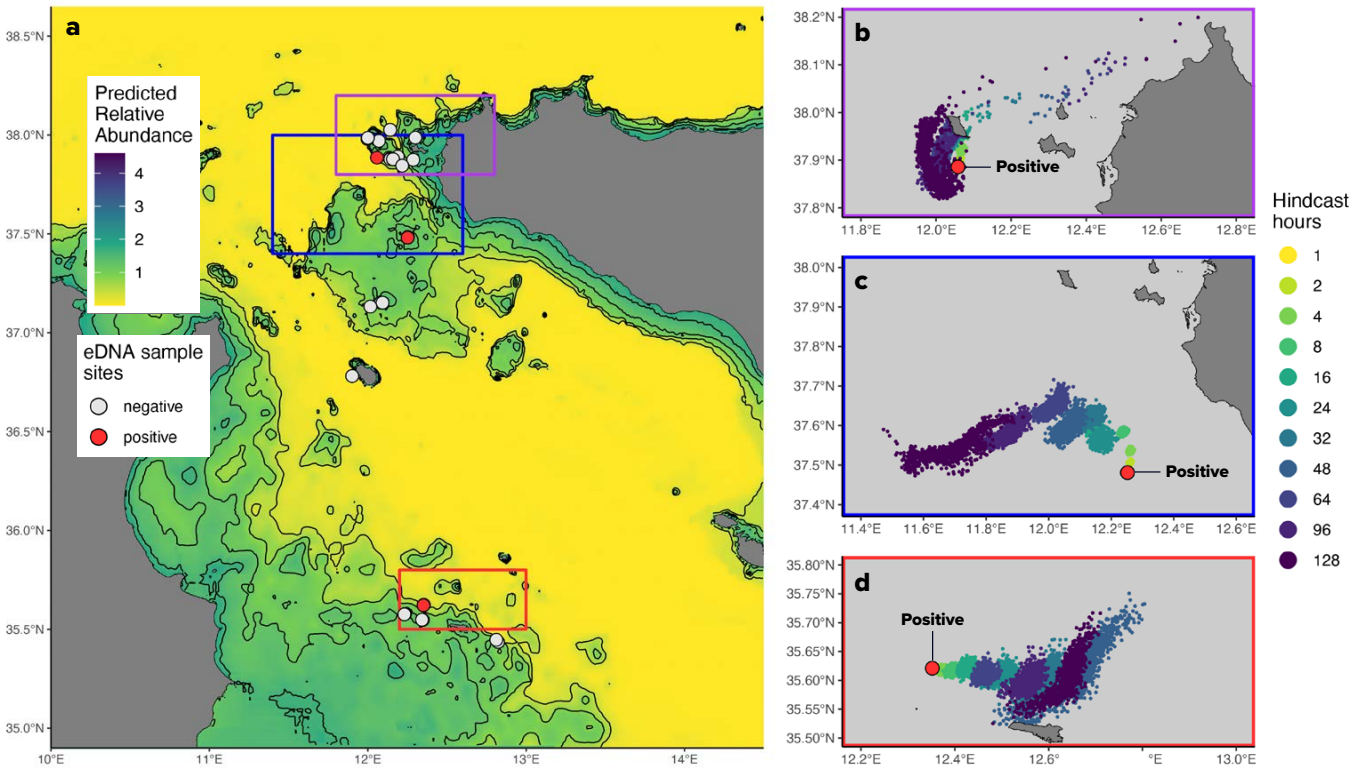

FIGURE 3. (a) We predicted relative abundance of white sharks in the Sicilian Channel during May–June. (b–d) Particle tracking hindcasts show predicted locations of the white shark eDNA molecules prior to detection. For hindcasted hours, yellow indicates the most recent predicted location of eDNA molecules (one hour prior to detection), and purple indicates the location of eDNA molecules 128 hours prior to detection. Red indicates the sample location where white shark eDNA was detected.

We are currently establishing a network of sailing partners in the Mediterranean Sea and have developed cost-efficient and easy-to-use kits for sampling and filtering surface water and preserving eDNA to be shipped back to our laboratory for processing. To teach citizens about the best sampling practices, we created a short instructional document and a step-by-step video to help them collect water, sterilize the equipment, and work area with diluted bleach; use latex gloves; and preserve eDNA. As the network expands, kits should be upgraded to sample at depth to help reveal the population distribution of white sharks in the Mediterranean.

In summary, detecting the DNA of Critically Endangered white shark individuals allowed us to extrapolate their spatiotemporal presence and develop a surveying strategy in a data-poor region. Expanded systematic eDNA monitoring is a promising tool for revealing the otherwise cryptic behavior of white sharks in the region. This will be crucial for developing conservation and management policies to protect the last strongholds of Mediterranean white sharks.

SUPPLEMENTARY MATERIALS

The supplementary materials can be found online at https://doi.org/10.5670/oceanog.2023.s1.28.

REFERENCES

Andruszkiewicz, E.A., J.R. Koseff, O.B. Fringer, N.T. Ouellette, A.B. Lowe, C.A. Edwards, and A.B. Boehm. 2019. Modeling environmental DNA transport in the coastal ocean using Lagrangian particle tracking. *Frontiers in Marine Science* 6:477, https://doi.org/10.3389/fmars.2019.00477.

Chavez, F.P., M. Min, K. Pitz, N. Truelove, J. Baker, D. LaScala-Grunewald, M. Blum, K. Walz, C. Nye, A. Djurhuus, and others. 2021. Observing life in the sea using environmental DNA. *Oceanography* 34(2):102–119, https://doi.org/10.5670/oceanog.2021.218.

Lafferty, K.D., K.C. Benesh, A.R. Mahon, C.L. Jerde, and C.G. Lowe. 2018. Detecting southern California's white sharks with environmental DNA. *Frontiers in Marine Science* 5:355, https://doi.org/10.3389/fmars.2018.00355.

Moro, S., G. Jona-Lasinio, B. Block, F. Micheli, G. De Leo, F. Serena, M. Bottaro, U. Scacco, and F. Ferretti. 2020. Abundance and distribution of the white shark in the Mediterranean Sea. *Fish and Fisheries* 21(2):338–349, https://doi.org/10.1111/faf.12432.

Truelove, N.K., E.A. Andruszkiewicz, and B.A. Block. 2019. A rapid environmental DNA method for detecting white sharks in the open ocean. *Methods in Ecology and Evolution* 10(8):1,128–1,135, https://doi.org/10.1111/2041-210X.13201.

ACKNOWLEDGMENTS

We acknowledge the following funding sources: The Explorers Club, The Discovery Channel, the Center for Coastal Studies, and the Acorn Alcinda Foundation.

ARTICLE DOI. https://doi.org/10.5670/oceanog.2023.s1.28

Toward Identifying the Critical Ecological Habitat of Larval Fishes: An Environmental DNA Window into Fisheries Management

By Erin V. Satterthwaite, Andrew E. Allen, Robert H. Lampe, Zachary Gold, Andrew R. Thompson, Noelle Bowlin, Rasmus Swalethorp, Kelly D. Goodwin, Elliott L. Hazen, Steven J. Bograd, Stephanie A. Matthews, and Brice X. Semmens

Environmental DNA (eDNA)-based ecological co-occurrence networks can provide a valuable tool for fisheries and conservation management. In the past, it was nearly impossible to explore the microscopic world of larval fishes in one sampling event. Now, eDNA data and ecological co-occurrence network modeling provide windows into ecosystems that support larval fishes and upon which subsequent fisheries rely. Thus, there is great potential for eDNA methods coupled with ecological network analyses to provide a holistic understanding of community composition and species interactions and to develop indicators for fisheries and ecosystem-based management.

Marine larvae are important to marine ecosystems and fisheries, but predicting recruitment remains a fundamental challenge in fisheries science. Most marine fishes and invertebrates produce many larvae that reside in the pelagic ocean for weeks to months, depending on the species. Mortality is high for most fishes during the larval stage, often upward of 99%, but because most species are highly fecund, small changes in larval survival can significantly alter survival to adult stages (i.e., recruitment; Houde, 1987). For this reason, elucidating the mechanisms that affect larval survival is an integral component of fisheries management. Despite over a century of recruitment research, accurately estimating the parameters that control larval survival has been difficult, and predicting conditions that facilitate recruitment remains a fundamental challenge in fisheries management (Hare, 2014).

In recent years, populations of the northern anchovy *Engraulis mordax* have undergone unprecedented recruitment variability. *E. mordax* is a major forage species in the California Current Ecosystem (CCE), serving as key prey for birds, marine mammals, and fishes, including commercially important fisheries species. Adult *E. mordax* abundance changed dramatically from 2014 to 2022 in the CCE. In 2014, adult anchovy abundance was among the lowest on record. Large recruitment classes, beginning in 2015, fueled a rapid rise in abundance, and by 2022 adult anchovy abundance approached a record high throughout the CCE. Surprisingly, this unparalleled population expansion occurred during the largest marine heatwave on record (Thompson et al., 2022), the opposite of the cool water conditions conventionally believed to favor anchovy (Chavez et al., 2003). Clearly, understanding the drivers of anchovy recruitment variability remains one of the greatest challenges in their assessment and management.

FIGURE 1. Image of a larval anchovy postflexion from the NOAA Southwest Fisheries Science Center archives.

Ecological aspects of the larval habitat can be examined through biomolecular techniques. Environmental conditions hypothesized to influence larval fish have been extensively studied and used to predict fish stocks. Examples include temperature and large-scale climate modes such as the Pacific Decadal Oscillation and the North Pacific Gyre Oscillation (Chavez et al., 2003). Nonetheless, these basin-scale parameters have been insufficient to predict observed variability in recruitment, likely because biophysical mechanisms are the primary drivers of recruitment. Therefore, the species that the larvae interact with in vivo (e.g., predators, prey, commensals, parasites) are likely key to understanding recruitment success or failure (Robert et al., 2014). However, understanding the ecosystem at this level has been difficult because plankton are patchily distributed, microscopic, often poorly characterized, and require extensive expertise and time to sort and identify. In addition, because larval predators can be numerous, it is difficult to quantify ecological interactions, and studying them requires extensive and diverse sampling and quantification techniques.

Fortunately, modern genetic tools provide a robust, rapid, and cost-effective way to characterize marine ecosystems more holistically and to help assess the biological factors that drive larval fish growth and survival. DNA-based approaches applied to individual tissues, filtered water, or sample preservatives can augment traditional sampling methods (e.g., visual enumeration from samples or flow-through systems) to provide enhanced spatial, temporal, or taxonomic resolution, especially for microscopic species that may be important for larval fishes but that cannot be easily sampled with conventional methods (e.g., nets, submersibles) or identified by morphological

examination (e.g., cryptic species). The resulting data can be examined using ecological co-occurrence network analysis, which can provide insight into potentially important species interactions for larval fish.

Previous work has characterized the set of physical conditions associated with the critical oceanic habitats for important fisheries as well as individual prey items, but the complex network of ecological associations that define the larval habitat are still largely unexplored (Thompson et al., 2022). Using *E. mordax* larvae as a case study (Figure 1), the goal of this paper is to examine how eDNA data can be coupled with traditionally sampled larval fish abundance data to develop ecological co-occurrence networks that provide insight into the microscopic world of larvae and work toward elucidating communities, species, and mechanisms that control larval dynamics.

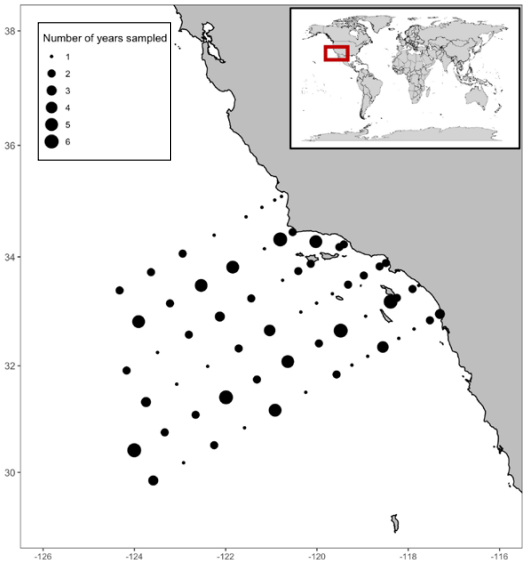

FIGURE 2. Map displaying sampling locations of concurrent eDNA observations from bottle samples (DNA sequences 16S and 18S) and visually enumerated ichthyoplankton from net tows. Circle size indicates the number of years each station was sampled for eDNA between 2014 and 2020. The samples in the core CalCOFI grid were regularly sampled for eDNA (black circles).

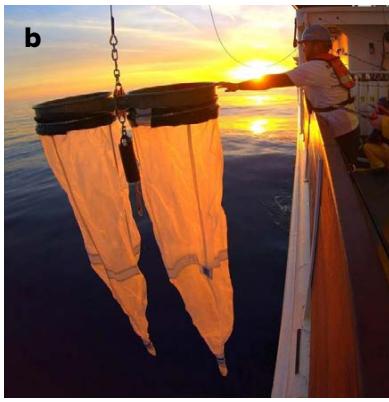

FIGURE 3. Collection devices are shown for (a) seawater, using a CTD rosette for eDNA, and (b) ichthyoplankton specimens, employing a bongo net tow.

eDNA in the Southern California Current Ecosystem reveals potentially important ecological interactions for *E. mordax*. We examine this subject within the Southern California Bight region, which is situated in the southern portion of the CCE, a productive upwelling system that supports important fisheries. In addition, the CCE is home to one of the longest running integrated marine ecosystem monitoring programs in the world, the California Cooperative Oceanic Fisheries Investigations (CalCOFI), which has systematically sampled the physics, chemistry, and biology of the system since 1951.

In 2014, the NOAA-CalCOFI Ocean Genomics (NCOG) program began collecting DNA samples to molecularly identify bacterioplankton, phytoplankton, and zooplankton (Figures 2 and 3a). NCOG has sequenced nearly 1,000 DNA samples from two depths (~10 m and the subsurface chlorophyll *a* maximum) across 2014–2020, enumerating over ~80,000 amplicon sequence variants (ASVs), unique DNA sequences, from 16S and 18S (James et al., 2022). ASVs from the domains Bacteria, Archaea, and Eukarya were taxonomically annotated with the SILVA and PR^2 databases. Additionally, ichthyoplankton have been visually identified from net tow samples throughout CalCOFI's history (Figure 3b). These rich data sets provide an avenue for exploring the ecological networks that potentially control the dynamics of the early life stages of marine fishes.

Here, we integrated larval fish and eDNA data from the core CalCOFI grid (Figure 2) over seven years (2014–2020) to generate an ecological co-occurrence network using methods adapted from Steinhauser et al. (2008). Ecological co-occurrence network analyses were used because they provide information on potential interactions between taxa in large, complex data sets, which may be more challenging to detect using diversity metrics or other types of multivariate community analyses (Barberán et al., 2012).

We correlated the presence/absence (P/A) of ASVs from biomolecular 16S and 18S data with visually enumerated counts of larval fishes. P/A data (reads > 0) were used for the ASVs because it is challenging to interpret metabarcoding data quantitatively. P/A analyses can provide more accurate estimates of taxon correlations in the absence of robust abundance estimates or when abundance data are uncertain (Mainali et al., 2017), but they can introduce error in cases where there are spurious, low read assignments.

All analyses were conducted using the statistical software R (R Core Team, 2021). Taxa with little to no variance were removed from analyses and positive Pearson's product moment correlations ($\rho > 0.237$) with strongly significant *p*-values (Benjamini and Hochberg adjusted *p*-values $< 3.3 \times 10^{-6}$) were identified among all remaining taxa. This resulted in a correlation matrix that was then visualized and explored using a network visualization package (igraph; Csardi and Nepusz, 2006). This analysis revealed a complex

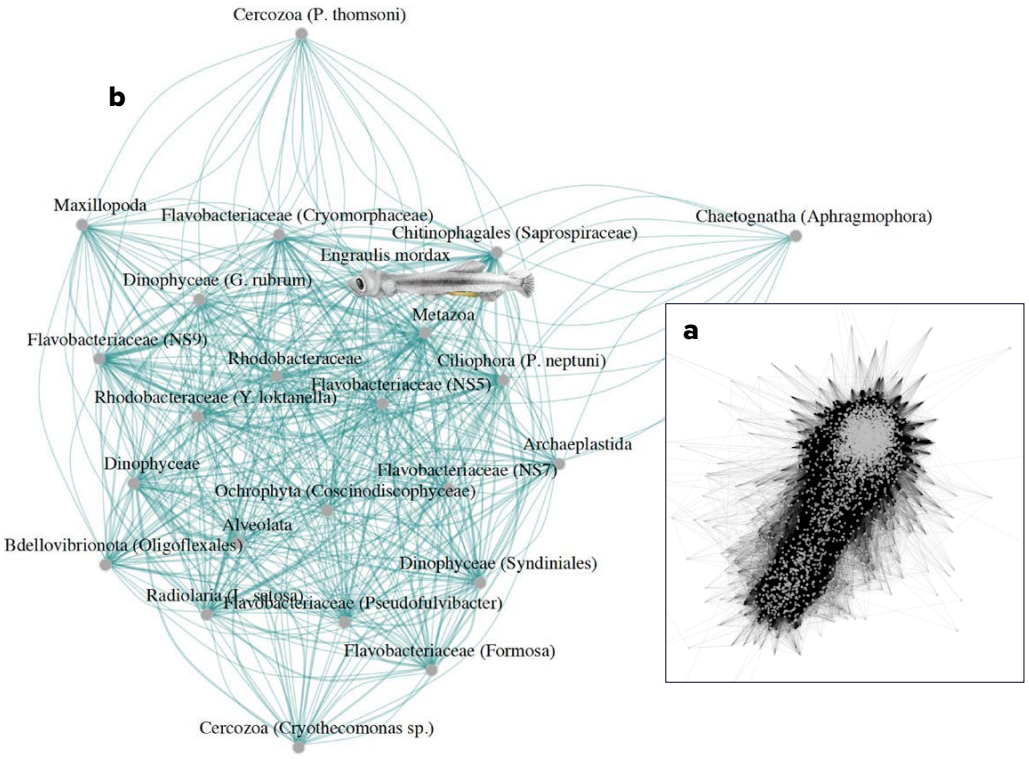

FIGURE 4. (a) Simplified ecological co-occurrence network between counts of larval fishes and presence/absence data of zooplankton, phytoplankton, and bacterioplankton taxa. Nodes represent clusters of plankton using the fast greedy modularity optimization algorithm. Exploring all strong correlations revealed a "hairball" network of dense connections. Thus, the data set was filtered to produce (b) a sub-network displaying only the ecological co-occurrence network of grouped amplicon sequence variants (ASVs) positively associated with larval anchovy (the "anchovy water"). For both networks, links represent positive Pearson's product moment correlations ($\rho > 0.237$) with strongly significant *p*-values (Benjamini and Hochberg adjusted *p*-values $< 3.3 \times 10^{-6}$).

"hairball" network of correlations that were mined to reveal potential ecological interactions among plankton taxa, including larvae of important fisheries species (Figure 4a).

Given the complexity of the network, we focused on a sub-network of taxa that had significant positive associations with larval *E. mordax* abundance. This could be used to characterize the potential ecological habitat of larval anchovies (the "anchovy water"; Alvariño, 1980) and could lend insight into drivers of anchovy recruitment dynamics from 2014 to 2020. The larval anchovy sub-network revealed 45 ASVs that clustered into 24 distinct taxa (Figure 4b). Taxa co-occurrence could be due to direct interactions (e.g., predation, parasitism, mutualism, or commensalism) or to indirect relationships via associations with similar water masses or environmental characteristics. Although co-occurrences do not prove ecological interactions, they identify hypotheses for future testing (Faust, 2021).

Anchovy water can be characterized by eDNA analysis to reveal potential prey field, predators, and microbiome associates. This analysis of 18S amplicons revealed a potential prey field for larval anchovy that included ciliates (*Pelagostrobilidium neptuni*), cercozoans (*Cryothecomonas* sp., *Protocystis thomsoni*), radiolarians (*Lithomelissa setosa*), maxillopods (likely copepods), and phytoplankton that included diatoms (Bacillariophyceae) and dinoflagellates (e.g., Syndiniales and *Gyrodinium rubrum*). Most of these broader taxa groups have been identified as important food sources for larval anchovies (Arthur, 1976), although Syndiniales is an order of parasitic dinoflagellates, so could be parasitic to either the fish larvae or potential prey. The network analysis identified chaetognaths (Aphragmophora) as potential predators or competitors (Alvarino, 1980). Five 18S ASVs (19%) were classified as eukaryotic with no lower taxonomic classification, four 18S ASVs (15%) were classified only to the level of Archaeplastida, and one 18S ASV (4%) to the level of Metazoa, suggesting that more research is needed to uncover the "dark matter" of larval fish habitats.

Several uncultured bacterial taxa showed co-occurrence with *E. mordax* larvae in this analysis (Figure 4b). The majority of 16S amplicons (72%) were assigned to the order *Flavobacteriales* with representatives from *Flavobacteriaceae* (marine group NS5, *Formosa*, and *Pseudofulvibacter*), *Cryomorphaceae*, and marine groups NS7 and NS9. *Rhodobacteraceae*, *Saprospiraceae*, and *Oligoflexales* were among the other taxonomic assignments. Many of the ASVs represented taxa that have been found in association with fish intestines/feces, gills, or skin (Senhal et al., 2021).

Biomolecular approaches provide insight into the larval habitats of important fisheries species and provide working hypotheses to explore through future research. Overall, the taxa found here provide candidate indicators to help understand the complex ecosystem of interactions that make up larval anchovy habitat (Figure 5). Co-occurrence networks, from coupled molecular and abundance data, provide tools for identifying the key ecological characteristics of larval fish habitats more extensively, and could be used to identify species interactions that have the potential to influence larval dynamics and perhaps recruitment success. Integrating biomolecular data with traditional survey tools represents an important

advancement in applying eDNA analysis for fisheries management by informing the essential mechanisms operating on larval fish and thus on the resulting fisheries.

Moving forward, observational data are needed to verify important interactions and the taxa involved to better constrain eDNA-based indicators for important fisheries. Specifically, future studies could: (1) validate the results of this study with additional surveys concurrently sampling eDNA and fish, (2) examine the broad suite of planktonic taxa that co-occur with other important individual fisheries species (e.g., sardines, Pacific halibut) or suites of species (e.g., coastal pelagic species), (3) leverage the taxonomic richness of eDNA-based monitoring products in efforts to improve fisheries prediction models (e.g., recruitment forecasting), (4) "fingerprint" quality larval habitats and provide indices of their spatial extents, (5) explore the potential to use broad network metrics in ecosystem-based fisheries management approaches, such as ecosystem status reports and as triggers for decision-making, (6) conduct targeted studies to test the connections found through these types of ecological co-occurrence studies, such as gut contents studies, and (7) develop more detailed reference databases to better resolve ASV taxonomy and inform essential mechanisms.

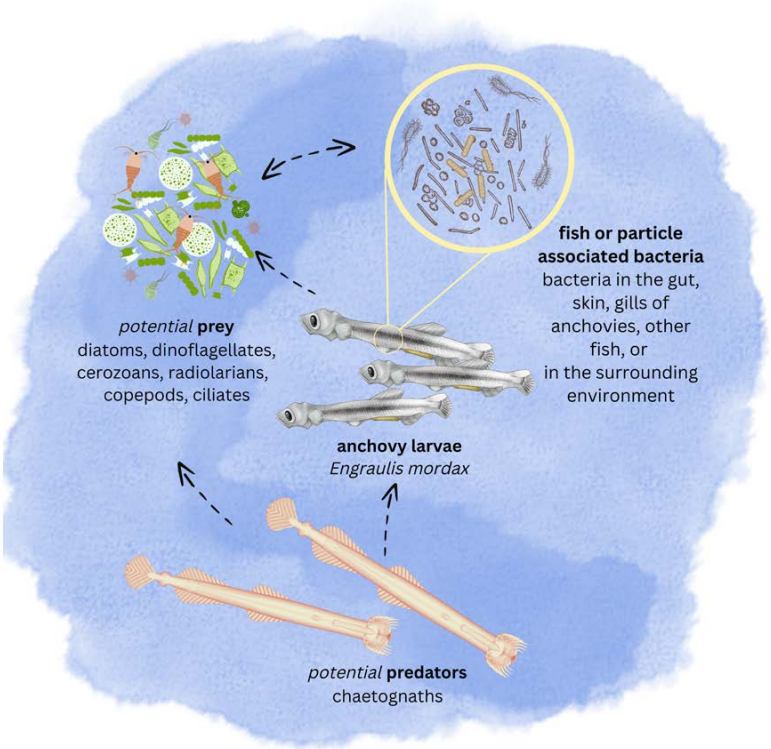

FIGURE 5. Conceptual diagram of the proposed ecological habitat of larval anchovy, or "anchovy water" (Alvariño, 1980), in the California Current Ecosystem. The relationships (dashed arrows) implied from eDNA-derived co-occurrence networks and supporting literature provide hypotheses that can be validated with additional research.

REFERENCES

Alvariño, A. 1980. The relation between the distribution of zooplankton predators and anchovy larvae. *Reports California Cooperative Oceanic Fisheries* 21:150–160.

Arthur, D.K. 1976. Food and feeding of larvae of three fishes occurring in the California Current, *Sardinops sagax*, *Engraulis mordax*, and *Trachurus symmetricus*. *Fishery Bulletin* 74(3):517–530.

Barberán, A., S.T. Bates, E.O. Casamayor, and N. Fierer. 2012. Using network analysis to explore co-occurrence patterns in soil microbial communities. *The ISME Journal* 6(2):343–351, https://doi.org/10.1038/ismej.2011.119.

Chavez, F.P., J. Ryan, S.E. Lluch-Cota, and M. Niquen. 2003. From anchovies to sardines and back: Multidecadal change in the Pacific Ocean. *Science* 299:217–221, https://doi.org/10.1126/science.1075880.

Csardi, G., and T. Nepusz. 2006. The igraph software package for complex network research. *InterJournal Complex Systems* 1695.

Faust, K. 2021. Open challenges for microbial network construction and analysis. *The ISME Journal* 15(11):3,111–3,118, https://doi.org/10.1038/s41396-021-01027-4.

Hare, J.A. 2014. The future of fisheries oceanography lies in the pursuit of multiple hypotheses. *ICES Journal of Marine Science* 71(8):2,343–2,356, https://doi.org/10.1093/icesjms/fsu018.

Houde, E.D. 1987. Fish early life dynamics and recruitment variability. *American Fisheries Society Symposium Series* 2:17–29.

James, C.C., A.D. Barton, L.Z. Allen, R.H. Lampe, A. Rabines, A. Schulberg, H. Zheng, R. Goericke, K.D. Goodwin, and A.E. Allen. 2022. Influence of nutrient supply on plankton microbiome biodiversity and distribution in a coastal upwelling region. *Nature Communications* 13(1):2448, https://doi.org/10.1038/s41467-022-30139-4.

Mainali, K.P., S. Bewick, P. Thielen, T. Mehoke, F.P. Breitwieser, S. Paudel, A. Adhikari, J. Wolfe, E.V. Slud, D. Karig, and W.F. Fagan. 2017. Statistical analysis of co-occurrence patterns in microbial presence-absence datasets. *PLoS ONE* 12(11):e0187132, https://doi.org/10.1371/journal.pone.0187132.

Robert, D., H.M. Murphy, G.P. Jenkins, and L. Fortier. 2014. Poor taxonomical knowledge of larval fish prey preference is impeding our ability to assess the existence of a "critical period" driving year-class strength. *ICES Journal of Marine Science* 71:2,042–2,052, https://doi.org/10.1093/icesjms/fst198.

R Core Team. 2021. R: A language and environment for statistical computing. R Foundation for Statistical Computing, Vienna, Austria, https://www.R-project.org/.

Sehnal, L., E. Brammer-Robbins, A.M. Wormington, L. Blaha, J. Bisesi, I. Larkin, C.J. Martyniuk, M. Simonin, and O. Adamovsky. 2021. Microbiome composition and function in aquatic vertebrates: Small organisms making big impacts on aquatic animal health. *Frontiers in Microbiology* 12:567408, https://doi.org/10.3389/fmicb.2021.567408.

Steinhauser, D., L. Krall, C. Müssig, D. Büssis, and B. Usadel. 2008. Correlation networks. Pp. 305–333 in *Analysis of Biological Networks*. B.H. Junker and F. Schreiber, eds, John Wiley & Sons, Inc. https://doi.org/10.1002/9780470253489.ch13.

Thompson, A.R., E.P. Bjorkstedt, S.J. Bograd, J.L. Fisher, E.L. Hazen, A. Leising, J.A. Santora, E.V. Satterthwaite, W.J. Sydeman, M. Alksne, and others. 2022. State of the California Current Ecosystem in 2021: Winter is coming? *Frontiers in Marine Science* 9:958727, https://doi.org/10.3389/fmars.2022.958727.

ACKNOWLEDGMENTS

This work was supported by NOAA grants NA15OAR4320071 and NA19NOS4780181 to AEA. ES was supported by a partnership among CalCOFI participants, including Scripps Institution of Oceanography (SIO), NOAA Southwest Fisheries Science Center (SWFSC), California Department of Fish and Wildlife, and California Sea Grant. EH was supported by NOAA's Integrated Ecosystem Assessment program. SAM was supported by CCE-LTER and an NSF Graduate Research Fellowship. KDG was supported by NOAA's Oceanic and Atmospheric Research 'Omics program. We are grateful to Bryce Ellman at SIO for the genomics sampling photo, Megan Human at SWFSC for the bongo net and larval anchovy postflexion photos, and Claudia Traboni for the larval anchovy drawing.

ARTICLE DOI. https://doi.org/10.5670/oceanog.2023.s1.29

The Use of eDNA to Monitor Pelagic Fish in Offshore Floating Wind Farms

By Thomas G. Dahlgren, Jon Thomassen Hestetun, and Jessica Ray

After nearly 30 years of experience with offshore wind energy (OWE), the industry is moving past the initial learning phase and into large-scale development. One of the strongest motivations for OWE is that projects are large enough to replace fossil-fueled electricity production that we know is a primary contributor to the ongoing climate crisis. Environmental concerns are therefore also at the core of OWE development, and environmental research and impact monitoring have been central parts of the industry since its inception. A large volume of science-based knowledge is available about the environmental impacts of OWE on marine ecosystems, from effects on the seafloor sediment infauna beneath the turbines to those on marine mammals that roam the developed seas.

In the next couple of years, we will see a large increase in OWE development, with single projects such as Dogger Bank in the North Sea coming online as well as larger projects that produce several gigawatts of energy from thousands of square kilometers devoted to OWE production. Because they can be deployed in deep water, floating wind turbines play a significant role in these long-term developmental plans, but their environmental impacts are not well understood, including the possible impacts on pelagic ecosystems. With large projects covering ever more area, including deep waters, we may see cumulative effects on upper ocean stratification as projected by oceanographic models of lee effects (Broström, 2008). Turbulence introduced by the foundation structures and anchoring lines may add to the forces that result in increased mixing of upper water layers with potential downstream consequences on productivity (Floeter et al., 2017).

Another knowledge gap concerns the general impact on pelagic fish from floating OWE. Trawl surveys are typically used to monitor pelagic fish; however, trawling is difficult in areas with large structures such as turbine foundations and their anchor lines. While demersal species of fish are relatively well researched in OWE installations, often using passive gear such as bottom set gill nets or fyke nets, the impact of the structures on behavior and distribution of pelagic species is less known (Methratta et al., 2020).

To address these knowledge gaps and assess a new method for impact monitoring at large offshore wind installations, we developed and tested a strategy for sampling environmental DNA in the pelagic ecosystem surrounding a floating OWE installation (Figure 1). Environmental DNA (or eDNA) is DNA shed from animals and plants to the soil, air, sediment, or water environment where it can be sampled by filtration with pore sizes in the range of one micrometer or smaller. The captured eDNA can be assessed in various ways. Here, we wanted to assess species composition of pelagic metazoan communities, with an emphasis on fish species. To accomplish this, we used metabarcoding with the relatively slowly evolving gene 18S (V1–V2), which amplifies a range of eukaryote taxa, and the fish-specific MiFish assay based on a fragment of the faster evolving, species-specific 12S mitochondrial gene. We also wanted to estimate the abundances of two of the commercially most important pelagic species in the area, Atlantic herring (*Clupea harengus*) and Atlantic mackerel (*Scomber scombrus*). For these quantitative analyses we used herring- and mackerel-specific primers in assays optimized for droplet digital PCR (ddPCR), a technology that permits estimates of the number of target gene copies in a sample.

The test was carried out in August 2021 at Equinor's pilot installation Hywind Scotland, situated 25 km east of Peterhead in northeastern Scotland and operational since 2017 (Figure 1a). The wind farm consists of five floating 6 MW turbines installed at 95–120 m depth,

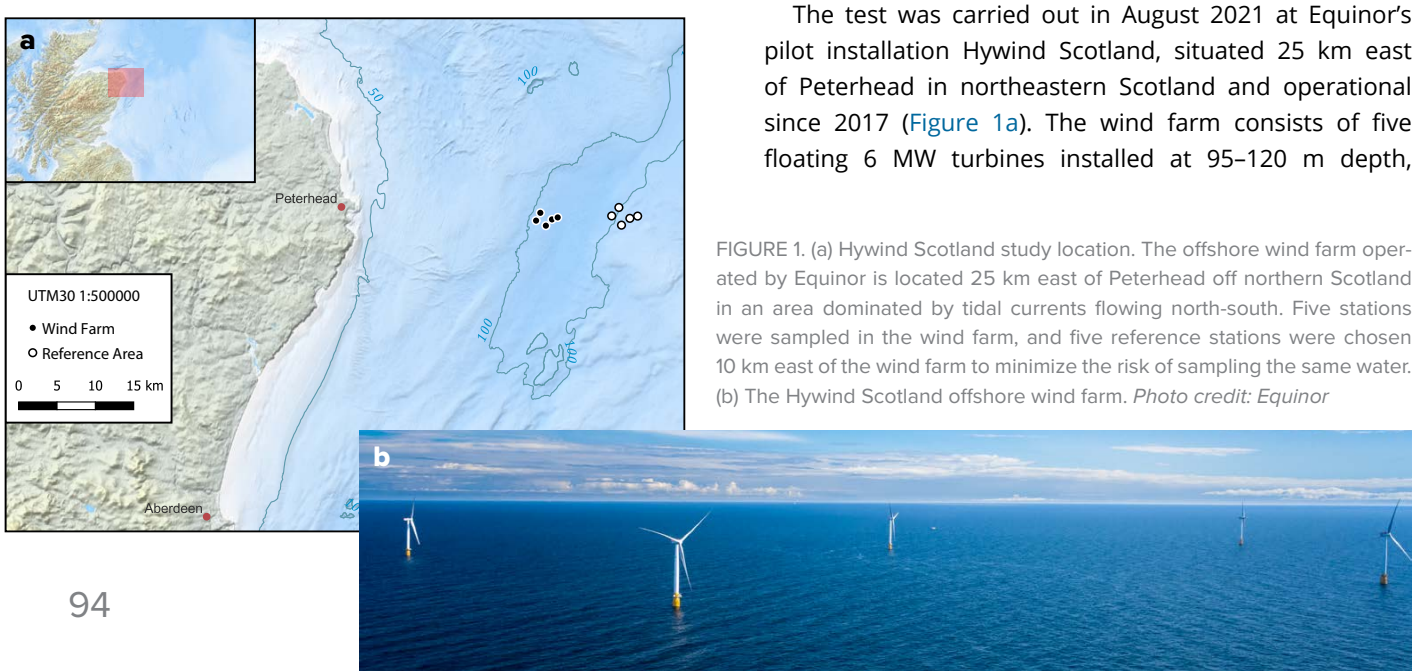

FIGURE 1. (a) Hywind Scotland study location. The offshore wind farm operated by Equinor is located 25 km east of Peterhead off northern Scotland in an area dominated by tidal currents flowing north-south. Five stations were sampled in the wind farm, and five reference stations were chosen 10 km east of the wind farm to minimize the risk of sampling the same water. (b) The Hywind Scotland offshore wind farm. *Photo credit: Equinor*

spaced 800–1,600 m apart, and attached to the seafloor with three-point mooring systems (Figure 1b). We used a similar sized reference area with the same depth range located approximately 10 km east of the wind farm. Five stations in each of these areas were sampled at 10 m and 50 m depths. Each sample consisted of 3 × 1 liter of water. The samples were immediately filtered and preserved on board and kept dark and cool to reduce eDNA decay prior to sample analysis.

The most striking result from the fish community composition analysis, using MiFish metabarcoding data, was the strong signal from demersal species (Figure 2). While the highest abundances were indicated for the three pelagic species herring, sprat, and mackerel, the data also included at least 22 bottom-dwelling species (Table S1). The signal was highest at 50 m depth, but some demersal species were also detected at 10 m. There was no significant difference between the installation and the reference area, but the two depths were consistently different from each other in the 20 sampled stations. While not a target species in this analysis, a faint eDNA signal from harbor porpoise was detected in the MiFish data from one of the wind-farm stations. Previous reports suggest that porpoises actively seek out offshore wind installations for foraging (Fernandez-Betelu et al., 2022). This shows that optimizing eDNA markers for marine mammals could facilitate inclusion of such species in future eDNA surveys.

Sampling was completed on one day only, so any attracting or repelling effects from the turbine foundations and mooring lines may have been masked by variations caused by dynamically moving schools of fish. More conclusive results would require sampling over time, including collecting diurnal and seasonal data. No signals from the target species were detected in relatively large fractions of ddPCR analyses, indicating that it would be advantageous to use larger volumes of filtered water than the 1 liter chosen for this study to limit time spent in the field. Given these caveats, species-specific abundance estimates (ddPCR data) indicated a higher abundance of herring in the wind farm relative to the reference site (Figure 2). This was true for both the 10 m and 50 m sampled depths. The mackerel data indicated a higher abundance at 10 m than 50 m in both areas, with no difference between the areas. Both results were supported by the number of reads from the metabarcoding data (Figure 2).

In our eukaryotic metabarcoding analysis, protists comprised the majority of sequence reads. As with the MiFish data, cluster analyses of the 18S data indicate no difference between the two areas, but there is a strong clustering of data based on depth. As this study represents a snapshot at a specific point in time, and plankton typically migrate

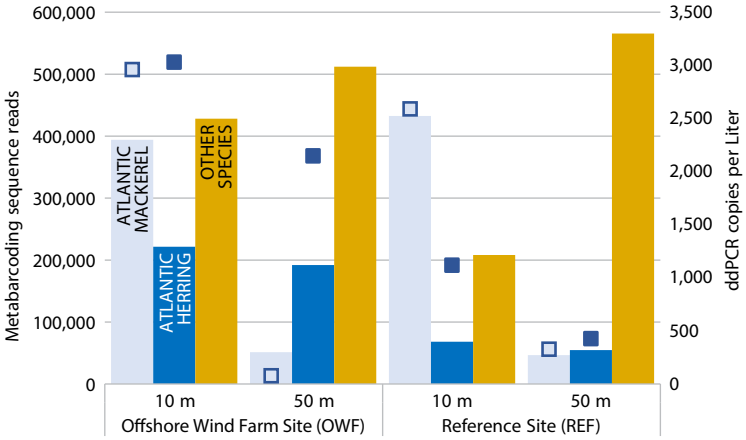

FIGURE 2. Hywind Scotland eDNA MiFish metabarcoding and ddPCR data. Bars represent number of reads from the 12S MiFish metabarcoding sequence data from the offshore wind park and the reference area. Most abundant pelagic species are named and other species are merged (see Table S1).

vertically in the water column over a 24-hour period, a sampling campaign would ideally extend over at least one full migratory cycle.

Our multi-pronged eDNA approach offers a powerful tool for identifying spatial and temporal structuring of pelagic communities. This will facilitate monitoring of change in hard-to-reach areas such as OWE installations where traditional methods are difficult to use. It may also increase the possibilities for identifying ecosystem changes at regional scales and over a broad range of taxons in a way that traditional sampling cannot do.

Pairing metabarcoding for broad-scale community level assessment with ddPCR to obtain quantitative information regarding important target species is a powerful approach for characterizing the structures of pelagic communities.

SUPPLEMENTARY MATERIALS

Supplementary Table S1 is available online at https://doi.org/10.5670/oceanog.2023.s1.30.

REFERENCES

Broström, G. 2008. On the influence of large wind farms on the upper ocean circulation. *Journal of Marine Systems* 74:585–591, https://doi.org/10.1016/j.jmarsys.2008.05.001.

Fernandez-Betelu, O., I.M. Graham, and P.M. Thompson. 2022. Reef effect of offshore structures on the occurrence and foraging activity of harbour porpoises. *Frontiers in Marine Science* 9:980388, https://doi.org/10.3389/fmars.2022.980388.

Floeter, J., J.E.E. van Beusekom, D. Auch, U. Callies, J. Carpenter, T. Dudeck, S. Eberle, A. Eckhardt, D. Gloe, K. Hänselmann, and others. 2017. Pelagic effects of offshore wind farm foundations in the stratified North Sea. *Progress in Oceanography* 156:154–173, https://doi.org/10.1016/j.pocean.2017.07.003.

Methratta, E.T., A. Hawkins, B.R. Hooker, A. Lipsky, and J.A., Hare. 2020. Offshore wind development in the Northeast US Shelf Large Marine Ecosystem. *Oceanography* 33(4):16–27, https://doi.org/10.5670/oceanog.2020.402.

ARTICLE DOI. https://doi.org/10.5670/oceanog.2023.s1.30

Deep-Sea Predator-Prey Dynamics Revealed by Biologging and eDNA Analysis

By Véronique J. Merten, Fleur Visser, and Henk-Jan T. Hoving

At depths below 200 m, the pelagic deep sea comprises the largest, but least explored, part of the ocean. In this vast environment, animals are hard to find, and interactions among them are even harder to investigate (Robison, 2009). Climate change and industrial exploitation are exerting increasing pressure on deep-sea ecosystems, causing a decline in global ecosystem health and ecosystem services. Many of these changes occur outside of the range of human observation and are unrecognized so that effective conservation is limited. Such changes can include interactions between elusive and sometimes giant deep-sea predators such as cetaceans and their prey. The use of on-animal recorders has revealed that multiple species of cetaceans make extensive use of the deep sea, specifically the meso- (200–1,000 m depth) and bathypelagic (1,000–4,000 m depth) zones, to hunt for diverse, often cephalopod-dominated prey populations (Tyack et al., 2006). Because their dives to remote depths are energy consuming, the prey reward needs to be substantial to make the dives profitable. Thus, we expect that deep-diving cetaceans selectively target distinct foraging zones that hold specific prey communities to optimize their foraging performance.

FIGURE 1. Cetacean biologging off Terceira Island, Azores, in the North Atlantic. A tagging pole holds a tag at left, and Risso's dolphins are shown being tagged at right. *Photo credit: Machiel Oudejans*

Cephalopods are extremely abundant and play a pivotal role in marine food webs as both predators and prey (Hoving et al., 2014). For instance, it is estimated that sperm whales alone annually feed on as many cephalopods in terms of biomass as human fisheries catch worldwide. Yet deep-sea cephalopods, in particular, are understudied, and many have never been observed alive in their habitats or captured as adults (Hoving et al., 2014). Traditional methods for studying cetacean prey include net capture, optical methods, or stomach content analysis. Physical and optical sampling face the challenge that cephalopods show avoidance behavior and are patchily distributed. This results in a sampling bias toward less mobile, less sensorially equipped, and abundant specimens (Wormuth and Roper, 1983). Stomach content analysis of cetaceans is rare and requires stranding or capture, and does not typically represent a good average of the population. An alternative method for assessing regional cephalopod diversity and hence potential prey spectra of cetaceans is environmental DNA (eDNA) analysis, a relatively novel tool for studying deep-sea communities. This method exploits the phenomenon that every organism leaves genetic information in the form of DNA particles behind. These DNA particles can stem from shed cells, mucus, or feces and have the potential to reveal the identity of the source organism. eDNA analysis has been successfully used to reconstruct the horizontal distribution, diversity, and migration of open-ocean nekton (Beng and Corlett, 2020). Yet, to the best of our knowledge, eDNA analysis has not been used to investigate cephalopod biodiversity in the deep sea prior to the study presented here, which is adapted from Visser et al. (2021).

TOOTHED WHALE PREDATORS WITH ALTERNATIVE DEEP-SEA FEEDING GROUNDS

We were particularly interested in the foraging behavior of Risso's dolphins *Grampus griseus* and Cuvier's beaked whales *Ziphius cavirostris*, two species of deep-diving toothed whales that co-occur off the Azores but exhibit two distinct deep-sea foraging strategies. Risso's dolphins target cephalopods in epi- and mesopelagic waters, while Cuvier's beaked whales dive deeper to meso- and bathypelagic waters to forage—indeed, the Cuvier's beaked whale holds the record for the deepest and longest dive, which lasted more than two hours to a depth of 2,992 m (Schorr et al., 2014). Despite this segregation in hunting

habitat, stomach content analyses of both species show partially overlapping prey populations dominated by deep-sea squids. A generally accepted but poorly studied hypothesis is that cetacean predators occupy different niches because they target different prey communities. This hypothesis remains largely untested, due to the methodological challenges of reaching and sampling the extreme deep-sea environment in which these animals forage.

To overcome these challenges, we pioneered the assessment of prey community composition via cephalopod eDNA analysis in combination with data on deep-sea predator foraging behavior obtained from biologging of Cuvier's beaked whales and Risso's dolphins. With biologging, we are tagging animals with small, animal-mounted instruments that record depth and sound to measure cetacean diving and acoustic behavior. This approach allowed us to test the hypotheses that Risso's dolphins and Cuvier's beaked whales exploit entirely discrete deep-sea foraging niches and that these niches hold specific prey spectra.

CETACEAN BIOLOGGING

We conducted shore- and vessel-based observations to identify the foraging habitats of Cuvier's beaked whales and Risso's dolphins off Terceira Island, Azores, in the North Atlantic. To determine the foraging depths of the two species, individuals were tagged with noninvasive, high-resolution digital acoustic recording tags (Figure 1). The tags were attached using suction cups and released automatically. They record dive and acoustic data. Risso's dolphins and Cuvier's beaked whales both detect and track prey by emission of echolocation click series, so-called biosonar. Depending on the click rate and amplitude of click series emitted by the cetaceans, we can differentiate between search phases for prey (broadband click series at regular intervals) and prey capture attempts ("buzzes" when the clicks transition into discrete, rapid click series at lower amplitude). Buzzes therefore accurately indicate prey capture attempts and foraging efforts. The tag data revealed a clear niche segregation of foraging habitat and zone between Risso's dolphins and Cuvier's beaked whales. Risso's dolphins hunt close to shore at depths between the surface and 600 m, while Cuvier's beaked whales hunt further offshore at deeper depths, below 900 m in the pelagic and above the bathyal seafloor.

CEPHALOPOD DIVERSITY IDENTIFIED FROM eDNA

After identifying the foraging habitats and zones of Risso's dolphins and Cuvier's beaked whales, we collected seawater at the respective sites throughout the water column from the surface to the seafloor (maximum depth of

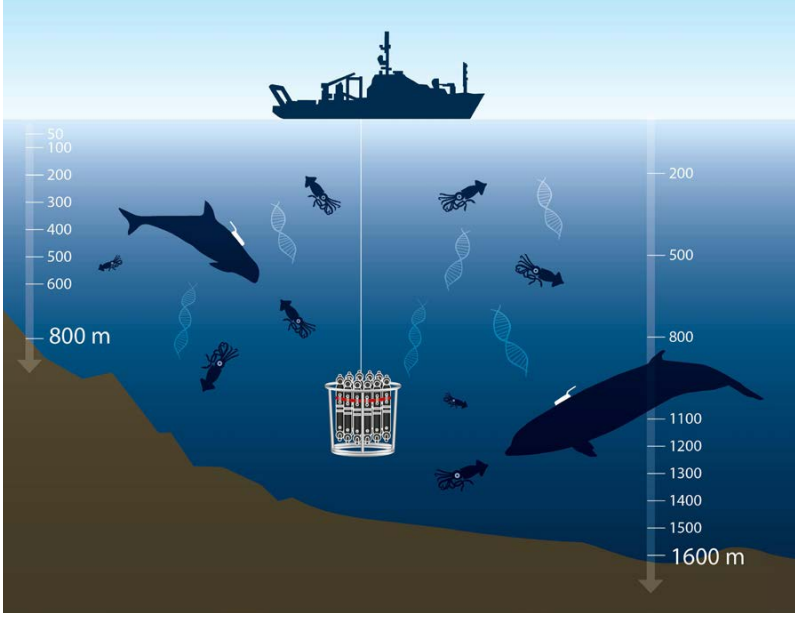

FIGURE 2. Illustration shows targeted sampling for cephalopod eDNA across the foraging zones of two cetacean deep-sea predators, Risso's dolphin (*G. griseus*, left) and Cuvier's beaked whale (*Z. cavirostris*, right), as determined from biologging of their diving and biosonar foraging behavior using noninvasive sound and movement recording tags. *From Visser et al. (2021). © The Authors, some rights reserved; exclusive licensee AAAS. Distributed under a CC BY-NC 4.0 license (https://creativecommons.org/licenses/by-nc/4.0/). Reprinted with permission from AAAS.*

1,600 m) in 100 m depth intervals (Figure 2). The collected seawater was then filtered to retrieve the eDNA. For each depth, we collected and filtered two liters in triplicate. After extracting the DNA from the filters, we amplified it via polymerase chain reaction (PCR) using two universal cephalopod primer pairs. A primer is a short piece of single-strand DNA that flanks the target region to be amplified. This target region or amplicon is later used to identify the taxa. Because a perfect primer that amplifies every species equally well does not exist, we used two primer pairs that target different gene regions to increase the number of taxa detections. We used one primer pair that targets the mitochondrial 16S rRNA gene (Jarman et al., 2006) and another that targets the nuclear 18S rRNA gene of cephalopods. The latter primer pair was developed by our lab (de Jonge et al., 2021).

After PCR and cleaning steps, the amplified DNA was sequenced, resulting in unique genetic barcodes that can be used to identify the taxa present in the filtered water sample. Each generated eDNA barcode is then compared to a reference sequence based on a voucher specimen that has been identified. In addition to primer bias, another bottleneck in eDNA metabarcoding is the incompleteness of reference databases: if species are missing from the reference database, they cannot be identified in the eDNA data. To complement existing cephalopod reference databases, we barcoded 32 additional species that are known to occur in the North Atlantic and have been captured there

in nets. Using public databases along with the one we created, we assigned taxa to the obtained eDNA sequences. As a result, we were able to identify 39 cephalopod taxa in the foraging habitats of Cuvier's beaked whales and Risso's dolphins, including 35 taxa that occurred in the foraging zones of both predators (Figure 3). The most widely detected taxa were *Enoploteuthis leptura* and *Liocranchia reinhardti* (Figure 4). Of the 39 cephalopod taxa, 21 could be identified to species level, which is equal to 25% of the species known to occur off the Azores. We also detected the elusive giant squid *Architeuthis* and two new species for this region: *Chiroteuthis mega* and *Cycloteuthis sirventi.* eDNA analysis proved to be an efficient technique for establishing diversity and distribution patterns of cephalopods in the deep sea. Our results also suggest that cephalopod eDNA is not a homogeneous mixture of DNA particles in the ocean but shows biologically meaningful distribution patterns when compared to cephalopod distributions reported in the literature. For example, strictly deep-sea taxa such as *Planctoteuthis levimana* and *Chtenopteryx* sp. were detected exclusively at great depths, while veined squid (*Loligo forbesii*) were only detected over the island slope at relatively shallow depths, matching its known habitat.

DEEP-SEA PREDATOR-PREY DYNAMICS

With biologging of Cuvier's beaked whales and Risso's dolphins, we were able to confirm our first hypothesis, that the two co-occurring cetaceans exploit two entirely discrete deep-sea foraging niches. By analyzing cephalopod eDNA, including use of a newly developed universal cephalopod primer pair (de Jonge et al., 2021) and the complementation of existing reference databases for cephalopods, we have provided the first reconstruction of cephalopod communities in the pelagic deep sea. Our second hypothesis,

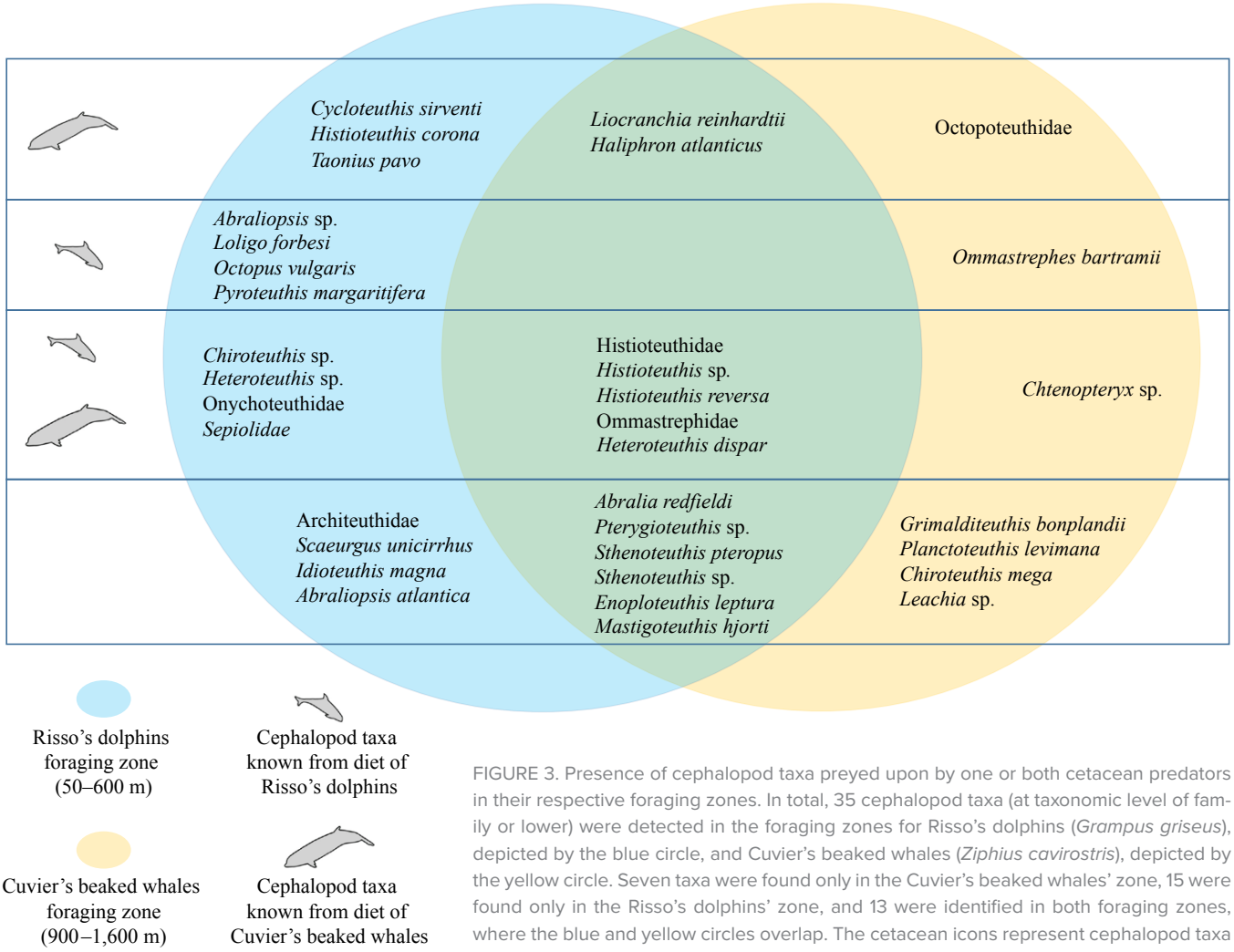

FIGURE 3. Presence of cephalopod taxa preyed upon by one or both cetacean predators in their respective foraging zones. In total, 35 cephalopod taxa (at taxonomic level of family or lower) were detected in the foraging zones for Risso's dolphins (*Grampus griseus*), depicted by the blue circle, and Cuvier's beaked whales (*Ziphius cavirostris*), depicted by the yellow circle. Seven taxa were found only in the Cuvier's beaked whales' zone, 15 were found only in the Risso's dolphins' zone, and 13 were identified in both foraging zones, where the blue and yellow circles overlap. The cetacean icons represent cephalopod taxa known from the diet of either Risso's dolphins (small contour) or Cuvier's beaked whales (large contour). *From Visser et al. (2021). © The Authors, some rights reserved; exclusive licensee AAAS. Distributed under a CC BY-NC 4.0 license (https://creativecommons.org/licenses/by-nc/4.0/). Reprinted with permission from AAAS.*

that the niches of the whales hold specific prey spectra, was not confirmed. Instead, the target zones of both cetacean species were occupied by diverse, overlapping cephalopod communities largely composed of known preferred prey. Thus, the cephalopod community composition did not explain the strict niche segregation. These findings raised the question of why Cuvier's beaked whales dive so deep to forage when they could find the same prey species in shallower waters.

The answer came from the tagging data, which revealed that Cuvier's beaked whales, on average, target seven to 21 fewer prey per hour than Risso's dolphins. As Cuvier's beaked whales are larger than Risso's dolphins and need more energy due to their more extensive diving behavior, they must prey on larger, more calorific prey than Risso's dolphins, which make fewer prey target attempts. eDNA analysis does not provide information on animal size, body mass, or stage of maturity. Five of the seven prey families detected through eDNA analysis, along with an additional four families in Cuvier's beaked whale diet, are known to undergo ontogenetic migration. That is, paralarvae and juvenile cephalopods reside in surface layers to profit from increased primary productivity but descend to deeper layers as they grow to hide from predators and to reproduce (Hoving et al., 2014). Targeting different ontogenetic stages of the same prey species would reduce competition between Cuvier's beaked whales and Risso's dolphins. Hunting for mature and reproducing cephalopods that are more calorific than their paralarval and juvenile stages would also allow Cuvier's beaked whales to meet their increased energetic requirements with fewer prey capture attempts. Cuvier's beaked whales are cryptic flight strategists that form small, temporary groups with limited ability for competition or defense (Aguilar de Soto et al., 2020). Risso's dolphins, on the other hand, are highly social and travel in large groups, which makes it easier for them to compete with other predators for resources (Hartman et al., 2008). Whereas the shallower foraging zones of Risso's dolphins are accessible to many other cetacean species and marine top predators, resulting in increased competition, only a few predators have the ability to target prey at beaked whale foraging depths.

Interactions between cetaceans and cephalopods play a key ecological role in marine deep-sea food webs. As top predators, cetaceans may shape the population size, structure, and distribution of cephalopods. They contribute to carbon flux by predation and defecation. Combined data on potential prey spectra in foraging zones of cetaceans contribute to the understanding of marine top predator foraging behavior and of their resilience to anthropogenic noise and/or climate change. The combination of biologging and eDNA analysis demonstrated here can be applied to other predator-prey systems and help to unravel open-ocean and deep-sea food web processes.

FIGURE 4. The deep-sea squid *Liocranchia reinhardti* lives in shallow waters when young and moves into deeper waters as it matures. This squid species is one of the known prey species of Cuvier's beaked whales. *Photo credit: Solvin Zankl*

REFERENCES

Aguilar de Soto, N., F. Visser, P.L. Tyack, J. Alcazar, G. Ruxton, P. Arranz, P.T. Madsen, and M. Johnson. 2020. Fear of killer whales drives extreme synchrony in deep diving beaked whales. *Scientific Reports* 10:13, https://doi.org/10.1038/s41598-019-55911-3.

Beng, K.C., and R.T. Corlett. 2020. Applications of environmental DNA (eDNA) in ecology and conservation: Opportunities, challenges and prospects. *Biodiversity and Conservation* 29:2,089–2,121, https://doi.org/10.1007/s10531-020-01980-0.

de Jonge, D., V. Merten, T. Bayer, O. Puebla, T.B.H. Reusch, and H.-J.T. Hoving. 2021. A novel metabarcoding primer pair for environmental DNA analysis of Cephalopoda (Mollusca) targeting the nuclear 18S rRNA region. *Royal Society Open Science*, https://doi.org/10.1098/rsos.201388.

Hartman, K.L., F. Visser, and A.J.E. Hendriks. 2008. Social structure of Risso's dolphins (*Grampus griseus*) at the Azores: A stratified community based on highly associated social units. *Canadian Journal of Zoology* 86:294–306, https://doi.org/10.1139/Z07-138.

Hoving, H.J.T., J.A.A. Perez, K.S.R. Bolstad, H.E. Braid, A.B. Evans, D. Fuchs, H. Judkins, J.T. Kelly, J.E.A.R. Marian, R. Nakajima, and others. 2014. The study of deep-sea cephalopods. Pp. 235–359 in *Advances in Cephalopod Science: Biology, Ecology, Cultivation, and Fisheries*. E.A.G. Vidal, ed., Oxford, UK, https://doi.org/10.1016/B978-0-12-800287-2.00003-2.

Jarman, S.N., K.S. Redd, and N.J. Gales. 2006. Group-specific primers for amplifying DNA sequences that identify Amphipoda, Cephalopoda, Echinodermata, Gastropoda, Isopoda, Ostracoda and Thoracica. *Molecular Ecology Notes* 6:268–271, https://doi.org/10.1111/j.1471-8286.2005.01172.x.

Robison, B. 2009. Conservation of deep pelagic biodiversity. *Conservation Biology* 23:847–858, https://doi.org/10.1111/j.1523-1739.2009.01219.x.

Schorr, G.S., E.A. Falcone, D.J. Moretti, and R.D. Andrews. 2014. First long-term behavioral records from Cuvier's beaked whales (*Ziphius cavirostris*) reveal record-breaking dives. *PLoS ONE* 9:e92633, https://doi.org/10.1371/journal.pone.0092633.

Tyack, P.L., M. Johnson, N.A. Soto, A. Sturlese, and P.T. Madsen. 2006. Extreme diving of beaked whales. *Journal of Experimental Biology* 209:4,238–4,253, https://doi.org/10.1242/jeb.02505.

Visser, F., V.J. Merten, T. Bayer, M.G. Oudejans, D.S.W. de Jonge, O. Puebla, T.B.H. Reusch, J. Fuss, and H.J.T. Hoving. 2021. Deep-sea predator niche segregation revealed by combined cetacean biologging and eDNA analysis of cephalopod prey. *Science Advances* 7:eabf5908, https://doi.org/10.1126/sciadv.abf5908.

Wormuth, J.H., and C.F.E. Roper. 1983. Quantitative sampling of oceanic cephalopods by nets: Problems and recommendations. *Biological Oceanography* 2(2–4):357–377.

ARTICLE DOI. https://doi.org/10.5670/oceanog.2023.s1.31

Evaluating Connectivity of Coastal Marine Habitats in the Gulf of Maine by Integrating Passive Acoustics and Metabarcoding

By Grant Milne, Jennifer Miksis-Olds, Alyssa Stasse, Bo-Young Lee, Dylan Wilford, and Bonnie Brown

Ecological connectivity among coastal marine habitats—linkage in the movement of organisms and natural processes across habitat boundaries—has significant implications for the health and resilience of commercially important or threatened species in the Gulf of Maine (GOM), off the coast of the northeastern United States. Methods designed to efficiently assess connectivity are vital for identifying and managing critical habitats (Perry et al., 2018). Paired use of passive acoustic monitoring (PAM) and metabarcoding seawater samples (MSS) for observing biological and functional connectivity at various spatiotemporal scales in the marine environment is largely unexplored and may provide an efficient alternative or supplement to existing strategies.

Passive acoustic recordings are non-invasive, can identify sound sources, and can quantify spatial, temporal, and frequency attributes of an environment, collectively referred to as the soundscape. Sound sources contributing to the underwater soundscape are categorized as biological (e.g., fish vocalizations, feeding sounds), anthropogenic (e.g., vessels, underwater construction), and geophysical (e.g., breaking waves, precipitation, earthquakes). PAM enables assessment of soundscapes over extended temporal periods with minimal environmental disturbance. This permits detection of sound source presence, individual source identification, taxa detection, and quantification of properties of the acoustic environment. However, PAM is only able to detect sources that are actively producing sound and cannot confirm sound producer absence. PAM also is limited by sound recording hardware constraints, high intensity acoustic masking conditions, and generation of large quantities of data that are resource intensive to store and analyze.

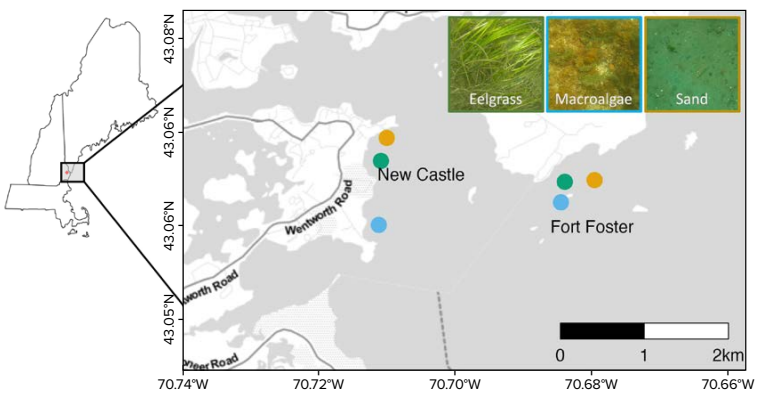

FIGURE 1. Location of hydrophone deployments in eelgrass (green), macroalgae (blue), and sand/mud (orange) habitats.

Metabarcoding analyses involve extracting genetic material from particles in the environment. Using MSS, genetic material is selectively amplified with primers that target certain taxa, the amplicons are sequenced, and the reads are compared against reference databases to assign sequences to taxonomic groups. This strategy enables detection of organism presence across a broad taxonomic range. MSS has limitations, including the inability to confirm absence of taxa, biases associated with the amplification process, and diminishing DNA detectability over time.

Coupling PAM observations of biological, anthropogenic, and geophysical activity with MSS detection of taxa that may or may not produce sound provides a more complete picture of biological connectivity in terms of ecology and function. Combined characterization of soundscapes and metagenomes of similar habitat types in different geographic locations affords the opportunity to determine whether habitat type or geographic location is more influential for either platform and indicates where the strongest localized functional connectivity operates within the GOM, for example, whether sound pollution is disrupting functional connectivity among habitats.

As part of a feasibility study of biological and acoustic connectivity of marine habitats, three habitat types in the shallow (<10 m depth) subtidal GOM were sampled. Target habitats, defined by biogenic and geologic components of the bottom substrate and including the water column located vertically above these substrates, were (1) eelgrass (*Zostera marina*) beds on soft substrates, (2) macroalgae colonizing hard substrates, and (3) soft sand/mud substrates with low biogenic cover. Two separate locations, each containing all three target habitat types, were sampled near New Castle, New Hampshire, and Fort Foster, Maine (Figure 1). These two locations were separated by ~2 km, and habitats within each were situated ≤1 km apart.

Acoustic recordings were made with SoundTrap ST500 hydrophones deployed 0.5–1 m above the substrate at all habitats. The sample rate was 144 kHz at a 50% duty cycle for a two- to three-week deployment period. Recordings collected over the deployment period were subsampled for 1 h at dawn, noon, dusk, and midnight, totaling 4 h from each day. Calculated acoustic measurements provided quantitative descriptions of the uniformity, impulsivity, and amplitude of the soundscapes in each habitat (Wilford et al., 2021). Measurements of these properties allowed for rapid, comprehensive soundscape comparisons.

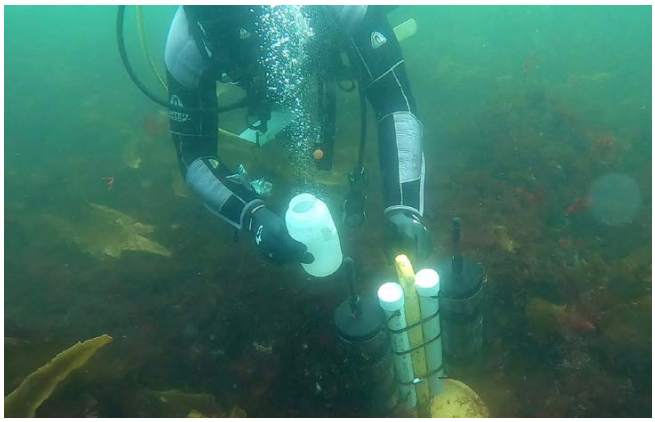

FIGURE 2. A diver collects water samples for metabarcoding near a hydrophone deployed in a macroalgae habitat. *Photo credit: J. Hamilton*

During each hydrophone deployment period, 3 L water samples were collected at two- to five-day intervals near the hydrophones from 1 m above the substrate (Figure 2). These samples were stored on ice for transport to the laboratory, filtered to concentrate particles ≥5 µm, and the filters were frozen until extracted with a QIAGEN PowerWater kit. The resulting genetic material was amplified using cytochrome c oxidase subunit I (COI) and V9 primer sets that targeted metazoan and macroalgae/macrophyte DNA, respectively. Subsequently, the array of DNA sequences for each sample was determined to the genus level (Jeunen et al., 2019).

Non-metric multidimensional scaling ordination (NMS) calculated with Bray-Curtis distance for genetic and acoustic data revealed that more variation is accounted for by geographic location than by habitat type. NMS of marine taxon presence revealed clear dissimilarities among coastal metagenomes by geographic location but showed no clear grouping by habitat (Figure 3a). These preliminary results contradict previous findings that coastal habitats in New Zealand connected by water movement exhibit distinct groupings in metagenomes (Jeunen et al., 2019) potentially due to the extreme proximity and comparatively narrow taxonomic focus (metazoans, macrophytes, macroalgae) of this preliminary study, which will be expanded to include detection of additional taxa (fish, marine mammals) in future work. For soundscape measurements, NMS ordination of $\log_{10}(x+1)$ transformed medians and central 95th percentages (C95) of each metric for each habitat showed clear grouping of soundscapes by geographic location, with some degree of separation by habitat (Figure 3b).

These preliminary results illustrate biological and functional connectivity among habitats at local scales and dissimilarity among the soundscapes and metagenomes of similar habitats at larger geographic scales. The MSS analyses complemented PAM by revealing the presence of taxa that are negligible sound producers, but that may modify the acoustic environment either by serving as sound attenuators or through association with substrates expected

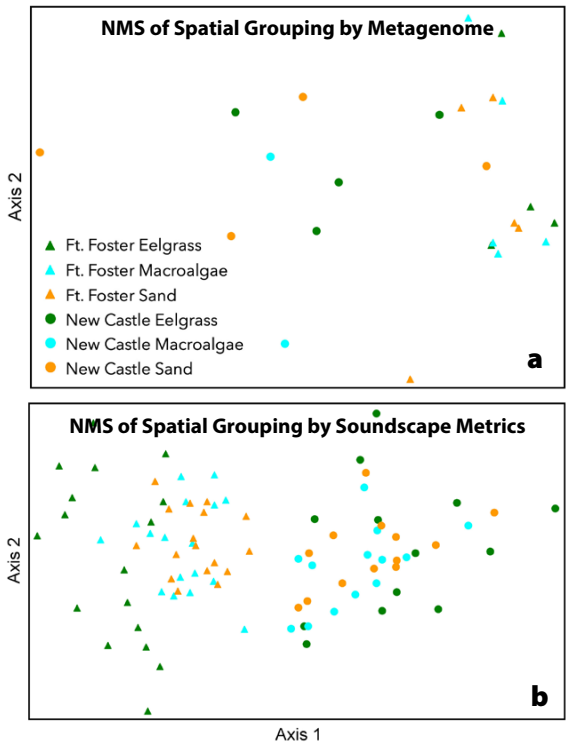

FIGURE 3. (a) Non-metric multidimensional scaling ordination (NMS) ordination of marine metagenomes, where each point represents one water sample collected from a habitat. Shapes indicate geographic location; triangles and circles represent Fort Foster and New Castle samples, respectively. Colors indicate habitat type: green, blue, and orange correspond to eelgrass, macroalgae, and sand habitats, respectively. (b) NMS ordination of median and central 95th percentage (C95) values for each soundscape metric. Each point represents four hours of acoustic data collected during one day of recording in a habitat.

to differentially impact sound propagation. PAM complemented MSS by detecting anthropogenic and geophysical sound sources expected to impact the functional connectivity of habitats that would be overlooked using MSS alone. The combination of these minimally invasive observation techniques allows for more complete detection of factors contributing to both sound production and propagation than would be possible with either technique individually. Future research will involve identifying drivers of acoustic and genetic variation among geographic locations, as well as identification of indicators of similar habitat types.

REFERENCES

Jeunen, G.J., M. Knapp, H.G. Spencer, M.D. Lamare, H.R. Taylor, M. Stat, M. Bunce, and N.J. Gemmell. 2019. Environmental DNA (eDNA) metabarcoding reveals strong discrimination among diverse marine habitats connected by water movement. *Molecular Ecology Resources* 19(2):426–438, https://doi.org/10.1111/1755-0998.12982.

Perry, D., T.A.B. Staveley, and M. Gullström. 2018. Habitat connectivity of fish in temperate shallow-water seascapes. *Frontiers in Marine Science* 4:440, https://doi.org/10.3389/fmars.2017.00440.

Wilford, D.C., J.L. Miksis-Olds, S.B. Martin, D.R. Howard, K. Lowell, A.P. Lyons, and M.J. Smith. 2021. Quantitative soundscape analysis to understand multidimensional features. *Frontiers in Marine Science* 8:672336, https://doi.org/10.3389/fmars.2021.672336.

ARTICLE DOI. https://doi.org/10.5670/oceanog.2023.s1.32

AUTHORS

INTRODUCTION

PAGE 1. **Ellen S. Kappel** (ekappel@geo-prose.com), Geosciences Professional Services Inc., Bethesda, MD, USA. **Mark John Costello**, Nord University, Bodø, Norway. **Luisa Galgani**, GEOMAR Helmholtz Center for Ocean Research Kiel, Germany. **Cesc Gordó-Vilaseca**, Nord University, Bodø, Norway. **Annette Govindarajan**, Woods Hole Oceanographic Institution, Woods Hole, MA, USA. **Soroush Kouhi**, Ocean Networks Canada, Victoria, BC, Canada. **Charles Lavin**, Nord University, Bodø, Norway. **Luke McCartin**, Lehigh University, Bethlehem, PA, USA. **Jens Daniel Müller**, ETH Zürich, Zürich, Switzerland. **Benoît Pirenne**, Ocean Networks Canada, Victoria, BC, Canada. **Toste Tanhua**, GEOMAR Helmholtz Center for Ocean Research Kiel, Germany. **Qianshuo Zhao**, Ocean University of China, Shandong, China. **Shiye Zhao**, Japan Agency for Marine-Earth Science and Technology, Yokosuka, Japan.

OCEAN CLIMATE NEXUS

PAGE 2. **Philip W. Boyd*** (philip.boyd@utas), Institute for Marine and Antarctic Studies, University of Tasmania, Hobart, TAS, Australia. **Hervé Claustre*** (herve.claustre@imev-mer.fr), **Louis Legendre*** (legendre@imev-mer.fr), and **Jean-Pierre Gattuso**, Sorbonne University, CNRS, Laboratoire d'Océanographie de Villefranche (LOV), Villefranche-sur-Mer, France. **Pierre-Yves Le Traon**, Mercator Ocean International, Ramonville-Saint-Agne, France.

PAGE 11. **Catherine Garcia** (cathy.garcia@hawaii.edu), **Benedetto Barone**, **Sara Ferrón**, and **David Karl**, University of Hawai'i at Mānoa, Honolulu, HI, USA.

PAGE 14. **Philip J. Bresnahan** (bresnahanp@uncw.edu), **Elizabeth Farquhar**, **Daniel Portelli**, and **Michael Tydings**, Department of Earth and Ocean Sciences, University of North Carolina Wilmington, Wilmington, NC, USA. **Taylor Wirth** and **Todd Martz**, Scripps Institution of Oceanography, University of California San Diego, La Jolla, CA, USA.

PAGE 16. **Chester J. Sands** (cjsan@bas.ac.uk), British Antarctic Survey, Cambridge, UK. **Nadescha Zwerschke**, Greenland Institute of Natural Resources, Nuuk, Greenland. **Narissa Bax**, South Atlantic Environment Research Institute, Stanley, Falkland Islands, and Centre for Marine Socioecology, Institute for Marine and Antarctic Studies, University of Tasmania, Hobart, Australia. **David K.A. Barnes**, British Antarctic Survey, Cambridge, UK. **Camille Moreau**, Université Libre de Bruxelles, Brussels, Belgium. **Rachel Downey**, Australian National University, Canberra, Australia. **Bernabé Moreno**, Institute of Oceanology Polish Academy of Sciences, Sopot, Poland. **Christoph Held**, Alfred Wegener Institute Helmholtz Centre for Polar and Marine Research, Bremerhaven, Germany. **Maria Paulsen**, Aahus Universitet, Aahus, Denmark.

PAGE 18. **Anya Waite**, **Mike Smit**, **Eric Siegel**, **Greg Hanna** (greg.hanna@dal.ca), and **Sara Leslie**, Ocean Frontier Institute, Dalhousie University, Halifax, NS, Canada.

*Equal first authors

ECOSYSTEMS AND THEIR DIVERSITY

PAGE 20. **Tzu-Hao Lin** (lintzuhao@gate.sinica.edu.tw), Biodiversity Research Center, Academia Sinica, Taiwan. **Frederic Sinniger** (fredsinniger@hotmail.com) and **Saki Harii**, Tropical Biosphere Research Center, University of Ryukyus, Japan. **Tomonari Akamatsu**, The Ocean Policy Research Institute, The Sasakawa Peace Foundation, Japan.

PAGE 28. **Stephen B. Brandt** (stephen.brandt@oregonstate.edu), Department of Fisheries, Wildlife, and Conservation Sciences, Oregon State University (OSU), Corvallis, OR, USA. **Sarah E. Kolesar**, Oregon Sea Grant, OSU, Corvallis, OR, USA. **Cassandra N. Glaspie**, Department of Oceanography and Coastal Sciences, Louisiana State University, Baton Rouge, LA, USA. **Arnaud Laurent**, Department of Oceanography, Dalhousie University, Halifax, NS, Canada. **Cynthia E. Sellinger**, Department of Fisheries, Wildlife and Conservation Sciences, OSU, Corvallis, OR, USA. **James J. Pierson**, **Michael R. Roman**, and **William C. Boicourt**, Horn Point Laboratory, University of Maryland Center for Environmental Science, Cambridge, MD, USA.

PAGE 31. **Suzanne Strom** (stroms@wwu.edu), Shannon Point Marine Center, Western Washington University, Anacortes, WA, USA, and the **Northern Gulf of Alaska Long-Term Ecosystem Research Team**.

PAGE 34. **Amy Leigh Mackintosh** (amy.mackintosh@nord.no), **Griffin Goldstein Hill**, **Mark John Costello**, and **Alexander Jueterbock**, Faculty of Biosciences and Aquaculture, Nord University, Bodø, Norway. **Jorge Assis**, Centre of Marine Sciences, CCMAR, University of Algarve, Faro, Portugal.

PAGE 36. **David R. Williamson** (david.williamson@ntnu.no), Norwegian University of Science and Technology (NTNU), and SINTEF Ocean, Trondheim, Norway. **Glaucia M. Fragoso**, **Sanna Majaneva**, **Alberto Dallolio**, **Daniel Ø. Halvorsen**, **Oliver Hasler**, **Adriënne E. Oudijk**, **Dennis D. Langer**, **Tor Arne Johansen**, **Geir Johnsen**, **Annette Stahl**, **Martin Ludvigsen**, and **Joseph L. Garrett**, NTNU, Trondheim, Norway.

PAGE 38. **Lillian R. Aoki**, Department of Ecology and Evolutionary Biology, Cornell University, Ithaca, NY, USA, now at Data Science Initiative, University of Oregon, Eugene, OR, USA. **Bo Yang**, Department of Urban and Regional Planning, San Jose State University, San Jose, CA, USA. **Olivia J. Graham**, Department of Ecology and Evolutionary Biology, Cornell University, Ithaca, NY, USA. **Carla Gomes** and **Brendan Rappazzo**, Department of Computer Science, Cornell University, Ithaca, NY, USA. **Timothy L. Hawthorne**, Department of Sociology and College of Sciences GIS Cluster, University of Central Florida, Orlando, FL, USA. **J. Emmett Duffy**, Tennenbaum Marine Observatories Network, Smithsonian Institution, Edgewater, MD, USA. **Drew Harvell** (cdh5@cornell.edu), Department of Ecology and Evolutionary Biology, Cornell University, Ithaca, NY, USA.

PAGE 40. **Xiaobo Ni*** (xiaoboni@sio.org.cn), **Feng Zhou***, **Dingyong Zeng**, **Dewang Li**, **Tao Zhang**, **Kui Wang**, **Yunlong Ma**, **Qicheng Meng**, **Xiao Ma**, **Qianjiang Zhang**, **Daji Huang**, and **Jianfang Chen**, Second Institute of Oceanography, Ministry of Natural Resources, Hangzhou, Peoples Republic of China.

OCEAN POLLUTANTS

PAGE 42. **Lixin Zhu***, Department of Marine and Environmental Sciences, Northeastern University, Boston, MA, USA. **Nicola Gaggelli***, Department of Biotechnology, Chemistry and Pharmacy, University of Siena, Siena, Italy. **Amedeo Boldrini**, Department of Biotechnology, Chemistry and Pharmacy, CSGI, University of Siena, Siena, Italy. **Aron Stubbins** (a.stubbins@northeastern.edu), Department of Marine and Environmental Sciences, Civil and Environmental Engineering, and Chemistry and Chemical Biology, Northeastern University, Boston, MA, USA. **Steven Arthur Loiselle** (loiselle@unisi.it), Department of Biotechnology, Chemistry and Pharmacy, CSGI, University of Siena, Siena, Italy.

PAGE 49. **Daniel Koestner** (daniel.koestner.optics@gmail.com), Department of Physics and Technology, University of Bergen, Bergen, Norway. **Robert Foster** and **Ahmed El-Habashi**, Remote Sensing Division, US Naval Research Laboratory, Washington, DC, USA.

PAGE 52. **Luisa Galgani** (lgalgani@geomar.de), GEOMAR Helmholtz Center for Ocean Research Kiel, Germany, and Harbor Branch Oceanographic Institute of Florida Atlantic University, USA. **Helmke Hepach**, **Kevin W. Becker**, and **Anja Engel**, GEOMAR Helmholtz Center for Ocean Research Kiel, Germany.

PAGE 54. **Jun She** (js@dmi.dk), Danish Meteorological Institute, Copenhagen, Denmark. **Asbjørn Christensen**, National Institute of Aquatic Resources, Lyngby, Denmark. **Francesca Garaventa**, Institute for the Study of Anthropic Impacts and Sustainability in the Marine Environment, National Research Council of Italy, Rome, Italy. **Urmas Lips**, Tallinn University of Technology, Tallinn, Estonia. **Jens Murawski**, Danish Meteorological Institute, Copenhagen, Denmark. **Manolis Ntoumas** and **Kostas Tsiaras**, Institute of Oceanography, Hellenic Center for Marine Research, Heraklion, Crete, Greece.

*Equal first authors

PAGE 58. **Juan Carlos Herguera** (herguera@cicese.mx), **Edward M. Peters**, **Julio Sheinbaum**, **Paula Pérez-Brunius**, **Vanesa Magar**, **Enric Pallàs-Sanz**, and **Sheila Estrada Allis**, Centro de Investigación Científica y Educación Superior de Ensenada, CICESE, México. **M. Leopoldina Aguirre-Macedo** and **Victor Manuel Vidal-Martinez**, Centro de Investigación y de Estudios Avanzados, CINVESTAV-Mérida, México. **Cecilia Enriquez** and **Ismael Mariño Tapia**, Escuela Nacional de Estudios Superiores ENES-UNAM Unidad Mérida, México. **Hector García Nava** and **Xavier Flores Vidal**, Universidad Autónoma de Baja California (UABC)-Instituto de Investigaciones Oceanológicas, México. **Tomas Salgado**, Centro de Ingeniería y Desarrollo Industrial CIDESI, México. **Rosario Romero-Centeno** and **Jorge Zavala-Hidalgo**, UNAM-Instituto de Ciencias de la Atmósfera y Cambio Climático, México. **Eduardo Amir Cuevas Flores**, Centro de Investigación y de Estudios Avanzados, CINVESTAV-Mérida, México. **Abigail Uribe Martínez**, Laboratorio de Ingeniería y procesos Costeros, Unidad Académica Sisal, UNAM, México. **Laura Carrillo**, El Colegio de la Frontera Sur-Chetumal (ECOSUR), México.

PAGE 64. **Brian M. Phillips** (brian.phillips@essie.ufl.edu), Department of Civil and Coastal Engineering, and **Forrest J. Masters**, School of Sustainable Infrastructure & Environment, University of Florida, Gainesville, FL, USA. **Britt Raubenheimer**, Applied Ocean Physics and Engineering, Woods Hole Oceanographic Institution, Woods Hole, MA, USA. **Maitane Olabarrieta**, Department of Civil and Coastal Engineering, and **Elise S. Morrison**, Department of Environmental Engineering Sciences, University of Florida, Gainesville, FL, USA. **Pedro L. Fernández-Cabán**, Department of Civil and Environmental Engineering, Florida A&M University-Florida State University, Tallahassee, FL, USA. **Christopher C. Ferraro**, **Justin R. Davis**, **Taylor A. Rawlinson**, and **Michael B. Rodgers**, Department of Civil and Coastal Engineering, University of Florida, Gainesville, FL, USA.

PAGE 66. **Tom Spencer** (ts111@cam.ac.uk), Cambridge Coastal Research Unit, University of Cambridge, Cambridge, UK. **Mike Dobson**, Arup Liverpool, Liverpool, UK. **Elizabeth Christie**, Cambridge Coastal Research Unit, University of Cambridge, Cambridge, UK. **Richard Eyres**, Cada Consulting, Liverpool, UK. **Sue Manson**, UK Environment Agency, Kingston upon Hull, UK. **Steve Downie**, Arup Liverpool, Liverpool, UK. **Angela Hibbert**, National Oceanography Centre and British Oceanographic Data Centre, Liverpool, UK.

PAGE 69. **Gianna Milton** (gmilton@tamu.edu), **Steven F. DiMarco** (sdimarco@tamu.edu), and **Anthony H. Knap**, Department of Oceanography and Geochemical and Environmental Research Group, Texas A&M University, College Station, TX, USA. **John Walpert**, Geochemical and Environmental Research Group, Texas A&M University, College Station, TX, USA. **Roee Diamant**, Underwater Acoustic and Navigation Laboratory, Department of Marine Technology, Leon H. Charney School of Marine Sciences, University of Haifa, Haifa, Israel.

PAGE 70. **Eduardo Pereira** (eduardo.pereira@civil.uminho.pt) and **Marcos Tieppo**, University of Minho, Braga, Portugal. **João Faria**, DSTelecom, Braga, Portugal. **Douglas Hart** and **Pierre Lermusiaux**, Massachusetts Institute of Technology, Cambridge, MA, USA. **K2D PROJECT TEAM ALSO INCLUDES: Tiago Miranda**, **Luís Gonçalves**, **Marcos Martins**, and **Filipe Costa**, University of Minho, Braga, Portugal. **Laura Gonzáles Garcia** and **Margarida Rolim**, University of the Azores, Ponta Delgada, Portugal. **Emanuel Castanho**, **José Moutinho**, and **Tânia Chen**, Atlantic International Research (AIR) Center, Angra do Heroísmo, Portugal. **Aníbal Matos**, **Bruno Ferreira**, and **Nuno Cruz**, Institute for Systems and Computer Engineering, Technology and Science (INESC TEC), University of Porto, Porto, Portugal. **Sérgio Jesus**, **António Silva**, **Friedrich Zabel**, and **Rúben Viegas**, Centro de Investigação Tecnológica do Algarve (CINTAL) – University of Algarve, Faro, Portugal. **John Leonard**, Massachusetts Institute of Technology, Cambridge, MA, USA.

PAGE 72. **Cassandra Bosma** (cbosma26@uvic.ca), **Adrienne Shumlich**, **Mark Rankin**, **Soroush Kouhi**, and **Reza Amouzgar**, Ocean Networks Canada, Victoria, BC, Canada.

PAGE 74. **Soroush Kouhi** (skouhi@uvic.ca), **Reza Amouzgar**, **Mark Rankin**, **Cassandra Bosma**, and **Adrienne Shumlich**, Ocean Networks Canada, Victoria, BC, Canada.

PAGE 76. **Fatemeh Nemati** (fnemati@uvic.ca) and **Lucinda Leonard**, University of Victoria, Victoria, BC, Canada. **Gwyn Lintern**, **Camille Brillon**, and **Andrew Schaeffer**, Natural Resources Canada, Sidney, BC, Canada. **Richard Thomson**, Fisheries and Oceans Canada, Sidney, BC, Canada.

PAGE 78. **Vitalijus Kondrat** (vitalijus.kondrat@ku.lt), **Ilona Šakurova**, **Eglė Baltranaitė**, and **Loreta Kelpšaitė-Rimkienė**, Klaipeda University's Marine Research Institute, Klaipėda, Lithuania.

*Equal first authors

PAGE 80. **Annette F. Govindarajan** (afrese@whoi.edu), Biology Department, Woods Hole Oceanographic Institution (WHOI), Woods Hole, MA, USA. **Allan Adams**, Aquatic Laboratories, Cambridge, MA, USA, and Department of Applied Ocean Physics and Engineering, WHOI, Woods Hole, MA, USA. **Elizabeth Allan**, School of Marine and Environmental Affairs, University of Washington, Seattle, WA, USA. **Santiago Herrera**, Department of Biological Sciences, Lehigh University, Bethlehem, PA, USA. **Andone Lavery**, Department of Applied Ocean Physics and Engineering, WHOI, Woods Hole, MA, USA. **Joel Llopiz**, Biology Department, WHOI, Woods Hole, MA, USA. **Luke McCartin**, Department of Biological Sciences, Lehigh University, Bethlehem, PA, USA. **Dana R. Yoerger** and **Weifeng Zhang**, Department of Applied Ocean Physics and Engineering, WHOI, Woods Hole, MA, USA.

PAGE 87. **Jeremy F. Jenrette** (jjeremy1@vt.edu), Department of Fish and Wildlife Conservation, Virginia Tech, Blacksburg, VA, USA. **Jennifer L. Jenrette**, Genomics Sequencing Center, Virginia Tech, Blacksburg, VA, USA. **N. Kobun Truelove**, Monterey Bay Aquarium Research Institute, Monterey, CA, USA. **Stefano Moro**, Sapienza University of Rome, Rome, Italy, and Stazione Zoologica Anton Dohrn, Naples, Italy. **Nick I. Dunn**, Institute of Zoology, The Zoological Society of London, London, UK. **Taylor K. Chapple**, Coastal Oregon Marine Experiment Station, Oregon State University, Newport, OR, USA. **Austin J. Gallagher**, Beneath the Waves Inc., Herndon, VA, USA. **Chiara Gambardella**, Stazione Zoologica Anton Dohrn, Naples, Italy. **Robert Schallert**, Stanford University, Palo Alto, CA, USA. **Brendan D. Shea**, Department of Fish and Wildlife Conservation, Virginia Tech, Blacksburg, VA, USA, and Beneath the Waves Inc., Herndon, VA, USA. **David J. Curnick**, Institute of Zoology, The Zoological Society of London, London, UK. **Barbara A. Block**, Stanford University, Palo Alto, CA, USA. **Francesco Ferretti**, Department of Fish and Wildlife Conservation, Virginia Tech, Blacksburg, VA, USA.

PAGE 90. **Erin V. Satterthwaite** (esatterthwaite@ucsd.edu), California Cooperative Oceanic Fisheries Investigations (CalCOFI) and California Sea Grant, Scripps Institution of Oceanography, University of California San Diego (UCSD), La Jolla, CA, USA. **Andrew E. Allen** and **Robert H. Lampe**, Scripps Institution of Oceanography, UCSD, and J. Craig Venter Institute, La Jolla, CA, USA. **Zachary Gold**, Scripps Institution of Oceanography, UCSD, La Jolla, CA, USA; Southern California Coastal Watershed Research Project, Costa Mesa, CA, USA; NOAA Southwest Fisheries Science Center (SWFSC), La Jolla, CA, USA; and Pacific Marine Environmental Laboratory, Seattle, WA, USA. **Andrew R. Thompson** and **Noelle Bowlin**, NOAA SWFSC, La Jolla, CA, USA. **Rasmus Swalethorp**, Scripps Institution of Oceanography, UCSD, La Jolla, CA, USA. **Kelly D. Goodwin**, NOAA SWFSC, La Jolla, CA, USA, and NOAA Atlantic Oceanographic & Meteorological Laboratory, Miami, FL, USA. **Elliott L. Hazen** and **Steven J. Bograd**, NOAA SWFSC, Monterey, CA, USA. **Stephanie A. Matthews** and **Brice X. Semmens**, Scripps Institution of Oceanography, UCSD, La Jolla, CA, USA.

PAGE 94. **Thomas G. Dahlgren** (thda@norceresearch.no), NORCE Climate & Environment, Bergen, Norway, and Department of Marine Sciences, University of Gothenburg, Gothenburg, Sweden. **Jon Thomassen Hestetun** and **Jessica Ray**, NORCE Climate & Environment, Bergen, Norway.

PAGE 96. **Véronique J. Merten** (vmerten@geomar.de), Deep-Sea Biology Research Group, GEOMAR Helmholtz Centre for Ocean Research Kiel, Germany. **Fleur Visser**, University of Amsterdam and the Netherlands Institute for Sea Research, Amsterdam, the Netherlands. **Henk-Jan T. Hoving**, Deep-Sea Biology Research Group, GEOMAR Helmholtz Centre for Ocean Research Kiel, Germany.

PAGE 100. **Grant Milne** (grant.milne@unh.edu), **Jennifer Miksis-Olds**, **Alyssa Stasse**, **Bo-Young Lee**, **Dylan Wilford**, and **Bonnie Brown**, University of New Hampshire, Durham, NH, USA.

*Equal first authors

ACRONYMS

ACDP.....Acoustic Doppler Current Profiler

AUV.....Autonomous Underwater Vehicle

BGC-Argo.....Biogeochemical Argo

CDR.....Carbon Dioxide Removal

CO_2.....Carbon Dioxide

CTD.....Conductivity-Temperature-Depth

DEM.....Digital Elevation Model

DO.....Dissolved Oxygen

DOC.....Dissolved Organic Carbon

DOM.....Dissolved Organic Matter

eDNA.....Environmental DNA

EOV.....Essential Ocean Variable

GRP.....Growth Rate Potential

IOP.....Inherent Optical Properties

IPPC.....Intergovernmental Panel on Climate Change

LTER.....Long Term Ecological Research

mCDR.....Marine Carbon Dioxide Removal

NOAA.....National Oceanic and Atmospheric Administration

NSF.....National Science Foundation

ONC.....Ocean Networks Canada

OTZ.....Ocean Twilight Zone

PCR.....Polymerase Chain Reaction

POGO.....Partnership for Observation of the Global Ocean

TA.....Total Alkalinity

UN.....United Nations

UAV.....Uncrewed Aerial Vehicle

USV.....Uncrewed Surface Vehicle

WHOI.....Woods Hole Oceanographic Institution

OPPOSITE PAGE. A live dive onboard Canadian Coast Guard Vessel *John P. Tully* during a 2022 expedition to maintain and install infrastructure and instrumentation at Ocean Network Canada's NEPTUNE and VENUS observatories located off the west and east coasts of Vancouver Island. *Photo credit: ONC*

An earthquake early warning sensor—a Titan accelerometer—is encased in a glass sphere to withstand the pressure in water depths of 850 m at Barkley Canyon, located at Ocean Network Canada's NEPTUNE observatory off the west and east coasts of Vancouver Island. *Photo credit: ONC/WHOI*

Publisher

The Oceanography Society

1 Research Court, Suite 450-117
Rockville, MD 20850 USA
https://tos.org

Sponsors

Support for this publication is provided by Ocean Networks Canada, the National Oceanic and Atmospheric Administration's Global Ocean Monitoring and Observing Program, and the Partnership for Observation of the Global Ocean.